Ghent University Faculty of Sciences – Department of Plant Biotechnology and Bioinformatics

Identification and characterization of E3 ubiquitin ligases involved in jasmonate signalling

Astrid Nagels Durand

Thesis submitted in partial fulfilment of requirements for the degree of
Doctor (PhD) in Sciences: Biotechnology

July 2015

Promotors:

Prof. Dr. Alain Goossens
Faculty of Sciences, Department Plant Biotechnology and Bioinformatics, Ghent University, Belgium
VIB Department of Plant Systems Biology, Secondary Metabolism group, B-9052 Ghent, Belgium

Dr. Laurens Pauwels
Faculty of Sciences, Department Plant Biotechnology and Bioinformatics, Ghent University, Belgium
VIB Department of Plant Systems Biology, Secondary Metabolism group, B-9052 Ghent, Belgium

This research was performed in the Department of Plant Systems Biology of the Flanders Institute for Biotechnology

This work was supported by The Research Foundation-Flanders (FWO) through the projects GA13111N and G005212N.

EXAM COMMISSION

Chairman

Prof. Dr. Lieven De Veylder	Department of Plant Biotechnology and Bioinformatics Faculty of Sciences Ghent University

Promotors

Prof. Dr. Alain Goossens (Secretary)	Department of Plant Biotechnology and Bioinformatics Faculty of Sciences Ghent University
Dr. Laurens Pauwels (Secretary)	Department of Plant Biotechnology and Bioinformatics Faculty of Sciences Ghent University

Promotion commission

Prof. Dr. Rudi Beyaert	Department of Biomedical Molecular Biology Faculty of Sciences Ghent University
Dr. Steven Spoel *	Institute of Molecular Plant Sciences School of Biological Sciences University of Edinburgh (UK)
Prof. Dr. Steven Maere	Department of Plant Biotechnology and Bioinformatics Faculty of Sciences Ghent University
Prof. Dr. Tina Kyndt *	Department of Molecular Biotechnology Faculty of Bioscience Engineering Ghent University
Dr. Barbara De Coninck *	Centre of Microbial and Plant Genetics Katholieke Universiteit Leuven
Dr. Jefri Heyman *	Department of Plant Biotechnology and Bioinformatics Faculty of Sciences Ghent University

*Members of the reading committee

Summary

Ubiquitination, the covalent attachment of ubiquitin (Ub) to a target protein, is a post-translational modification that is involved in most, if not all, biological processes in eukaryotic organisms. Ubiquitination of a target protein requires the consecutive action of three enzymes (E1, E2 and E3). The E3 Ub ligase is of special interest because it is responsible for recruiting the target protein, determining the specificity of this modification. The Ub system contributes to the regulation of the production, perception and signal transduction of plant hormones. These hormones are critical for correct plant development and adaptation to the variable environmental conditions plants are exposed to during their life cycle.

Jasmonic acid and its derivatives, known as jasmonates (JAs), act as signalling compounds regulating plant development and plant responses to various biotic and abiotic stress conditions. Even though more than 1500 E3 ligases are encoded by the genome of the model plant *Arabidopsis thaliana*, very few have been associated with JA biosynthesis or signal transduction. Best characterized is the SCF^{COI1} E3 ligase, a component of the JA-receptor. Making use of transcriptomic data and a bio-informatics approach, we have identified a set of 22 E3 ligases with a putative role in JA-signalling (see Chapter 3), further extending the connection between the Ub system and JA-signalling.

Despite the large number of E3s present in plants, very few ubiquitination targets have been associated with a specific E3 ligase. Here, we used a customized Tandem Affinity Purification (TAP) platform to identify E3-interacting proteins that constitute potential ubiquitination substrates. Customization consisted of inactivation of the Ub-ligase activity of the E3s by introduction of specific mutations in their RING domain, preventing target ubiquitination and resulting in stabilization of the E3-target interaction. Mutated E3s where then used as baits in purification experiments. This approach led to the identification of potential targets of several E3 ligases with a predicted function in JA-signalling, including AE31, ATL23, BRIZ1/2, KEG and RGLG3/4 (see Chapter 3 and 5).

To cope with the restraints that *in vitro* ubiquitination assays impose on the ability to demonstrate ubiquitination of a protein by a specific E3 ligase, we attempted to develop an alternative *in vivo* assay. The yeast *S. cerevisiae* was chosen as a heterologous host to maintain modification of the potential target protein by related or unrelated E3s to a minimum. The principle of this assay is based on the assembly of plant E3 ligases with the yeast ubiquitination machinery. Upon expression of the suspected target-E3 couple, the target would be ubiquitinated, and this should be dependent on co-expression of the (functional) E3. Because yeast is relatively resistant to proteasome inhibition, and target ubiquitination in most cases leads to proteasome mediated degradation of the latter, we first engineered a strain that had increased sensitivity to proteasome inhibition and determined which treatment was most efficient to attain this inhibition (see Chapter 3). We also generated a set of MultiSite Gateway compatible vectors for the expression of genes in *S. cerevisiae*, as this cloning technology is

widely used by plant researchers (see Chapter 4). The assay was tested using the heterodimeric E3 ligase BRIZ1/2 and its candidate target LARP6b. Although we could not detect ubiquitination of the LARP6b protein after purification of the protein under denaturing conditions, we did detect a modified form of the protein and this was dependent on co-expression of both BRIZ1 and BRIZ2 (see Chapter 3).

Further work focussed on the redundant E3 ligases RGLG3/4 that were reported to be involved in JA-signalling. We identified PKC-θ INTERACTING PROTEIN COUSIN OF THIOREDOXIN 1 (PICOT1/GRXS17) and HEMOGLOBIN 3 (GLB3) as potential targets of RGLG3/4 using the customized TAP approach described above, followed by confirmation of direct interaction using yeast two-hybrid (Y2H). We further demonstrated RGLG3/4 mediate PICOT1 poly-ubiquitination and subsequent proteasomal degradation. PICOT1 is an iron-sulfur (Fe-S) cluster binding glutathioredoxin that localizes to the nucleus and the cytoplasm in Arabidopsis. The use of PICOT1 as a bait in TAP experiments further showed that PICOT1 forms a protein complex with nearly all components of the cytosolic Fe-S assembly pathway as well as with some other known Fe-S proteins. In contrast to the human and yeast orthologs of PICOT1, which function in Fe-homeostasis and Fe-S cluster assembly, the activity of the PICOT1-interacting Fe-S protein XANTHINE DEHYDROGENASE 1 was only marginally affected in *picot1* seedlings. In addition to Fe-S proteins, PICOT1 interacted with several proteins involved in tRNA thiolation. Accordingly, plants carrying mutations in genes involved in tRNA modification were found to resemble *picot1* plants phenotypically (see Chapter 5).

Our most remarkable finding, however, was that PICOT1 potentially regulates the JA-receptor F-box component COI1. The thioredoxin domain of PICOT1 mediates direct interaction with COI1 in the nucleus. In addition, the short-root phenotype of *picot1* seedlings was partially rescued in *coi1-16picot1* lines. Despite their physical and genetic interaction however, *picot1* seedlings did not show alterations in their response to JA. Transcriptome analysis of *picot1, coi1-16* and *coi1-16picot1* seedlings revealed a set of genes are upregulated in *coi1-16* in a PICOT1-dependent manner. These genes were not related to JA-signalling, and included a set of co-regulated genes that are expressed in response to infection with *Hyaloperonospera arabidopsidis* (previously known as *H. parasitica*). We therefore propose PICOT1 regulates the JA-independent function of COI1 (see Chapter 6).

In conclusion, a bio-informatics approach combined with customized protein-protein interaction mining was effective in extending our knowledge on the role of the Ub system in JA-signalling. Additionally, we have identified the E3 ligases RGLG3/4 and their target PICOT1 as molecular players in COI1-dependent but JA-independent signalling.

Samenvatting

Ubiquitinatie, de covalente binding van ubiquitine (Ub) aan een substraateiwit, is een post-translationele modificatie die betrokken is in bijna alle biologische processen in eukaryote organismen. Ubiquitinatie van een substraat vereist de opeenvolgende werking van drie enzymen (E1, E2 en E3). Het E3 ligase is van uitzonderlijk belang omdat het verantwoordelijk is voor de rekrutering van het substraateiwit en op die manier de specificiteit van de modificatie bepaalt. Het Ub systeem draagt bij aan de regulatie van de aanmaak, de perceptie en de signaaltransductie van plantenhormonen. Deze hormonen zijn van cruciaal belang voor de correcte ontwikkeling en voor aanpassing van planten aan de wisselende omstandigheden waaraan deze gedurende hun levenscyclus worden blootgesteld.

Jasmijnzuur en derivaten, gekend als jasmonaten (JAs), werken als signaalmoleculen die plantenontwikkeling en verdedigingsresponsen tegen verscheidene biotische en abiotische stresscondities reguleren. Hoewel er meer dan 1500 E3 ligasen gecodeerd zijn in het genoom van de modelplant Arabidopsis thaliana (zandraket), zijn er slechts enkelen geassocieerd met JA-biosynthese of signaaltransductie. Het best gekarakteriseerde E3 ligase hierbij is SCF^{COI1}, dat deel uitmaakt van de JA-receptor. We hebben tijdens dit onderzoek de link tussen het Ub systeem en JA-signalisatie verder versterkt door 22 nieuwe E3 ligasen te identificeren die mogelijk een rol spelen in JA-signalisatie, via een bio-informatica analyse van transcriptoom data (zie Hoofdstuk 3).

Ondanks het grote aantal E3s aanwezig in planten, zijn er slechts weinig substraten geassocieerd met een specifiek E3 ligase. We hebben hier gebruik gemaakt van een aangepast platform voor Tandem Affiniteitszuivering (TAP) om eiwitten te identificeren die met E3s interageren en dus potentiele substraten vormen. De aanpassing bestond uit het inactiveren van de Ub-ligase activiteit van de E3s door het gericht invoeren van mutaties binnen het RING domein waardoor ubiquitinatie van het substraat verstoord wordt, wat resulteert in stabilisatie van de E3-substraat interactie. Deze aanpak leidde tot het ontdekken van potentiele substraten van verschillende E3 ligasen met een voorspelde functie in JA-signalisatie waaronder AE31, ATL23, BRIZ1/2, KEG en RGLG3/4 (zie Hoofdstuk 3 en 5).

Om komaf te maken met de beperkingen die door in vitro ubiquitinatie-assays opgelegd worden op de mogelijkheid om ubiquitinatie van een substraateiwit door een specifiek E3 ligase aan te tonen, werd een poging ondernomen om een alternatieve in vivo assay te ontwikkelen. Om de modificatie van potentiële substraateiwitten door (on)gerelateerde E3s tot een minimum te beperken werd de gist S. cerevisiae gekozen als heterologe gastheer. Het principe achter deze assay is dat planten E3s in staat zijn om te assembleren met de ubiquitinatie uitrusting van gist. Bij expressie van het verdachte substraat-E3 koppel zou het substraat geübiquitineerd worden, afhankelijk van de aanwezigheid van het (functionele) E3. Omdat gist relatief resistent is tegen proteasoom-inhibitie, en ubiquitinatie van een substraat meestal leidt tot de proteasoom-afhankelijke

afbraak ervan, werd er eerst een giststam ontwikkeld die verhoogde gevoeligheid vertoont aan proteasoom-inhibitie, en werd er bepaald welke behandelingen resulteerden tot de hoogste graad van inhibitie (zie Hoofdstuk 3). Daarnaast werd een set MultiSite Gateway-compatibele vectoren gegenereerd voor de expressie van genen in S. cerevisiae, gezien deze kloneringsmethode veel gebruikt wordt binnen het plantenonderzoek (zie Hoofdstuk 4). De assay werd getest met het heterodimeer E3 ligase BRIZ1/2 en zijn kandidaatsubstraat LARP6b. Hoewel we geen ubiquitinatie van LARP6b konden detecteren na zuivering van het eiwit onder denaturerende condities, werd er wel een gemodificeerde vorm van het eiwit gedetecteerd die afhankelijk was van co-expressie met zowel BRIZ1 als BRIZ2 (zie Hoofdstuk 3).

Het verdere werk concentreerde zich op de redundante E3 ligasen RGLG3/4 waarvan de functie in JA-signalisatie reeds gerapporteerd werd. Gebruik makend van de hierboven beschreven aangepaste TAP procedure identificeerden we twee kandidaatsubstraten: PKC-θ INTERACTING PROTEIN COUSIN OF THIOREDOXIN 1 (PICOT1/GRXS17) en HEMOGLOBIN 3 (GLB3). Directe interactie werd vervolgens bevestigd aan de hand van yeast two-hybrid (Y2H). We toonden verder aan dat RGLG3/4 de ubiquitinatie en vervolgens proteasoom-afhankelijke degradatie van PICOT1 mediëren. PICOT1 is een ijzer-zwavel (Fe-S) cluster bindend glutathioredoxine dat in de celkern en het cytoplasma lokaliseert in Arabidopsis. Wanneer PICOT1 gebruikt werd als aas in TAP experimenten vonden we dat PICOT1 eiwitcomplexen vormt met bijna alle componenten van de cytosolische Fe-S assemblage pathway en ook met andere gekende Fe-S eiwitten. In tegenstelling tot de orthologen van *PICOT1* in mensen en gist, die een functie hebben in Fe-homeostase en Fe-S samenstelling, was de activiteit van het Fe-S enzym XANTHINE DEHYDROGENASE 1 nauwelijks verminderd in *picot1* zaailingen. Naast Fe-S eiwitten, interageerde PICOT1 ook met verschillende eiwitten betrokken bij tRNA thiolatie. Overeenkomstig hiermee vertoonden planten die mutaties dragen in genen betrokken bij tRNA modificatie een gelijkaardig fenotype als *picot1* planten (zie Hoofdstuk 5).

Onze meest opmerkelijke bevinding was echter dat PICOT1 een potentiele regulator is van de JA-receptor component COI1. Het thioredoxinedomein van PICOT1 medieert rechtstreekse interactie met COI1 in de celkern. Bovendien werd het korte-wortel-fenotype van *picot1* zaailingen gedeeltelijk ongedaan gemaakt in *coi1-16picot1* lijnen. Ondanks hun fysieke en genetische interactie, vertoonden *picot1* zaailingen echter geen gewijzigde JA-respons. Transcriptoomanalyse van *picot1*, *coi1-16* en *coi1-16picot1* onthulde een set genen die opgereguleerd waren in *coi1-16* op PICOT1-afhankelijke wijze. Deze genen waren niet gerelateerd aan JA-signalisatie en bevatten een set van co-gereguleerde genen die geëxpresseerd worden als reactie op infectie met *Hyaloperonospera arabidopsidis* (vroeger gekend als *H. parasitica*). Op basis hiervan stellen we PICOT1 voor als een regulator van de JA-onafhankelijke functie van COI1 (zie Hoofdstuk 6).

Tot besluit kunnen we stellen dat bio-informatica gecombineerd met aangepaste eiwit-eiwit-interactieonderzoek een effectieve aanpak was om onze kennis over de rol van het Ub systeem in JA-signalisatie te versterken. Daarnaast hebben we aangetoond dat de E3 ligasen RGLG3/4 en hun substraateiwit PICOT1 moleculaire componenten zijn van de COI1-afhankelijke maar JA-onafhankelijke signaaltransductie.

Contents

Abbreviations

3AT	3-amino-1,2,4-triazole
ABA	abscisic acid
ABI	abscisic acid insensitive
AFB	auxin signalling F-box
AFP	ABI5 binding protein
AIP2	ABI3 interacting protein-2
AOC	ALLENE OXIDE CYCLASE
AOS	ALLENE OXIDE SYNTHASE
APC	Anaphase promoting complex
ASK1	ARABIDOPSIS SKP1 HOMOLOG 1
ATG	AUTOPHAGY
ATL	Arabidopsis Toxicos en Levadura
AXR1/ECR1	AUXIN RESISTANT 1
bHLH	basic helix-loop-helix
BiFC	bimolecular fluorescence complementation
BIN2	BRASSINOSTEROID INSENSITIVE 2
BOI	BOTRYTIS SUSCEPTIBLE1 INTERACTOR
BOS1	BOTRYTIS SUSCEPTIBLE1
BRAP	BRCA1-associated protein
BRG	BOI related gene
BRIZ	BRAP2 RING ZNF UBP DOMAIN-CONTAINING PROTEIN
BRs	brassinosteroids
CaMV	cauliflower mosaic virus
CC	coiled coil
CHX	cycloheximide
CIA	cytosolic iron-sulfur cluster assembly
CIPK	Calcineurin B-like interacting protein kinase
CNX	COFACTOR OF NITRATE REDUCTASE AND XANTHINE DEHYDROGENASE
COI1	CORONATINE-INSENSITIVE 1
COR	coronatine
CRL	Cullin-RING ligase
CTU	CYTOPLASMIC THIOURIDYLASE
CUL	cullin
DAD1	DEFICIENT IN ANTHER DEHISCENCE 1
DAF	DAD1-ACTIVATING FACTOR
DDB1	DNA DAMAGE-BINDING PROTEIN1
DMSO	dimethyl sulfoxide
dTM	deleted trans-membrane domain
DUB	de-ubiquitinase
DWD	DDB1-BINDING/WD-40 DOMAIN CONTAINING
E1	ubiquitin activating enzyme
E2	ubiquitin conjugating enzyme

E3	ubiquitin ligase
EAR	ERF-associated amphiphilic repression
ELO	ELONGATA
ELP	elongator acetyltransferase complex subunit
ERF	ETHYLE RESPONSE FACTOR
ET	ethylene
FAD	flavin adenine dinucleotide
FAD	FATTY ACID DESATURASE
FB1	Fumonisin B1
Fe-S	iron-sulfur
FL	full length
GA	gibberellic acid/gibberellins
GLB3	HEMOGLOBIN 3
Grx	glutaredoxin domain
GST	Glutathion S-transferase
HA	hemagglutinin
HECT	Homologous to the E6-AP Carboxyl Terminus
HERC	HECT and RCC1-like
HUB	HOMOLOGY TO UBIQUITIN
HUbA	Heterologous Ubiquitination Assay
ICE	INDUCER OF CBP EXPRESSION
IMAC	immobilized-metal affinity chromatography
JA	jasmonic acid / jasmonate
JAI	JASMONATE INSENSITIVE
JA-Ile	(+)-7-iso-jasmonyl-L-isoleucine
JAR1	JASMONATE RESISTANT1
JAV1	JASMONATE-ASSOCIATED VQ MOTIF GENE 1
JAZ	JASMONATE ZIM-DIOMAIN
JIN	JASMONATE INSENSITIVE
KEG	KEEP ON GOING
KO	knock-out
La	Lupus auto-antigen
LARP	La-related protein
LC-MS	liquid chromatography-mass spectrometry
LOX	LIPOXIGENASE
LRR	leucine rich repeat
LSA	La and S1 associated
LURP	late upregulated in response to *Hyaloperonospora parasitica*
MAX	MORE AXILLARY BRANCHES
MBP	Maltose-binding protein
mcm^5	5-methoxycarbonyl-methyluridine
MED	Mediator complex
MeJA	Methyl jasmonic acid
Moco	molybdenum cofactor
mRING	mutated RING domain
MS	mass spectrometry

MUB	MEMBRANE ANCHORED UBIQUITIN
NADH	nicotinamide adenine dinucleotide
NADPH	nicotinamide adenine dinucleotide phosphate
Nedd8	Neural precursor cell expressed, developmentally down-regulated 8 (=RUB)
NES	nuclear export signal
NINJA	NOVEL INTERACTOR OF JAZ
NLS	nuclear localization signal
OE	overexpression
OPDA	12-oxo-phytodienoic acid
ORA59	OCTADECANOID-RESPONSIVE ARABIDOPSIS AP2/ERF59
PAGE	polyacrylamide gel electrophoresis
PCD	programmed cell death
PGHG	peptidyl-glutamyl peptide-hydrolysing
PICOT	PKC-θ interacting protein cousin of thioredoxin
PKC	protein kinase C
PTGS	post-transcriptional gene silencing
qRT-PCR	quantitative real-time PCR
R:FR	red:far-red ratio
RBX1	RING-BOX 1
RCD1	RADICAL INDUCED CELL DEATH 1
RCE	RUB-CONJUGATING ENZYME
RGLG	RING DOMAIN LIGASE
RING	Really interesting new gene
RRM	RNA recognition motif
RUB	Related to ubiquitin (=Nedd8)
SA	salicylic acid
SAE	SUMO-ACTIVATING ENZYME
SAM	S-adenosyl methionine
SCE	SUMO-CONJUGATING ENZYME
SCF	Skp1-Cullin-F-box ligase
SDS	sodium dodecyl sulfate
SEM	standard error of the mean
SIS	Sugar insensitive
SL	strigolactone
SR	Ser/Arg-rich
SRPK4	SR PROTEIN SPECIFIC KINASE 4
SUMO	SMALL UBIQUITIN-LIKE MODIFIER
TAP	tandem affinity purification
TEV	tobacco etch virus
TF	transcription factor
TGN/EE	trans-Golgi/Early endosome
TGS	transcriptional gene silencing
TIA	terpenoid indole alkaloid
TIC	TIME FOR COFFEE
TPL	TOPLESS
TPR	TOPLESS-RELATED

Trx	thioredoxin domain
TtcA	Two-thio-cytidine
Ub	ubiquitin
UBC	ubiquitin conjugating enzyme-domain
UBL	ubiquitin-like modifier
UFM	UBIQUITIN-FOLD MODIFIER
URE	UREASE
UREG	UREASE ACCESSORY PROTEIN G
URH1/2	URIDINE RIBOHYDROLASE 1/2
URM	UBIQUITIN-RELATED MODIFIER
UV	ultraviolet
VBC	VHL/Elongin B,C/CUL2
VHL	Von Hippel–Lindau
vWA	von Willebrand Factor type A
Vwaint	vWA/Hedgehog protein intein-like
WT	wild-type
XDH1	XANTHINE DEHYDROGENASE 1
Y2H	yeast two-hybrid
Y3H	yeast three-hybrid
ZIM	Zinc-finger expressed in the inflorescence meristem
ZML	ZIM-like

Chapter 1:
Introduction:
The ubiquitin system and jasmonate signalling in plants

Astrid Nagels Durand

PREFACE

Plants harvest energy from the sun and provide both food and habitat for other organisms, placing them at the basis of our ecosystem. The maintenance of plant homeostasis depends on a finely orchestrated balance between protein synthesis and protein breakdown. In the past, researchers focussed mainly on the mechanism and regulation of protein synthesis. However, pathways regulating protein degradation have gained interest in the last couple of decades (Smalle and Vierstra, 2004; Callis, 2014).

Protein synthesis during organism development or in response to changing environmental conditions is often regulated by the production of signalling molecules such as hormones. Jasmonates (JA) are fatty-acid derived compounds that act as signalling molecules during plant development, and during plant responses to biotic and abiotic stress. Upon perception of JAs, plants will activate gene expression and protein production to arm themselves against threats, including pathogenic bacteria and herbivores.

Conversely, targeted protein breakdown can influence how a plant adapts to new environmental conditions, or to attack by other organisms, directly by facilitating the degradation of rate-limiting enzymes. Alternatively, plants can be dependent on protein degradation for turning on the production of proteins that are required only under specific conditions. In many cases this is achieved by removal of transcriptional repressors that block specific responses at times when they are not required. For example, defence artillery against pathogens is costly for the plant, at the expense of resources that could otherwise be used for growth and reproduction, and should therefore only be employed at the appropriate occasion.

In this introduction we will give an overview on the role of two strongly intertwined pathways influencing plant homeostasis. We will describe one of the most important pathways leading to protein breakdown in eukaryotic organisms, the “ubiquitin system” and how this system influences plant hormonal signalling cascades, focussing on the JA signalling pathway.

THE UBIQUITIN SYSTEM

The ubiquitin conjugation pathway: E1 – E2 – E3

Ubiquitin (Ub) is a polypeptide (76 amino acids) present in all eukaryotes. Its protein sequence is highly conserved and plant Ub differs from human Ub by only three amino acids (Callis et al., 1989). Ub and Ub-like polypeptides have a characteristic fold conferring tight packing and high structural stability (Ciechanover et al., 1980). Ub is encoded by multiple genes as a poly-Ub multimer or as a translational fusion between Ub and a different protein. Production of functional Ub-monomers therefore requires post-translational processing, achieved by Ub-specific proteases known as de-ubiquitinases (DUBs). These enzymes recognize the C-terminal end of Ub and cleave specifically after Ub's amino acid 76 (Callis, 2014).

At least three enzymes are required for Ub-conjugation to a target protein (Figure 1-1). First, Ub is activated by the Ub activating enzyme (E1). This step requires ATP hydrolysis and yields a complex (E1~Ub) where Ub is covalently bound to the E1 active-site Cys residue through a thioester bond. The Arabidopsis genome encodes two E1s (*UBA1-2*) (Smalle and Vierstra, 2004).

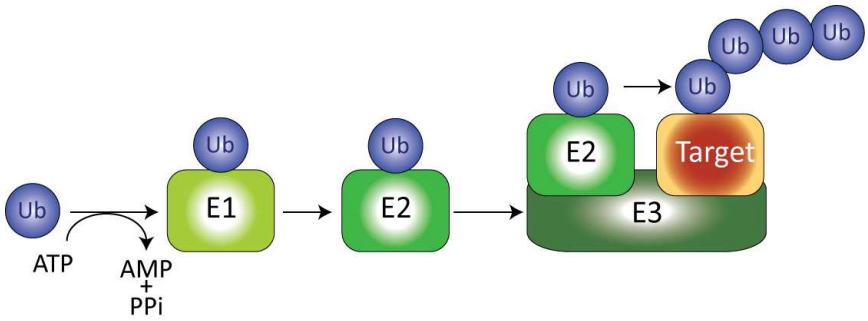

Figure 1-1. Enzymatic steps in the ubiquitin conjugation pathway.

Ubiquitin (Ub) is activated and bound by the E1 in an ATP-dependent reaction through a thioester bond. Ub is then transferred to E2 where it is also bound through a thioester bond. The E3 interacts simultaneously with the target and the E2~Ub conjugate, facilitating transfer of Ub to the target.

The second step in the Ub-conjugation cascade involves a Ub-conjugating enzyme (E2). During this step, Ub is transferred from E1~Ub to the E2, where it is again covalently bound to the active site Cys residue through a thioester bond. Arabidopsis encodes 48 proteins with a typical Ub conjugating enzyme (UBC) domain, of which 8 lack the active site Cys and three are involved in conjugation of Ub-like proteins (Kraft et al., 2005).

Finally, the Ub ligase or E3 interacts forms a complex with E2~Ub and target, facilitating transfer of Ub to the target where it is covalently bound to a Lys residue. In most cases E2~Ub and E3 interact non-covalently, although exceptions where Ub is first covalently bound to the E3 through a thioester bond also occur. Because the E3 is responsible for target recognition,

it constitutes the main specificity determinant of the Ub system. More than 1,500 E3s are encoded in the genome of Arabidopsis (Hua and Vierstra, 2011).

Classes of Ub ligases (E3s)

Ub ligases can be subdivided into three mechanistic types that in most cases correlate with the presence of a conserved domain that mediates interaction with the E2~Ub. While RING-type and U-box type E3 ligases do not interact covalently with the E2-bound Ub, HECT (Homologous to the E6-AP Carboxyl Terminus) type E3s form a thioester-bound E3~Ub intermediary before Ub-transfer to the target protein.

The RING (REALLY INTERESTING NEW GENE) family of E3 ligases is characterized by the presence of a conserved RING domain, which mediates interaction with the E2~Ub. The RING domain contains 8 conserved His or Cys metal binding residues that coordinate two Zn atoms forming a cross-brace secondary structure (Stone et al., 2005). A similar structure that also serves as the E2 docking site is present in U-box type E3s. The U-box domain, however, does not coordinate Zn atoms and thanks its protein fold to a network of hydrogen bonds that is further stabilized by hydrophobic interactions and salt bridges (Andersen et al., 2004). The model plant Arabidopsis encodes 490 proteins that contain a RING domain and 64 U-box proteins (Callis, 2014).

To mediate interaction with the target, protein-protein interaction domains are often present in addition to the RING/U-box domain. Alternatively, multi-protein complexes containing a RING protein, a CULLIN protein and one or more adaptor modules also function as complex RING-type E3 ligases and are known as CRLs (CULLIN-RING ligases, Figure 1-2). The structural organization of CRLs is highly conserved between plants and animals. In Arabidopsis, a CULLIN isoform (CUL1/3/4) functions as a scaffold and accommodates the RING-domain containing protein RBX1a (RING BOX1) and one of three types of substrate interacting module.

The most abundant type of CRL in plants are SCF CRLs characterized by the presence of CUL1 and a substrate-recognition module composed of ASK1/2 (ARABIDOPSIS SKP1 HOMOLOG 1 / 2) in combination with an F-box protein (Figure 1-2). In contrast to the situation in yeast or humans where a low number of F-box proteins is present (20 and 69, respectively), the Arabidopsis F-box family is very large and contains at least 700 members. A second related CRL complex is the BTB CRL that contains CUL3 and a member of the BTB (broad complex/tram track/bric-a-brac) family (Figure 1-2). Finally, CRLs containing CUL4 and a substrate adaptor molecule composed of a DDB1 (DNA DAMAGE-BINDING PROTEIN 1) and a DWD (DDB1-BINDING/WD-40 DOMAIN CONTAINING) family protein are known as DWD CRLs (Figure 1-2). No relatives of CUL2 or CUL5 have been found in plants yet, however, in animals they each define an additional CRL type. In these organisms, Elongin C connects CUL2 to a VHL (Von Hippel–Lindau) family protein in VBC (VHL/Elongin B,C/CUL2) CRLs. Alternatively, Elongin C

can also connect CUL5 with a SOCS-box protein in SOCS CRLs. Although a sequence orthologue of Elongin C is universally present, no proteins related to CUL2, CUL5, VHL nor SOCS have been identified in plants (Hua and Vierstra, 2011).

Finally, the Anaphase Promoting Complex (APC) is an atypical mega-subunit CRL-type E3 ligase. This complex is essential for the transition from metaphase to anaphase during mitosis and is highly conserved. In plants, the APC has been shown to be required for plant development, controlling both cell division and cell differentiation. The Arabidopsis APC consists of at least 11 core subunits of which APC11 contains a RING-domain and APC2 shows sequence similarity to cullin proteins (Heyman and De Veylder, 2012).

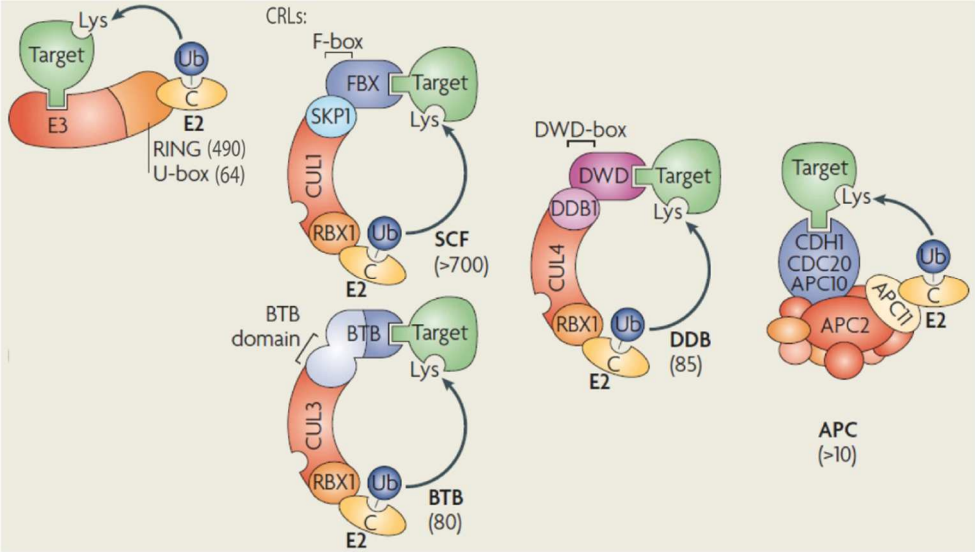

Figure 1-2. RING-type E3 ligases identified in plants.

The structural organization and components of single subunit (left) or complex RING-type E3 ligases. Cullin-RING ligases (CRLs) are composed of a RING-protein (RBX1) a CULLIN (CUL1/3/5) and a target recognition module. The Anaphase-Promoting-Complex (APC) is a mega-subunit E3 ligase that is classified as a member of the CRLs due to the presence of a RING-protein (APC11) and a CULLIN-like protein (APC2). The numbers in parentheses indicate the predicted number of *A.thaliana* genes that encode the target recognition component in each E3 type. Figure adapted fromVierstra (2009).

Versatility of the ubiquitin system

During Ub conjugation, a covalent bond is formed between the C-terminal Gly residue of Ub and the ε-amino group of a Lys residue in the target protein, termed an isopeptide bond. Exceptions have been observed in mammals where Ub was found to be ligated to alternative amino acid residues (Ser, Thr or Cys) or to the N-terminal amino group of the target protein. The attachment of one Ub entity is referred to as mono-ubiquitination. Additional Lys residues within a single target protein can be modified with Ub resulting in multi-monoubiquitination (Figure 1-3). Reversible mono-ubiquitination of histones H2A and H2B has been associated with transcriptional repression or activation, respectively (Feng and Shen, 2014).

Ub contains 7 Lys residues (K6, K11, K27, K29, K33, K48 and K63) that can be modified with Ub themselves, giving rise to the formation of Ub-chains. Modification of a protein by covalent attachment of Ub-chains is known as poly-ubiquitination. In addition, Ub can also form chains by attachment to the N-terminal amino group of the previous Ub moiety, forming linear Ub-chains. The Ub-packing in a chain is determined by the internal Ub Lys residue used for chain assembly (i.e. the Ub "linkage", Figure 1-3). This structural difference is thought to be the basis for the different roles of the different linkage-types of poly-Ub. A final factor that further increases the complexity of the Ub system is the formation of mixed linkage chains and branched poly-Ub chains on target proteins, of which the role is still not well understood. The different signals arising by various structurally different forms of ubiquitination can be recognized and interpreted by proteins containing an array of ubiquitin binding domains (Dikic et al., 2009).

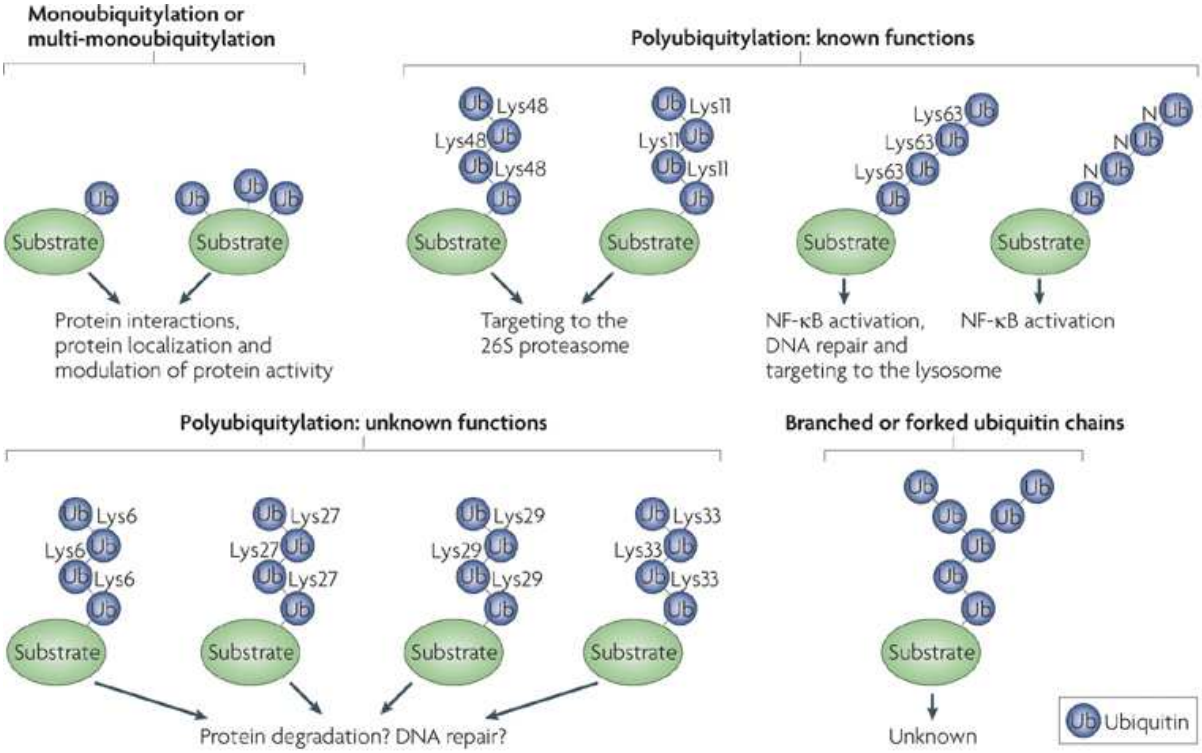

Figure 1-3. Versatility of the Ub system.

Attachment of a single Ub to one or multiple Lys residues in the target protein is referred to mono-ubiquitination or multi-monoubiquitination, respectively. Attachment of Ub to one of the seven Lys residues present in Ub itself, leads to the assembly of Ub chains with varying linkages. In addition, the N-terminal amino group of Ub can also serve as a Ub-acceptor resulting in the formation of linear Ub chains. The versatility of the ubiquitin system can further be increased by the generation of mixed-linkage chains or forked/branched Ub chains that result from the attachment of two Ub moieties to two different Lys residues within a single Ub molecule. These differences in Ub chain topology lead to structural variations, forming the basis for functional diversification in the ubiquitin system. Figure adapted from Ye and Rape (2009).

Much effort has been invested to identify motifs for Ub addition by examining Ub-attachment sites through proteome-wide Ub analysis. However, identification of such a consensus sequence has failed, indicating a universal Ub-motif does not exist. Instead, the

mechanism of E3 ligases recruiting E2~Ub and the target protein, results in the creation of a "hot zone" in the target protein that is in close proximity to the Ub moiety (Meierhofer et al., 2008; Xu et al., 2009; Kim et al., 2013).

While Ub proteomic studies have succeeded to detect all 8 possible Ub-linkage types in yeast and humans (Meierhofer et al., 2008; Xu et al., 2009), K27-linked Ub chains and linear Ub-chains have not been detected in plants (Kim et al., 2013). The best characterized and most abundant linkage-type arises from K48-linked Ub-chains. Modification of a target protein with K48-linked poly-Ub marks the protein for proteolytic degradation (Fu et al., 1998). The Ub system therefore plays a crucial role in regulated protein turnover.

The second most abundant linkage type of poly-Ub identified on target proteins is K63-linked. In yeast and mammalian cells K63 poly-Ub has been associated to regulatory non-proteolytic functions such as DNA repair and kinase activation, and particularly to intracellular trafficking events. Although K63-linkage is poorly understood in plants, it has been implicated in intracellular trafficking by mediating endocytosis and subsequent vacuolar targeting of the auxin efflux carrier protein PIN2 (Leitner et al., 2012). K63 Ub-chains have also been shown to be involved in plant iron homeostasis (Li and Schmidt, 2010).

The third most abundant Ub linkage type in plants is K11-linked Ub (Kim et al., 2013). In yeast and animals, K11 poly-ubiquitination is thought to target proteins to the proteasome, and its formation has been shown to play a role in cell cycle progression, mediated by the APC E3 ligase (Matsumoto et al., 2010; Wickliffe et al., 2011). The function of K11 linked Ub-chains has not been studied in plants. However, treatment of seedlings with the proteasome inhibitor MG132 increases the amount of K11 Ub-modified proteins detected in proteome wide analysis indicating their function in proteasomal degradation is conserved in plants. The remaining Ub-linkage types found in plants were much less abundant than K48, K63 or K11, and their function is still unknown (Kim et al., 2013).

The proteasome

In all organisms studied so far, it has been shown that proteins that are poly-ubiquitinated with K48-linked Ubs are eventually degraded by a 2 MDa proteolytic complex: the 26S proteasome. This ATP-dependent multi-subunit protease is similarly organized in yeasts, mammals and plants and can be divided in two particles: the 20S core particle and the 19S regulatory particle (Figure 1-4). The 20S core particle consists of four heptameric rings of α and β subunits. The α subunits restrict entrance to the active site by creating a narrow gated channel that is only accessible to unfolded proteins (Vierstra, 2009). Enzymatic activity is conferred by the β1, β2 and β5 subunits. Each subunit has a specific proteolytic activity. The β1-subunit (encoded in yeast by *Pre3*) confers peptidyl-glutamyl peptide-hydrolysing (PGHG)-like activity, the β2 subunit (encoded in yeast by *Pup1*) confers trypsin-like activity and the β5

subunit (encoded in yeast by *Pre2*) is responsible for the chymotrypsin-like activity (Heinemeyer et al., 1997).

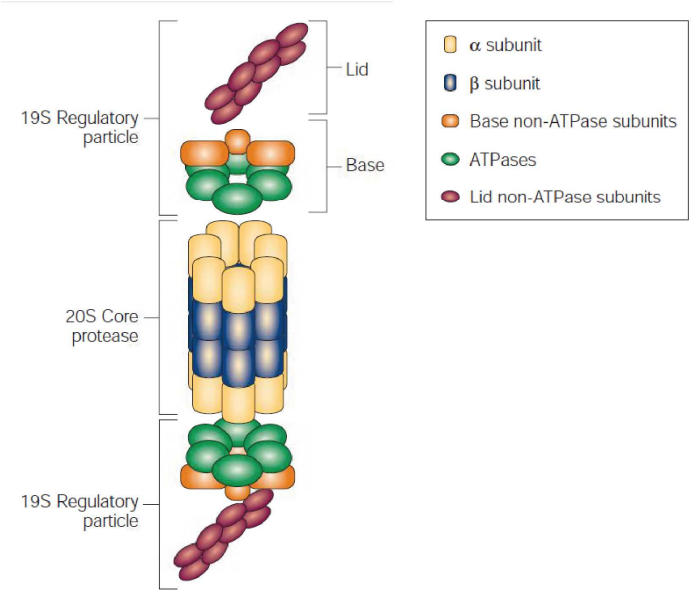

Figure 1-4. Structure of the plant 26S proteasome.

Schematic overview of the plant 26S proteasome, existing of a 20S Core particle capped at both ends by the 19S regulatory particle. The latter can further be subdivided into a Lid and a Base complex. Figure adapted from Sullivan et al. (2003).

Each end of the 20S core particle is capped by a 19S regulatory particle. This particle can be further subdivided into a Lid and a Base complex. The Lid is thought to assist in the recognition of poly-ubiquitinated proteins and to release poly-Ub from substrates. The Base contains ATP-dependent subunits that probably help to unfold the substrate and to transport it into the 20S core particle (Vierstra, 2009).

UBIQUITIN-LIKE MODIFIERS

Ub structure is characterized by a core β-grasp fold where a 5-stranded β sheet appears to grasp a diagonally held α helix (Figure 1-5). This structure is referred to as the Ubiquitin-fold. Several polypeptides have been identified that, despite their low sequence homology, show high structural similarity to Ub and share the common Ub-fold. In plants these Ubiquitin-like modifiers (UBLs) currently include RUB/Nedd8 (related to Ub), SUMO (small Ub-like modifier), URM1 (Ub-related modifier-1), ATG8/12 (autophagy 8/12), MUB (membrane anchored Ub), UFM1 (Ub-fold modifier-1) and HUB1 (homology to Ub-1). Like in the case of Ub, UBL-conjugation generally depends on a E1-E2-E3 cascade and targets the ε-amino acid group of Lys residues (Vierstra, 2012).

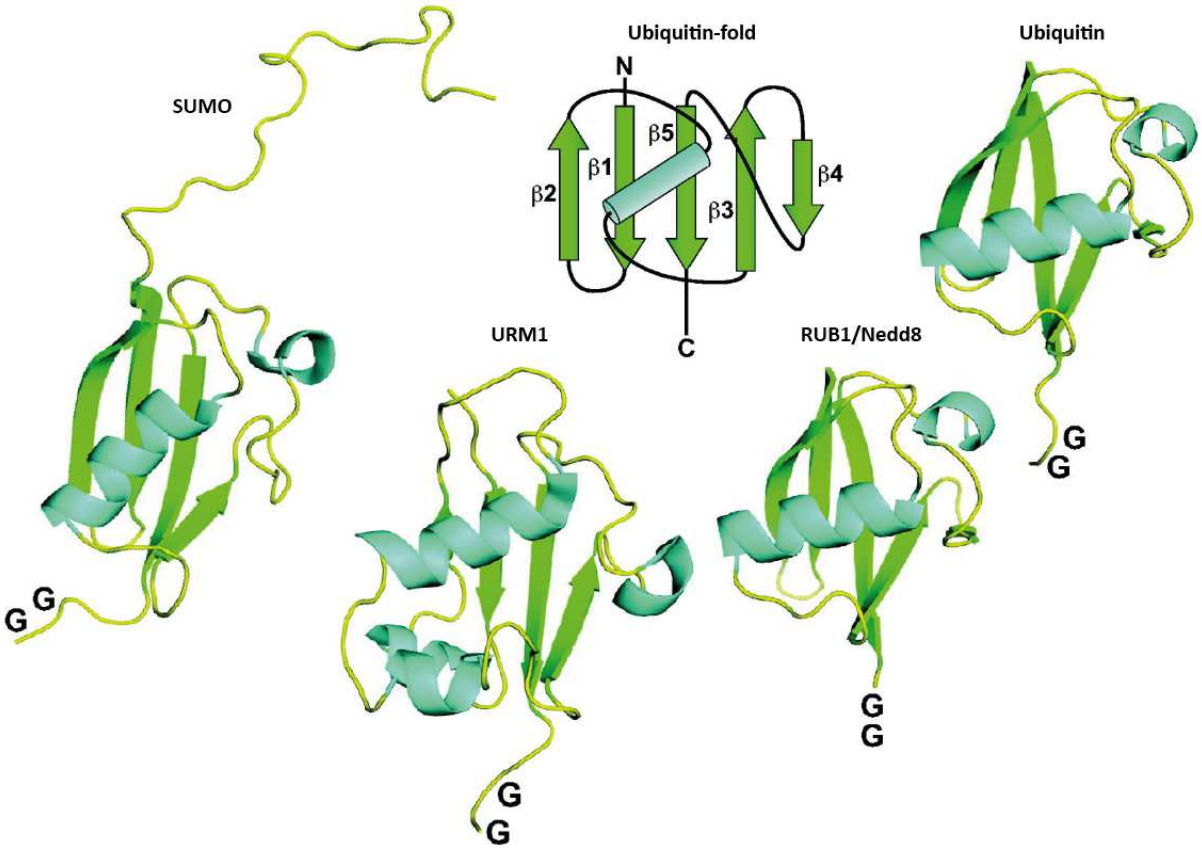

Figure 1-5. Structure of Ub-like polypeptides.

The schematic structure of the Ub-fold and the ribbon structure of Ub and four UBLs: SUMO, small ubiquitin-like modifier; URM1, ubiquitin-related modifier-1; RUB1/Nedd8, related to ubiquitin-1. Figure adapted from Vierstra (2012).

Although UBLs share a similar fold, their functions and properties differ from Ub and from each other. Little is known about the function or conjugation of UFM1, MUB, HUB1 and ATG8/12 in plants. While knowledge on UFM1 is completely missing in plants, E1-E2-E3 enzymes for UFM1 conjugation have been characterized in mammals (Komatsu et al., 2004; Tatsumi et al., 2010). MUB is anchored to the membrane owing to the presence of a prenylation signal at its C-terminus instead of the usual di-Gly motif (Downes et al., 2006). In yeast and mammals HUB1 functions non-covalently. Accordingly, no E1-E2-E3 cascade has

been identified for this UBL. Finally, ATG8 and ATG12 are UBLs with an essential role in autophagy and this role is conserved in yeast, humans and plants (Ohsumi, 2001; Li and Vierstra, 2012).

Related to Ub - Nedd8/RUB

Amongst the UBLs, Nedd8/RUB is most closely related to Ub and is strongly conserved across species (Vierstra, 2012). Three copies of Nedd8 are encoded in the Arabidopsis genome (RUB1-3), and neddylation is essential for plant growth and development (Bostick et al., 2004). In Arabidopsis, ECR1/AXR1 form a heterodimeric Nedd8 activating enzyme (E1, del Pozo et al., 2002) while *RCE1* and *RCE2* (for RUB-CONJUGATING ENZYME) encode two Nedd8-specific conjugating enzymes (E2s, del Pozo and Estelle, 1999).

The best characterized Nedd8 conjugated proteins in all eukaryotic organisms are CULs, the scaffold proteins of CRLs. Remarkably, the RING-component of CRLs, RBX1, was found to be necessary not only for the ubiquitination of CRL targets but also as a Nedd8 E3 ligase to catalyse CUL neddylation (Kamura et al., 1999; Morimoto et al., 2003). Neddylation of CUL is essential for the activation of CRL complexes and is crucial for regulating their activity (Hua and Vierstra, 2011). In mammals and yeast, several other RING-type E3 ligases have recently been reported to function in Nedd8 conjugation, in addition to RBX1 (Enchev et al., 2015). Only two non-CUL neddylation substrates are known in plants: DDB1, a CUL4-CRL subunit and ML3, a protein involved in pathogen responses whose exact function is not well understood (Mergner and Schwechheimer, 2014).

Small Ub-like modifier - SUMO

The SUMO pathway is essential for plants and mutations cause embryo lethality. The SUMO conjugation cascade in plants involves a heterodimeric E1 (SAE1a/b and SAE2, for SUMO ACTIVATING ENZYME) and the SUMO conjugating enzyme SCE1 (E2). At least two SUMO-specific E3 ligases are known in plants, SIZ1 and HYP2/MMS21 (Saracco et al., 2007; Novatchkova et al., 2012). In addition, SUMO can also form chains, generating poly-SUMOylated proteins. This modification does not serve as a signal for proteolytic degradation by the proteasome but rather seems involved in modulating the ability of substrates to interact with other proteins (Melchior, 2000). In plants, various forms of abiotic stress cause a dramatic rise of SUMO conjugates, mainly in the nucleus (Kurepa et al., 2003; Saracco et al., 2007; Miller et al., 2013). Accordingly, in yeast and mammals SUMO-modification has been shown to activate transcription factors or to cause translocation of cytosolic factors to the nucleus (Melchior, 2000). SUMOylation is therefore thought to help shift the plant from growth to a protective mode (Saracco et al., 2007).

Ub-related modifier-1 - URM1

The URM1 pathway is thought to be reminiscent of the ancient roles of UBLs in prokaryotic sulfur chemistry. This UBL has been shown to be involved in the thio-modification of transfer RNAs (tRNAs). In this context, URM1 is activated by an E1 (CNX5 in Arabidopsis) resulting in formation of a thioester linked E1~URM1 where URM1 is thiocarboxylated and the sulfur atom is donated by a desulfurase (Nakai et al., 2008; Van der Veen et al., 2011; Nakai et al., 2012). Subsequently, a highly conserved complex formed by CTU1-CTU2 (named Ncs6/Tuc1-Ncs2/Tuc2 in yeast) mediates transfer of the sulfur atom from URM1 to the uridine at the first anticodon position of Glu, Lys and Gln tRNAs (Dewez et al., 2008; Philipp et al., 2014). This process is dependent on the cytosolic and mitochondrial assembly of iron-sulfur cofactors, although it remains to be determined which protein possesses this cofactor (Shigi, 2014).

Alternatively, URM1 has been shown to be conjugated to Lys residues in target proteins in yeast and mammals. This process is dependent on both thioester formation with the E1 and thiocarboxylation of URM1. Attachment of URM1 to a target protein results in release of the sulfur moiety. The respective E2 and E3 involved in this process remain unknown (Goehring et al., 2003; Van der Veen et al., 2011).

JASMONATES: PLANT STRESS HORMONES

Jasmonic acid (JA) together with its precursors and derivatives, referred to in general as jasmonates (JAs), are plant-specific signalling molecules. These phyto-hormones are produced upon wounding or pathogen infection and support the establishment of adequate defence responses against these threats. Induction of secondary metabolism by JAs contributes to a large part of this response. In addition, JAs are also important for plant development and resistance to abiotic stress (Browse, 2009; Wasternack and Hause, 2013). The wide range of processes influenced by JAs is reflected in a marked alteration of the plant transcriptome upon treatment with JAs (Pauwels et al., 2008; Pauwels et al., 2009).

Biosynthesis of jasmonates

The production of JAs is triggered by wounding, caused mechanically or by herbivore attack, by infection with necrotrophic pathogens or by exposure to several abiotic stress conditions(Browse, 2009). JAs are cyclic oxylipins derived from fatty acid catabolism through the octadecanoid pathway (Browse and Howe, 2008). Membrane damage causes release of α-linolenic acid and this is used as a substrate for JA biosynthesis. The first part of this process takes place in the chloroplast whereas the final production of JA takes place in the peroxisome (Browse, 2009). JA is then further metabolized into various derivatives, including the volatile compound methyl jasmonic acid (MeJA) (Wasternack, 2007; Wasternack and Hause, 2013). Another JA derivative is formed by conjugation of JA with an amino acid. *JASMONATE RESISTANT1 (JAR1*) encodes the JA-amino synthetase responsible for the conjugation of JA to isoleucine and *jar1* mutants are defective in the JA response (Staswick and Tiryaki, 2004; Westfall et al., 2012). JA-Ile has two chiral centres and the isomer (+)-7-iso-Jasmonyl-L-isoleucine was identified as the endogenous bioactive form of the hormone (Fonseca et al., 2009). It is noteworthy that most of the genes coding for enzymes of the JA-Ile biosynthesis pathway are upregulated by wounding as well as by JA itself suggesting that JA production is regulated by a positive feedback mechanism (Wasternack, 2007; Browse, 2009). The metabolic fate of JA and JA-Ile is diverse, and new JA-metabolites are still being identified. It remains to be determined whether these metabolites show biological activity independent of JA-Ile or function solely as a storage or inactivation mechanism for JA-Ile (Figure 1-6, Wasternack and Hause, 2013).

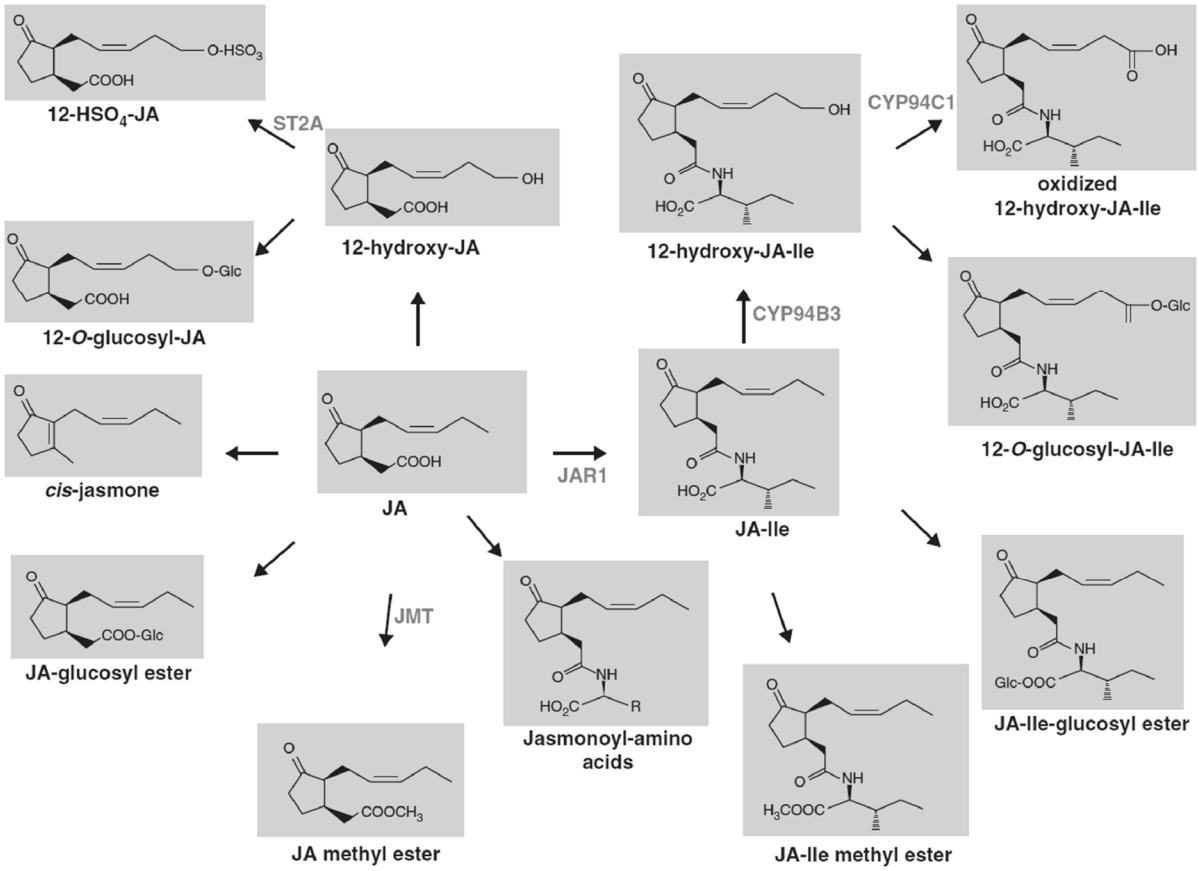

Figure 1-6. Metabolic derivatives of jasmonic acid (JA) and JA-Ile.

The chemical structure of JA-related compounds is shown. JAR1, JA-amino acid synthetase; JMT, JA methyl transferase; ST2A, sulfotransferase 2A. Figure adapted from Wasternack and Hause (2013).

Jasmonates function in defence responses

JAs regulate the wound response and the defence response against herbivore insects. Mechanical wounding together with the involuntary release of elicitors in oral secretions of herbivore insects during feeding trigger JA production at the site of attack (Koo et al., 2009). JA accumulation at the site of wounding leads to the synthesis of JA-Ile and volatile MeJA. In addition, the JA biosynthesis intermediate 12-oxo-phytodienoic acid (OPDA) has also been shown to have a signalling function in the defence response (Howe and Jander, 2008).

In response to tissue injury, JA-Ile triggers transcription of JA responsive defence-related genes. Direct responses include induction of proteinase inhibitors, as well as other proteins depending on the plant species, which target the insect's food consumption, leading to restriction of insect growth and development (Howe and Jander, 2008). Next to this local response, MeJA and other volatile compounds which are produced upon wound-induced JA accumulation act as signals that can reach distal tissues in the same plant as well as neighbouring plants, as was demonstrated in tobacco and tomato (Heil and Ton, 2008; Howe and Jander, 2008). Perception of this volatile compounds leads to direct activation of defence or can prime the defence response (Heil and Ton, 2008). Subsequent insect attack will induce

a more rapid or stronger defence response in primed tissues. In addition, release of volatiles can help establish tritrophic interactions which are beneficial for the plant. For example, the plant volatiles can attract predators of the herbivore insect under whose attack it is (Howe and Jander, 2008). MeJA has been suggested to be involved in the systemic induction of resistance in the plant, based on tomato grafting experiments (Heil and Ton, 2008). Finally, the JA-dependent broad-spectrum response to feeding insects is further modulated by crosstalk with several other phyto-hormones (Erb et al., 2012).

The defence response against necrotrophic pathogens is also regulated by JAs. In contrast to biotrophic pathogens, who feed on living tissue, necrotrophs kill host tissue and feed on what's left over. While the response to biotrophic pathogens is regulated by salicylic acid (SA), resistance to necrotrophic pathogens is regulated by JA as well as by ethylene (ET), and this response shows considerable overlap with the wound response described above (Glazebrook, 2005). Arabidopsis plants defective in JA biosynthesis or perception show severely compromised resistance to necrotrophic fungi (Vijayan et al., 1998).

JA biosynthesis is increased upon perception of necrotroph attack. Accumulation of JA triggers the expression of defensive effector genes. Induction of some of these genes, such as *PDF1.2*, depend on both JA and ET signalling in Arabidopsis (Thomma et al., 2002; Glazebrook, 2005). This crosstalk between JA and ET is thought to be mediated by two APETALA2/Ethylene Response Factor (AP2/ERF)-domain transcription factors (TFs) *ERF1* (*ETHYLENE RESPONSE FACTOR 1*) and *ORA59* (Lorenzo et al., 2003; Zarei et al., 2011).

Jasmonates function in abiotic stress resistance

JAs further contribute to plant plasticity by regulating responses to abiotic stresses. Tolerance to cold/freezing stress is mediated by the bHLH TFs ICE1 and ICE2. In the absence of JAs, expression of *ICE1* and *ICE2* is repressed by the JA signalling machinery. Exposure to cold leads to elevated biosynthesis and accumulation of JAs in the plant, triggering *ICE1/2* expression (Hu et al., 2013b). Alternatively, JAs also function as positive regulators of heat stress tolerance. While JA and SA-signalling are generally regarded as antagonistic pathways, JAs function synergistically with SA to promote tolerance to excess heat (Clarke et al., 2009).

JAs have also been implicated in the responses to drought stress. One method plants employ to cope with drought is to induce stomatal closure, preventing further water loss due to transpiration. The JA-precursor OPDA, but not JA, was found to accumulate during drought treatment and to induce stomatal closure independent of abscisic acid (ABA) signalling, thus functioning as a positive regulator of drought tolerance (Savchenko et al., 2014). JAs were also shown to contribute to drought tolerance by increasing the root capacity to take up water from soil with limited moisture (Kazan, 2015).

Abiotic stress caused by high salinity is another factor compromising plant growth and productivity. JAs have recently been implicated as positive regulators of salt stress tolerance (Kazan, 2015). Overexpression of wheat JA-biosynthesis genes in Arabidopsis increases salt tolerance. Accordingly, JA accumulation in wheat confers salt stress tolerance. Remarkably this process is ABA-dependent or ABA-independent, depending on which gene is overexpressed (Dong et al., 2013; Zhao et al., 2014). The Mediator complex is a multi-subunit complex, conserved in eukaryotes, involved in the transcription of protein coding genes. The complex can link DNA-binding proteins (i.e. TFs) to the transcription machinery as well as to numerous other coactivators and corepressors to regulate gene transcription. The Mediator complex also connects JA-signalling to salt tolerance. The Mediator subunit MED25 positively regulates JA-dependent gene expression (Cevik et al., 2012; Chen et al., 2012). In addition, MED25 interacts with the TF DREB2A, a positive regulator of salt tolerance, independent of ABA-signalling (Elfving et al., 2011).

In addition to the stress-types mentioned above, JAs are involved in the response to several other types of abiotic stress including ozone-triggered cell death and UV radiation (Wasternack and Hause, 2013; Kazan, 2015).

Jasmonates steer secondary metabolite production

JAs also trigger the induction of secondary metabolism in response to wounding, herbivore attack or pathogen infection. Secondary metabolites are small organic compounds which, in contrast to primary metabolites, are not essential for plant growth and development. The presence of different classes of secondary metabolites can therefore be restricted to different groups of plant families. These compounds fulfil diverse roles during the plant life cycle. Amongst other functions, they contribute to plant defence against predators and pathogens. Many of these compounds are toxic to insects or have antibiotic activity. Various secondary metabolites are constitutively produced in the plant and form a basal defence mechanism, but the synthesis of many of these secondary metabolites is induced during responses established by JAs. Plant secondary metabolites can be categorized into three major classes (terpenoids, alkaloids and phenylpropanoids) although more exist. Exogenous administration of JAs induces production of secondary metabolites in all these classes (De Geyter et al., 2012). This profound alteration of secondary metabolism is accomplished by extensive transcriptional reprogramming in response to JA accumulation (Pauwels et al., 2009).

In *Arabidopsis*, JAs trigger the synthesis of glucosinolates, phenylpropanoids including flavonoids and anthocyanins, isoprenoids and the indole alkaloid camalexin (Pauwels et al., 2009; De Geyter et al., 2012). While many of these compounds are toxic to chewing insects or pathogens, others protect plants by filtering UV-radiation or stimulate plant development by

attracting pollinators or symbionts (Bednarek et al., 2009; Chamam et al., 2013; Emiliani et al., 2013). In tobacco, JAs have been shown to induce expression of genes involved in synthesis of alkaloids and phenylpropanoids (Goossens et al., 2003; Heil and Ton, 2008; Zhang and Memelink, 2009). In periwinkle (*Catharanthus roseus*), JAs also induce expression of all genes involved in terpenoid indole alkaloid (TIAs) synthesis. Several of this TIAs have pharmaceutical applications, for example, vinblastine and vincristine are potent antitumor drugs. Remarkably, MeJA also induces genes involved in production of primary metabolites that form precursors for TIA biosynthesis (Memelink et al., 2001; Zhang and Memelink, 2009; De Geyter et al., 2012). Defence-related secondary metabolites can also be toxic to the plant, and are therefore often stored as non-toxic precursors until they are activated by herbivore detection (Howe and Jander, 2008).

Jasmonates are necessary for plant development

Next to their clearly defined role in defence responses to biotic and abiotic stresses, JAs are also essential for normal plant development and growth. Many of the functions of JAs were discovered by analysing the phenotype of wild type (WT) plants grown on medium containing JAs or coronatine (COR), as well as by analysing JA biosynthesis and perception mutants. COR is a bacterial phytotoxin, produced by strains of *Pseudomonas syringae*, that structurally and functionally mimics JA-Ile (Wasternack, 2007; Fonseca et al., 2009, Figure 1-7).

The JA-insensitive mutant, *coi1-1* (*coronatine-insensitive 1*), the JA-receptor mutant (see next section) and the *fad3-2 fad7-2 fad8* triple mutant, which is deficient in the JA biosynthesis precursor linolenic acid, show deficiency in flower development and are male sterile. In the *fad3-2 fad7-2 fad8* triple mutant the male sterility phenotype can be rescued by exogenous application of JA to the flower buds. JAs therefore seem to be essential in Arabidopsis for correct stamen development by regulating filament elongation, anther dehiscence and the final stages of pollen development (Feys et al., 1994; McConn and Browse, 1996; Pauwels et al., 2009; Shih et al., 2014).

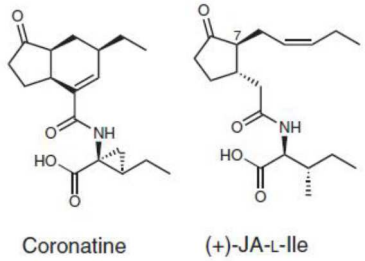

Figure 1-7. Coronatine functionally and structurally resembles JA-Ile.

The phytotoxin coronatine functionally and structurally resembles the functional hormone (+)-7-iso-L-JA-Ile. Figure adapted from Fonseca et al. (2009).

When WT plants are grown on medium supplemented with JAs or with COR, they undergo root growth inhibition. Because JA-insensitive mutants do not show this phenotype upon treatment, it is often used to screen for mutants that have reduced sensitivity to JAs (Feys et al., 1994; Wasternack, 2007; Wasternack and Hause, 2013). This root growth inhibition is the result of reduction of meristem activity and decreased cell elongation in the root differentiation zone by JAs (Chen et al., 2011; Acosta et al., 2013).

Seed germination is inhibited by JAs and ABA. However, this is not achieved by JA-Ile but by the jasmonate precursor OPDA, in a COI1-independent manner (Dave et al., 2011). Another developmental process regulated by JAs is the onset of leaf senescence, a developmental program that causes a type of slow, programmed cell death. This program is regulated both by intrinsic factors, such as hormones, and by external factors, such as environmental conditions. JA production is increased during leaf senescence and JAs have been shown to positively regulate the onset of natural and dark induced senescence. This effect is at least partially dependent on ethylene signalling (Kim et al., 2015) and is antagonized by auxin signalling (Jiang et al., 2014).

Glandular trichomes are often involved in the defence response to herbivores as they produce high amounts of secondary metabolites and defence proteins. In addition, together with non-glandular trichomes they provide a physical barrier against insects (Wasternack and Hause, 2013). Gibberellins (GAs) and JAs synergistically regulate trichome initiation in Arabidopsis by targeting the activation of TF complexes required for this process (Qi et al., 2011; Qi et al., 2014).

In the last five years, research concerning the integration of light signals into developmental responses through JA-signalling has made significant progress. Plants possess several photoreceptors that allow them to fine-tune their development in response to light quantity, quality, direction and periodicity. Shade caused by plant growth under dense canopies is perceived as a reduction in the red:far-red (R:FR) light ratio. Low R:FR ratios promote plant growth to outcompete neighbours, known as the shade avoidance response. Low R:FR ratios were found to negatively regulate JA-dependent defence responses, including the production of secondary metabolites and green leaf volatiles. In this way, plants prioritize resource allocation to growth over immune responses during the shade avoidance response (Cerrudo et al., 2012; Kegge et al., 2013; Cargnel et al., 2014).

In addition to the key function of JAs in the processes mentioned above, JAs also function during development during lateral and adventious root formation, in growth inhibition of above-ground plant parts, in the induction of tuber formation in potato, regulation of tendril coiling in Bryonia, leaf movements (nyctinasty and hyponasty) in Albizzia, fruit ripening and the modulation of symbiotic interactions (Wasternack, 2007; Balbi and Devoto, 2008; Wasternack and Hause, 2013).

THE JA-SIGNALLING PATHWAY

As described above, JAs are involved in numerous plant defence and developmental processes. Because of the large impact of this phyto-hormone on different cellular and developmental programs, considerable research effort has been spent to the characterization of the JA signal transduction pathway.

Until recently, the core JA signalling module was defined as composed by: MYC2, a key transcription factor regulating expression of JA-responsive genes (Lorenzo et al., 2004), JAZ proteins, repressors that inhibit MYC2 activity in the absence of the hormone (Chini et al., 2007; Thines et al., 2007) and COI1 that acts as the JA receptor *in vivo* and, in response to JA-Ile, targets the repressor for proteolytic degradation (Fonseca et al., 2009; Yan et al., 2009). The co-repressors NINJA and TPL were later identified as members of the core JA-signalling complex, mediating the repressor-effect of JAZ proteins (Pauwels et al., 2010, Figure 1-8). The components of the core JA signalling module are considered essential for JA signal transduction as mutations affecting this complex disturb many (or all) JA responses (Wasternack, 2007; Chico et al., 2008; Browse, 2009).

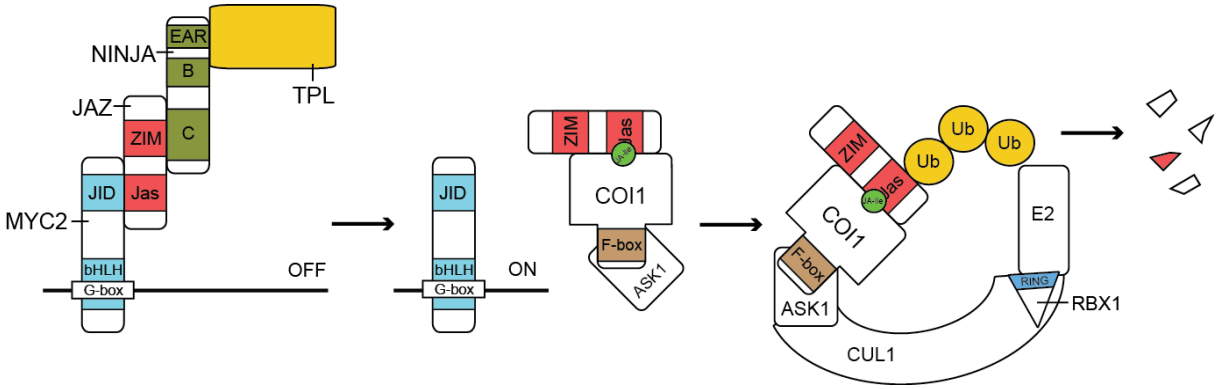

Figure 1-8. Overview of the JA-signalling pathway.

In the absence of JA-Ile, the activity of transcription factor MYC2, bound to the G-box of jasmonate (JA) responsive promotors, is repressed by interaction with JAZ proteins. JAZ proteins bind to the JAZ-interacting domain (JID) of MYC2 through their Jas domain. Simultaneously JAZ proteins interact through their ZIM domain with the C-domain of NINJA. Finally, NINJA recruits the co-repressor TOPLESS (TPL) to the promotors of JA-responsive genes through its EAR domain. Upon perception of the hormone, the CRL E3 ligase with F-box component COI1 binds and ubiquitinates JAZ proteins. Subsequently, JAZ proteins are degraded and MYC2 activates transcription of JA-responsive genes eventually resulting in a JA-response. Figure adapted from Pauwels and Goossens (2011).

MYC2 regulates the transcription of JA-responsive genes

The transcription factor MYC2 plays a central role in regulating the transcriptional reprogramming in response to JAs. *MYC2* was first identified as *JASMONATE INSENSITIVE-1* (*JIN1/JAI1*) in two different screens for mutants with a reduced JA sensitivity. The *jin1/jai1/myc2* mutant shows reduced root growth inhibition and anthocyanin production when treated with MeJA compared to WT plants. *MYC2* expression is induced by JAs or

wounding and overexpression (OE) of the TF renders plants hypersensitive to JAs (Berger et al., 1996; Lorenzo et al., 2004).

MYC2 encodes a nuclear localized basic helix-loop-helix-leucine zipper (bHLH)-type TF. This TF specifically regulates (at least) two branches of the JA response, in an antagonistic manner. One branch includes JA-responsive genes with a role in defence against pathogens or a role in secondary metabolism. Expression of these genes is repressed by MYC2 upon JA-treatment, and their induction requires activation of both JA and ET signalling. A second branch includes genes responsive to mechanic or biotic wounding and genes involved in flavonoid metabolism or oxidative stress tolerance. Expression of genes in this branch is activated by MYC2 in response to JA (Lorenzo et al., 2004; Kazan and Manners, 2013). Furthermore, MYC2 has been shown to be a positive regulator of JA-mediated oxidative stress tolerance, flavonoid biosynthesis and anthocyanin biosynthesis, and of the ABA-mediated drought response. As a negative regulator, MYC2 represses JA-dependent Trp metabolism and the subsequent biosynthesis of indole glucosinolates (Dombrecht et al., 2007; Kazan and Manners, 2013).

MYC2 binds to the G-box, a CACGTG palindrome hexamer, and G-box related motifs present in the promoters of a great number of genes that are activated by JA through its basic amino acids (Toledo-Ortiz et al., 2003; Dombrecht et al., 2007; Godoy et al., 2011). The MYC2 promoter itself also contains a G-box motif and the TF regulates its own transcription (Dombrecht et al., 2007). The HLH-domain is required for the formation of homo or heterodimers with other related TFs (Fernandez-Calvo et al., 2011). The N-terminal part of MYC2 contains a transcriptional activation domain, that mediates interaction with the Mediator complex subunit MED25 for transcription initiation (Fernandez-Calvo et al., 2011; Cevik et al., 2012; Chen et al., 2012), and a JAZ interaction domain (JID) that mediates interaction with the JAZ repressors (Chini et al., 2007; Fernandez-Calvo et al., 2011).

The transcriptional reprogramming induced by JAs has been shown to enclose two different transcriptional waves. An early transcriptional wave induces expression of genes encoding primary regulators of JA signalling such as the JAZ proteins and MYC2. A subsequent wave consists of both positive and negative regulation of genes including other TFs (Pauwels et al., 2009). *Jin1/jai1* mutants are not fully impaired in all JA-mediated responses. For that reason, the transcriptional reprogramming following JA perception cannot be entirely performed by MYC2 (Chico et al., 2008). Indeed, the TFs MYC3/ATR2 and MYC4 that are closely related to MYC2 were also shown to activate JA-dependent transcription upon perception of the hormone. Similarly to MYC2, MYC3/4 transcriptional activity was directly inhibited by binding with JAZ proteins. Finally, loss-of-function mutations in any of the two TFs rendered the plants partially insensitive to JA and aggravated the JA-insensitive phenotype when combined with the *jin1/jai1* mutant (Fernandez-Calvo et al., 2011).

JAZ proteins repress JA-signalling

Jasmonate ZIM-domain (JAZ) proteins have recently been shown to constitute the missing link between the transcriptional regulation of JA responses and the perception of JA. In the absence of jasmonates, members of the JAZ protein family repress expression of JA-responsive genes by inhibiting MYC2 activity. Upon treatment with the hormone, JAZ proteins are degraded by the 26S proteasome, thereby allowing transcriptional activation of JA-responsive genes. This degradation is dependent on direct interaction between JAZ and COI1 (Chini et al., 2007; Thines et al., 2007; Sheard et al., 2010).

The JAZ protein family has 13 members in Arabidopsis (Chini et al., 2007; Thireault et al., 2015) and homologues have been identified in several plant species, both dicotyledons and monocotyledons, but not outside the plant kingdom (Chini et al., 2007; Ye et al., 2009; Thireault et al., 2015). Null mutations in JAZ proteins do not have a clear phenotypic effect suggesting JAZ proteins are functionally redundant (Thines et al., 2007; Chico et al., 2008; Grunewald et al., 2009).

JAZ proteins contain three conserved domains: the ZIM domain, a region of weak homology at the N-terminus and the C-terminal Jas domain which is most strongly conserved (Figure 1-9). The Jas domain is essential for JAZ stability, as it constitutes the interaction platform between JAZ and COI1 upon hormone treatment (Chini et al., 2007; Thines et al., 2007; Melotto et al., 2008). Mutation of essential amino acid residues within the Jas domain generates plants with a JA-insensitive phenotype similar to that of *coi1-1* (Melotto et al., 2008). The ZIM domain refers to a 36-amino acid domain, containing a conserved motif, shared by Zinc-finger expressed in the inflorescence meristem (ZIM) and ZIM-like (ZML) proteins. Within the ZIM domain, a strongly conserved amino acid pattern forms the TIFY motif (Vanholme et al., 2007). The ZIM domain mediates hormone-independent homo- and hetero-dimerization of JAZ proteins (Chini et al., 2009; Chung and Howe, 2009). The newest member of the JAZ family (JAZ13), contains a divergent TIFY-motif and Jas domain. This protein was shown to be a functional member of the JAZ family and to repress JA-responses through interaction with the TF MYC2. However, the divergent TIFY-motif does not mediate hetero-dimerization of JAZ13 with other members of the JAZ-family (Thireault et al., 2015).

Finally, a negative feedback loop is induced during JA-signalling as JAZ proteins have a G-box (or a variant of it) overrepresented in their promoter. JA-mediated induction of JAZ expression results in a pulsed response followed by subsequent desensitization, avoiding a harmful runaway response (Chini et al., 2007; Thines et al., 2007).

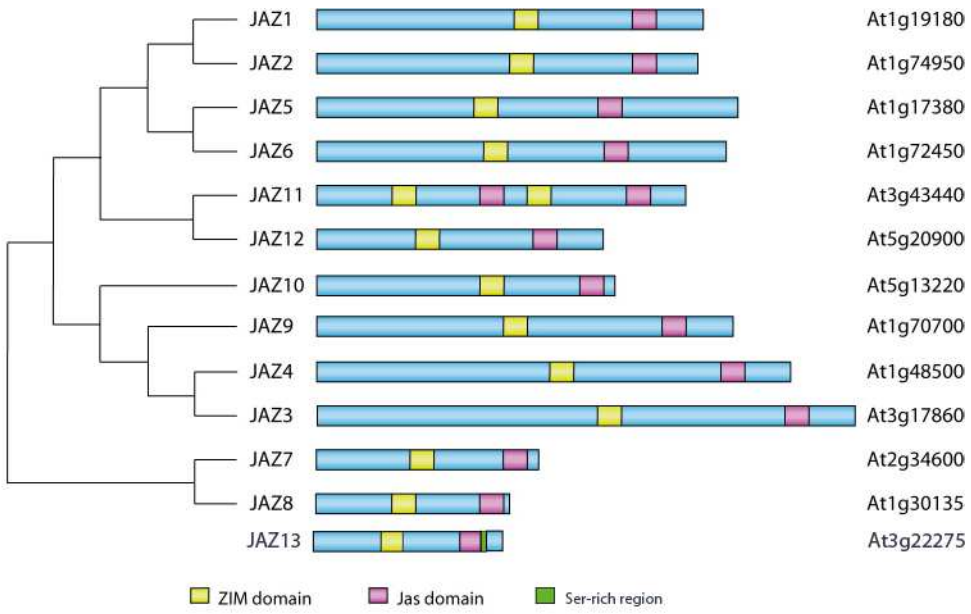

Figure 1-9. Structure and phylogeny of Arabidopsis JAZ proteins

JAZ proteins contain three conserved domains: the N-terminal ZIM domain (yellow), the C-terminal Jas domain (pink) and a region of weak homology at the N-terminus (not shown). In addition, JAZ13 contains an additional Ser-rich C-terminal tail. Figure adapted from Browse (2009) and Thireault et al. (2015).

NINJA and TOPLESS are negative regulators of JA-responses

The molecular mechanism by which JAZ proteins manage to repress transcription of JA-inducible genes was discovered recently. JAZ proteins were shown to bind a previously unknown protein designated NOVEL INTERACTOR OF JAZ (NINJA) that functions as an adaptor protein to recruit the co-repressor TOPLESS (TPL) and TPL related (TPR) proteins to the MYC-JAZ complex (Pauwels et al., 2010).

NINJA is related to the family of ABI5 binding proteins (AFPs, Pauwels et al., 2010). This small, plant-specific protein family contains four highly conserved members that play a role in ABA-signalling by regulating the TF ABI5 (Garcia et al., 2008). AFPs are localized in the nucleus and possess three conserved domains - A, B and C – as is the case for NINJA (Garcia et al., 2008; Pauwels et al., 2010). NINJA interacts directly with JAZ proteins through its C-domain. Reversibly, JAZs do not bind to the C-domain of AFPs, suggesting the specificity of JAZ proteins for NINJA. This interaction is dependent on the presence of the TIFY motif within the ZIM domain of JAZ proteins. The ZIM domain, consequently, has a dual function: it is not only necessary for dimerization of JAZ proteins but also for binding of these proteins to the NINJA/TPL complex. NINJA therefore acts as a negative regulator of JA signalling (Pauwels et al., 2010).

NINJA exerts its co-repressor activity by interacting with TOPLESS (TPL). TPL is a Groucho/Tup1-type co-repressor that has been shown to play a role in the auxin signalling pathway (Long et al., 2006; Szemenyei et al., 2008). It is recruited by repressors of the auxin

response through an Ethylene Response Factor (ERF)-associated amphiphilic repression motif (EAR motif, Szemenyei et al., 2008). The EAR motif is present on several repressors and is essential for their repressor activity (Ohta et al., 2001). This motif is also present within the A domain of NINJA which thereby recruits the TPL co-repressor to the MYC-JAZ complex, bound to promoters of JA-responsive genes. NINJA therefore functions as an adaptor protein between JAZ repressors and the TPL and TPR co-repressors. JAZ8 and JAZ13 contain an EAR motif themselves, and this EAR motif mediates direct interaction with the TPL co-repressor without the need for the adaptor NINJA (Shyu et al., 2012; Thireault et al., 2015).

The EAR motif is also present on AFP proteins, and these were shown to interact with TPL as well. TPL and TPR therefore probably act as general co-repressors that are recruited to different signalling pathways by specific adaptor proteins (Pauwels et al., 2010). Recently, the identification of new *ninja* mutants revealed the role of NINJA as a co-repressor of JA-signalling was predominant in hypocotyls and in the root, where a functional NINJA-complex is necessary to repress basal JA-signalling and allow cell elongation and root growth under standard conditions (Acosta et al., 2013).

COI1 links the Ubiquitin system to JA-signalling

As mentioned earlier, coronatine (COR) is a phytotoxin produced by *Pseudomonas syringae* that structurally and functionally resembles JA-Ile. Based on the property of COR and JAs to inhibit seedling root and shoot growth, a screen for COR-insensitive mutants led to the discovery of the *CORONATINE-INSENSITIVE1* (*COI1*) gene. *Coi1-1* loss-of-function mutants are insensitive to COR/JA and are male sterile in Arabidopsis (Feys et al., 1994). In addition, *coi1-1* mutants are resistant to *P. syringae* infection (Vijayan et al., 1998; Glazebrook, 2005; Howe and Jander, 2008). Because COR is a molecular mimic of JA-Ile, both are perceived by the same receptor and, in WT plants, COR triggers JA-signalling, which antagonizes SA-dependent defence mechanisms that are normally needed to limit *P. syringae* growth. This explains why *coi1-1* plants are resistant to *P. syringae* (Glazebrook, 2005; Browse, 2009).

The COI1 protein was characterized as an F-box protein that, next to its N-terminal F-box domain, also contains 16 leucine rich repeats (LRRs, Xie et al., 1998). The F-box domain of COI1 is characteristic for proteins that associate with SCF ubiquitin-ligase complexes and the protein is closely related to other F-box proteins with a function in hormone signalling (Figure 1-10A). Accordingly, COI1 has been shown to associate with RBX1, CUL1, and either ASK1 or ASK2 to assemble functional SCF^{COI1} complexes in Arabidopsis (Dai et al., 2002) and plants deficient in other components or regulators of SCF complexes also show impaired JA responses (Lorenzo et al., 2004; Chico et al., 2008).

In 2010, (Sheard et al., 2010) published the crystal structure of COI1 in complex with ASK1, JA-Ile and the JAZ1 degron, the region of JAZ1 necessary to mediate its SCF^{COI1}-

dependent degradation (Figure 1-10 B-C). This finally revealed the exact mechanism for JA-perception. The overall structure of COI1 resembles that of the auxin receptor F-box protein TIR1. The 18 tandem LRRs of COI1 form a horseshoe-shaped solenoid domain, housing the JA-Ile binding pocket. High affinity JA-Ile binding however requires both COI1 and the JAZ degron, thus implying JA-perception is mediated by a co-receptor complex existing of COI1 and JAZ. Part of the JAZ1 degron interacts with JA-Ile while the other part interacts with COI1. The JAZ1 degron is therefore referred to as a bi-partite degron. Four loops (loop-2,-12,-14 and loop-C) protrude at the top surface of the COI1 LRR domain and are important for JA-Ile and JAZ binding. Finally, inositol-pentakisphosphate was identified as a COI1 cofactor, binding at the centre of the protein, underneath the JA-Ile binding pocket, and crucial for the formation of a high-affinity co-receptor complex (Sheard et al., 2010).

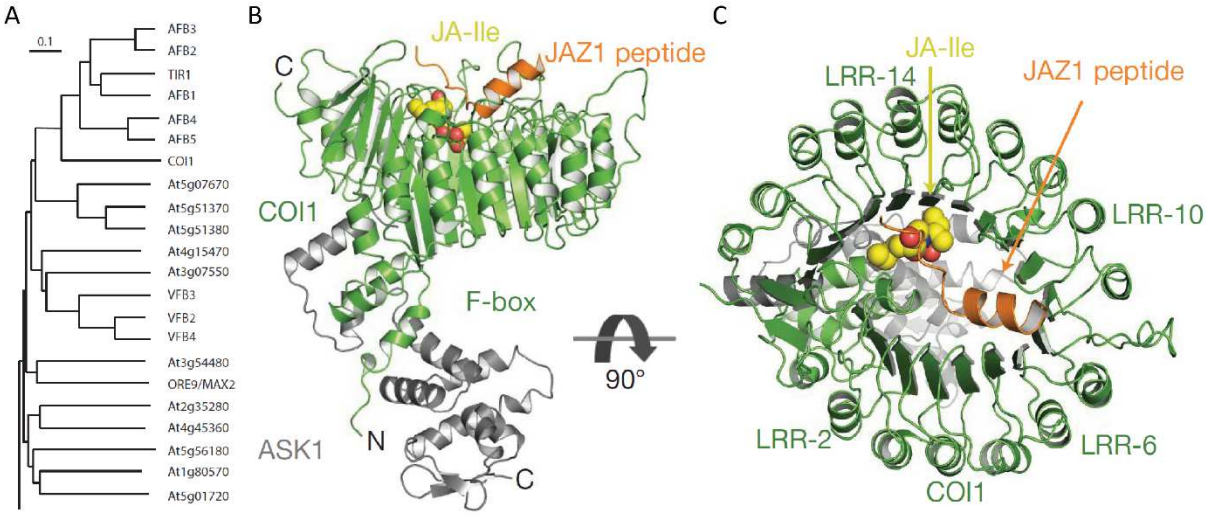

Figure 1-10. COI1 phylogeny and crystal structure.

A. Phylogenetic tree showing part of the C4 F-box subfamily. This subfamily includes TIR1 and AFB1-5 (involved in auxin perception) and MAX2 (involved in strigolactone perception). Bars represent the branch length equivalent to a 0.1 amino acid change per residue. Figure adapted from Gagne et al. (2002). B, C. COI1 structure (green ribbon) in complex with ASK1 (grey ribbon), the JAZ1 degron peptide (orange ribbon) and (3*R*,7*S*)-JA-Ile (yellow space-fill representation). Figure adapted from Sheard et al. (2010).

The presence of ASK1 in complex with COI1 during crystallization was later found to be essential, as COI1 turned out to be an unstable protein when dissociated from the SCF-complex. COI1 instability is, again, mediated by the ubiquitin system as its degradation was proteasome dependent and involved ubiquitination at Lys297 (Yan et al., 2013). COI1 protein levels are thus strictly regulated and maintained at a level essential for proper activation of JA-responses.

SCF^{COI1}, thus, links the Ub system to JA perception by forming a co-receptor complex with JAZ for the bioactive JA-Ile as well as for its molecular mimic COR. Perception of the phyto-hormone by the F-box protein COI1 leads to ubiquitination of JAZ repressors by SCF^{COI1} and their subsequent degradation in the proteasome. This causes de-repression of TFs involved in the activation of JA-mediated responses. The variety of phenotypes associated

with the *coi1-1* mutation, however, suggest that SCF^{COI1} might have multiple targets (Xu et al., 2002). In addition, as the *jar1* mutant, defect in the enzyme responsible for JA-Ile production, does not display all the defects that are observed in the *coi1* mutant (Kazan and Manners, 2008), other signals than JA-Ile might be recognized by the same or a different receptor to activate JA signalling. On the other hand, there might be redundancy in JA-Ile conjugating enzymes.

Beyond the core JA-signalling module

In addition to all known JAZ proteins, MYC3/4 and the Mediator complex subunit MED25, MYC2 interacts with several other proteins. These include AHP5 (HISTIDINE CONTAINING PHOSPHOTRANSFER FACTOR 5), implicated in cytokinin signalling, TIC (TIME FOR COFFEE) involved in circadian signalling, SGB3 (SUPRESSOR OF G BETA 3) implicated in heterotrimeric G-protein signalling, the stress response regulator RCD1 (RADICAL INDUCED CELL DEATH 1) protein and all members of the DELLA protein family (Kazan and Manners, 2013). Many of the MYC2 interacting proteins form points of crosstalk with other signalling pathways, further fine-tuning the JA-response.

During JA-signalling, MYC2 negatively regulates genes involved in pathogen defence, as well as positive regulators of these genes. Expression of these genes in response to JA is dependent on two of these positive regulators: the TFs *ORA59* (*OCTADECANOID-RESPONSIVE ARABIDOPSIS AP2/ERF59)* and *ERF1* (Kazan and Manners, 2013). Remarkably, activation of the SA-signalling pathway causes degradation of ORA59, thus suppressing JA-signalling during SA-JA antagonism (Van der Does et al., 2013). Finally, ABA differentially affects the two branches of JA-responsive gene expression similarly to the dual effect of MYC2 (Kazan and Manners, 2013).

As mentioned earlier, JAs are also involved in light signalling, including circadian signalling. Both *MYC2* expression and protein accumulation seem to be under control of the circadian clock. Rhythmic MYC2 accumulation is regulated by the Ub system, as interaction of MYC2 with TIC, a component of the circadian clock, leads to proteasome-dependent degradation of MYC2. In addition, JA-perception is also regulated in a circadian manner as the expression of *COI1* is also controlled by TIC (Shin et al., 2012).

DELLA proteins, repressors of GA-responses, interact with both MYC2 and JAZ proteins to modulate JA-responses. These interactions are especially important during shade avoidance responses (see above) when resource allocation is primarily directed from defence to growth. At low GA concentrations, DELLAs compete with MYC2 for JAZ-binding, modulating the JA-response. Low R:FR ratios (i.e. shade) trigger GA-mediated degradation of DELLAs increasing the capacity of JAZ proteins to bind and inactivate MYC-type TFs. Moreover, low R:FR light conditions increase the stability of several JAZs while increasing MYC2/3/4 turnover,

resulting in increased repression of the JA-response. In addition, one DELLA protein (RGL3) was shown to positively regulate MYC2 and thus be required for full activation of JA-responses (Pieterse et al., 2014).

Since the discovery of JAZ proteins in 2007, a wide array of additional TFs that are capable to interact with JAZ proteins have been identified (Pauwels and Goossens, 2011; Sasaki-Sekimoto et al., 2013; Toda et al., 2013; Fonseca et al., 2014; Sasaki-Sekimoto et al., 2014), often involved in specific processes, an overview is given in Figure 1-11. These TFs are also necessary to integrate signals generated by alternate hormonal signalling pathways, in addition to JA-signalling, to fine-tune the different responses that are mediated by JAs to allow optimal adaptation or response to diverse environmental and developmental cues.

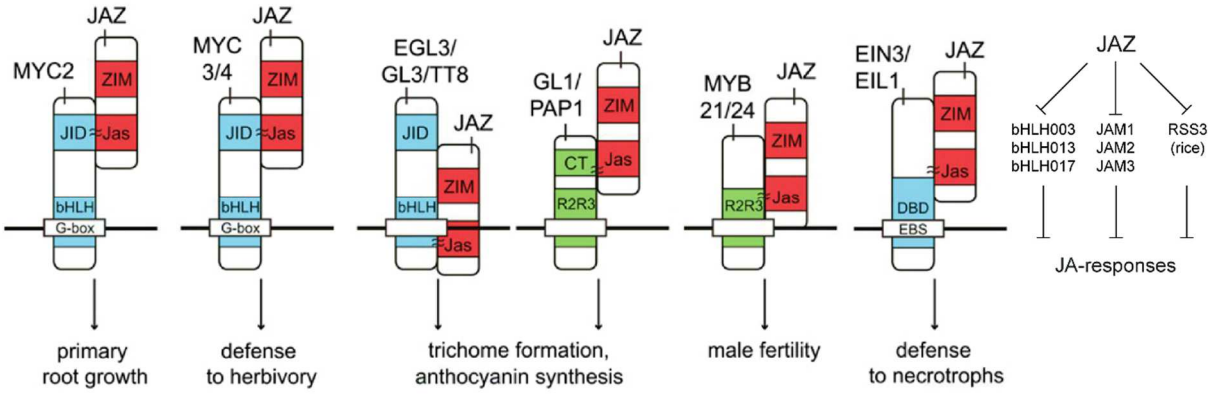

Figure 1-11. Alternative transcription factors involved in JA-signalling.

Overview of different transcription factors that are repressed by JAZ proteins (and domains mediating their interactions) and their role in JA-signalling responses. Figure adapted from Pauwels and Goossens (2011).

Recently, the VQ-motif containing protein JAV1 (JASMONATE-ASSOCIATED VQ MOTIF GENE 1) was identified as a negative regulator of JA-mediated plant defence responses against pathogens and herbivore insects. In addition, COI1-dependent JA perception leads to JAV1 protein degradation. This degradation is proteasome dependent and thus regulated by the Ub system. Because SCF^{COI1} does not interact directly with JAV1, the E3 Ub ligase responsible for JAV1 ubiquitination and subsequent degradation remains to be identified (Hu et al., 2013a).

The phospholipase A1 protein DAD1 (DEFICIENT IN ANTHER DEHISCENCE1) catalyses the initial step of JA-biosynthesis, the release of α-linolenic acid from chloroplast membranes. *Dad1* mutants are deficient in anther dehiscence and in pollen maturation, eventually resulting in a male-sterile phenotype, which can be rescued by exogenous application of JA to the flower buds (Ishiguro et al., 2001). Similar phenotypes were observed when expression of the E3 Ub ligase DAF/*ATL73* (*DAD1-ACTIVATING FACTOR*) was suppressed (Peng et al., 2013). DAF belongs to the ATL sub-group of RING-type E3 Ub ligases (Serrano et al., 2006), linking the Ub system to JA-biosynthesis. DAF was shown to act upstream of DAD1, and to be necessary for the expression of DAD1 to enable correct JA-mediated flower development. The function

of DAF was dependent on the integrity of its RING-domain, however, no DAF ubiquitination target has been identified yet (Peng et al., 2013).

Two additional E3 Ub ligases have been associated to JA-signalling. *RGLG3* and *RGLG4* belong to the *RGLG* (*RING DOMAIN LIGASE*) family of E3 ligases that contains five members in Arabidopsis (Stone et al., 2005; Zhang et al., 2012). *RGLG3* and *RGLG4* were reported to function redundantly as positive regulators of JA-responses (Zhang et al., 2012). Additionally, recent research involucrated RGLG3 and RGLG4 in the regulation of crosstalk between SA and JA in response to infection with the fungal pathogen *Fusarium moniliforme* (Zhang et al., 2015). The molecular mechanisms underlying RGLG3 and RGLG4 function in these processes and the ubiquitination target(s) of RGLG3 and RGLG4 remain to be identified.

THE UBIQUITIN SYSTEM AND OTHER PLANT HORMONE SIGNALLING PATHWAYS

Auxin

There is a striking parallelism between auxin and JA signalling. The auxin receptor TIR1 is an F-box protein closely related to COI1 and assembles into SCF^{TIR1}. Bioactive auxin forms a molecular glue between TIR1 and the auxin repressor proteins AUX/IAA that recruit the co-repressor TPL to promoters of auxin responsive genes. Degradation of AUX/IAA repressors eventually leads to de-repression of auxin responsive genes and activation of the auxin response (Cuéllar Pérez and Goossens, 2013; Figure 1-12).

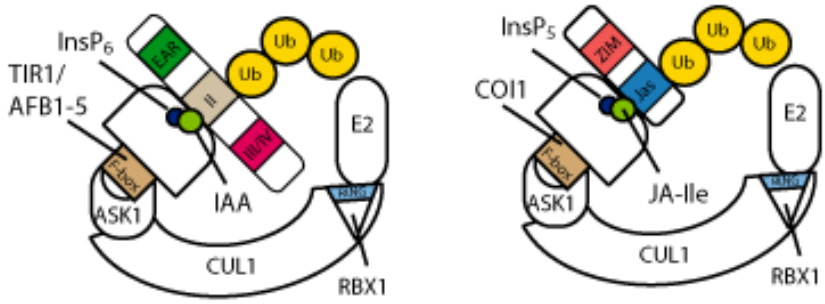

Figure 1-12. Parallelism between the auxin and the JA signalling pathways.

Formation of the co-receptor complexes in the presence of the hormone and inositol polyphosphates leads to ubiquitination of the Aux/IAA repressors by $SCF^{TIR1/AFB1-5}$ (left) or JAZ repressors by SCF^{COI1} (right). EAR, ETHYLENE RESPONSE FACTOR (ERF)-associated amphiphilic repression; IAA, indole-acetic acid; $InsP_5$, inositol pentakisphosphatephosphate; $InsP_6$, inositol hexakisphosphate; ZIM, Zinc-finger protein expressed in Inflorescence Meristems. Figure adapted from Cuéllar Pérez and Goossens (2013).

Gibberellic acid

Gibberellins are best known as growth promoting hormones and in the absence of the hormone gibberellin responses are negatively regulated by DELLA proteins. Perception of gibberellin by GID1 leads to its interaction with DELLA proteins. This interaction enhances the affinity of the F-box protein SLY1/GID2 towards DELLAs. Subsequent ubiquitination of DELLAs by $SCF^{SLY1/GID2}$ leads to their degradation and de-repression of the gibberellin response (Wang and Deng, 2011; Figure 1-13).

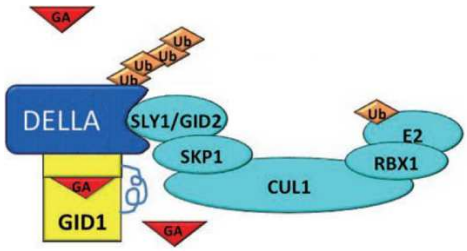

Figure 1-13. Gibberellic acid (GA) induced DELLA protein degradation.

In the presence of GA, formation of the GA-GID1-DELLA complex promotes the recruitment of DELLAs by the $SCF^{SLY1/GID2}$ E3 complex. DELLA protein degradation enables GA responsive genes to become activated. Figure adapted from Wang and Deng (2011).

Ethylene

Ethylene (ET) is a gaseous hormone that, in addition to its role in the defense response to necrotrophic pathogens (see above), is also involved in cell expansion, senscence and fruit ripening and abscission (An et al., 2010). In contrast to auxin, JA and gibberellins, perception of ET leads to stabilization of positive transcriptional regulators by inhibition of the F-box component of SCF^{EBF1} and SCF^{EBF2}. In the absence of ET, these E3 ligases are responsible for the degradation of (at least) two master TFs ETHYLENE INSENSITIVE3 (EIN3) and EIN3-LIKE1 (EIL1) that positively regulate the ET-response (An et al., 2010). In addition, ET biosynthesis is also regulated by the Ub system. The BTB protein Ethylene-Overproducer 1 (ETO1), the target recognition module of a CUL3-type CRL, regulates the stability of a key enzyme involved in ethylene production (Wang et al., 2004; Figure 1-14A).

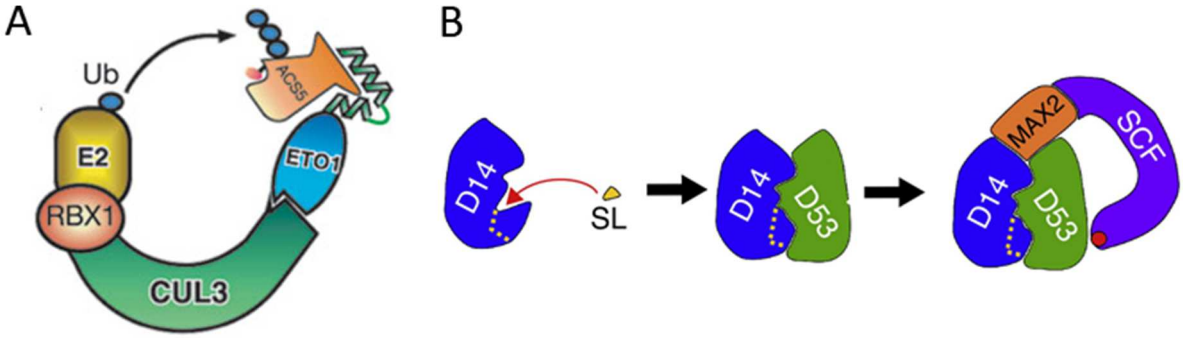

Figure 1-14. Involvement of the Ub system in ET biosynthesis and SL signalling.

A. Regulation of ET biosynthesis by the E3 ligase component ETO1. ETO1 recognizes the ET biosynthetic enzyme ACS5. ETO1 is a BTB protein and is part of a CUL3-type E3 ligase, interaction with ACS5 leads to proteasome-dependent degradation of the latter. Figure adapted from Wang et al. (2004). B. Hypothetical model of SL signalling. Binding of SL to D14 causes a conformational change that enables tight interaction of D14 with D53. The D14/D53 complex forms a substrate for ubiquitination by SCF^{MAX2} (purple). Figure adapted from Bennett and Leyser (2014).

Strigolactone

Although strigolactones (SLs) are an ancient class of plant hormones, they have been noticed by researches only recently. Nevertheless, their signalling pathway has partly been identified and resembles that of JA and auxin. Upon SL perception, the CRL-type E3 ligase SCF^{MAX2} targets the ubiquitination of the SL repressor proteins D14 and D53 (SMXL6/7 in *Arabidopsis*). SMXL proteins contain EAR motifs that could possibly recruit TPL and repress the activation of SL-responsive genes in the absence of the hormone (Bennett and Leyser, 2014; Figure 1-14B).

Salicylic acid

Salicylic acid (SA) is essential for plant immune responses against biotrophic pathogens. Recently, the BTB proteins NPR2 and NPR3 were shown to act as SA receptors. The CRL-type E3 ligases BTB^{NPR2} and BTB^{NPR3} regulate NPR1, stability in an SA-dependent manner. NPR1 is the key regulator of SA-responses (Fu et al., 2012).

Abscisic acid

Abscisic acid (ABA) is involved in plant responses to numerous types of abiotic stresses. The abundance of two ABA-responsive TFs is regulated by two RING-type E3 ligases: AIP2 (ABI3-Interacting Protein-2) and KEG (Keep on Going). Remarkably, ABA differentially regulates the activity of these E3 ligases towards their targets (Stone and Callis, 2007).

Brassinosteroids

Brassinosteroids (BRs) are plant hormones critical to plant growth and development. In the absence of BRs, the kinase BRASSINOSTEROID-INSENSITIVE 2 (BIN2) accumulates and negatively regulates BR signalling. Exogenous application of active BRs trigger the proteasome-dependent degradation of BIN2, allowing activation of BR responsive gene expression (Peng et al., 2008). In addition, the TF CES (CESTA or 'basket' in Spanish), a phosphorylation target of BIN2 and regulator of BR responses, is regulated by sumoylation. Sumoylation of CES controls the subnuclear localization of the TF and is antagonized by CES phosphorylation mediated by BIN2 (Khan et al., 2014).

REFERENCES

Acosta IF, Gasperini D, Chetelat A, Stolz S, Santuari L, Farmer EE (2013) Role of NINJA in root jasmonate signaling. Proceedings of the National Academy of Sciences of the United States of America **110:** 15473-15478

An FY, Zhao QO, Ji YS, Li WY, Jiang ZQ, Yu XC, Zhang C, Han Y, He WR, Liu YD, et al (2010) Ethylene-Induced Stabilization of ETHYLENE INSENSITIVE3 and EIN3-LIKE1 Is Mediated by Proteasomal Degradation of EIN3 Binding F-Box 1 and 2 That Requires EIN2 in Arabidopsis. The Plant cell **22:** 2384-2401

Andersen P, Kragelund BB, Olsen AN, Larsen FH, Chua NH, Poulsen FM, Skriver K (2004) Structure and biochemical function of a prototypical Arabidopsis U-box domain. The Journal of biological chemistry **279:** 40053-40061

Balbi V, Devoto A (2008) Jasmonate signalling network in Arabidopsis thaliana: crucial regulatory nodes and new physiological scenarios. New Phytologist **177:** 301-318

Bednarek P, Pislewska-Bednarek M, Svatos A, Schneider B, Doubsky J, Mansurova M, Humphry M, Consonni C, Panstruga R, Sanchez-Vallet A, et al (2009) A Glucosinolate Metabolism Pathway in Living Plant Cells Mediates Broad-Spectrum Antifungal Defense. Science **323:** 101-106

Bennett T, Leyser O (2014) Strigolactone signalling: standing on the shoulders of DWARFs. Current opinion in plant biology **22:** 7-13

Berger S, Bell E, Mullet JE (1996) Two Methyl Jasmonate-Insensitive Mutants Show Altered Expression of AtVsp in Response to Methyl Jasmonate and Wounding. Plant physiology **111:** 525-531

Bostick M, Lochhead SR, Honda A, Palmer S, Callis J (2004) Related to ubiquitin 1 and 2 are redundant and essential and regulate vegetative growth, auxin signaling, and ethylene production in Arabidopsis. The Plant cell **16:** 2418-2432

Browse J (2009) Jasmonate Passes Muster: A Receptor and Targets for the Defense Hormone. Annual review of plant biology **60:** 183-205

Browse J, Howe GA (2008) New weapons and a rapid response against insect attack. Plant physiology **146:** 832-838

Callis J (2014) The ubiquitination machinery of the ubiquitin system. The Arabidopsis book / American Society of Plant Biologists **12:** e0174

Callis J, Pollmann L, Shanklin J, Wettern M, Vierstra RD (1989) Sequence of a cDNA from Chlamydomonas reinhardii encoding a ubiquitin 52 amino acid extension protein. Nucleic acids research **17:** 8377

Cargnel MD, Demkura PV, Ballare CL (2014) Linking phytochrome to plant immunity: low red : far-red ratios increase Arabidopsis susceptibility to Botrytis cinerea by reducing the biosynthesis of indolic glucosinolates and camalexin. New Phytologist **204:** 342-354

Cerrudo I, Keller MM, Cargnel MD, Demkura PV, de Wit M, Patitucci MS, Pierik R, Pieterse CMJ, Ballare CL (2012) Low Red/Far-Red Ratios Reduce Arabidopsis Resistance to Botrytis cinerea and Jasmonate Responses via a COI1-JAZ10-Dependent, Salicylic Acid-Independent Mechanism. Plant physiology **158:** 2042-2052

Cevik V, Kidd BN, Zhang PJ, Hill C, Kiddle S, Denby KJ, Holub EB, Cahill DM, Manners JM, Schenk PM, et al (2012) MEDIATOR25 Acts as an Integrative Hub for the Regulation of Jasmonate-Responsive Gene Expression in Arabidopsis. Plant physiology **160:** 541-555

Chamam A, Sanguin H, Bellvert F, Meiffren G, Comte G, Wisniewski-Dye F, Bertrand C, Prigent-Combaret C (2013) Plant secondary metabolite profiling evidences strain-dependent effect in the Azospirillum-Oryza sativa association. Phytochemistry **87:** 65-77

Chen Q, Sun JQ, Zhai QZ, Zhou WK, Qi LL, Xu L, Wang B, Chen R, Jiang HL, Qi J, et al (2011) The Basic Helix-Loop-Helix Transcription Factor MYC2 Directly Represses PLETHORA Expression during Jasmonate-Mediated Modulation of the Root Stem Cell Niche in Arabidopsis. The Plant cell **23:** 3335-3352

Chen R, Jiang HL, Li L, Zhai QZ, Qi LL, Zhou WK, Liu XQ, Li HM, Zheng WG, Sun JQ, et al (2012) The Arabidopsis Mediator Subunit MED25 Differentially Regulates Jasmonate and Abscisic Acid Signaling through Interacting with the MYC2 and ABI5 Transcription Factors. The Plant cell **24:** 2898-2916

Chico JM, Chini A, Fonseca S, Solano R (2008) JAZ repressors set the rhythm in jasmonate signaling. Current opinion in plant biology **11:** 486-494

Chini A, Fonseca S, Chico JM, Fernandez-Calvo P, Solano R (2009) The ZIM domain mediates homo- and heteromeric interactions between Arabidopsis JAZ proteins. The Plant journal : for cell and molecular biology **59:** 77-87

Chini A, Fonseca S, Fernandez G, Adie B, Chico JM, Lorenzo O, Garcia-Casado G, Lopez-Vidriero I, Lozano FM, Ponce MR, et al (2007) The JAZ family of repressors is the missing link in jasmonate signalling. Nature **448:** 666-671

Chung HS, Howe GA (2009) A critical role for the TIFY motif in repression of jasmonate signaling by a stabilized splice variant of the JASMONATE ZIM-domain protein JAZ10 in Arabidopsis. The Plant cell **21:** 131-145

Ciechanover A, Elias S, Heller H, Ferber S, Hershko A (1980) Characterization of the heat-stable polypeptide of the ATP-dependent proteolytic system from reticulocytes. The Journal of biological chemistry **255:** 7525-7528

Clarke SM, Cristescu SM, Miersch O, Harren FJM, Wasternack C, Mur LAJ (2009) Jasmonates act with salicylic acid to confer basal thermotolerance in Arabidopsis thaliana. New Phytologist **182:** 175-187

Cuéllar Pérez A, Goossens A (2013) Jasmonate signalling: a copycat of auxin signalling? Plant Cell Environ **36:** 2071-2084

Dai L, Xu L, Huang D, Li X, Luo K, Guan C (2002) ASK1 physically interacts with COI1 and is required for male fertility in Arabidopsis. Science in China Series C, Life sciences / Chinese Academy of Sciences **45:** 631-636

Dave A, Hernandez ML, He Z, Andriotis VM, Vaistij FE, Larson TR, Graham IA (2011) 12-oxo-phytodienoic acid accumulation during seed development represses seed germination in Arabidopsis. The Plant cell **23:** 583-599

De Geyter N, Gholami A, Goormachtig S, Goossens A (2012) Transcriptional machineries in jasmonate-elicited plant secondary metabolism. Trends in plant science **17:** 349-359

del Pozo JC, Dharmasiri S, Hellmann H, Walker L, Gray WM, Estelle M (2002) AXR1-ECR1-dependent conjugation of RUB1 to the Arabidopsis Cullin AtCUL1 is required for auxin response. The Plant cell **14:** 421-433

del Pozo JC, Estelle M (1999) The Arabidopsis cullin AtCUL1 is modified by the ubiquitin-related protein RUB1. Proceedings of the National Academy of Sciences of the United States of America **96:** 15342-15347

Dewez M, Bauer F, Dieu M, Raes M, Vandenhaute J, Hermand D (2008) The conserved Wobble uridine tRNA thiolase Ctu1-Ctu2 is required to maintain genome integrity. Proceedings of the National Academy of Sciences of the United States of America **105:** 5459-5464

Dikic I, Wakatsuki S, Walters KJ (2009) Ubiquitin-binding domains - from structures to functions. Nature reviews Molecular cell biology **10:** 659-671

Dombrecht B, Xue GP, Sprague SJ, Kirkegaard JA, Ross JJ, Reid JB, Fitt GP, Sewelam N, Schenk PM, Manners JM, et al (2007) MYC2 differentially modulates diverse jasmonate-dependent functions in Arabidopsis. The Plant cell **19:** 2225-2245

Dong W, Wang MC, Xu F, Quan TY, Peng KQ, Xiao LT, Xia GM (2013) Wheat Oxophytodienoate Reductase Gene TaOPR1 Confers Salinity Tolerance via Enhancement of Abscisic Acid Signaling and Reactive Oxygen Species Scavenging. Plant physiology **161:** 1217-1228

Downes BP, Saracco SA, Lee SS, Crowell DN, Vierstra RD (2006) MUBs, a family of ubiquitin-fold proteins that are plasma membrane-anchored by prenylation. The Journal of biological chemistry **281:** 27145-27157

Elfving N, Davoine C, Benlloch R, Blomberg J, Brannstrom K, Muller D, Nilsson A, Ulfstedt M, Ronne H, Wingsle G, et al (2011) The Arabidopsis thaliana Med25 mediator subunit integrates environmental cues to control plant development. Proceedings of the National Academy of Sciences of the United States of America **108:** 8245-8250

Emiliani J, Grotewold E, Ferreyra MLF, Casati P (2013) Flavonols Protect Arabidopsis Plants against UV-B Deleterious Effects. Molecular plant **6:** 1376-1379

Enchev RI, Schulman BA, Peter M (2015) Protein neddylation: beyond cullin-RING ligases. Nature reviews Molecular cell biology **16:** 30-44

Erb M, Meldau S, Howe GA (2012) Role of phytohormones in insect-specific plant reactions. Trends in plant science **17:** 250-259

Feng J, Shen WH (2014) Dynamic regulation and function of histone monoubiquitination in plants. Frontiers in plant science **5**

Fernandez-Calvo P, Chini A, Fernandez-Barbero G, Chico JM, Gimenez-Ibanez S, Geerinck J, Eeckhout D, Schweizer F, Godoy M, Franco-Zorrilla JM, et al (2011) The Arabidopsis bHLH transcription factors MYC3 and MYC4 are targets of JAZ repressors and act additively with MYC2 in the activation of jasmonate responses. The Plant cell **23:** 701-715

Feys BJF, Benedetti CE, Penfold CN, Turner JG (1994) Arabidopsis Mutants Selected for Resistance to the Phytotoxin Coronatine Are Male-Sterile, Insensitive to Methyl Jasmonate, and Resistant to a Bacterial Pathogen. The Plant cell **6:** 751-759

Fonseca S, Chini A, Hamberg M, Adie B, Porzel A, Kramell R, Miersch O, Wasternack C, Solano R (2009) (+)-7-iso-Jasmonoyl-L-isoleucine is the endogenous bioactive jasmonate. Nature chemical biology **5:** 344-350

Fonseca S, Fernandez-Calvo P, Fernandez GM, Diez-Diaz M, Gimenez-Ibanez S, Lopez-Vidriero I, Godoy M, Fernandez-Barbero G, Van Leene J, De Jaeger G, et al (2014) bHLH003, bHLH013 and bHLH017 Are New Targets of JAZ Repressors Negatively Regulating JA Responses. PloS one **9**

Fu H, Sadis S, Rubin DM, Glickman M, van Nocker S, Finley D, Vierstra RD (1998) Multiubiquitin chain binding and protein degradation are mediated by distinct domains within the 26 S proteasome subunit Mcb1. The Journal of biological chemistry **273:** 1970-1981

Fu ZQ, Yan SP, Saleh A, Wang W, Ruble J, Oka N, Mohan R, Spoel SH, Tada Y, Zheng N, et al (2012) NPR3 and NPR4 are receptors for the immune signal salicylic acid in plants. Nature **486:** 228-+

Gagne JM, Downes BP, Shiu SH, Durski AM, Vierstra RD (2002) The F-box subunit of the SCF E3 complex is encoded by a diverse superfamily of genes in Arabidopsis. Proceedings of the National Academy of Sciences of the United States of America **99:** 11519-11524

Garcia ME, Lynch T, Peeters J, Snowden C, Finkelstein R (2008) A small plant-specific protein family of ABI five binding proteins (AFPs) regulates stress response in germinating Arabidopsis seeds and seedlings. Plant molecular biology **67:** 643-658

Glazebrook J (2005) Contrasting mechanisms of defense against biotrophic and necrotrophic pathogens. Annu Rev Phytopathol **43:** 205-227

Godoy M, Franco-Zorrilla, Perez-Perez J, Oliveros JC, Lorenzo O, Solano R (2011) Improved protein-binding microarrays for the identification of DNA-binding specificities of transcription factors. Plant Journal **66:** 700-711

Goehring AS, Rivers DM, Sprague GF, Jr. (2003) Urmylation: a ubiquitin-like pathway that functions during invasive growth and budding in yeast. Molecular biology of the cell **14:** 4329-4341

Goossens A, Hakkinen ST, Laakso I, Seppanen-Laakso T, Biondi S, De Sutter V, Lammertyn F, Nuutila AM, Soderlund H, Zabeau M, et al (2003) A functional genomics approach toward the understanding of secondary metabolism in plant cells. Proceedings of the National Academy of Sciences of the United States of America **100:** 8595-8600

Grunewald W, Vanholme B, Pauwels L, Plovie E, Inze D, Gheysen G, Goossens A (2009) Expression of the Arabidopsis jasmonate signalling repressor JAZ1/TIFY10A is stimulated by auxin. EMBO reports **10:** 923-928

Heil M, Ton J (2008) Long-distance signalling in plant defence. Trends in plant science **13:** 264-272

Heinemeyer W, Fischer M, Krimmer T, Stachon U, Wolf DH (1997) The active sites of the eukaryotic 20 S proteasome and their involvement in subunit precursor processing. The Journal of biological chemistry **272:** 25200-25209

Heyman J, De Veylder L (2012) The anaphase-promoting complex/cyclosome in control of plant development. Molecular plant **5:** 1182-1194

Howe GA, Jander G (2008) Plant immunity to insect herbivores. Annual review of plant biology **59:** 41-66

Hu P, Zhou W, Cheng ZW, Fan M, Wang L, Xie DX (2013a) JAV1 Controls Jasmonate-Regulated Plant Defense. Molecular cell **50:** 504-515

Hu YR, Jiang LQ, Wang F, Yu DQ (2013b) Jasmonate Regulates the INDUCER OF CBF EXPRESSION-C-REPEAT BINDING FACTOR/DRE BINDING FACTOR1 Cascade and Freezing Tolerance in Arabidopsis. The Plant cell **25:** 2907-2924

Hua Z, Vierstra RD (2011) The cullin-RING ubiquitin-protein ligases. Annual review of plant biology **62:** 299-334

Ishiguro S, Kawai-Oda A, Ueda J, Nishida I, Okada K (2001) The DEFECTIVE IN ANTHER DEHISCENCE1 gene encodes a novel phospholipase A1 catalyzing the initial step of jasmonic acid biosynthesis, which synchronizes pollen maturation, anther dehiscence, and flower opening in Arabidopsis. The Plant cell **13:** 2191-2209

Jiang YJ, Liang G, Yang SZ, Yu DQ (2014) Arabidopsis WRKY57 Functions as a Node of Convergence for Jasmonic Acid- and Auxin-Mediated Signaling in Jasmonic Acid-Induced Leaf Senescence. The Plant cell **26:** 230-245

Kamura T, Conrad MN, Yan Q, Conaway RC, Conaway JW (1999) The Rbx1 subunit of SCF and VHL E3 ubiquitin ligase activates Rub1 modification of cullins Cdc53 and Cul2. Genes & development **13:** 2928-2933

Kazan K (2015) Diverse roles of jasmonates and ethylene in abiotic stress tolerance. Trends in plant science **20:** 219-229

Kazan K, Manners JM (2008) Jasmonate signaling: Toward an integrated view. Plant physiology **146:** 1459-1468

Kazan K, Manners JM (2013) MYC2: The Master in Action. Molecular plant **6:** 686-703

Kegge W, Weldegergis BT, Soler R, Vergeer-Van Eijk M, Dicke M, Voesenek LACJ, Pierik R (2013) Canopy light cues affect emission of constitutive and methyl jasmonate-induced volatile organic compounds in Arabidopsis thaliana. New Phytologist **200:** 861-874

Kim DY, Scalf M, Smith LM, Vierstra RD (2013) Advanced proteomic analyses yield a deep catalog of ubiquitylation targets in Arabidopsis. The Plant cell **25:** 1523-1540

Khan M, Rozhon W, Unterholzner SJ, Chen T, Eremina M, Wurzinger B, Bachmair A, Teige M, Sieberer T, Isono E, Poppenberger B (2014) Interplay between phosphorylation and SUMOylation events determines CESTA protein fate in brassinosteroid signalling. Nature communications **5**

Kim J, Chang C, Tucker ML (2015) To grow old: regulatory role of ethylene and jasmonic acid in senescence. Frontiers in plant science **6**

Komatsu M, Chiba T, Tatsumi K, Iemura S, Tanida I, Okazaki N, Ueno T, Kominami E, Natsume T, Tanaka K (2004) A novel protein-conjugating system for Ufm1, a ubiquitin-fold modifier. The EMBO journal **23:** 1977-1986

Koo AJK, Gao XL, Jones AD, Howe GA (2009) A rapid wound signal activates the systemic synthesis of bioactive jasmonates in Arabidopsis. Plant Journal **59:** 974-986

Kraft E, Stone SL, Ma L, Su N, Gao Y, Lau OS, Deng XW, Callis J (2005) Genome analysis and functional characterization of the E2 and RING-type E3 ligase ubiquitination enzymes of Arabidopsis. Plant physiology **139:** 1597-1611

Kurepa J, Walker JM, Smalle J, Gosink MM, Davis SJ, Durham TL, Sung DY, Vierstra RD (2003) The small ubiquitin-like modifier (SUMO) protein modification system in Arabidopsis. Accumulation of SUMO1 and -2 conjugates is increased by stress. The Journal of biological chemistry **278:** 6862-6872

Leitner J, Petrasek J, Tomanov K, Retzer K, Parezova M, Korbei B, Bachmair A, Zazimalova E, Luschnig C (2012) Lysine63-linked ubiquitylation of PIN2 auxin carrier protein governs hormonally controlled adaptation of Arabidopsis root growth. Proceedings of the National Academy of Sciences of the United States of America **109:** 8322-8327

Li F, Vierstra RD (2012) Autophagy: a multifaceted intracellular system for bulk and selective recycling. Trends in plant science **17:** 526-537

Li W, Schmidt W (2010) A lysine-63-linked ubiquitin chain-forming conjugase, UBC13, promotes the developmental responses to iron deficiency in Arabidopsis roots. The Plant journal : for cell and molecular biology **62:** 330-343

Long JA, Ohno C, Smith ZR, Meyerowitz EM (2006) TOPLESS regulates apical embryonic fate in Arabidopsis. Science **312:** 1520-1523

Lorenzo O, Chico JM, Sanchez-Serrano JJ, Solano R (2004) JASMONATE-INSENSITIVE1 encodes a MYC transcription factor essential to discriminate between different jasmonate-regulated defense responses in Arabidopsis. The Plant cell **16:** 1938-1950

Lorenzo O, Piqueras R, Sanchez-Serrano JJ, Solano R (2003) ETHYLENE RESPONSE FACTOR1 integrates signals from ethylene and jasmonate pathways in plant defense. The Plant cell **15:** 165-178

Matsumoto ML, Wickliffe KE, Dong KC, Yu C, Bosanac I, Bustos D, Phu L, Kirkpatrick DS, Hymowitz SG, Rape M, et al (2010) K11-linked polyubiquitination in cell cycle control revealed by a K11 linkage-specific antibody. Molecular cell **39:** 477-484

McConn M, Browse J (1996) The critical requirement for linolenic acid is pollen development, not photosynthesis, in an arabidopsis mutant. The Plant cell **8:** 403-416

Meierhofer D, Wang X, Huang L, Kaiser P (2008) Quantitative analysis of global ubiquitination in HeLa cells by mass spectrometry. Journal of proteome research **7:** 4566-4576

Melchior F (2000) SUMO--nonclassical ubiquitin. Annual review of cell and developmental biology **16:** 591-626

Melotto M, Mecey C, Niu Y, Chung HS, Katsir L, Yao J, Zeng W, Thines B, Staswick P, Browse J, et al (2008) A critical role of two positively charged amino acids in the Jas motif of Arabidopsis JAZ proteins in mediating coronatine- and jasmonoyl isoleucine-dependent interactions with the COI1 F-box protein. The Plant journal : for cell and molecular biology **55:** 979-988

Memelink J, Verpoorte R, Kijne JW (2001) ORCAnization of jasmonate - responsive gene expression in alkaloid metabolism. Trends in plant science **6:** 212-219

Mergner J, Schwechheimer C (2014) The NEDD8 modification pathway in plants. Frontiers in plant science **5:** 103

Miller MJ, Scalf M, Rytz TC, Hubler SL, Smith LM, Vierstra RD (2013) Quantitative proteomics reveals factors regulating RNA biology as dynamic targets of stress-induced SUMOylation in Arabidopsis. Molecular & cellular proteomics : MCP **12:** 449-463

Morimoto M, Nishida T, Nagayama Y, Yasuda H (2003) Nedd8-modification of Cul1 is promoted by Roc1 as a Nedd8-E3 ligase and regulates its stability. Biochemical and biophysical research communications **301:** 392-398

Nakai Y, Harada A, Hashiguchi Y, Nakai M, Hayashi H (2012) Arabidopsis molybdopterin biosynthesis protein Cnx5 collaborates with the ubiquitin-like protein Urm11 in the thio-modification of tRNA. The Journal of biological chemistry **287:** 30874-30884

Nakai Y, Nakai M, Hayashi H (2008) Thio-modification of yeast cytosolic tRNA requires a ubiquitin-related system that resembles bacterial sulfur transfer systems. The Journal of biological chemistry **283:** 27469-27476

Novatchkova M, Tomanov K, Hofmann K, Stuible HP, Bachmair A (2012) Update on sumoylation: defining core components of the plant SUMO conjugation system by phylogenetic comparison. The New phytologist **195:** 23-31

Ohsumi Y (2001) Molecular dissection of autophagy: two ubiquitin-like systems. Nature reviews Molecular cell biology **2:** 211-216

Ohta M, Matsui K, Hiratsu K, Shinshi H, Ohme-Takagi M (2001) Repression domains of class II ERF transcriptional repressors share an essential motif for active repression. The Plant cell **13:** 1959-1968

Pauwels L, Barbero GF, Geerinck J, Tilleman S, Grunewald W, Perez AC, Chico JM, Bossche RV, Sewell J, Gil E, et al (2010) NINJA connects the co-repressor TOPLESS to jasmonate signalling. Nature **464:** 788-791

Pauwels L, Goossens A (2011) The JAZ proteins: a crucial interface in the jasmonate signaling cascade. The Plant cell **23:** 3089-3100

Pauwels L, Inze D, Goossens A (2009) Jasmonate-inducible gene: what does it mean? Trends in plant science **14:** 87-91

Pauwels L, Morreel K, De Witte E, Lammertyn F, Van Montagu M, Boerjan W, Inze D, Goossens A (2008) Mapping methyl jasmonate-mediated transcriptional reprogramming of metabolism and cell cycle progression in cultured Arabidopsis cells. Proceedings of the National Academy of Sciences of the United States of America **105:** 1380-1385

Peng P, Yana Z, Zhua Y, Lia J (2008) Regulation of the Arabidopsis GSK3-like Kinase BRASSINOSTEROID-INSENSITIVE 2 through Proteasome-Mediated Protein Degradation. Molecular Plant **1(2):** 338-346

Peng YJ, Shih CF, Yang JY, Tan CM, Hsu WH, Huang YP, Liao PC, Yang CH (2013) A RING-type E3 ligase controls anther dehiscence by activating the jasmonate biosynthetic pathway gene DEFECTIVE IN ANTHER DEHISCENCE1 in Arabidopsis. Plant Journal **74:** 310-327

Philipp M, John F, Ringli C (2014) The cytosolic thiouridylase CTU2 of Arabidopsis thaliana is essential for posttranscriptional thiolation of tRNAs and influences root development. BMC plant biology **14:** 109

Pieterse CMJ, Pierik R, van Wees SCM (2014) Different shades of JAZ during plant growth and defense. New Phytologist **204:** 261-264

Qi TC, Huang H, Wu DW, Yan JB, Qi YJ, Song SS, Xie DX (2014) Arabidopsis DELLA and JAZ Proteins Bind the WD-Repeat/bHLH/MYB Complex to Modulate Gibberellin and Jasmonate Signaling Synergy. The Plant cell **26:** 1118-1133

Qi TC, Song SS, Ren QC, Wu DW, Huang H, Chen Y, Fan M, Peng W, Ren CM, Xie DX (2011) The Jasmonate-ZIM-Domain Proteins Interact with the WD-Repeat/bHLH/MYB Complexes to Regulate Jasmonate-Mediated Anthocyanin Accumulation and Trichome Initiation in Arabidopsis thaliana. The Plant cell **23:** 1795-1814

Saracco SA, Miller MJ, Kurepa J, Vierstra RD (2007) Genetic analysis of SUMOylation in Arabidopsis: conjugation of SUMO1 and SUMO2 to nuclear proteins is essential. Plant physiology **145:** 119-134

Sasaki-Sekimoto Y, Jikumaru Y, Obayashi T, Saito H, Masuda S, Kamiya Y, Ohta H, Shirasu K (2013) Basic Helix-Loop-Helix Transcription Factors JASMONATE-ASSOCIATED MYC2-LIKE1 (JAM1), JAM2, and JAM3 Are Negative Regulators of Jasmonate Responses in Arabidopsis. Plant physiology **163:** 291-304

Sasaki-Sekimoto Y, Saito H, Masuda S, Shirasu K, Ohta H (2014) Comprehensive analysis of protein interactions between JAZ proteins and bHLH transcription factors that negatively regulate jasmonate signaling. Plant signaling & behavior **9:** e27639

Savchenko T, Kolla VA, Wang CQ, Nasafi Z, Hicks DR, Phadungchob B, Chehab WE, Brandizzi F, Froehlich J, Dehesh K (2014) Functional Convergence of Oxylipin and Abscisic Acid Pathways Controls Stomatal Closure in Response to Drought. Plant physiology **164:** 1151-1160

Serrano M, Parra S, Alcaraz LD, Guzman P (2006) The ATL gene family from Arabidopsis thaliana and Oryza sativa comprises a large number of putative ubiquitin ligases of the RING-H2 type. Journal of molecular evolution **62:** 434-445

Sheard LB, Tan X, Mao H, Withers J, Ben-Nissan G, Hinds TR, Kobayashi Y, Hsu FF, Sharon M, Browse J, et al (2010) Jasmonate perception by inositol-phosphate-potentiated COI1-JAZ co-receptor. Nature **468:** 400-405

Shigi N (2014) Biosynthesis and functions of sulfur modifications in tRNA. Frontiers in genetics **5:** 67

Shih CF, Hsu WH, Peng YJ, Yang CH (2014) The NAC-like gene ANTHER INDEHISCENCE FACTOR acts as a repressor that controls anther dehiscence by regulating genes in the jasmonate biosynthesis pathway in Arabidopsis. Journal of experimental botany **65:** 621-639

Shin J, Heidrich K, Sanchez-Villarreal A, Parker JE, Davis SJ (2012) TIME FOR COFFEE Represses Accumulation of the MYC2 Transcription Factor to Provide Time-of-Day Regulation of Jasmonate Signaling in Arabidopsis. The Plant cell **24:** 2470-2482

Shyu C, Figueroa P, DePew CL, Cooke TF, Sheard LB, Moreno JE, Katsir L, Zheng N, Browse J, Howe GA (2012) JAZ8 Lacks a Canonical Degron and Has an EAR Motif That Mediates Transcriptional Repression of Jasmonate Responses in Arabidopsis. The Plant cell **24:** 536-550

Smalle J, Vierstra RD (2004) The ubiquitin 26S proteasome proteolytic pathway. Annual review of plant biology **55:** 555-590

Staswick PE, Tiryaki I (2004) The oxylipin signal jasmonic acid is activated by an enzyme that conjugates it to isoleucine in Arabidopsis. The Plant cell **16:** 2117-2127

Stone SL, Callis J (2007) Ubiquitin ligases mediate growth and development by promoting protein death. Current opinion in plant biology **10:** 624-632

Stone SL, Hauksdottir H, Troy A, Herschleb J, Kraft E, Callis J (2005) Functional analysis of the RING-type ubiquitin ligase family of Arabidopsis. Plant physiology **137:** 13-30

Sullivan JA, Shirasu K, Deng XW (2003) The diverse roles of ubiquitin and the 26S proteasome in the life of plants. Nature reviews Genetics **4:** 948-958

Szemenyei H, Hannon M, Long JA (2008) TOPLESS mediates auxin-dependent transcriptional repression during Arabidopsis embryogenesis. Science **319:** 1384-1386

Tatsumi K, Sou YS, Tada N, Nakamura E, Iemura S, Natsume T, Kang SH, Chung CH, Kasahara M, Kominami E, et al (2010) A novel type of E3 ligase for the Ufm1 conjugation system. The Journal of biological chemistry **285:** 5417-5427

Thines B, Katsir L, Melotto M, Niu Y, Mandaokar A, Liu G, Nomura K, He SY, Howe GA, Browse J (2007) JAZ repressor proteins are targets of the SCF(COI1) complex during jasmonate signalling. Nature **448:** 661-665

Thireault C, Shyu C, Yoshida Y, St.Aubin B, Campos ML, Howe GA (2015) Repression of jasmonate signaling by a non-TIFY JAZ protein in Arabidopsis. The Plant Journal**:** n/a-n/a

Thomma BPHJ, Cammue BPA, Thevissen K (2002) Plant defensins. Planta **216:** 193-202

Toda Y, Tanaka M, Ogawa D, Kurata K, Kurotani K, Habu Y, Ando T, Sugimoto K, Mitsuda N, Katoh E, et al (2013) RICE SALT SENSITIVE3 Forms a Ternary Complex with JAZ and Class-C bHLH Factors and Regulates Jasmonate-Induced Gene Expression and Root Cell Elongation. The Plant cell **25:** 1709-1725

Toledo-Ortiz G, Huq E, Quail PH (2003) The Arabidopsis basic/helix-loop-helix transcription factor family. The Plant cell **15:** 1749-1770

Van der Does D, Leon-Reyes A, Koornneef A, Van Verk MC, Rodenburg N, Pauwels L, Goossens A, Korbes AP, Memelink J, Ritsema T, et al (2013) Salicylic Acid Suppresses Jasmonic Acid Signaling Downstream of SCFCOI1-JAZ by Targeting GCC Promoter Motifs via Transcription Factor ORA59. The Plant cell **25:** 744-761

Van der Veen AG, Schorpp K, Schlieker C, Buti L, Damon JR, Spooner E, Ploegh HL, Jentsch S (2011) Role of the ubiquitin-like protein Urm1 as a noncanonical lysine-directed protein modifier. Proceedings of the National Academy of Sciences of the United States of America **108:** 1763-1770

Vanholme B, Grunewald W, Bateman A, Kohchi T, Gheysen G (2007) The tify family previously known as ZIM. Trends in plant science **12:** 239-244

Vierstra RD (2009) The ubiquitin-26S proteasome system at the nexus of plant biology. Nature reviews Molecular cell biology **10:** 385-397

Vierstra RD (2012) The expanding universe of ubiquitin and ubiquitin-like modifiers. Plant physiology **160:** 2-14

Vijayan P, Shockey J, Levesque CA, Cook RJ, Browse J (1998) A role for jasmonate in pathogen defense of Arabidopsis. Proceedings of the National Academy of Sciences of the United States of America **95:** 7209-7214

Wang F, Deng XW (2011) Plant ubiquitin-proteasome pathway and its role in gibberellin signaling. Cell Res **21:** 1286-1294

Wang KLC, Yoshida H, Lurin C, Ecker JR (2004) Regulation of ethylene gas biosynthesis by the Arabidopsis ETO1 protein. Nature **428:** 945-950

Wasternack C (2007) Jasmonates: An update on biosynthesis, signal transduction and action in plant stress response, growth and development. Ann Bot-London **100:** 681-697

Wasternack C, Hause B (2013) Jasmonates: biosynthesis, perception, signal transduction and action in plant stress response, growth and development. An update to the 2007 review in Annals of Botany. Ann Bot-London **111:** 1021-1058

Westfall CS, Zubieta C, Herrmann J, Kapp U, Nanao MH, Jez JM (2012) Structural Basis for Prereceptor Modulation of Plant Hormones by GH3 Proteins. Science **336:** 1708-1711

Wickliffe KE, Williamson A, Meyer HJ, Kelly A, Rape M (2011) K11-linked ubiquitin chains as novel regulators of cell division. Trends in cell biology **21:** 656-663

Xie DX, Feys BF, James S, Nieto-Rostro M, Turner JG (1998) COI1: an Arabidopsis gene required for jasmonate-regulated defense and fertility. Science **280:** 1091-1094

Xu LH, Liu FQ, Lechner E, Genschik P, Crosby WL, Ma H, Peng W, Huang DF, Xie DX (2002) The SCFCOI1 ubiquitin-ligase complexes are required for jasmonate response in Arabidopsis. The Plant cell **14:** 1919-1935

Xu P, Duong DM, Seyfried NT, Cheng D, Xie Y, Robert J, Rush J, Hochstrasser M, Finley D, Peng J (2009) Quantitative proteomics reveals the function of unconventional ubiquitin chains in proteasomal degradation. Cell **137:** 133-145

Yan J, Li H, Li S, Yao R, Deng H, Xie Q, Xie D (2013) The Arabidopsis F-box protein CORONATINE INSENSITIVE1 is stabilized by SCFCOI1 and degraded via the 26S proteasome pathway. The Plant cell **25:** 486-498

Yan J, Zhang C, Gu M, Bai Z, Zhang W, Qi T, Cheng Z, Peng W, Luo H, Nan F, et al (2009) The Arabidopsis CORONATINE INSENSITIVE1 protein is a jasmonate receptor. The Plant cell **21:** 2220-2236

Ye HY, Du H, Tang N, Li XH, Xiong LZ (2009) Identification and expression profiling analysis of TIFY family genes involved in stress and phytohormone responses in rice. Plant molecular biology **71:** 291-305

Ye Y, Rape M (2009) Building ubiquitin chains: E2 enzymes at work. Nature reviews Molecular cell biology **10:** 755-764

Zarei A, Korbes AP, Younessi P, Montiel G, Champion A, Memelink J (2011) Two GCC boxes and AP2/ERF-domain transcription factor ORA59 in jasmonate/ethylene-mediated activation of the PDF1.2 promoter in Arabidopsis. Plant molecular biology **75:** 321-331

Zhang H, Memelink J (2009) Regulation of Secondary Metabolism by Jasmonate Hormones. *In* AE Osbourn, V Lanzotti, eds, Plant-derived Natural Products: Synthesis, Function, and Application. Springer Science

Zhang X, Wu Q, Cui S, Ren J, Qian W, Yang Y, He S, Chu J, Sun X, Yan C, et al (2015) Hijacking of the jasmonate pathway by the mycotoxin fumonisin B1 (FB1) to initiate programmed cell death in Arabidopsis is modulated by RGLG3 and RGLG4. Journal of experimental botany

Zhang X, Wu Q, Ren J, Qian WQ, He SP, Huang KW, Yu XC, Gao Y, Huang P, An CC (2012) Two Novel RING-Type Ubiquitin Ligases, RGLG3 and RGLG4, Are Essential for Jasmonate-Mediated Responses in Arabidopsis. Plant physiology **160:** 808-822

Zhao Y, Dong W, Zhang NB, Ai XH, Wang MC, Huang ZG, Xiao LT, Xia GM (2014) A Wheat Allene Oxide Cyclase Gene Enhances Salinity Tolerance via Jasmonate Signaling. Plant physiology **164:** 1068-1076

Chapter 2:
Research scope and objectives

Astrid Nagels Durand

The ubiquitin (Ub) system is involved in most, if not all, biological processes in eukaryotes. The major specificity determinants of this system are the E3 ligases, as they are responsible for target recruitment to the ubiquitination machinery. Based on the large number of E3 ligases encoded in the model plant Arabidopsis (>1500), it is unlikely that SCF^{COI1} is the only E3 ligase involved in jasmonate (JA) signalling. The aim of this research was to further investigate the connection between the Ub system and JA-signalling through identification and target characterization of novel E3 ligases involved in this pathway. In addition, we aimed to improve the methodology for specific identification and characterization of plant E3 ligase targets.

A first step to strengthen the link between JA-signalling and the Ub system, constitutes of the identification of additional E3 ligases with a putative role in JA-signalling. A bio-informatics screen will be performed, based on available transcriptomic data, to identify E3 ligases with a potential function in JA-signalling. Subsequent identification of possible ubiquitination targets of these E3s is crucial for their functional characterization. Despite the large number of E3 ligases present in plants, ubiquitination of only few proteins has been specifically associated with a certain E3. We therefore will use a specific experimental approach to identify putative E3 substrates. This approach is based on protein-interaction studies using Tandem Affinity Purification (TAP) in combination with targeted mutation of E3 ligases (see Chapter 3).

Another reason why only few E3-specific targets are known in plants is because this relationship is difficult to proof based on the currently available methods. Hence, we will set up an innovative *in vivo* platform to unambiguously validate target ubiquitination by a specific plant-derived E3 ligase using a heterologous yeast host system. To allow efficient expression of plant proteins in this system, we also need to generate a set of yeast vectors that is compatible with the -by plant researchers frequently used- Gateway cloning system (see Chapter 4).

Finally, we will extensively characterize the RING-type E3 ligases RGLG3 and RGLG4, which were reported to function in JA-signalling during the course of this PhD (Zhang et al., 2012; Zhang et al., 2015). The above mentioned TAP strategy, will allow identification of a putative target of these E3 ligases (PICOT1). Identification of PICOT1 interacting proteins will be used to investigate in which biological processes the protein is involved. This knowledge will then enable us to look into more detail at the function of PICOT1 in specific molecular processes (see Chapter 5). The function of *PICOT1* in JA-signalling (see Chapter 6) will be investigated using a reverse genetics approach, based on phenotypic characterization of plants with altered *PICOT1* expression.

REFERENCES

Zhang X, Wu Q, Cui S, Ren J, Qian W, Yang Y, He S, Chu J, Sun X, Yan C, et al (2015) Hijacking of the jasmonate pathway by the mycotoxin fumonisin B1 (FB1) to initiate programmed cell death in Arabidopsis is modulated by RGLG3 and RGLG4. Journal of experimental botany

Zhang X, Wu Q, Ren J, Qian WQ, He SP, Huang KW, Yu XC, Gao Y, Huang P, An CC (2012) Two Novel RING-Type Ubiquitin Ligases, RGLG3 and RGLG4, Are Essential for Jasmonate-Mediated Responses in Arabidopsis. Plant physiology **160:** 808-822

Chapter 3: Identification of E3 ubiquitin ligase target proteins

Astrid Nagels Durand[1], Jonas Goossens, Sabrina Iñigo, Andres Ritter, Patricia Fernandez-Calvo, Steven Maere, Geert De Jaeger, Laurens Pauwels and Alain Goossens

Aspects of this chapter are incorporated in the manuscript:

Laurens Pauwels, Andres Ritter, Astrid Nagels Durand, Jonas Goossens, Honxia Liu, Jan Geerinck, Marta Boter, Robin Vanden Bossche, Rebecca De Clercq, Kris Gevaert, Geert De Jaeger, Roberto Solano, Sophia Stone, Judy Callis and Alain Goossens. **The RING E3 ligase KEEP ON GOING regulates JAZ12 stability.** Submitted to Plant Physiology.

[1] Author contributions: bio-informatics screen analysis, cloning and mutagenesis, tandem affinity purifications, yeast two-hybrid analyses, yeast strain engineering, HUbA, data interpretation and writing.

SUMMARY

Several E3 ligases have been associated to phytohormone signalling pathways. However, only one E3 ligase (SCF^{COI1}) has a well characterized function in jasmonate (JA)-signalling. To identify new E3 ligases with a possible function in JA-signalling, we performed a transcriptomics-based bio-informatics screen. Subsequently, we looked for candidate targets of these E3 ligases by identifying proteins that can interact with them using tandem affinity purification (TAP). Direct interaction was confirmed between a number of E3 ligases and candidate targets. Finally, we developed an *in vivo* heterologous ubiquitination assay using the yeast *Saccharomyces cerevisiae* as a host. This assay was used to investigate the relationship between a heterodimeric E3 ligase (BRIZ1/2) and its candidate target protein (LARP6b). We found that LARP6b is post-translationally modified in yeast when co-expressed with BRIZ1/2.

INTRODUCTION

The ubiquitin (Ub) system has been shown to be involved in phytohormone signalling at multiple levels (Kelley and Estelle, 2012). The specificity of the system is guaranteed by target recruitment through dedicated E3 ligases. According to the sequenced *Arabidopsis* genome, more than 1,500 different E3 ligases can be assembled (Hua and Vierstra, 2011). However, SCF^{COI1} remains to date the only E3 ligase with a well characterized function in JA-signalling. The F-box component COI1 functions together with JAZ and inositol pentakisphosphate ($InsP_5$) as a three-molecule co-receptor complex for the bioactive JA-hormone (+)-7-jasmonyl-L-isoleucine (Fonseca et al., 2009; Sheard et al., 2010). Formation of the receptor complex is believed to trigger SCF^{COI1}-mediated poly-ubiquitination of JAZ proteins leading to their degradation, eventually resulting in de-repression of JA-responsive genes (Chini et al., 2007; Thines et al., 2007).

Despite the vast number of E3 ligases encoded by the Arabidopsis genome, only a few targets have been associated with a specific E3 ligase. Current approaches for the identification of ubiquitinated proteins can be divided in targeted and non-targeted approaches. Non-targeted proteomic approaches are based on affinity purification of ubiquitinated proteins followed by MS-analysis of the purified proteins. Enrichment of ubiquitinated proteins is achieved by expressing ubiquitin (Ub) with a tag (e.g. 6xHIS-Ub, Peng et al., 2003) or by making use of Ub-binding motifs attached to a resin (e.g. TUbEs, Hjerpe et al., 2009). Alternatively, the total protein content can first be digested with trypsin, which will also digest Ub leaving a di-Gly rest on the formerly ubiquitinated peptide, followed by purification with specific antibodies against this di-Gly rest. Unfortunately, Ub-related modifiers will also leave a di-Gly hallmark after trypsin digest (Udeshi et al., 2013). The main disadvantage of non-targeted approaches, however, is their inability to link a specific E3 ligase to its target. Targeted approaches, on the other hand, are low-throughput and have yielded satisfying results only sporadically.

In our group, the composition of the JA core signalling complex was studied using Tandem Affinity Purification (TAP) in Arabidopsis PSB-D cell cultures. When COI1-GS was used as bait, we could identify multiple components of the core JA-signalling pathway including JAZ12 (Pauwels *et al*., submitted). Therefore, TAP is a suitable technique to identify transient E3-target interactions (Yumimoto et al., 2012). However, once the E3 and target interact, the latter will probably be ubiquitinated and eventually degraded. Stabilization of the E3-target interaction can overcome this hazard and can be achieved by disturbing the E3-E2 interaction. In the case of F-box proteins, this could be done by simply deleting the F-box domain of the bait (Salahudeen et al., 2009). Deletion of the F-box domain of COI1 was however shown to destabilize the protein (Zhou et al., 2013) and this approach is likely not to work for COI1.

The largest group of single-subunit E3 ligases is the RING-type. Interaction with the Ub-charged E2 is mediated by the characteristic RING domain, which contains eight conserved residues (Cys or His) that together coordinate two Zn ions resulting in a conserved cross-brace tertiary structure. RING-type E3 ligases can be further classified based on the distance between the conserved metal binding residues and the number of His-residues. The interaction between RING-type E3s and corresponding E2s can be easily disturbed by mutating at least one of the metal binding residues (Stone et al., 2005) thus abolishing E3 ligase activity.

Four RING-type E3 ligases are being studied in our group because of a possible link with JA signalling: BOTRYTIS SUSCEPTIBLE 1 INTERACTOR (BOI), KEEP ON GOING (KEG) and the BRAP2 RING ZnF UBP domain-containing proteins 1 and 2 (BRIZ1 and BRIZ2). Besides sharing a conserved RING domain these E3s have very different domain structures (Figure 3-1).

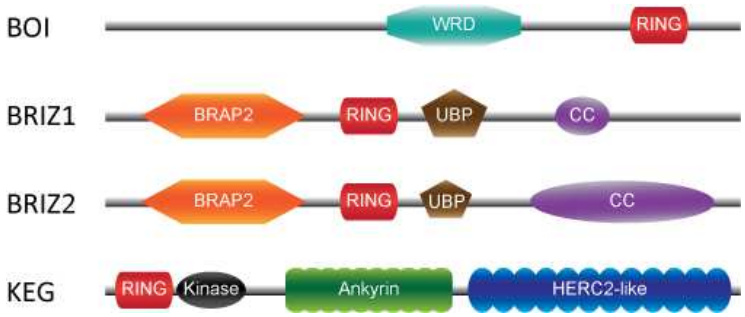

Figure 3-1. Structure of E3 ligases with putative function in JA-signalling

Structure of four RING-type E3 ligases: BOTRYTIS SUSCEPTIBLE1 INTERACTOR (BOI), BRAP2 RING ZNF UBP DOMAIN-CONTAINING PROTEINS 1 and 2 (BRIZ1 and BRIZ2) and KEEP-ON-GOING (KEG). Protein domain abbreviations: WRD, a central domain conserved in BOI and *BOI-RELATED GENES*; BRAP2, BRCA1-associated protein 2; UBP, zinc finger Ub-binding protein; CC, coiled-coil region; HERC2-like, HECT and RCC1 like.

BOI is a RING-type E3 ligase being studied in our group because it negatively regulates pathogen and stress-induced cell death, thereby contributing to plant disease resistance and abiotic stress tolerance. In addition to a C-terminal RING domain, BOI contains a central WRD domain that is essential for interaction with the MYB transcription factor BOTRYTIS SUSCEPTIBLE1 (BOS1/MYB108). BOS1 has been shown to be a ubiquitination target of BOI *in vitro* (Luo et al., 2010). Interestingly, the pathway leading to disease or stress-induced cell death that is regulated by BOI-BOS1 is, at least partially, controlled by JA (Mengiste et al., 2003; Luo et al., 2010). BOI and its homologs BOI-RELATED GENE1-3 (BRG1-3) also negatively regulate GA-responses through association with DELLA proteins, although DELLA protein stability was not affected in quadruple *boibrg1-3* KO mutants when compared to WT plants. Instead, the authors showed BOI can bind a subset of GA responsive gene promoters and repress their expression levels (Park et al., 2013).

Two other RING-type E3 ligases that caught our attention are BRIZ1 and BRIZ2. These E3s are essential for normal seed germination and post-germination growth in *Arabidopsis.* Both proteins are closely related and share four common domains with the mammalian BRCA1 Associated Protein 2 (BRAP2): a BRAP2-domain, a RING domain, a zinc finger (ZnF) Ub-binding

protein (UBP) domain and a coiled-coil (CC) region. BRIZ1 and BRIZ2 were shown to form dimers through their CC region with preference for assembly into hetero-dimers. Both proteins showed Ub ligase activity *in vitro*, which was dependent on the integrity of their RING domain, but only BRIZ2 could bind Ub *in vitro.* Despite their similarity, loss of function mutations in either *BRIZ1* or *BRIZ2* lead to defects in germination and post-germination arrest, implying BRIZ1 and BRIZ2 are both essential for these processes and do not function redundantly but rather function together in the same complex (Hsia and Callis, 2010). The targets of BRIZ1 and BRIZ2 are currently unknown. Nevertheless, a genetic interaction has been observed with ABA signalling (Hsia and Callis, in preparation). The ABA and JA signalling pathways share some similarities. For example, the co-repressor protein NINJA is related to the family of ABI5 binding proteins, that play a role in ABA signalling by regulating the TF ABI5. In addition, our group recently characterized the specific interaction between a JAZ protein and an E3 ligase involved in ABA signalling (see below). Because of this parallel structure of ABA and JA signalling pathways, the BRIZ E3 ligases might also influence JA signalling.

A fourth and last RING-type E3 ligase of interest to our research group is KEG. *KEG* encodes a 178kDa-large protein assembled from the combination of four different types of functional domains. KEG thanks its dual enzymatic activity to the presence of an N-terminal RING domain that accounts for KEG's E3-ligase activity, followed by a serine/threonine protein kinase domain. Large protein-protein interaction platforms offer docking sites for KEG substrates and consist of nine consecutive ankyrin repeats followed by twelve consecutive repeats of a HERC2-like protein domain (Figure 3-1). In the absence of ABA, KEG interacts with and ubiquitinates the transcription factor ABSCISIC ACID INSENSITIVE5 (ABI5) in the cytosol, thereby mediating ABI5 proteasome dependent degradation (Stone et al., 2006; Liu and Stone, 2013). The ABI5 related TFs ABF1 and ABF3 can interact with ABI5 and like ABI5, they are unstable proteins that accumulate in the presence of ABA. ABF1 and ABF3 are degraded *in vivo* in a proteasome-dependent manner and were also shown to be ubiquitinated *in vitro* by KEG (Chen et al., 2013). ABI5, ABF1 and ABF3 positively regulate ABA-responses including ABA-induced post-germinative growth arrest under adverse environmental conditions (Stone et al., 2006; Chen et al., 2013; Liu and Stone, 2013).

Seedlings carrying loss of function mutations in *KEG* (*keg-1*, *keg-2* and *keg-3,* here collectively referred to as keg^{KO}) arrest growth soon after germination. This seedling-lethal phenotype is mediated, at least partly by ABA-hypersensitivity in these mutants (Stone et al., 2006). Upon treatment of plants with ABA, KEG preferentially self-ubiquitinates and, as a result, is degraded by the 26S proteasome. KEG is also phosphorylated *in vivo* but the degree of phosphorylation does not differ before or after ABA treatment. Nevertheless, (auto-) phosphorylation is a prerequisite for KEG self-ubiquitination, and the specific site of phosphorylation is thought to switch the E3 ligase activity of KEG towards itself or towards alternative targets such as ABI5, ABF1 and ABF3 (Liu and Stone, 2010). In keg^{KO} seedlings,

ABI5/ABF1/ABF3 accumulate even in the absence of ABA, blocking post-germinative growth under normal growth conditions. Loss of function mutations in ABI5, ABF1 or ABF3 can partially complement the *keg*^{KO} phenotype (Stone et al., 2006; Chen et al., 2013). However, restoring ABA-sensitivity in *keg*^{KO} seedlings does not complement all mutant phenotypes. Indeed, KEG has been shown to play additional roles in the plant cell.

In 2008, a new allele of *KEG* was identified (*keg-4*) during a screen for suppression of the *enhanced disease resistance1* (*edr1*) mutation. This mutation confers resistance to powdery mildew, to drought-induced growth inhibition and to ethylene-induced senescence. In addition, *edr1* mutants are hypersensitive to ABA. All these phenotypes were suppressed by the *keg-4* mutation which carries a missense mutation (G1144S) in one of the HERC2-like repeats of KEG. Surprisingly, *keg-4* seedlings do not show hypersensitivity to ABA nor glucose, as was previously described for *keg*^{KO} alleles, but supressed the ABA hypersensitivity of the *edr1* mutant (Wawrzynska et al., 2008). Further studies showed that the HERC2-like repeats of KEG were essential for its interaction with EDR1 in the trans-golgi network/early endosomes (TGN/EE). In plants, the TGN and EE cannot be distinguished from each other. The TGN/EE is necessary for protein sorting to the vacuole and the plasma membrane as well as for endocytic trafficking (Gu and Innes, 2011). KEG was shown to be required for transport of certain plasma membrane proteins to the vacuole through ARA6-associated multi-vesicular bodies that originated from the TGN/EE. *Keg*^{KO} seedlings develop defects in vacuole formation, which in turn leads to defects in cell expansion. These defects are reflected in the smaller size of *keg*^{KO} cells, together with alterations in the cell wall structure. Finally, KEG is also required for apoplastic protein secretion. Remarkably, during powdery mildew infection, KEG localizes at fungal penetration sites where it seems to be degraded, emphasizing KEG is involved in regulating responses to both biotic and abiotic stress (Gu and Innes, 2012).

Recently, we found JAZ12 to interact with KEG. JAZ12 belongs to the JAZ family that consists out of 13 members in Arabidopsis. The level of redundancy or specificity amongst these members is currently not well understood. In addition to KEG, JAZ12 also interacted during TAP experiments with SCF^{COI1} components, matching with observed *in vivo* ubiquitination and with rapid degradation after treatment with JA. JAZ12, encoded by the most highly expressed *JAZ* gene, was further characterized in our group. This member of the JAZ family interacted with the transcription factors MYC2, MYC3 and MYC4 *in vivo* and repressed MYC2 activity, two properties characteristic for members of the this protein family. To study the functional role of the interaction between JAZ12 and KEG, we circumvented the lethality of *keg* mutants by knocking down *KEG* using an amiRNA approach. Both ABA treatment and knock down of *KEG* led to a decrease in JAZ12 protein levels. Correspondingly, *KEG* overexpression was capable of partially inhibiting COI1-mediated JAZ12 degradation. Our results provide additional evidence for KEG as an important factor in plant hormone signalling and a positive regulator of JAZ12 stability (Pauwels *et al*., submitted).

Here, we used a bio-informatics approach based on existing transcriptomics data to identify additional E3 ligases with a possible role in JA-signalling resulting in a list of 22 candidate E3 ligases. A selected group of candidate E3 ligases, together with E3 ligases that are already being studied in our group, were subsequently mutated to inactivate their intrinsic E3 ligase activity and used as baits in tandem affinity purification (TAP) experiments. Mass spectrometry (MS)-based identification of co-purifying proteins resulted in identification of co-purifying proteins for a number of E3 ligases. These E3 ligase interacting proteins constitute a list of potential Ub-targets for the respective E3s. Finally, we developed a novel heterologous yeast ubiquitination assay (HUbA) to further investigate plant E3-target couples. The BRIZ1/2 interacting protein LARP6b was found to be post-translationally modified when co-expressed with the respective E3 ligases in yeast.

RESULTS AND DISCUSSION

Putative E3s involved in JA-signalling

The E3 ligase SCF^{COI1} was the only E3 ligase complex reported to play a role in JA-signalling at the start of this project. To identify additional E3 ligases that could be involved in JA-signalling, we performed a bio-informatics screen. This screen was based on transcriptome data, which due to the rise of transcript-profiling technologies (e.g. micro-array experiments) is readily available within the research community. First, co-expression networks were established based on transcriptomics data. The 'guilt by association' principle states that differentially co-expressed genes are often involved in similar or related biological processes. This principle can therefore be used for new functional annotation of proteins based on the function of their neighbours in the network.

We started our screen based on four established sampling compendia. Three of these compendia contain expression data obtained in perturbational experiments, where a treatment or growth condition was compared to a control condition, and were related to cell-cycle processes, plant Environmental Ontology (EO) term 'methyl jasmonate' or EO term 'abscisic acid regimen', respectively (further referred to as 'CC', 'MeJA' and 'ABA' compendia). The fourth compendium contains expression data of three different wild-type Arabidopsis accessions that were grown under the same macroscopic conditions, in six different labs. Accession, lab and lab x accession effects were removed from this dataset and the residual expression variation was retained. This sampling compendium is referred to as "Agronomics residuals" compendium and has proven to be a valuable tool to infer the function of yet uncharacterized genes in a certain process, including the JA-response (Massonnet et al., 2010; Bhosale et al., 2013).

ENIGMA (Expression Network Inference and Global Module Analysis) was used on each of these compendia to assemble four networks of co-regulated differentially expressed genes, i.e. genes whose expression is regulated similarly over a subset of perturbations (Maere et al., 2008). Finally, the obtained networks of differentially co-expressed genes were subsequently analysed with the Cytoscape plug-in PiNGO (Smoot et al., 2011). PiNGO is a tool that can be used to screen biological networks for candidate genes, allowing the prediction of their functional annotation, based on the annotation of their neighbours. More precisely, we looked for Ub E3 ligases that are co-expressed with genes involved in JA-signalling. This approach targeted the identification of E3 ligases involved in secondary or tertiary JA-responses, as E3 ligases involved in primary JA-responses are probably not transcriptionally regulated by JA, as is the case for COI1. This resulted in a list of 22 E3 ligase encoding genes with a potential function in JA-signalling (p-value<0.05, Table 3-1). Additionally, substantial overlap between the genes identified over the four different networks (Figure 3-2) underscores the robustness of this method.

The list of 22 candidate genes was further narrowed down based on literature mining and manual curation. Characteristics taken into account were, amongst others, the availability of Arabidopsis T-DNA insertion lines in the gene and the amount of redundancy expected due to the presence of homologous genes. Homologous genes appearing as tandem repeats on the genome were also discarded due to the inability to make double knock-out lines. We preferentially selected genes with unknown function. Accordingly, genes being currently investigated by other research groups were also discarded. As RING-type E3 ligases can easily be made inactive we preferentially retained RING-type E3 ligases in our final list of candidates (Table 3-1).

Table 3-1. E3 ligases with a putative role in JA-signalling

AGI	Name	E3-type	Compendium
At1g08050	AE31*	RING	CC
At3g05200	ATL6	RING	CC, ABA, Agronomics residuals
At5g42200	ATL23*	RING	Agronomics residuals
At5g27420	ATL31/CNI1	RING	CC, JA, Agronomics residuals
At1g66160	CMPG1	U-box	CC, ABA
At5g64660	CMPG2	U-box	CC, ABA, JA, Agronomics residuals
At3g07360	PUB9	U-box	CC
At3g46510	PUB13	U-box	Agronomics residuals
At1g60190	PUB19	U-box	CC, ABA
At3g52450	PUB22	U-box	CC
At2g35930	PUB23	U-box	CC, ABA
At3g11840	PUB24	U-box	CC, ABA, JA
At3g19380	PUB25	U-box	CC
At5g10380	ATL55/RING1*	RING	CC, ABA
At2g22010	RKP	RING	CC
At4g03510	RMA1	RING	CC
At3g47990	SIS3*	RING	Agronomics residuals
At1g21410	SKP2A	F-box	CC
At1g77000	SKP2B	F-box	CC
At5g61560		U-box	ABA
At3g49060		U-box	Agronomics residuals
At5g67340		U-box	JA

Asterisks indicate E3 ligases that were selected for further characterization.

Our screen identified several members of the ARABIDOPSIS TOXICOS EN LEVADURA (ATL) family of H2-type RING E3 ligases as being putatively involved in JA-signalling. The ATL family comprises 80 members in *Arabidopsis* and is characterized by a conserved Proline residue within the RING H2 motif. In addition, ATL family members have a conserved N-terminal hydrophobic stretch and a GLD-motif which is located between the hydrophobic stretch and the C-terminal RING domain. Several of these genes have been shown to be induced by fungal or bacterial elicitors, including ATL6 and ATL31 which were also identified in our screen (Maekawa et al., 2012). The tomato ortholog of Arabidopsis ATL6 (LeATL6) was shown to possess E3 ligase activity and is also thought to contribute to JA-mediated elicitor-activated defence responses triggered by the bio-control agent *Pythium oligandrum* (Hondo

et al., 2007). In addition, at least one (ATL43) shows altered responses to ABA treatment (Serrano et al., 2006).

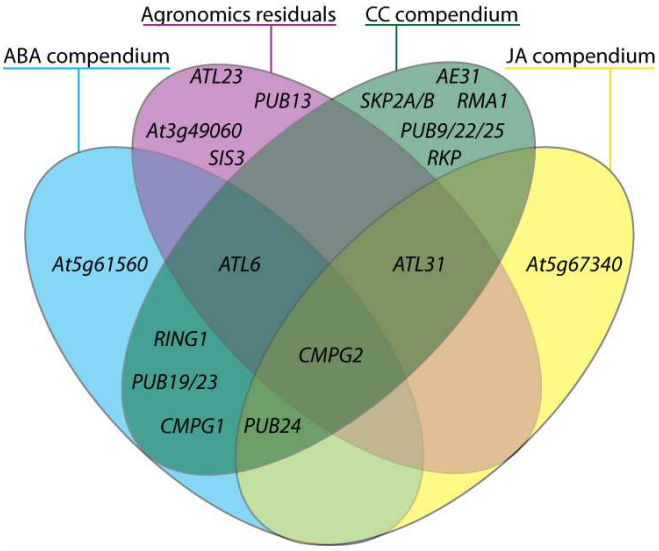

Figure 3-2. E3-ligases identified using PiNGO.

Numbers indicate the identified number of genes encoding E3 ligases that are co-regulated with JA-responsive genes ($p<0.05$) in the four different ENIGMA-generated networks.

Two members of the ATL family were chosen for further analysis: ATL23 and ATL55/RING1. RING1 was previously shown to possess E3 ligase activity and this activity is dependent on the integrity of the RING-domain. It is a relatively unstable protein whose expression is up-regulated after treatment with fungal elicitors or after pathogen infection. The resulting up-regulation of RING1 expression and stability leads to the onset of programmed cell death. Because RING1 associates with lipid rafts in the plasma membrane, it is thought to function as a signalling molecule to trigger programmed cell death, therefore contributing to plant defence against biotic stress (Lin et al., 2008).

A third E3 ligase selected for further studies is *SUGAR-INSENSITIVE 3* (*SIS3*). *SIS3* was first identified in a screen for mutants resistant to the detrimental effects of high exogenous sugar levels on early seedling development. While most WT seeds grown on medium supplemented with high levels of glucose or sucrose arrest growth early after germination, *sis3* KO seeds often develop into seedlings with relatively normal shoot systems. SIS3 was therefore suggested to have a positive regulatory role on sugar signalling during early seedling development (Huang et al., 2010). SIS3 possesses E3-ligase activity *in vitro* and this activity is dependent on the presence of a H2-type RING domain (Stone et al., 2005; Huang et al., 2010). The target protein(s) for ubiquitination by SIS3 remain unknown. Although germination has been linked to ABA and GA signalling, *sis3* KO seedlings do not exhibit altered ABA or GA-responses when compared to WT, indicating SIS3 affects germination through a signalling pathway differing from ABA or GA signalling (Huang et al., 2010). Unfortunately, the sensitivity of *sis3* KO seeds to the inhibitory effect of JA on germination was not investigated during this study.

Finally, a yet uncharacterized E3 ligase identified in our screen, which we named *Astrid's E3 ligase-1* (*AE31*, At1g08050), was also selected for further characterization. *AE31* encodes a 641 amino-acid (AA) long protein with an N-terminal H2-type RING-domain (AA68-113, Stone et al., 2005). In addition, AE31 contains both a von Willebrand Factor type A domain (AA204-AA376, vWA) and a vWA / Hedgehog protein intein-like domain (551-623, Vwaint, Burglin, 2008). While the function of the Vwaint-domain is unknown, the vWA-domain is thought to function as a protein-protein interaction platform. Although vWA-domain proteins appeared early during evolution and were originally intracellular proteins, most vWA-containing proteins in humans are extracellular. Indeed, the domain is found in various blood plasma proteins and mutations lead to a number of known human diseases. Remarkably, in *Arabidopsis* only one fifth of the 25 vWA-domain proteins are predicted to be localized outside the cell. Finally, thirteen of the predicted intracellular vWA-proteins also contain a RING-domain. Proteins that have this domain architecture include the RING Ligase family that contains five members in Arabidopsis (*RGLG1-5*) and is characterized by an additional RING domain C-terminal of the vWA domain. The remaining eight proteins contain an N-terminal RING-domain in addition to the vWA domain. Four members have been involved in the gravitropic response (WAV3, WAVH1-2 and EDA40) while the remaining four (including AE31) have not been characterized yet and contain a metal ion binding motif in their vWA domain (Whittaker and Hynes, 2002).

Differential Tandem Affinity Purification for the identification of E3 targets

Identification of E3 ligase substrates is essential to unravel the biological function or contribution of an E3 ligase to a process of interest, in our case the JA-signalling pathway. We therefore sought to identify targets of the E3 ligases selected from our bio-informatics screen, or of E3 ligases that were already being studied in our group due to their possible role in JA-signalling. In first instance, we looked for proteins interacting with the respective E3 ligase, as interaction with the E3 is required to be a candidate target.

In contrast to stable protein-protein interactions, the interaction of an E3-ligase with its target is thought to be transient, as ubiquitination in most cases will lead to recognition of the substrate by the proteasomal degradation machinery, eventually leading to the degradation of the target. Our group previously showed TAP is a suitable technique to identify both stable and transient protein-protein interactions and can be used to identify targets of E3 ligases. Indeed, JAZ was co-purified with SCF^{COI1} when COI1 was used as bait in cell cultures (Pauwels *et al*., submitted). For this reason, TAP was chosen to search for proteins that interact with the E3 ligases of interest, which then constitute putative targets of these E3 ligases.

To increase our chances to identify E3 ligase targets two modifications were introduced in bait proteins. First, mutations in the RING-domain of baits were introduced (referred to as mRING-variants) to avoid ubiquitination and subsequent degradation of target proteins during the course of the purification procedure. As mentioned earlier, the E3 ligase's main function is to bring the target and the Ub-charged E2 in close proximity to facilitate Ub-transfer from E2 to target. Mutation of at least one of the eight conserved metal-binding residues present in the RING-domain interferes with the formation of the typical cross-brace structure of the RING-domain, which is necessary to interact with the E2 conjugase. As a result, ubiquitination of the target protein following interaction with the corresponding mutated E3 ligase is prevented and enrichment of the target is achieved. In addition, disruption of the E3-E2 interaction will also lead to stabilization of the E3 ligase due to diminished auto-ubiquitination activity. A second modification was made to baits that were predicted to be localized at membranes, which could be the case for E3 ligases with a predicted trans-membrane domain. In that case, the trans-membrane domain was removed (referred to as dTM-variants) to avoid loss of the bait protein during protein extraction caused by reduced solubility due to the hydrophobic character of the trans-membrane domain.

The CDS of respective baits was fused carboxy(C) or amino(N) terminally to a TAP-tag. The GS TAP-tag was chosen as it has been previously shown to be superior in our system. This tag consists of two immunoglobulin G-binding domains of Protein G, combined with a streptavidin binding peptide, separated by a specific Tobacco Etch Virus (TEV) protease cleavage site (Burckstummer et al., 2006; Van Leene et al., 2008). During the course of this project, an improved version of this tag, where the TEV cleavage site was replaced by a double Rhinovirus3C protease cleavage site (GSrh, Van Leene et al., 2015), became available and was implemented in our experiments. The TAP-tagged bait was expressed in *Arabidopsis* PSB-D cells under a constitutive cauliflower mosaic virus 35S promoter (pCaMV35S). After expression of the bait was verified in cell cultures using Western Blot, purifications were performed both with WT and altered E3 ligases as baits and the results of TAP experiments are shown in Table 3-2.

A dozen variations of four E3 ligases identified during our bio-informatics screen were used as baits for TAP purifications, as described in Table 3-2. Unfortunately, SIS3 and BOI could not be expressed in our system to a level detectable on immunoblots when expressed as a TAP-tagged fusion in cell cultures. Our research on these two E3 ligases was therefore discontinued. Also, no RING1 interacting proteins could be identified yet, two constructs remain to be tested. When a mRING version of AE31 was used as bait, SRPK4 (SR PROTEIN SPECIFIC KINASE 4), co-purified with AE31mRING in all TAPs performed (Table 3-2, Supplementary File S1). SRPK4 was shown to interact and phosphorylate 12 Ser/Arg-rich (SR) splicing factors *in vitro*, implicating the kinase in RNA metabolism (de la Fuente van Bentem et al., 2006).

Several proteins could be co-purified with ATL23 when a specific variant was used (Table 3-2, Supplementary File S1). This ATL variant consisted of a truncated mRING bait where the first 54 amino-acids that constitute the hydrophobic stretch, typically found in ATL family proteins, were removed. *NIT1* and *NIT2* encode two nitrilases that are involved in auxin biosynthesis (Bartel and Fink, 1994) while *ACX2* encodes an acyl-CoA oxidase involved in peroxisomal oxidation and JA biosynthesis (Dave et al., 2011). *ERMO2/SEC24B* encodes a coat protein complex II (COPII) vesicle coat subunit involved in endoplasmic reticulum (ER)-to-Golgi trafficking in the early secretory pathway (Qu et al., 2014). ERMO2/SEC24B and SEC24C

Table 3-2. Summary of E3 ligase-interactors identified in TAP experiments

Bait	Construct	Alteration	TAP-tag	Expression	Interactors	Name	Score	
							-JA	+JA
RING1	FL	none	C-GSrh	Yes	No			
			N-GS	Yes	No			
	dTM	Δ1-62	C-GSrh	Yes	N/A			
			N-GSrh	No				
	mRING	C135A	C-GSrh	Yes	No			
		C138A	N-GSrh	No				
	dTMmRING	Δ1-62	C-GSrh	Yes	No			
		C135A C138A	N-GSrh	Yes	N/A			
ATL23	FL	none	C-GS	Yes	N/A			
			N-GS	No				
	dTM	Δ1-54	C-GSrh	No				
			N-GSrh	No				
	mRING	C104A	C-GSrh	Yes	No			
		C107A	N-GSrh	No				
	dTMmRING	Δ1-54	C-GSrh	Yes	AT5G65110	ACX2	1/1	1/1
		C104A			AT3G07100	ERMO2	1/1	1/1
		C107A			AT5G51970	SDH	1/1	1/1
					AT1G09300	unknown	1/1	1/1
					AT1G47128	RD21A	1/1	1/1
					AT3G09350*	FES1A*	1/1	0/1
					AT3G44310*	NIT1*	1/1	1/1
					AT3G44300*	NIT2*	0/1	1/1
					AT1G07750*	unknown*	1/1	1/1
			N-GSrh	No				
AE31	FL	none	C-GSrh	No				
			N-GSrh	Yes	No			
	mRING	C109A	C-GSrh	Yes	AT3G53030	SRPK4	2/2	2/2
		C112A	N-GSrh	No				
SIS3	FL	none	C-GSrh	No				
			N-GSrh	No				
	mRING	H258A	C-GSrh	No				
		C261A	N-GSrh	No				
BOI	FL	None	C-GSrh	No				
			N-GSrh	No				
	mRING	C275A	C-GSrh	No				
		C278A	N-GSrh	No				

FL, Full length; mRING, protein with mutated RING domain; dTM, protein without transmembrane domain; N/A, TAP not performed; *, possible background protein. The score indicates the incidence of protein identification out of the total number of experiments performed.

function redundantly during the development of plant reproductive cells (Tanaka et al., 2013). *FES1A* encodes a Hsp70-binding protein that prevents cytosolic Hsp70 degradation, thereby negatively regulating heat-shock transcription (Zhang et al., 2010). SDH (sorbitol dehydrogenase) oxidizes sorbitol, which functions as a means to translocate photo-assimilated carbon from source to sink, to metabolically accessible fructose (Aguayo et al., 2013). *AT1G09300* encodes a metallopeptidase M24 family protein of yet unknown function (The Arabidopsis Information Resource, TAIR, Lamesch et al., 2012). *RD21A* encodes a vacuole and ER-body localized protease that has been shown to provide immunity to the necrotrophic pathogen *Botrytis cinerea* and to be involved in the onset of senescence and the resistance to several biotic and abiotic stresses (Gu et al., 2012; Shindo et al., 2012; Lampl et al., 2013). *AT1G07750* encodes a protein of unknown function, characterized by the presence of an 11-S seed storage protein domain and an RmcI-like cupin domain (TAIR, Lamesch et al., 2012).

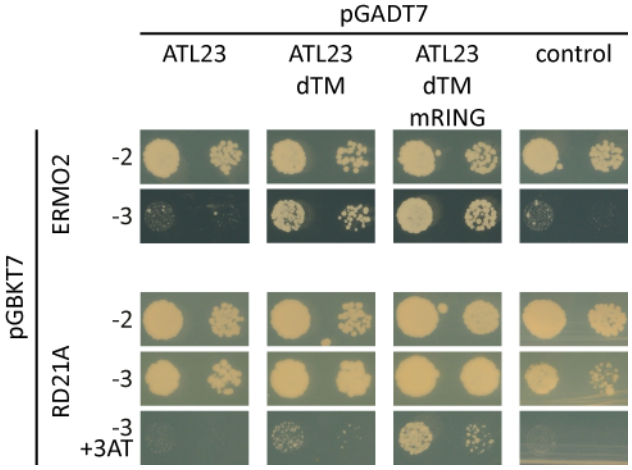

Figure 3-3. ERMO2 and RD21A interact directly with ATL23.

Y2H-assay of ATL23 interactions with ERMO2 and RD21A. ATL23-variants included ATL23 without trans-membrane domain (dTM) and/or with a mutated RING domain (mRING). Transformed yeasts were spotted in 10-fold and 100-fold dilutions on control medium (-2), selective medium (-3) or selective medium containing 500 µM 3-Amino-1,2,4-triazole (-3 +3AT).

To discriminate whether proteins identified in a complex with ATL23 are interacting directly or indirectly with the bait, yeast two-hybrid (Y2H) assays were performed between ATL23 or ATL23-variants and the interacting proteins. Only ERMO2 and RD21A were able to interact with ATL23 after deletion of its trans-membrane domain (ATL23dTM, Figure 3-3). Because RD21A fused to the DNA-binding domain of GAL4 was able to activate transcription of the reporter gene *HIS3* in the absence of additional proteins, a phenomenon referred to as auto-activation, the experiment was repeated in the presence of 3-amino-1,2,4-triazole (3AT). This compound acts as a quantitative inhibitor of the HIS3 reporter and can therefore be used to discriminate between a false-positive result due to low HIS3 activity caused by auto-activation or a true-positive result caused by high-affinity interaction between bait and prey proteins. In the presence of 500 µM 3AT, auto-activation was inhibited while the interaction between RD21A and ATL23dTM was still clearly positive. Additionally, mutations in the RING

domain of ATL23dTM (ATL23dTMmRING) seemed to positively affect the degree of interaction, with both ERMO2 and RD21A, which we also encountered when testing other E3 ligase-substrate interactions via this method. ERMO2 and RD21A therefore constitute two candidate targets of the E3 ligase ATL23. The relationship between ATL23 and ERMO2/RD21A is being further studied within our group and will not be discussed in this PhD thesis.

KEG interacts with a diverse set of proteins

To further unravel the role of KEG in JA signalling, we tried to identify new unknown (ubiquitination) substrates of KEG in a TAP experiment. We used N-terminally TAP-tagged KEGmRING (C29A, H31A, and C34A) as bait. The cultures were treated with 50 µM JA or a mock solution (100% ethanol) for 1 minute before harvesting. Proteins that co-purified with KEGmRING are shown in Table 3-3 (Supplementary File S1). Note that there was no overlap with the KEG-interacting proteins identified previously in our group when truncated versions of KEG were used as bait (Geerinck 2010, PhD thesis). However, neither EDR1 nor any of the previously identified ubiquitination targets of KEG were retrieved in the experiment using a truncated protein.

Table 3-3. Summary of GSrh-KEGmRING interacting proteins identified in TAP experiments.

Interactors	Name	Score /2	
		-JA	+JA
At1g05460	SDE3	0	2
At3g55620	eIF6A	0	2
At5g21326	CIPK26	0	2
At2g42810	PP5*	2	2
At4g29040	RPT2a*	2	2
At5g37130	Unknown*	2	2
At1g23900	γ-ADAPTIN1*	1	1
At1g60850	RPAC42*	1	2
At1g60620	RPAC43*	0	1

* Possible background protein. The score indicates the incidence of protein identification out of two experiments.

Four KEG interacting proteins could only be identified in JA-treated cells: SDE3, eIF6A, CIPK26 and RPAC43. Silencing Defective 3 (SDE3), facilitates the onset/maintenance of amplified cytoplasmic post-transcriptional gene silencing (PTGS) at specific transgenic and endogenous loci. Additionally, SDE3 might have a dual function where PTGS might provide an initial trigger for transition to TGS (Garcia et al., 2012). Remarkably, RPT2a which was also identified as a KEG-interacting protein, negatively regulates TGS at transgenes and endogenous loci through DNA methylation of target promoters (Sako et al., 2012). RPAC43 is an RNA polymerase subunit. RPAC42 and RPAC43 are orthologs of yeast RNA polymerase subunit AC40 of RNA Polymerase I and III, two of the three nuclear DNA-dependent RNA polymerases present in this organism (Ulmasov et al., 1995).

The eukaryotic Initiation Factor 6 protein eIF6A, which is involved in translation initiation, was also identified as a KEG interacting protein in the presence of JA. During mammalian ribosome biogenesis, eIF6 phosphorylation by activated protein kinase C (PKC) is mediated by interaction of both proteins with Receptor for Activated Protein Kinase 1 (RACK1).This contributes to 80S ribosome assembly and leads to initiation of translation elongation. eIF6A interacts with all Arabidopsis RACK1-orthologs *in vivo* and loss of function mutations in eIF6A cause an embryo-lethal phenotype. Remarkably, the expression of both RACK1 and eIF6A is negatively regulated by ABA. Since eIF6A was only co-purified with KEG in the presence of JA, interaction of KEG with eIF6A may influence the rate of translation elongation initiation at the post-transcriptional level depending on the presence of JA and/or ABA, as KEG was shown to self-ubiquitinate in the presence of ABA (Liu and Stone, 2010). eIF6A might therefore constitute a point of cross-talk for JA and ABA hormone signalling pathways. Further research is needed to verify if the KEG-eIF6A interaction is direct and depends on JA, and if so, what the biological outcome is.

Calcineurin B-like Interacting Protein Kinase 26 (CIPK26) was the fourth KEG-interacting protein that could only be identified in JA-treated cells via TAP. The group of Sophia Stone picked up the same protein in a Y2H screen using KEG as bait (Lyzenga et al., 2013). The interaction was localized to the cytoplasm and the TGN/EE. CIPK26 was proposed to be a ubiquitination target of KEG, as protein stability was influenced by KEG expression levels and by proteasomal activity. CIPK26 interacted with the protein phosphatases ABA Insensitive 1 and 2 (ABI1 and ABI2), both negative regulators of ABA-responses. In addition, CIPK26 also interacted with and was able to phosphorylate the transcription factor ABI5 thereby positively regulating ABA responses. KEG thus negatively regulates ABA responses by targeting CIPK26 and ABI5, both positive regulators of ABA signalling, for proteasomal degradation in the absence of the hormone (Lyzenga et al., 2013). Because we only identified CIPK26 via TAP of JA-treated cell cultures, our results slightly contradict above mentioned findings. Therefore, further investigation of the JA-dependency of the KEG-CIPK26 interaction should be carried out. It is worth mentioning, however, that in general, a higher number of interactors were identified in JA-treated cells than in mock-treated cells. It cannot be excluded that this difference could be due to an effect of JA on the stability of the bait rather than on its functionality.

Taken together, we identified a number of proteins that interacted with KEG *in planta*, among which the proposed E3 target CIPK26 (Lyzenga et al., 2013). Unfortunately, we did not identify additional proteins with a probable role in the JA-signalling pathway besides JAZ12. Therefore, further work on KEG during this PhD was discontinued.

LARP6b is a candidate target of the BRIZ1/2 E3 ligase complex

TAP with BRIZ2 or BRIZ2mRING (C186A, H188A) as bait was performed in an attempt to identify candidate targets of this E3 ligase (Table 3-4, Supplementary File S1). The E3 ligases BRIZ1 and BRIZ2 were previously reported to preferentially occur as heterodimeric complexes (Hsia and Callis, 2010). We were able to confirm the occurrence of BRIZ1 and BRIZ2 in biologically relevant complexes via TAP.

As expected, the introduction of mRING mutations in BRIZ2 allowed us to identify at least one additional interacting protein: the La-related protein 6b (LARP6b, Figure 3-4A). The La-motif was first identified in the Lupus auto-antigen (La) protein. Genuine La-proteins are RNA-binding proteins that function in the metabolism of nascent RNA Polymerase III transcripts or modulate the translation of certain mRNAs (Bayfield et al., 2010). Accordingly, they contain two RNA recognition motifs (RRMs), one of them immediately following the La-motif. Although La-related proteins (LARPs) do not have this classical La-RRM1-RRM2 organization, LARP6b has a conserved region at the place of RRM1 that is also predicted to adopt an RRM-like fold. In addition, the C-terminal stretch of the three LARP6 proteins present in Arabidopsis is highly conserved and shows homology to a motif present at the C-terminal end of Cold-shock Response Protein 1 (CSP1) from various animals, this motif is therefore called the La and S1 associated (LSA) motif (Bousquet-Antonelli and Deragon, 2009).

Table 3-4. Proteins co-purified with BRIZ2 in TAP experiments

Bait	Construct	Alteration	TAP-tag	Expression	Interactors	Name	Score /2
BRIZ2	FL	none	N-GS	Yes	AT2G42160	BRIZ1	2
	mRING	C186A	N-GS	Yes	AT2G42160	BRIZ1	2
		H188A			AT2G43970	LARP6b	2

FL, Full length, mRING, protein with mutated RING domain. The score indicates the incidence of protein identification out of two experiments.

In order for LARP6b to be a substrate of BRIZ1/2, direct interaction was assessed in a Y2H assay (Figure 3-4B). Due to the functional conservation of the RING domain in both yeasts and plants, heterologous E3 ligases expressed in yeast are thought to associate with the yeast ubiquitination machinery. Therefore, when the E3 ligase interacts with its substrate during Y2H, the substrate will probably be degraded, causing only very transient assembly of the GAL4 transcription factor, which might not be enough for the transcriptional activation of the reporter gene. Indeed, LARP6b interaction with full length BRIZ2 could only be observed when the mRING mutations were present in BRIZ2.

Truncated constructs of BRIZ1 and BRIZ2 were used to determine which region is responsible for LARP6b interaction. A construct comprising the BRAP2-domain and the RING-domain (BRIZ-BR) was sufficient for interaction of both E3s with LARP6b in yeast (Figure 3-4B). We also confirmed that a truncation containing only the coiled coil region of BRIZ1 (BRIZ1-C) is essential and sufficient for interaction with BRIZ2 (Hsia and Callis, 2010, Figure 3-4B).

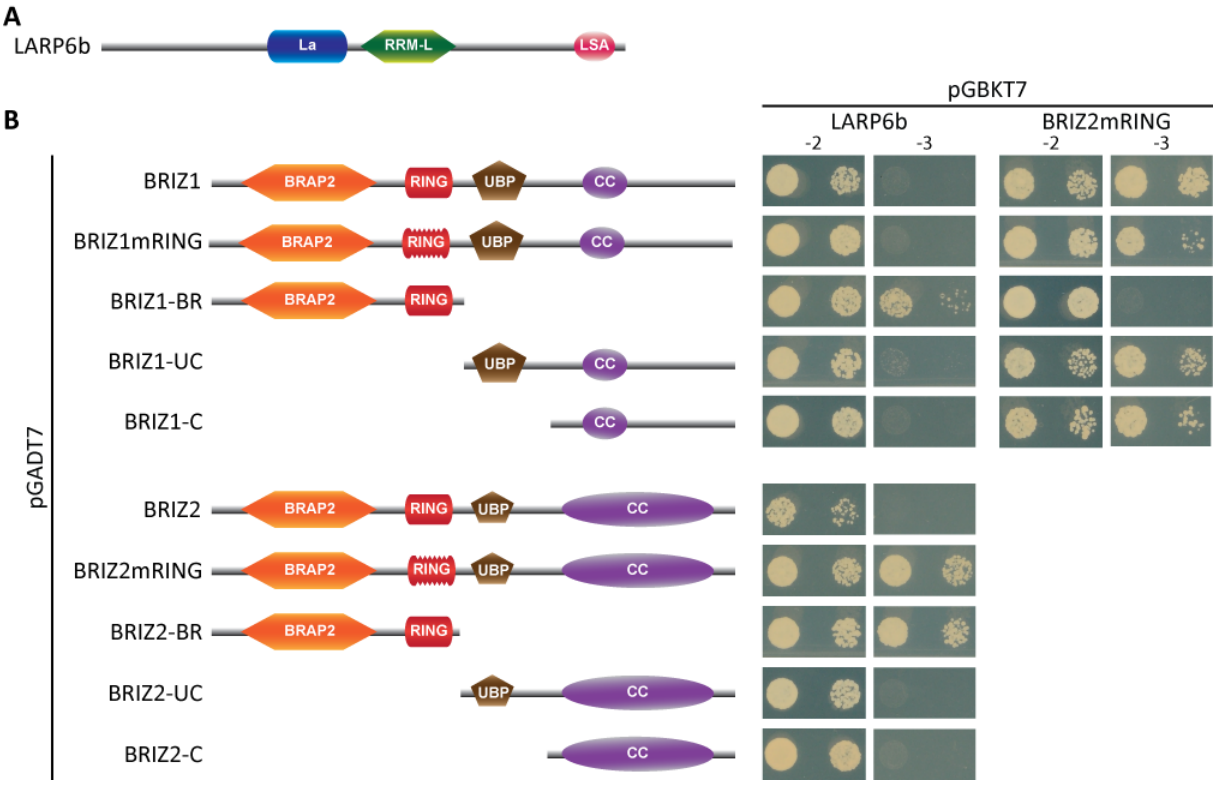

Figure 3-4. LARP6b interacts with the E3 ligases BRIZ1 and BRIZ2

A. Structure of LARP6b. The protein contains a La-motif (residues 193-270), an RNA recognition motif-like (RRM-L, residues 286-378) and a C-terminal La and S1-associated motif (LSA, residues 516-538). B. Y2H-assay of BRIZ-LARP6b interactions and BRIZ1-BRIZ2 heterodimerization. In addition to mRING-versions, also several truncated versions of the E3 ligases were used as shown in the left panel. Transformed yeasts were spotted in 10-fold and 100-fold dilutions on control medium (-2) or selective medium (-3).

Together, our results indicate that the BRIZ1/2 E3 ligase complex interacts directly with the LARP6b protein. In addition, the use of BRIZ2 containing RING mutations for Y2H assays stabilizes the interaction with LARP6b further supporting the possibility that LARP6b is a ubiquitination target of BRIZ1/2.

Heterologous Ubiquitination Assay development

In vitro ubiquitination assays are currently the best accepted assays to demonstrate the specific activity of a certain E3 ligase towards its substrate protein. These assays, however, require recombinant production of (at least) the E3 ligase and the substrate, what often can become a hurdle. In addition, since the Ub-linkage is determined by the E2 Ub-conjugase used, *in vitro* assays can be biased towards certain types of ubiquitination depending on the E2 used. Taking into account that the Arabidopsis genome encodes 37 E2s (Kraft et al., 2005), and that often *in vitro* ubiquitination assays are performed using commercially available human E2s, it would be preferable to have an alternative method.

One main advantage of the *in vitro* procedure, however, is that there is no background activity originating from similar E3 ligases and that simple omission of the E3 ligase from the

reaction mix is sufficient to investigate the relation between the E3 ligase and the ubiquitination-status of the suspected substrate. To obtain a comparable level of straight-forwardness, we decided to use yeast (*S. cerevisiae*) as a heterologous expression host for the study of our plant-derived E3-ligases. Due to the high degree of conservation of the ubiquitination machinery throughout different organisms, expression of only the heterologous F-box component of multi-subunit SCF-E3 ligases in this host is sufficient to assemble a functional E3 ligase complex, as the F-box domain will mediate assembly with the endogenous Skp1. The functionality of this approach has been demonstrated as expression of AtTIR1 in yeast leads to IAA-mediated degradation of a GFP equipped with the AUX/IAA degron motif (Nishimura et al., 2009).

The principle of the newly developed Heterologous Ubiquitination Assay (HUbA) is that co-expression of an E3 ligase together with its target leads to ubiquitination of the target. Treatment of the yeast cells with proteasome inhibitors prevents degradation of the ubiquitinated target which can then be purified and visualised in immunoblots with antibodies that detect (poly-) Ub or the target protein (Figure 3-5).

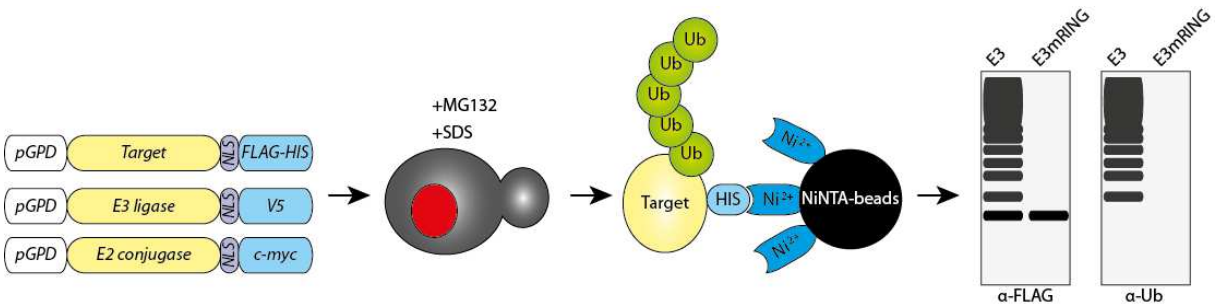

Figure 3-5. Principle of the Heterologous Ubiquitination Assay (HUbA)

The E3 ligase, corresponding target and optionally also the E2, are expressed in the *S. cerevisiae* strain *pre3pup1pdr5*. After growth in the presence of the proteasome inhibitor MG132 and 0.003% SDS in the medium, proteins are extracted and the ubiquitinated target is purified under denaturing conditions based on immobilized metal ion chromatography (e.g. Ni-NTA beads). The purified target protein and the ubiquitinated target proteins are detected in immunoblots using anti-FLAG and anti-Ub antibodies, respectively.

In first instance, we engineered a *S. cerevisiae* strain to increase its sensitivity to the proteasome inhibitor MG132 as WT yeast is relatively resistant to proteasome inhibitors. The yeast proteasome has three different proteolytic activities: a chymotrypsin-like, a trypsin-like and a caspase-like activity that correlate with the Pre2, the Pup1 and the Pre3 proteasomal subunits, respectively. Proteasome inhibitors like MG132 or Bortezomib, particularly block the chymotrypsin-like activity (Pre2) of the proteasome. However, in yeast, the two other proteasomal proteolytic activities are thought to compensate for proteasome function when the chymotrypsin-like activity is blocked. We therefore first obtained a strain (*pre3pup1*) where two of three proteolytic activities of the proteasome are disabled (Heinemeyer et al., 1997). Growth of the yeast strains in the presence of MG132 was used as a measure for the

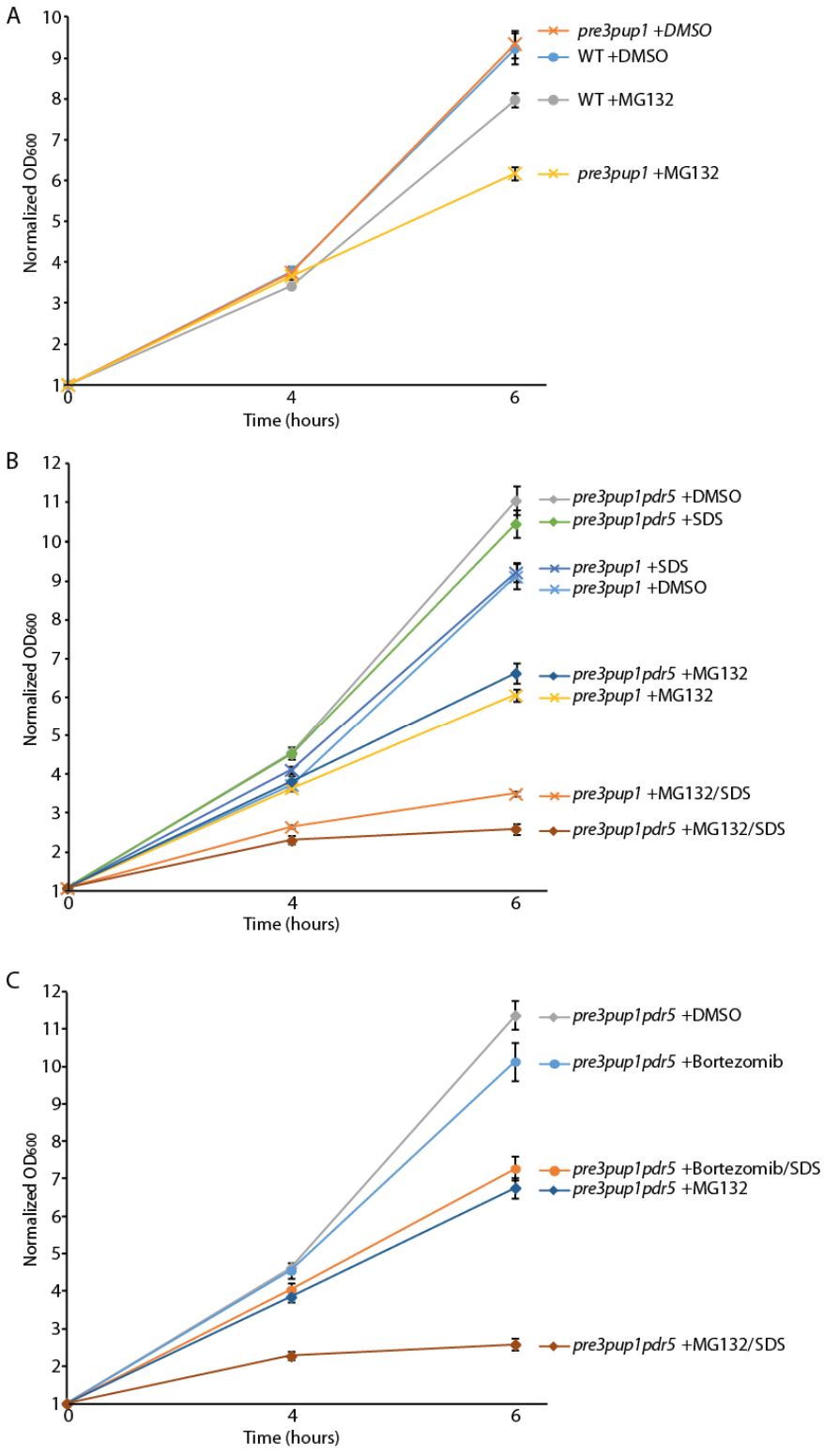

Figure 3-6. Yeast proteasome inhibition measured by growth rate.

The indicated yeast strains were pre-grown to stationary phase and then diluted to the same OD_{600} in YPD medium and incubated 6 hours in the presence of different compounds. The OD_{600} was measured at three different time points (0, 4 and 6 hours) after start of the treatment and normalized with respect to the OD_{600} at 0 hours. A. Growth rate inhibition by incubation with 50 µM MG132 or DMSO was compared between WT and *pre3pup1* yeast strains. B. Growth rate inhibition by incubation with 50 µM MG132 in the presence or absence of 0.003% SDS was compared between *pre3pup1* and *pre3pup1pdr5* stain. C. Growth rate inhibition by incubation with 50 µM MG132 or 50 µM Bortezomib was assessed in the *pre3pup1pdr5* yeast strain. Error bars represent ±SEM of 7 biological repeats.

inhibition of proteasomal activity. The *pre3pup1* strain grows at a similar rate as WT yeast under control (DMSO) conditions. However, growth of the *pre3pup1* strain is slowed down when incubated with MG132, while there was almost no growth inhibition by MG132 in the WT yeast strain (Figure 3-6A).

A second property that prevents efficient inhibition of yeast proteasomal activity, is the low permeability of yeast cell membranes. We therefore knocked-out the *PDR5* gene in the *pre3pup1* mutant background using homologous recombination with a KanMX disruption cassette (Guldener et al., 1996) yielding the *pre3pup1pdr5* strain. PDR5 functions as a drug-efflux pump and is thought to literally pump inhibitors/drugs back out of the yeast cell. In addition, including low amounts of SDS in the growth medium leads to mild permeabilization of the yeasts cells, resulting in higher uptake of MG132 (Collins et al., 2010). Accordingly, this treatment was included in our growth assays. Under control conditions (DMSO or SDS treatments), the *pre3pup1pdr5* strain showed no defects in growth when compared to the *pre3pup1* strain. Treatment with MG132 in the presence of SDS in the medium resulted in almost complete growth arrest in the *pre3pup1pdr5* strain. The effect of MG132 on cell growth in the presence of SDS was significantly stronger in this strain than in the parental *pre3pup1* strain (Figure 3-6B).

We also evaluated the use of an alternative 26S proteasome inhibitor, namely Bortezomib (Tsukamoto and Yokosawa, 2009), by comparing yeast growth in the presence of equimolar amounts of Bortezomib or MG132 (Figure 3-6C). Our results indicate MG132 treatment of the *pre3pup1pdr5* strain in combination with SDS has the most pronounced effect on yeast growth rate and are well-suited for our Heterologous Ubiquitination Assay (HUbA).

Finally, to efficiently express plant genes in the heterologous yeast host, we constructed a set of vectors that were compatible with expression in yeast, while making optimal use of the resources available for the cloning of plant genes. This resulted in the construction of a set of three-fragment MultiSite Gateway™ destination vectors (Nagels Durand et al., 2012, see Chapter 4). In addition, we constructed a number of tags that are optimized for the HUbA assay. First, a nuclear localization signal (NLS) was included in every tag in order to target all expressed proteins to the same subcellular compartment. Second, a HIS-tag that allows affinity purification under denaturing conditions, was combined with a sensitive epitope tag for specific immunodetection with low background. Under denaturing conditions, de-ubiquitinating enzymes and proteasomal subunits are unfolded, preventing de-ubiquitination or proteolytic degradation of the target during the purification procedure. This resulted in the construction of a NLS-V5-tag and a NLS-3x myc-tag for fusion to the E3 Ub-ligase, and a NLS-3x FLAG-6x HIS-tag for fusion to the substrate (Figure 3-5).

Taken together, we engineered a yeast host strain and determined adequate treatments that make it suitable for the study of ubiquitinated proteins due to increased sensitivity to MG132. In addition, we developed appropriate expression vectors that enable efficient expression of adequately tagged plant E3 ligase/target pairs in this host strain.

AtLARP6b is post-translationally modified by BRIZ1/2 during HUbA

To investigate if LARP6b is a target of BRIZ1/2, we performed a HUbA with these proteins. Because LARP6b was identified originally as a BRIZ2-interacting protein in Arabidopsis cell cultures, we compared LARP6b expression in yeast in the presence of BRIZ2 alone, or both BRIZ1 and BRIZ2, as both homologs were published to function together in a non-redundant manner (Hsia and Callis, 2010). We expressed the proteins in the HUbA yeast strain (*pre3pup1pdr5*), extracted total protein lysates and visualized the respective proteins on immunoblots (Figure 3-7A). Only when both E3 ligases were simultaneously co-expressed with their putative target LARP6b, a higher molecular weight band appeared on top of the band corresponding to LARP6b (marked with an asterisk in Figure 3-7A). As this higher molecular weight band was much less abundant than the unmodified LARP6b band, we included a cycloheximide (CHX) treatment in the next experiments. CHX inhibits translation and because LARP6b is expressed under control of a constitutive promoter, blocking synthesis of new LARP6b protein might result in relatively higher accumulation of the (presumably modified) higher molecular weight band. Yeasts expressing LARP6b together with BRIZ1 and BRIZ2 were upscaled and treated with MG132 in the presence of CHX, before being harvested for immobilized-metal affinity chromatography (IMAC) based purification of LARP6b. When an aliquot of the total protein extract was analysed on immunoblot, we indeed saw enrichment of the LARP6b higher molecular weight band. Additionally, the effect of MG132 treatment now became visible as the LARP6b protein accumulated in the presence of the proteasome inhibitor (Figure 3-7B). The higher molecular weight form co-purified with LARP6 during IMAC, confirming this protein is a modified form of HIS-tagged LARP6b. However, when the same blot was re-probed with anti-Ub antibodies, no ubiquitinated proteins could be detected. Because only one higher molecular weight band was present, it is possible that the sensitivity of the anti-Ub antibody we used is restricted to poly-Ub entities rather than mono-Ub. Alternatively, the covalent modification detected could be of a different nature than Ub.

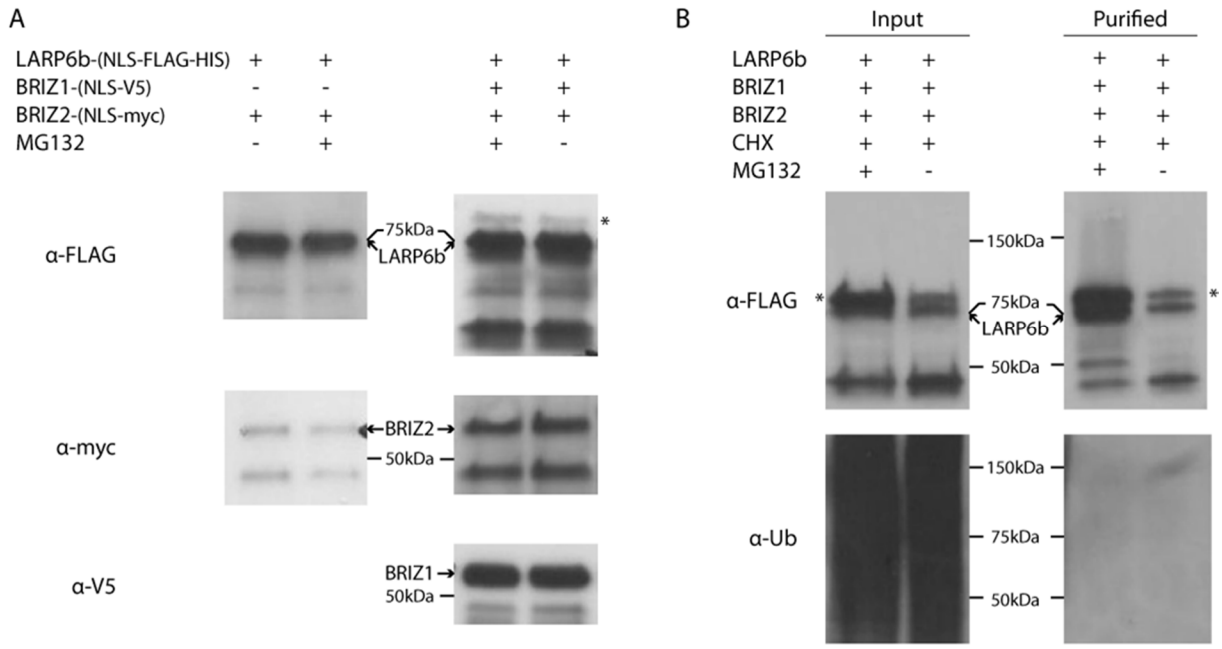

Figure 3-7. Heterologous Ubiquitination Assay of LARP6b by BRIZ1/2.

A. LARP6b was expressed in *pre3pup1pdr5* yeast in the presence of BRIZ2 alone, or both BRIZ1 and BRIZ2. The yeasts were grown at 30°C in selective medium and treated or not with 50 µM MG132, in the presence of 0.003% SDS for 1 hour before total protein extracts were analysed on immunoblots. B. LARP6b was expressed in *pre3pup1pdr5* yeast in the presence of both BRIZ1 and BRIZ2. The yeasts were grown at 25°C in selective medium and treated with 50 µM MG132 or DMSO in the presence of 0.003%SDS for 1 hour and additionally with 1 mg/ml CHX 30 minutes before harvesting. LARP6b was purified from total protein extracts using IMAC. LARP6b and Ub or Ub-conjugates were detected before and after purification on immunoblots using anti-Ub antibodies. LARP6b, BRIZ1 and BRIZ2 were detected using anti-FLAG, anti-myc or anti-V5 antibodies, respectively. Asterisks indicate a higher molecular weight form of LARP6b. Expected molecular weights including epitope tag: LARP6b 67kDa, BRIZ1 62kDa and BRIZ2 60kDa.

BIRZ1/2 are highly homologous, and also have high similarity to the mammalian BRAP2/IMP protein. BRAP2 contains a BRAP2-domain comprising an RNA-recognition motif (RRM, Marchler-Bauer et al., 2015), a RING domain followed by a ZnF UBP domain and a coiled coil domain. This domain architecture is remarkably similar to that of the BRIZ1 and BRIZ2 proteins (Hsia and Callis, 2010), (Figure 3-1). BRAP2 was first identified as a BRCA-1 interacting protein and shown to be a cytoplasmic protein that binds to the NLS motifs of BRCA-1 and several other proteins, functioning as a cytoplasmic retention factor for nuclear and nuclear-envelope localized proteins (Li et al., 1998; Fulcher et al., 2010; Davies et al., 2013). BRAP2 has also been involved in the control of NF-κB localization. NF-κB plays a crucial role in the regulation of diverse cellular functions including the inflammatory response. Under normal conditions, NF-κB is sequestered in the cytoplasm by IκB. Upon stimulation with inflammatory cytokines, IκB is degraded and NF-κB translocates to the nucleus. BRAP2 was shown to influence cytokine-mediated NF-κB nuclear translocation. Additionally the authors showed BRAP2 is able to bind tandem Nedd8 and Nedd8-conjugated proteins in a RING-dependent manner. Remarkably, BRAP2 itself is also neddylated *in vivo* (Takashima et al., 2013). No ubiquitination target of BRAP2 has been identified yet. Note that when BRIZ2 (but not BRIZ1) was expressed in yeast for HUbA assays, it was always detected as two bands on western blots

(Figure 3-7). The molecular weight of the yeast NEDD8 homolog is around 9 kDa. Although, the two BRIZ2-bands seem to have a larger difference in molecular weight, it is still possible that BRIZ2 is being modified with multiple NEDD8 entities. Alternatively, the two BRIZ2-bands can be originated by other post-translational modifications like proteolytic processing.

In animals, LARP6 proteins are involved in control of developmental decisions in neurons and muscle cells. The HsLARP6 (Acheron) contains both a NLS and a NES (nuclear export signal). HsLARP6 has been associated with enhanced breast tumour growth and vascularization when constitutively targeted to the nucleus, indicating controlled shuttling of HsLARP6 between the nucleus and the cytoplasm is crucial to properly exert its function (Shao et al., 2012).

To investigate if BRIZ1/2 could act as a cytoplasmic retention factor for LARP6b in plants, we first observed LARP6b localization by transiently expressing LARP6b-GFP under control of a constitutive pCaMV35S promotor in *Nicotiana benthamiana* mesophyll cells. LARP6b-GFP localization was nucleo-cytoplasmic (Figure 3-8 A), indicating it can shuttle between nucleus and cytoplasm analogous to the human HsLARP6 protein. The influence of BRIZ1/2 overexpression on LARP6b localization was then examined by transiently co-expressing BRIZ1/2 with LARP6b-GFP in *N. benthamiana.* We noticed no apparent alteration in LARP6b-GFP localization when co-expressed with BRIZ1/2 under the conditions tested (Figure 3-8 B).

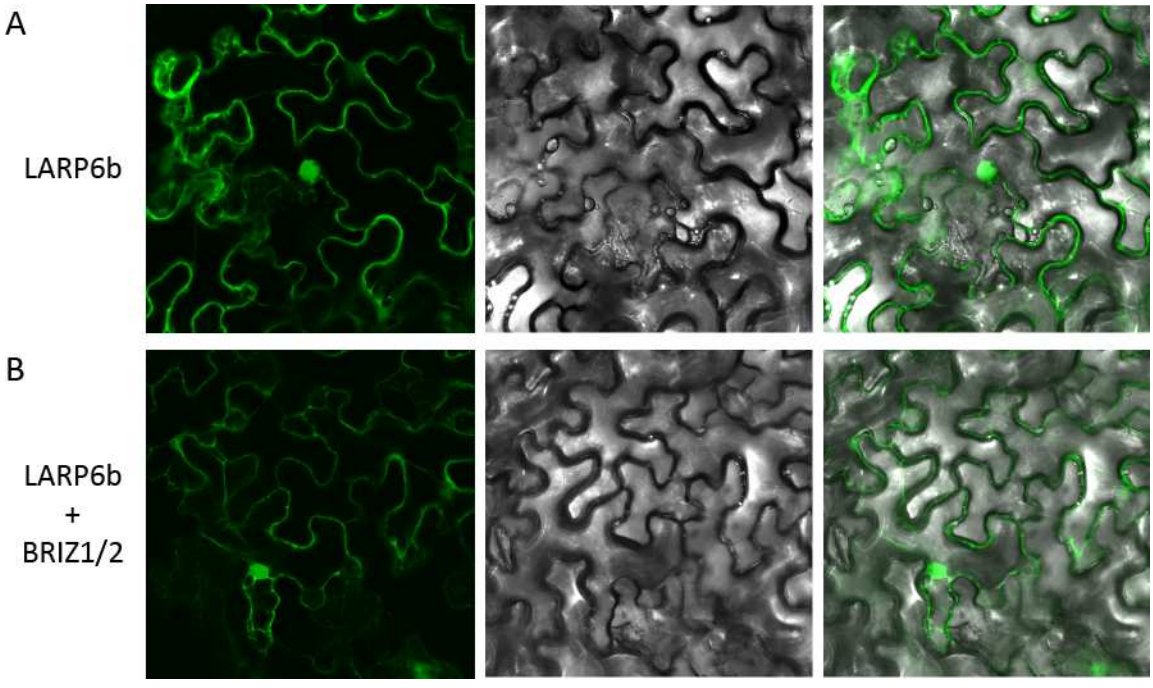

Figure 3-8. LARP6b subcellular localization is not influenced by BRIZ1/2 overexpression.

N. benthamiana leafs were transiently transfected with LARP6b-GFP alone or LARP6b-GFP and BRIZ1/2 in addition to a P19 expressing construct. Lower epidermal leaf cells were imaged 3-5 days after infiltration using a Leica SP2 upright confocal microscope.

Taken together, we have identified LARP6b that interacts directly with the heterodimeric E3 ligase BRIZ1/2. In addition, we have shown that LARP6b is modified in yeast when co-expressed with BRIZ1/2. We have failed, however, to identify the nature of this modification, as anti-Ub antibodies were unsuccessful in recognizing the modified LARP6b protein. Since BRIZ1/2 closely resemble the human BRAP2 protein, and this protein has been shown to bind neddylated proteins, it is possible that the covalent modification observed on LARP6b is not Ub but rather the Ub-related protein Nedd8. No Nedd8-specific E3 ligase has been identified yet, however, neddylation has been reported to be sometimes mediated (at least in the case of RBX1) by RING-type proteins (Scott et al., 2014). Because the RING domain of BRAP2 was reported to be essential for Nedd8 binding, and BRIZ1/2 and BRAP2 share high homology, it is tempting to state that they might function as Nedd8 E3 ligases. In accordance with this, we did not succeed in identifying an Arabidopsis Ub-conjugase (E2) that could interact with either BRIZ1 or BRIZ2 in Y2H (results not shown), further supporting BRIZ1/2 could function in a pathway other than Ub-ligation.

CONCLUSION

Our bio-informatics screen combined with TAP of E3 ligase interactors led to the successful identification of potential targets of at least four E3 ligases (ATL23, AE31, KEG and BRIZ1/2) with a possible function in JA-signalling. To further investigate ubiquitination we developed a new *in vivo* ubiquitination assay in yeast (HUbA). Although proof of concept for this assay is still missing, preliminary tests with BRIZ1/2 and their candidate target LARP6b indicate the assay might be useful for detecting Ub E3-ligase activity but also for Ub-like E3 ligase activity (e.g. Nedd8). Further experiments will be needed to discriminate between Ub or Ub-like E3 ligase activity of BRIZ1/2, which could be achieved by MS analysis of LARP6b after HUbA or by detection of the purified protein on western blot with antibodies against specific Ub-like modifications.

EXPERIMENTAL PROCEDURES

Bio-informatics screen

The raw microarray data was obtained from the AGRON-OMICS repository (http://www.agron-omics.eu) for the 'Agronomics residuals' compendium or from CORNET (De Bodt et al., 2010) for the 'CC', 'MeJA' and 'ABA' compendia. The Bioconductor R package, version 2.5 (Gentleman et al., 2004), was used to RMA (Robust Multi-array Average) normalize the raw data. Only the Affymetrix ATH1 probe sets present on the AGRONOMICS1 array were retained for calculating gene expression levels, to facilitate comparisons between this data set and the sample data sets for pooled plants. A linear model was fit to the expression levels using Limma (Linear Modelling of Microarray data) R package (Wettenhall and Smyth, 2004).

To categorize genes as being differentially (up or down) regulated the 'Agronomics residuals' data set was standardized using a log ratio threshold of 0.3498 while for the 'CC', 'MeJA' and 'ABA' datasets the log ratios were subjected to a moderated t-test ($p<0.01$). Co-differential expression networks and expression modules for the different data sets were obtained using ENIGMA 1.1 (Maere et al., 2008). The FDR (false discovery rate) level for detecting significant co-differential expression links was set to 0.01. For functional annotation on the level of expression modules, GO ontology information and annotations for Arabidopsis were obtained from the GO database (www.geneontology.org) and annotations with non-experimental evidence codes IEA, ISS, and RCA were discarded. GO enrichment of gene modules was assessed using hypergeometric tests, and the resulting p values were corrected for multiple testing using the Benjamini and Hochberg FDR correction at FDR = 0.05. Potential regulators of a module were predicted from the set of genes annotated to "biological regulation" in GO (GO:0065007) at FDR = 0.01. The remaining ENIGMA parameters were set to default values. For use in gene function predictions, negative correlation edges were removed from the co-differential expression networks. Basic network topology parameters (network density and clustering coefficient for the major connected component of each network) were obtained using NetworkX 2.6.4 (http://networkx.github.com/).

Ontology terms for PiNGO (Smoot et al., 2011) input were selected from AmiGO (http://amigo.geneontology.org/). Start GO's where 'ubiquitin-protein ligase activity' (GO: 0004842), 'protein ubiquitination' (GO: 0016567) or 'ubiquitin-dependent protein catabolic process' (GO: 0006511). Target GO's where 'jasmonic acid mediated signalling pathway' (GO: 0009867) or 'response to jasmonic acid stimulus' (GO: 0009753).

Generation of Entry-clones

ORFs were amplified from a cDNA template by PCR using Phusion High-fidelity Polymerase (NEB), with specific primers including *att*B sites and subsequently recombined with pDONR207. Forward primers annealing after transmembrane regions including *att*B1 and a new start codon were used for the construction of dTM variants. For the creation of C-terminal fusions, reverse primers did not include a stop codon. For the construction of mRING variants, corresponding full-length Entry vectors were amplified using Pfu DNA polymerase (Promega) and primers containing the mutations. The PCR product was digested using *Dpn*I before transformation to *E. coli*. Positive colonies were picked and sequence verified. All primers used are listed in Supplementary Table S1.

Entry vectors encoding KEGmRING, BRIZ1, BRIZ2 and BRIZ truncations were kindly provided by Judy Callis. BRIZ truncations contained ORF of BRIZ encoding amino-acids (AA) as follows: BRIZ1-BR AA 1-229 , BRIZ1-UC AA 231-488 , BRIZ1-C AA 277-488 , BRIZ2-BR AA 1-241, BRIZ2-UC AA 207-479 and BRIZ2-C AA 240-479.

Tandem affinity purification

N or C-terminally tagged TAP constructs (GS or GSrh tag) were generated as described (Van Leene et al., 2015), used for the transformation of Arabidopsis PSB-D cell suspension cultures without callus selection and further grown and subcultured as described (Van Leene et al., 2011). Stably transformed cultures were scaled up and harvested 6 days after subculturing. Cells were treated with 50 µM JA (Duchefa) for 1 min before harvesting. Purifications were performed as described (Van Leene et al., 2015) with the exception that no Benzonase treatment was performed on the cell extracts. Expression of TAP-tagged constructs in stably transformed Arabidopsis PSB-D cultures was verified on an aliquot of total protein extract before purification.

Immunodetection of proteins

Yeasts were pre-cultured over-night to stationary phase, diluted to OD_{600} 0.1 and grown to exponential phase (OD_{600}>0.3). Total yeast protein extracts were obtained under denaturing conditions as described (Hampton and Rine, 1994). Cells were washed with 0.1% NaN_3 and resuspended in 100 µl SUTE buffer (8 M urea, 1% SDS, 10 mM Tris, 10 mM EDTA, pH 7.5) containing protease inhibitor cocktail (cOmplete ULTRA, Roche). 100 µl of acid-washed 0.5mm glass beads were added and the mixture was vortexed at maximum speed for 2.5 min. 100 µl of USB buffer (8 M urea, 4% SDS, 125 mM Tris, 10% β-mercapto-ethanol, pH 6.8) was added and the mixture was incubated 10 min at 65°C. Protein lysates were finally obtained by centrifuging 1 min at 10 000 rpm.

Protein concentrations were quantified using the Bradford Protein Assay (Bio-Rad). Samples were combined with 5x Laemmli loading buffer and denatured for 10 min at 95°C. Subsequently, 30 µg total protein was separated on a 4–15% Mini-PROTEAN TGX Precast Gel (Bio-Rad) and transferred to a PVDF membrane using the Trans-Blot Turbo transfer system (Bio-Rad). Detection was performed using the following primary antibodies: Peroxidase anti-peroxidase (Sigma-Aldrich), anti-FLAG (Sigma), anti-myc-HRP (Invitrogen), anti-V5 (Sigma) and anti-Ubiquitin (VU-1, LifeSensors).

Immobilized Metal Affinity Chromatography

Yeasts were pre-cultured over-night to stationary phase, diluted to OD_{600} 0.1 and grown to OD_{600}>0.8. Cells were washed with ice-cold water and resuspended in 200 µl buffer A (8 M urea, 50 mM NaH_2PO_4, 300 mM NaCl, 0.5% Triton X-100, pH 8). 100 µl of acid-washed 0.5mm glass beads were added and the mixture was vortexed at maximum speed for 2.5 min. Protein lysates were obtained by centrifuging 5 min at 14 000 rpm and incubated with 25 µl effective volume Ni-NTA resin (Ni-NTA Superflow, Qiagen) for 2 h at room temperature on a rotating wheel. Resin-bound proteins were washed in a Mobicol column (ImTec Diagnostics NV, Belgium) first with 250 µl Buffer A and then with 250 µl buffer A containing 20mM imidazole. Bound proteins were eluted by incubating the resin for 5 minutes with 50 µl 1x Laemmli loading buffer containing 150 mM imidazole. An aliquot of the total protein lysate (before purification) was taken to estimate protein concentrations based on Coomassie staining after electrophoresis.

Yeast transformation and Yeast two-hybrid

Expression clones for yeast two-hybrid were generated by LR Gateway recombination between respective Entry-clones and pGADT7 or pGBKT7 and co-transformed in competent yeast cells of the *S. cerevisiae* strain PJ69-4A using the LiAc/SS carrier DNA/PEG method (Gietz and Schiestl, 2007). Transformants were selected on SD media lacking Leu and Trp (-2). Dropping was performed as described (Cuéllar Pérez et al., 2013).

Yeast strain construction and treatments

The *pre3pup1* strain (YWO1641:pre3-T20A pup1-T30A) was kindly provided by Dieter Wolf and described in (Heinemeyer et al., 1997). A KanMX disruption cassette (Guldener et al., 1996) was PCR-amplified using primers that included regions homologous to the PDR5 gene. The PCR product was purified and transformed into the *pre3pup1* strain, followed by selection on YPD containing 200 µg/ml geneticin (G-418). Disruption of the PDR5 gene was verified by PCR. This resulted in the isolation of the *pre3pup1pdr5* strain. The *pre3pup1* and *pre3pup1pdr5* strain are isogenic with the WT strain WCG4a, kindly provided by Dieter Wolf (YWO0898:MATα *leu2-3,112 ura3 his3-11,15 Can^s GAL)*. For treatments, yeasts were pre-grown at 30°C in YPD or selective medium until stationary phase, diluted to OD_{600} 0.1 and grown to exponential phase (OD_{600}> 0.3). Then, 50 µM MG132, 50 µM Bortezomib, 0.003% SDS and/or 1mg/ml CHX were included in the medium for the indicated time.

Agorbacterium mediated transient expression in Nicotiana benthamiana

WT *N. benthamiana* plants (3–4 weeks old) were used for transient expression of constructs by *Agrobacterium tumefaciens*-mediated transient transformation of lower epidermal leaf cells as previously described (Boruc et al., 2010) using a modified infiltration buffer (10 mM $MgCl_2$, Merck; 10 mM MES pH 5.7, Duchefa; 100 µM Acetosyringone, Sigma-Aldrich) and addition of a P19 expressing *Agrobacterium* strain to boost protein expression (Voinnet et al., 2003). All *Agrobacterium* strains were grown for 2 days, diluted to OD 1 in infiltration buffer and incubated for 2-4 h at room temperature before mixing in a 1:1 ratio with other strains and injecting. Lower epidermal leaf cells were imaged 3-5 days after infiltration using a Leica SP2 upright confocal microscope.

REFERENCES

Aguayo MF, Ampuero D, Mandujano P, Parada R, Munoz R, Gallart M, Altabella T, Cabrera R, Stange C, Handford M (2013) Sorbitol dehydrogenase is a cytosolic protein required for sorbitol metabolism in Arabidopsis thaliana. Plant science : an international journal of experimental plant biology **205-206:** 63-75

Bartel B, Fink GR (1994) Differential regulation of an auxin-producing nitrilase gene family in Arabidopsis thaliana. Proceedings of the National Academy of Sciences of the United States of America **91:** 6649-6653

Bayfield MA, Yang R, Maraia RJ (2010) Conserved and divergent features of the structure and function of La and La-related proteins (LARPs). Biochimica et biophysica acta **1799:** 365-378

Bhosale R, Jewell JB, Hollunder J, Koo AJ, Vuylsteke M, Michoel T, Hilson P, Goossens A, Howe GA, Browse J, et al (2013) Predicting gene function from uncontrolled expression variation among individual wild-type Arabidopsis plants. The Plant cell **25:** 2865-2877

Boruc J, Inze D, Russinova E (2010) A high-throughput bimolecular fluorescence complementation protein-protein interaction screen identifies functional Arabidopsis CDKA/B-CYCD4/5 complexes. Plant signaling & behavior **5:** 1276-1281

Bousquet-Antonelli C, Deragon JM (2009) A comprehensive analysis of the La-motif protein superfamily. Rna **15:** 750-764

Burckstummer T, Bennett KL, Preradovic A, Schutze G, Hantschel O, Superti-Furga G, Bauch A (2006) An efficient tandem affinity purification procedure for interaction proteomics in mammalian cells. Nature methods **3:** 1013-1019

Burglin TR (2008) Evolution of hedgehog and hedgehog-related genes, their origin from Hog proteins in ancestral eukaryotes and discovery of a novel Hint motif. BMC genomics **9:** 127

Chen YT, Liu H, Stone S, Callis J (2013) ABA and the ubiquitin E3 ligase KEEP ON GOING affect proteolysis of the Arabidopsis thaliana transcription factors ABF1 and ABF3. The Plant journal : for cell and molecular biology **75:** 965-976

Chini A, Fonseca S, Fernandez G, Adie B, Chico JM, Lorenzo O, Garcia-Casado G, Lopez-Vidriero I, Lozano FM, Ponce MR, et al (2007) The JAZ family of repressors is the missing link in jasmonate signalling. Nature **448:** 666-671

Collins GA, Gomez TA, Deshaies RJ, Tansey WP (2010) Combined chemical and genetic approach to inhibit proteolysis by the proteasome. Yeast **27:** 965-974

Cuéllar Pérez A, Pauwels L, De Clercq R, Goossens A (2013) Yeast two-hybrid analysis of jasmonate signaling proteins. Methods in molecular biology **1011:** 173-185

Dave A, Hernandez ML, He Z, Andriotis VM, Vaistij FE, Larson TR, Graham IA (2011) 12-oxo-phytodienoic acid accumulation during seed development represses seed germination in Arabidopsis. The Plant cell **23:** 583-599

Davies RG, Wagstaff KM, McLaughlin EA, Loveland KL, Jans DA (2013) The BRCA1-binding protein BRAP2 can act as a cytoplasmic retention factor for nuclear and nuclear envelope-localizing testicular proteins. Biochimica et biophysica acta **1833:** 3436-3444

De Bodt S, Carvajal D, Hollunder J, Van den Cruyce J, Movahedi S, Inze D (2010) CORNET: A User-Friendly Tool for Data Mining and Integration. Plant physiology **152:** 1167-1179

de la Fuente van Bentem S, Anrather D, Roitinger E, Djamei A, Hufnagl T, Barta A, Csaszar E, Dohnal I, Lecourieux D, Hirt H (2006) Phosphoproteomics reveals extensive in vivo phosphorylation of Arabidopsis proteins involved in RNA metabolism. Nucleic acids research **34:** 3267-3278

Fonseca S, Chini A, Hamberg M, Adie B, Porzel A, Kramell R, Miersch O, Wasternack C, Solano R (2009) (+)-7-iso-Jasmonoyl-L-isoleucine is the endogenous bioactive jasmonate. Nature chemical biology **5:** 344-350

Fulcher AJ, Roth DM, Fatima S, Alvisi G, Jans DA (2010) The BRCA-1 binding protein BRAP2 is a novel, negative regulator of nuclear import of viral proteins, dependent on phosphorylation flanking the nuclear localization signal. FASEB journal : official publication of the Federation of American Societies for Experimental Biology **24:** 1454-1466

Garcia D, Garcia S, Pontier D, Marchais A, Renou JP, Lagrange T, Voinnet O (2012) Ago hook and RNA helicase motifs underpin dual roles for SDE3 in antiviral defense and silencing of nonconserved intergenic regions. Molecular cell **48:** 109-120

Geerinck J (2010) Dynamic protein complexes involved in plant secondary metabolism. UGhent, PhD Thesis.

Gentleman RC, Carey VJ, Bates DM, Bolstad B, Dettling M, Dudoit S, Ellis B, Gautier L, Ge YC, Gentry J, et al (2004) Bioconductor: open software development for computational biology and bioinformatics. Genome Biol **5**

Gietz RD, Schiestl RH (2007) High-efficiency yeast transformation using the LiAc/SS carrier DNA/PEG method. Nature protocols **2:** 31-34

Gu C, Shabab M, Strasser R, Wolters PJ, Shindo T, Niemer M, Kaschani F, Mach L, van der Hoorn RA (2012) Post-translational regulation and trafficking of the granulin-containing protease RD21 of Arabidopsis thaliana. PloS one **7:** e32422

Gu Y, Innes RW (2011) The KEEP ON GOING protein of Arabidopsis recruits the ENHANCED DISEASE RESISTANCE1 protein to trans-Golgi network/early endosome vesicles. Plant physiology **155:** 1827-1838

Gu Y, Innes RW (2012) The KEEP ON GOING protein of Arabidopsis regulates intracellular protein trafficking and is degraded during fungal infection. The Plant cell **24:** 4717-4730

Guldener U, Heck S, Fielder T, Beinhauer J, Hegemann JH (1996) A new efficient gene disruption cassette for repeated use in budding yeast. Nucleic acids research **24:** 2519-2524

Hampton RY, Rine J (1994) Regulated degradation of HMG-CoA reductase, an integral membrane protein of the endoplasmic reticulum, in yeast. The Journal of cell biology **125:** 299-312

Heinemeyer W, Fischer M, Krimmer T, Stachon U, Wolf DH (1997) The active sites of the eukaryotic 20 S proteasome and their involvement in subunit precursor processing. The Journal of biological chemistry **272:** 25200-25209

Hjerpe R, Aillet F, Lopitz-Otsoa F, Lang V, England P, Rodriguez MS (2009) Efficient protection and isolation of ubiquitylated proteins using tandem ubiquitin-binding entities. EMBO reports **10:** 1250-1258

Hondo D, Hase S, Kanayama Y, Yoshikawa N, Takenaka S, Takahashi H (2007) The LeATL6-associated ubiquitin/proteasome system may contribute to fungal elicitor-activated defense response via the jasmonic acid-dependent signaling pathway in tomato. Molecular plant-microbe interactions : MPMI **20:** 72-81

Hsia MM, Callis J (2010) BRIZ1 and BRIZ2 proteins form a heteromeric E3 ligase complex required for seed germination and post-germination growth in Arabidopsis thaliana. The Journal of biological chemistry **285:** 37070-37081

Hua Z, Vierstra RD (2011) The cullin-RING ubiquitin-protein ligases. Annual review of plant biology **62:** 299-334

Huang Y, Li CY, Pattison DL, Gray WM, Park S, Gibson SI (2010) SUGAR-INSENSITIVE3, a RING E3 ligase, is a new player in plant sugar response. Plant physiology **152:** 1889-1900

Kelley DR, Estelle M (2012) Ubiquitin-mediated control of plant hormone signaling. Plant physiology **160:** 47-55

Kraft E, Stone SL, Ma L, Su N, Gao Y, Lau OS, Deng XW, Callis J (2005) Genome analysis and functional characterization of the E2 and RING-type E3 ligase ubiquitination enzymes of Arabidopsis. Plant physiology **139:** 1597-1611

Lamesch P, Berardini TZ, Li DH, Swarbreck D, Wilks C, Sasidharan R, Muller R, Dreher K, Alexander DL, Garcia-Hernandez M, et al (2012) The Arabidopsis Information Resource (TAIR): improved gene annotation and new tools. Nucleic acids research **40:** D1202-D1210

Lampl N, Alkan N, Davydov O, Fluhr R (2013) Set-point control of RD21 protease activity by AtSerpin1 controls cell death in Arabidopsis. The Plant journal : for cell and molecular biology **74:** 498-510

Li S, Ku CY, Farmer AA, Cong YS, Chen CF, Lee WH (1998) Identification of a novel cytoplasmic protein that specifically binds to nuclear localization signal motifs. The Journal of biological chemistry **273:** 6183-6189

Lin SS, Martin R, Mongrand S, Vandenabeele S, Chen KC, Jang IC, Chua NH (2008) RING1 E3 ligase localizes to plasma membrane lipid rafts to trigger FB1-induced programmed cell death in Arabidopsis. The Plant journal : for cell and molecular biology **56:** 550-561

Liu H, Stone SL (2010) Abscisic acid increases Arabidopsis ABI5 transcription factor levels by promoting KEG E3 ligase self-ubiquitination and proteasomal degradation. The Plant cell **22:** 2630-2641

Liu H, Stone SL (2013) Cytoplasmic degradation of the Arabidopsis transcription factor abscisic acid insensitive 5 is mediated by the RING-type E3 ligase KEEP ON GOING. The Journal of biological chemistry **288:** 20267-20279

Luo H, Laluk K, Lai Z, Veronese P, Song F, Mengiste T (2010) The Arabidopsis Botrytis Susceptible1 Interactor defines a subclass of RING E3 ligases that regulate pathogen and stress responses. Plant physiology **154:** 1766-1782

Lyzenga WJ, Liu H, Schofield A, Muise-Hennessey A, Stone SL (2013) Arabidopsis CIPK26 interacts with KEG, components of the ABA signalling network and is degraded by the ubiquitin-proteasome system. Journal of experimental botany **64:** 2779-2791

Maekawa S, Sato T, Asada Y, Yasuda S, Yoshida M, Chiba Y, Yamaguchi J (2012) The Arabidopsis ubiquitin ligases ATL31 and ATL6 control the defense response as well as the carbon/nitrogen response. Plant molecular biology **79:** 217-227

Maere S, Van Dijck P, Kuiper M (2008) Extracting expression modules from perturbational gene expression compendia. BMC systems biology **2:** 33

Marchler-Bauer A, Derbyshire MK, Gonzales NR, Lu S, Chitsaz F, Geer LY, Geer RC, He J, Gwadz M, Hurwitz DI, et al (2015) CDD: NCBI's conserved domain database. Nucleic acids research **43:** D222-226

Massonnet C, Vile D, Fabre J, Hannah MA, Caldana C, Lisec J, Beemster GTS, Meyer RC, Messerli G, Gronlund JT, et al (2010) Probing the Reproducibility of Leaf Growth and Molecular Phenotypes: A Comparison of Three Arabidopsis Accessions Cultivated in Ten Laboratories. Plant physiology **152:** 2142-2157

Mengiste T, Chen X, Salmeron J, Dietrich R (2003) The BOTRYTIS SUSCEPTIBLE1 gene encodes an R2R3MYB transcription factor protein that is required for biotic and abiotic stress responses in Arabidopsis. The Plant cell **15:** 2551-2565

Nagels Durand A, Moses T, De Clercq R, Goossens A, Pauwels L (2012) A MultiSite Gateway vector set for the functional analysis of genes in the model Saccharomyces cerevisiae. BMC molecular biology **13:** 30

Nishimura K, Fukagawa T, Takisawa H, Kakimoto T, Kanemaki M (2009) An auxin-based degron system for the rapid depletion of proteins in nonplant cells. Nature methods **6:** 917-922

Park J, Nguyen KT, Park E, Jeon JS, Choi G (2013) DELLA proteins and their interacting RING Finger proteins repress gibberellin responses by binding to the promoters of a subset of gibberellin-responsive genes in Arabidopsis. The Plant cell **25:** 927-943

Peng J, Schwartz D, Elias JE, Thoreen CC, Cheng D, Marsischky G, Roelofs J, Finley D, Gygi SP (2003) A proteomics approach to understanding protein ubiquitination. Nature biotechnology **21:** 921-926

Qu X, Chatty PR, Roeder AH (2014) Endomembrane trafficking protein SEC24A regulates cell size patterning in Arabidopsis. Plant physiology **166:** 1877-1890

Sako K, Maki Y, Kanai T, Kato E, Maekawa S, Yasuda S, Sato T, Watahiki MK, Yamaguchi J (2012) Arabidopsis RPT2a, 19S proteasome subunit, regulates gene silencing via DNA methylation. PloS one **7:** e37086

Salahudeen AA, Thompson JW, Ruiz JC, Ma HW, Kinch LN, Li Q, Grishin NV, Bruick RK (2009) An E3 ligase possessing an iron-responsive hemerythrin domain is a regulator of iron homeostasis. Science **326:** 722-726

Scott DC, Sviderskiy VO, Monda JK, Lydeard JR, Cho SE, Harper JW, Schulman BA (2014) Structure of a RING E3 trapped in action reveals ligation mechanism for the ubiquitin-like protein NEDD8. Cell **157:** 1671-1684

Serrano M, Parra S, Alcaraz LD, Guzman P (2006) The ATL gene family from Arabidopsis thaliana and Oryza sativa comprises a large number of putative ubiquitin ligases of the RING-H2 type. Journal of molecular evolution **62:** 434-445

Shao R, Scully SJ, Jr., Yan W, Bentley B, Mueller J, Brown C, Bigelow C, Schwartz LM (2012) The novel lupus antigen related protein acheron enhances the development of human breast cancer. International journal of cancer Journal international du cancer **130:** 544-554

Sheard LB, Tan X, Mao H, Withers J, Ben-Nissan G, Hinds TR, Kobayashi Y, Hsu FF, Sharon M, Browse J, et al (2010) Jasmonate perception by inositol-phosphate-potentiated COI1-JAZ co-receptor. Nature **468:** 400-405

Shindo T, Misas-Villamil JC, Horger AC, Song J, van der Hoorn RA (2012) A role in immunity for Arabidopsis cysteine protease RD21, the ortholog of the tomato immune protease C14. PloS one **7:** e29317

Smoot M, Ono K, Ideker T, Maere S (2011) PiNGO: a Cytoscape plugin to find candidate genes in biological networks. Bioinformatics **27:** 1030-1031

Stone SL, Hauksdottir H, Troy A, Herschleb J, Kraft E, Callis J (2005) Functional analysis of the RING-type ubiquitin ligase family of Arabidopsis. Plant physiology **137:** 13-30

Stone SL, Williams LA, Farmer LM, Vierstra RD, Callis J (2006) KEEP ON GOING, a RING E3 ligase essential for Arabidopsis growth and development, is involved in abscisic acid signaling. The Plant cell **18:** 3415-3428

Takashima O, Tsuruta F, Kigoshi Y, Nakamura S, Kim J, Katoh MC, Fukuda T, Irie K, Chiba T (2013) Brap2 regulates temporal control of NF-kappaB localization mediated by inflammatory response. PloS one **8:** e58911

Tanaka Y, Nishimura K, Kawamukai M, Oshima A, Nakagawa T (2013) Redundant function of two Arabidopsis COPII components, AtSec24B and AtSec24C, is essential for male and female gametogenesis. Planta **238:** 561-575

Thines B, Katsir L, Melotto M, Niu Y, Mandaokar A, Liu G, Nomura K, He SY, Howe GA, Browse J (2007) JAZ repressor proteins are targets of the SCF(COI1) complex during jasmonate signalling. Nature **448:** 661-665

Tsukamoto S, Yokosawa H (2009) Targeting the proteasome pathway. Expert opinion on therapeutic targets **13:** 605-621

Udeshi ND, Mertins P, Svinkina T, Carr SA (2013) Large-scale identification of ubiquitination sites by mass spectrometry. Nature protocols **8:** 1950-1960

Ulmasov T, Larkin RM, Guilfoyle TJ (1995) Arabidopsis expresses two genes that encode polypeptides similar to the yeast RNA polymerase I and III AC40 subunit. Gene **167:** 203-207

Van Leene J, Eeckhout D, Cannoot B, De Winne N, Persiau G, Van De Slijke E, Vercruysse L, Dedecker M, Verkest A, Vandepoele K, et al (2015) An improved toolbox to unravel the plant cellular machinery by tandem affinity purification of Arabidopsis protein complexes. Nature protocols **10:** 169-187

Van Leene J, Eeckhout D, Persiau G, Van De Slijke E, Geerinck J, Van Isterdael G, Witters E, De Jaeger G (2011) Isolation of transcription factor complexes from Arabidopsis cell suspension cultures by tandem affinity purification. Methods in molecular biology **754:** 195-218

Van Leene J, Witters E, Inze D, De Jaeger G (2008) Boosting tandem affinity purification of plant protein complexes. Trends in plant science **13:** 517-520

Voinnet O, Rivas S, Mestre P, Baulcombe D (2003) An enhanced transient expression system in plants based on suppression of gene silencing by the p19 protein of tomato bushy stunt virus. The Plant journal : for cell and molecular biology **33:** 949-956

Wawrzynska A, Christiansen KM, Lan Y, Rodibaugh NL, Innes RW (2008) Powdery mildew resistance conferred by loss of the ENHANCED DISEASE RESISTANCE1 protein kinase is suppressed by a missense mutation in KEEP ON GOING, a regulator of abscisic acid signaling. Plant physiology **148:** 1510-1522

Wettenhall JM, Smyth GK (2004) limmaGUI: A graphical user interface for linear modeling of microarray data. Bioinformatics **20:** 3705-3706

Whittaker CA, Hynes RO (2002) Distribution and evolution of von Willebrand/integrin A domains: widely dispersed domains with roles in cell adhesion and elsewhere. Molecular biology of the cell **13:** 3369-3387

Yumimoto K, Matsumoto M, Oyamada K, Moroishi T, Nakayama KI (2012) Comprehensive identification of substrates for F-box proteins by differential proteomics analysis. Journal of proteome research **11:** 3175-3185

Zhang JX, Wang C, Yang CY, Wang JY, Chen L, Bao XM, Zhao YX, Zhang H, Liu J (2010) The role of Arabidopsis AtFes1A in cytosolic Hsp70 stability and abiotic stress tolerance. The Plant journal : for cell and molecular biology **62:** 539-548

Zhou W, Yao R, Li H, Li S, Yan J (2013) New perspective on the stabilization and degradation of the F-box protein COI1 in Arabidopsis. Plant signaling & behavior **8**

Chapter 4:
A MultiSite Gateway™ vector set for the functional analysis of genes in the model *Saccharomyces cerevisiae*

Astrid Nagels Durand[1], Tessa Moses, Alain Goossens and Laurens Pauwels

Published in:

Astrid Nagels Durand, Tessa Moses, Rebecca De Clercq, Alain Goossens and Laurens Pauwels. **A MultiSite Gateway™ vector set for the functional analysis of genes in the model *Saccharomyces cerevisiae*.** *BMC Molecular Biology* (2012), 13:30

[1] Author contributions: Molecular cloning, expression analysis, data interpretation and writing the manuscript.

SUMMARY

Recombinatorial cloning using the Gateway™ technology has been the method of choice for high-throughput omics projects, resulting in the availability of entire ORFeomes in Gateway™ compatible vectors. The MultiSite Gateway™ system allows combining multiple genetic fragments such as promoter, ORF and epitope tag in one single reaction. To date, this technology has not been accessible in the yeast *Saccharomyces cerevisiae*, one of the most widely used experimental systems in molecular biology, due to the lack of appropriate destination vectors. Here, we present a set of three-fragment MultiSite Gateway™ destination vectors that have been developed for gene expression in *S. cerevisiae* and that allow the assembly of any promoter, open reading frame, epitope tag arrangement in combination with any of four auxotrophic markers and three distinct replication mechanisms. As an example of its applicability, we used yeast three-hybrid to provide evidence for the assembly of a ternary complex of plant proteins involved in jasmonate signalling and consisting of the JAZ, NINJA and TOPLESS proteins. Our vectors make MultiSite Gateway™ cloning accessible in *S. cerevisiae* and implement a fast and versatile cloning method for the high-throughput functional analysis of (heterologous) proteins in one of the most widely used model organisms for molecular biology research.

INTRODUCTION

The model organism *Saccharomyces cerevisiae* has contributed greatly to our current understanding on eukaryotic genes, their products, and their functions. Decades of study have resulted in an extensive knowledge on yeast physiology, genetics, and the molecular functions and interactions of its proteins. Furthermore, this unicellular eukaryotic system is well suited for the study of basic cellular processes which are often conserved in higher eukaryotes. Because of its ease for genetic modification and fast growth, yeast became the system of choice for *in vivo* protein analyses from other eukaryotes. *S. cerevisiae* was used, for example, to perform proteome-wide analysis of the human protein-protein interaction networks (Rual et al., 2005), to systematically analyze protein-DNA interaction networks of the nematode *C. elegans* (Deplancke et al., 2006), and to produce high-value bioactive plant secondary metabolites through metabolic engineering approaches (Ro et al., 2006).

Large scale genomics approaches to uncover protein function are adopted more and more in the current era of systems biology research. To cope with the large amounts of constructs needed, scientists make use of high-throughput cloning technologies, such as the Gateway™ technology (Invitrogen; http://www.invitrogen.com/), which is based on the site-specific recombination system from the bacteriophage lambda that facilitates the integration of the phage's DNA into the *Escherichia coli* chromosome (Hartley et al., 2000). DNA segments that are flanked by the appropriate recombination sites in a standard vector (pENTR) can easily be transferred to a compatible vector (pDEST) for functional analysis (Figure 4-1A). MultiSite Gateway™ uses modified recombination sites to allow the combination of multiple DNA segments in one single *in vitro* recombination reaction. The segments are joined in a pDEST in a predefined order and orientation, maintaining the reading frame and with low risk for mutations (Hartley et al., 2000) (Figure 4-1B). Three-segment MultiSite Gateway™ makes it possible to easily make any combination of a promoter, gene and tag without the need of redesigning new destination vectors for each new experimental approach. The ability to choose a promoter allows varying temporal, spatial, and quantitative control of gene expression, while different possible tags enable the inclusion of fluorescent protein tags for localisation or epitope tags for detection or purification, or the creation of protein chimeras (Figure 4-2). The flexibility introduced by the MultiSite Gateway™ technology is illustrated by the large amount of "building blocks" already made available as pENTR clones by several research groups (Burckstummer et al., 2006; Karimi et al., 2007a; Kwan et al., 2007; Van Leene et al., 2007; Benhamed et al., 2008; Van Leene et al., 2008; Petersen and Stowers, 2011). Existing pENTR collections include ORFeomes from multiple prokaryotic and eukaryotic organisms (ATOME 1 and ATOME 2; Pathogen Functional Genomics Resource Center; The ORFeome Collaboration; Reboul et al., 2003; Dricot et al., 2004; Labaer et al., 2004; Lamesch et al., 2004; Brettin et al., 2005; Gelperin et al., 2005; Schroeder et al., 2005; Matsuyama et

al., 2006; von Brunn et al., 2007; de Chassey et al., 2008; Yilmaz et al., 2009; Rajagopala et al., 2010).

Single-segment pDEST vectors are available for virtually all commonly used systems, such as Drosophila (Akbari et al., 2009). Moreover, for plants an extensive repertoire of pDEST for two- and three-segment MultiSite Gateway™ has been established (Karimi et al., 2007b). Three-segment MultiSite Gateway™ destination vectors are also available for Gram-positive bacteria (Perehinec et al., 2007). In *S. cerevisiae*, single-segment pDEST vectors are available for yeast two-hybrid screens (Invitrogen), and two-segment (promoter::ORF) MultiSite Gateway™ vectors have been described (Cheo et al., 2004). An extensive set of single-fragment Gateway™ vectors was constructed, allowing N-terminal fusions with four fluorescent tags, and C-terminal fusions with five different fluorescent tags, an affinity tag and an epitope tag under the control of the inducible GAL1 or constitutive GPD promoter (Alberti et al., 2007). Alternatively, tags that are not present in this vector set can be fused to the gene of interest through 2-step PCR fusion (Atanassov et al., 2009) before performing the BP reaction. However, to our knowledge no three-segment MultiSite Gateway™ pDEST vectors exist for *S. cerevisiae* to date. As a consequence, a large number of commonly used protein tags already available as pENTR clones are not readily applicable in the organism that - together with *E. coli* - is the workhorse of molecular biology.

In this paper we present a set of eleven functionally validated three-segment MultiSite Gateway™ pDEST vectors for use in *S. cerevisiae*. The vector set features the four most commonly used auxotrophic markers for selection of yeast transformants combined with three different replication mechanisms. The presence of the CYC1 terminator in these vectors allows construction of any promoter::ORF:tag combination. In addition, a number of useful entry clones harbouring commonly used yeast promoters and entry clones with protein tags to be used with these pDESTs are presented and validated. These vectors have been appended to our collection of 'Gateway™ vectors for functional studies' and can be ordered through the website http://gateway.psb.ugent.be/. Finally, we illustrate the applicability of this vector set by confirming the formation of a ternary complex between the jasmonate ZIM-domain (JAZ), the Novel Interactor of JAZ (NINJA) and the TOPLESS (TPL) proteins, with NINJA acting as a bridging protein. This complex was previously shown to be involved in jasmonate signalling in the model plant Arabidopsis (*Arabidopsis thaliana*) (Pauwels et al., 2010).

RESULTS AND DISCUSSION

Construction of MultiSite Gateway™ vectors

The MultiSite Gateway™ cassette of pKm43GW (http://gateway.psb.ugent.be/) flanked by *attR4* and *attR3* sites, was PCR amplified adding *Xho*I and *Sac*I restriction sites (Supplementary Table S1). The amplification product was subsequently cloned into the *Xho*I and *Sac*I sites present in the backbones of the vectors of the pAG-series (Alberti et al., 2007). This step replaced the original Gateway™ cassette and the eukaryotic promoter from the pAG vectors, while maintaining the CYC1 terminator. Ligation products were transformed into *ccdB* resistant *E. coli* cells (One shot *ccdB* survival™, Invitrogen). The pAG vectors contain an ampicillin resistance gene for selection in *E. coli*, one of four different auxotrophic selection markers *(HIS3, LEU2, TRP1*, and *URA3*) and one of three different replication determinants (2µ ori, CEN, or Integrating) thus giving rise to a MultiSite Gateway™ vector set (Figure 4-1C) for expression in *S. cerevisiae* (see Table 4-1 for nomenclature). We did not succeed in creating the Integrating vector with the *HIS3* autotrophic marker (Table 4-1).

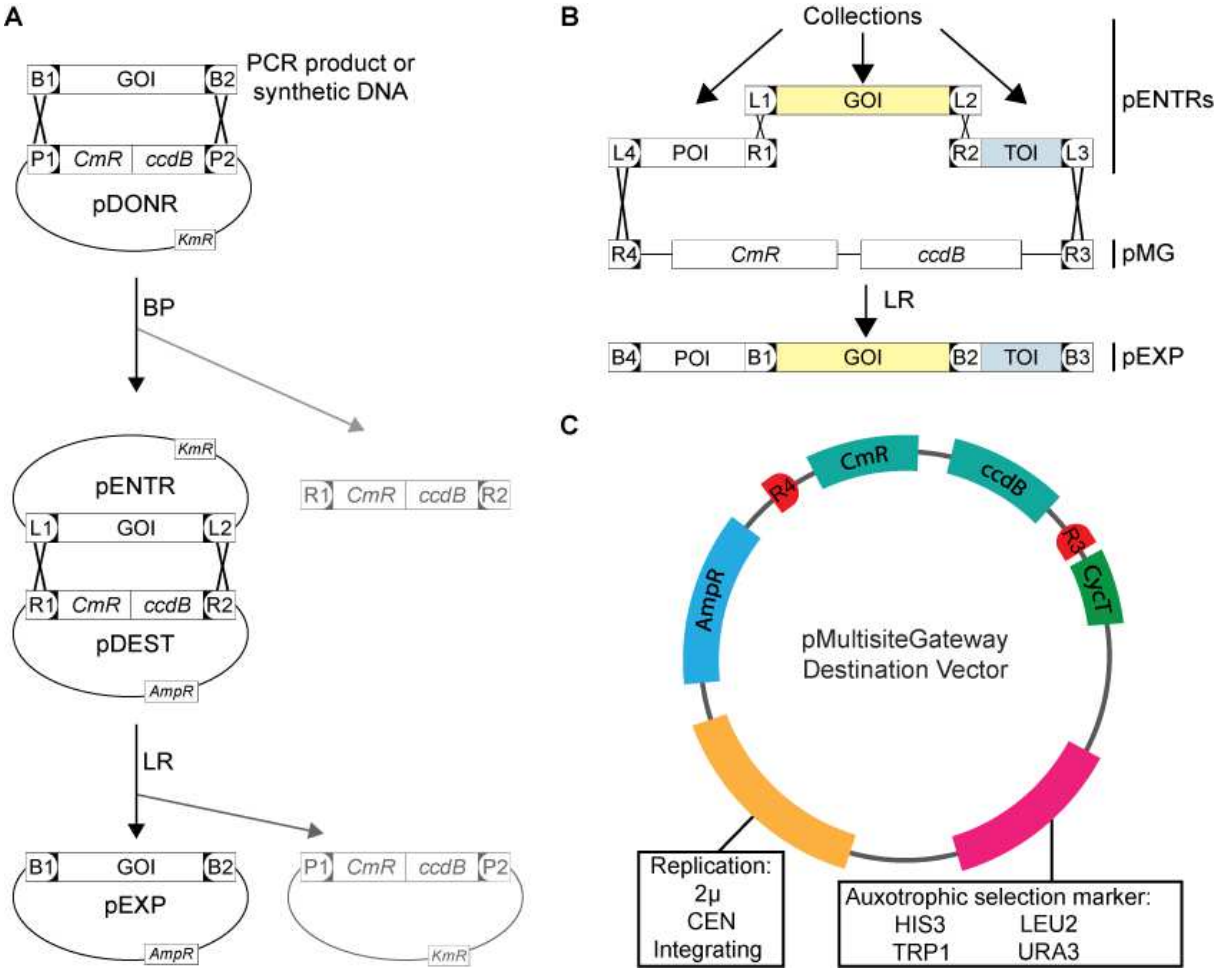

Table 4-1. Nomenclature of the *S. cerevisiae* MultiSite Gateway™ pDEST vectors.

Name*	Replication	Selectable marker
pMG304	Integrating	TRP1
pMG305	Integrating	LEU2
pMG306	Integrating	URA3
pMG413	CEN	HIS3
pMG414	CEN	TRP1
pMG415	CEN	LEU2
pMG416	CEN	URA3
pMG423	2µ	HIS3
pMG424	2µ	TRP1
pMG425	2µ	LEU2
pMG426	2µ	URA3

*pMG*XYZ* where MG indicates the presence of the MultiSite Gateway™ cassette; *X* stands for the presence (4) or absence (3) of replication determinants on the vector; *Y* stands for the replication determinant: Integrating (0), CEN (1) or 2µ (2); *Z* indicates the auxotrophic selection marker: HIS3 (3), TRP1 (4), LEU2 (5) or URA3 (6).

Testing the versatility of the system

To illustrate the flexibility of this vector collection, we took advantage of a few "building blocks" for MultiSite Gateway™ cloning that were available in-house as entry clones (Figure 4-2, http://gateway.psb.ugent.be/). One of the assets of MultiSite Gateway™ destination vectors is that any promoter of interest can be used, provided it is available as an entry clone flanked by *attL4* and *attR1* sites. To achieve this, we cloned two constitutively active promoters (pGPD/TDH3 and pADH1) and a galactose-inducible promoter (pGAL1) into pDONR P4-P1R (Invitrogen). The inducibility of the GAL1 promoter was verified by expression in yeast of a heterologous Arabidopsis gene fused to a NLS-FLAG-HIS tag under the control of the GAL1 promoter using pMG416 (Figure 4-3A).

Figure 4-1. Schematic overview of (MultiSite) Gateway™ cloning and properties of the constructed destination vectors. (A) Overview of the Gateway™ cloning procedure. Attachment of *attB* sites to a DNA segment of choice, often generated by PCR or as synthetic DNA, allows recognition by the BP Clonase™ and recombination into a donor vector (pDONR) containing *attP* sites, yielding an entry clone (pENTR) carrying *attL* sites. The DNA segment in the pENTR clone can then be transferred to a destination vector (pDEST) by recombination between *attL* and *attR* sites present on the pDEST vector mediated by the LR ClonaseTM. This yields an expression clone (pEXP) in which the DNA segment again becomes flanked by *attB* sites. Positive selection of pENTR and pEXP clones on medium containing appropriate antibiotics together with negative selection of starting products and by-products (shown in grey) based on the presence of a negative (*ccdB*) selection marker between the recombination sites (Gateway™ Cassette) further increases the efficiency of the system. (B) A combination of existing pENTRs, or new pENTRs, are easily assembled in a single MultiSite Gateway™ reaction catalyzed by the LR II Clonase™ Plus using pMG as destination vector. (C) Schematic representation of the MultiSite Gateway™ compatible vector set (pMG) for transformation of *S. cerevisiae.*

GOI, POI and TOI indicate gene, promoter and tag of interest, respectively. CmR, AmpR and KmR indicate chloramphenicol, ampicillin and kanamycin resistance, respectively. B1-B4, P1-P2, L1-L4 and R1-R4 stand for the respective *att* sites. CycT indicates the *CYC1* terminator on the vector's backbone.

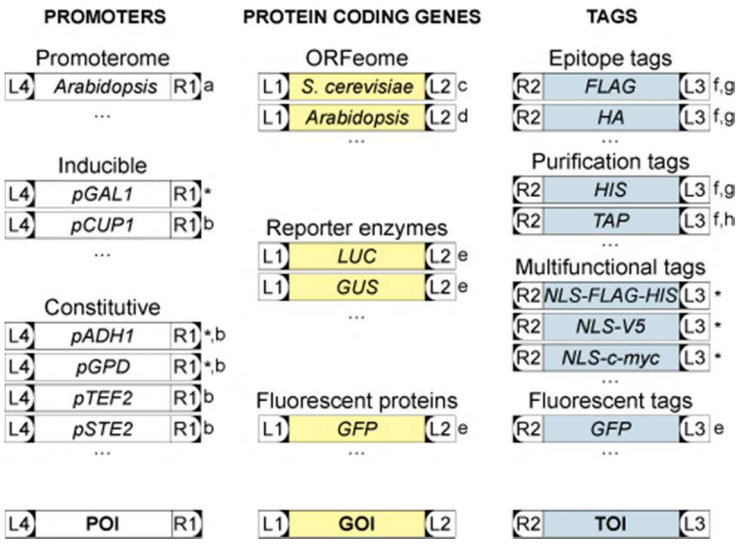

Figure 4-2. Flexibility of the MultiSite Gateway™ cloning system

The flexibility of the MultiSite Gateway™ system is illustrated by the ample possibilities to combine any gene of interest (GOI) with any promoter of interest (POI) and tag of interest (TOI), depending on the experimental needs. Many of such sequences, including whole ORFeomes (cloned without STOP codon) of several model organisms (ATOME 1 and ATOME 2; Gelperin et al., 2005; von Brunn et al., 2007; Yilmaz et al., 2009) and a broad range of tags (Burckstummer et al., 2006; Karimi et al., 2007a; Van Leene et al., 2007; Van Leene et al., 2008) are already available in suitable pDONR vectors. L1-L4 and R1-R2 stand for the *att* sites *attL1-attL4* and *attR1-attR2*, respectively.

Asterisks mark constructs generated in this study, lower case letters indicate constructs generated previously by others: a (Benhamed et al., 2008), b (Cheo et al., 2004), c (Gelperin et al., 2005), d (ATOME 1 and ATOME 2; Dricot et al., 2004), e (Karimi et al., 2007a), f (Van Leene et al., 2008), g (Van Leene et al., 2007), h (Burckstummer et al., 2006).

Another advantage of the MultiSite Gateway™ system is that several different tag sequences are readily available (Figure 4-2) and can easily be introduced to acquire translational fusions, since the *att* sites do not disturb the reading frame. For proof-of-concept, we cloned different plant genes (without STOP codon) in a C-terminal translational fusion with either a V5, c-myc, or FLAG-HIS tag. To make these constructs compatible with protein interaction studies in yeast, we additionally fused each epitope tag with a nuclear localization signal (NLS) derived from SV40, thereby creating the NLS-3xV5, NLS-3xc-myc, and NLS-3xFLAG-6xHIS tags, respectively. Such constructs allow avoiding false negative experimental outcomes that result from protein localisation in different cellular compartments, for instance. Tagged plant proteins were expressed in yeast under the control of the constitutive GPD or ADH1 promoters in different vectors from our set. Total protein extracts were obtained and the expressed proteins were visualized through immunoblot analysis (Figure 4-3B). The (NLS)FLAG-HIS tag is particularly suitable when protein purification under denaturing conditions is needed, while, at the same time, low background detection on immunoblots is desired.

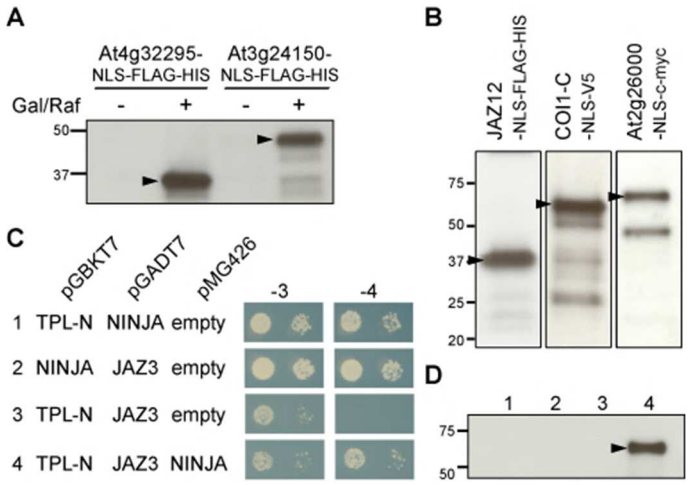

Figure 4-3. Versatility of the newly generated MultiSite Gateway™ vector set.

(A) Inducibility of the pGAL1 promoter. Arabidopsis genes At4g32295 and At3g24150 were expressed in yeast under the control of the pGAL1 promoter and fused with an NLS-FLAG-HIS tag using the pMG416 vector. After total protein extraction, expression was verified in inducing (+) and non-inducing (-) medium through immunoblot analysis with anti-FLAG antibodies. (B) Functionality of newly developed C-terminal translational fusion epitope tags. Yeasts were transformed with pMG425-ADH1::JAZ12:NLS-FLAG-HIS, pMG423-GPD::COI1-C:NLS-V5 where COI1-C is a truncated version of COI1, or pMG423-GPD::At2g26000:NLS-c-myc. Expression of the different constructs was verified with immunoblot analysis of total protein extracts with anti-FLAG, anti-V5 and anti-c-myc antibodies, respectively. (C) Interaction of proteins in the trimeric JAZ3-TPL-NINJA complex in Y3H assays. Transformed yeasts were spotted in 10-fold and 100-fold dilutions on control medium (-3: SD-Leu-Trp-Ura) and selective medium (-4: SD-His-Leu-Trp-Ura). Gene constructs in the pGBKT7 and pGADT7 vectors carry the DNA-binding domain or the transcription activation domain, respectively, in contrast to constructs expressed in pMG426, which do not carry DNA-binding or transcription activation domains. (D) Verification of expression of NINJA:NLS-FLAG-HIS in the Y3H set-ups shown in panel C. After total protein extraction, NINJA:NLS-FLAG-HIS was detected through immunoblot analysis with anti-FLAG antibodies. Arrowheads indicate the fusion protein.

To express C-terminal translational fusions by means of our promoters, tags and destination vectors, entry vectors containing the GOI should be cloned with a start codon and without a stop codon, and the manufacturer's guidelines regarding the reading frame should be adopted (http://www.invitrogen.com). Organisms for which ORFeome collections contain vectors that match these criteria include several bacterial collections [*Brucella melitensis* (Dricot et al., 2004), *Pseudomonas aeruginosa* (Labaer et al., 2004), *Bacillus anthracis*, *Francisella tularensis*, *Helicobacter pylori*, *Mycobacterium tuberculosis*, *Rickettsia prowazekii*, *Staphylococcus aureus*, *Streptococcus pneumoniae*, *Vibrio cholerae* (Pathogen Functional Genomics Resource Center)], human and mouse (The ORFeome Collaboration), plants [Arabidopsis (ATOME 1 and ATOME 2), maize, sorghum, sugarcane, rice (Yilmaz et al., 2009)], viruses (von Brunn et al., 2007) and yeasts [*S. cerevisiae* (Gelperin et al., 2005) and *Schizosaccharomyces pombe* (Matsuyama et al., 2006)]. Caution is advised since some ORFeome collections contain entry clones both with and without stop codon (The ORFeome Collaboration, ATOME1 and ATOME 2). ORFeome collections that comprise only GOI's provided with a stop codon, as is the case for some bacterial and viral ORFeomes [*Neisseria gonorrhoeae* (Brettin et al., 2005), *Sinorhizobium meliloti* (Schroeder et al., 2005), *Yersinia pestis* (Pathogen Functional Genomics Resource Center), and Hepatitis C (de Chassey et al.,

2008)] are not compatible with our vectors. Other ORFeomes in which the GOI is cloned without a start and without a stop codon [*Caenorhabditis elegans* (Reboul et al., 2003; Lamesch et al., 2004), *E. coli* (Rajagopala et al., 2010)], are not compatible with our current promoters but can be used for expression of C-terminal translational fusions with our vectors provided the promoter is cloned followed by a start codon. Since this ORFeome list is non-exhaustive and, as described above, different approaches are used when cloning the GOI, the compatibility of available pENTR collections should always be corroborated either *in silico* before assembling the different sequences into expression vectors or through epitope tag detection in immunoblots. Finally, the destination vector set presented here also allows expression of N-terminal fusions, provided the *att* sites flanking the different fusion components are adapted accordingly.

Value of the vector set

The value of this vector set was exemplified by a yeast three-hybrid (Y3H) experiment, in which we investigated the formation of the ternary protein complex by the Arabidopsis JAZ3, NINJA, and TPL proteins. We have proposed recently that the adaptor protein NINJA bridges the JAZ proteins to TPL proteins and thereby forms a repressor complex that blocks the cellular programs regulated by the jasmonates, ubiquitous plant hormones that regulate various aspects of plant growth, development, and survival (Pauwels et al., 2010). TPL interacts with the ETHYLENE RESPONSIVE FACTOR–associated amphiphilic repression (EAR) motif that is present in NINJA (Pauwels et al., 2010) but absent in most JAZ proteins, including JAZ3. Some JAZ proteins however, i.e. JAZ5 to JAZ8, contain EAR motifs themselves and are capable of direct interaction with TPL (Pauwels and Goossens, 2011; Causier et al., 2012; Shyu et al., 2012).

The N-terminal domain of TPL contains the LisE and CTHL domains and was previously shown to be essential for binding the EAR motif in Aux/IAA proteins (Szemenyei et al., 2008). Therefore we cloned this part (denominated TPL-N) as a bait protein for Y2H. In agreement with the proposed models, the interaction of TPL-N with NINJA was confirmed but TPL-N could not interact with JAZ3 (Figure 4-3C).

Commonly used Y2H vectors such as pGADT7 and pGBKT7 (Clontech) are designed such that the bait and prey fusion proteins are targeted to the same subcellular compartment (i.e. nucleus) and are equipped with an epitope tag, HA and c-myc, respectively, allowing easy confirmation of expression through immunoblot. To verify whether NINJA can connect EAR-lacking JAZs with TPL, as previously proposed (Pauwels et al., 2010), we performed a Y3H assay in which we expressed NINJA, under control of a constitutive promoter (pGPD), as a bridging protein. Hereby we used the MultiSite Gateway™ vector pMG426 (Table 4-1) that carries the URA3 auxotrophic marker that is often still available in yeast strains used for Y2H. As a C-

terminal tag we used the NLS-FLAG-HIS tag. Only when NINJA is co-expressed, yeast growth was observed on selective –His medium, indicating that interaction between JAZ3 and TPL requires the involvement of NINJA (Figure 4-3C and 4-3D).

DISCUSSION AND CONCLUSION

We have successfully constructed a set of three-segment MultiSite Gateway™ destination vectors for *S. cerevisiae*. Our findings make high-throughput recombinatorial cloning of multiple genetic segments in one single reaction accessible in one of the most widely used experimental model systems in molecular biology. The availability of different auxotrophic markers in this vector set, together with the large amount of existing compatible building blocks for MultiSite Gateway™ cloning already available in several research groups, creates a versatile utility for these vectors. In addition, we have cloned two constitutive and one inducible yeast promoter in appropriate pENTR vectors and constructed three novel epitope tags, each including a NLS, which are suitable for interaction studies in yeast.

The usefulness of the MultiSite Gateway™ vectors was demonstrated in a Y3H assay with which we corroborated the hypothesis that NINJA connects the JAZ proteins with the co-repressor TPL. This trimeric complex mediates repression of jasmonate responsive genes in the absence of the hormone (Pauwels et al., 2010).

Implementation of the vector set presented in this article, together with the cloning of more promoters and (epitope) tags according to personal experimental needs, will facilitate gene functional studies and contribute to the high-throughput versatile expression of heterologous (plant) proteins in yeast.

EXPERIMENTAL PROCEDURES

Strains and growth conditions

The *E. coli* strains used were either the *ccdB* resistant strain DB3.1 (Invitrogen) or the *ccdB* sensitive strain DH5α. Both were grown at 37°C in LB broth medium with appropriate antibiotics. Several different commonly used yeast lab-strains were grown at 30°C in synthetic defined medium (Clontech) lacking the appropriate amino acids.

MultiSite Gateway™ cloning and yeast transformation

MultiSite LR reactions were performed in 10 µL total volume containing 10 fmoles of each entry vector, 20 fmoles of destination vector, and 2 µL LR II Clonase™ Plus (Invitrogen). The reaction was incubated overnight at 25°C. After proteinase treatment, the mix was transformed into *E. coli* DH5α. Colonies that grew on selective medium were picked and the insert was sequenced using M13 forward and reverse primers (Additional file 1). To maintain the reading frame, necessary for expression of translational fusions, MultiSite Gateway™ cloning was carried out according to the manufacturer's guidelines (http://www.invitrogen.com). Note that in order to produce C-terminal translational fusions, the ORFs used should be without STOP codon. A convenient method to obtain simultaneously clones of ORFs with and without STOP codon has been described (Underwood et al., 2006).

Competent yeast cells were transformed using the LiAc/SS carrier DNA/PEG method (Gietz and Schiestl, 2007).

Promoter cloning

The *attB4* and *attB1* sites were introduced in the primers used for promoter amplification (Supplementary Table S1). A PCR was performed using Phusion High-Fidelity PCR Kit (Thermo Fisher Scientific) on 50 ng of pBEVY-A, pBEVY-GL (Miller et al., 1998), and pGAD424 (Clontech) as template for the GPD, GAL, and ADH1 promoters, respectively. PCR products were purified with the GeneJET Gel Extraction kit (Fermentas). BP reactions were performed in a total volume of 5 µl containing 1 µl enzyme, 300 ng pDONR P4-P1R (Invitrogen), and 30 ng of PCR product. Incubation and subsequent treatments were the same as those for MultiSite LR reactions.

Epitope-tag design and immunoblot analysis

Synthetic DNA encoding NLS-3xFLAG-6xHIS, NLS-3xV5, and NLS-3xc-myc flanked by *attB2R-attB3* sites were designed in Vector NTI® (Invitrogen) and ordered from GenScript as clones in the pUC57 vector. These tags were introduced into pDONR P2R-P3 through a BP reaction. The resulting entry vectors were transformed into *E. coli* and sequence verified.

Total yeast protein extracts were obtained as described (Hampton and Rine, 1994) and concentration quantified using the Bio-Rad Protein Assay (Bio-Rad). Samples were combined with 5x Laemmli loading buffer and denatured for 10 minutes at 95ºC. Subsequently, 30 µg total protein was loaded on a 4-15 % Mini-PROTEAN® TGX™ Precast Gel (Bio-Rad) and transferred to a PVDF membrane using the Trans-Blot Turbo transfer system (Bio-Rad). Detection was performed using the following primary antibodies: anti-FLAG (Sigma), anti-c-myc-HRP (Invitrogen), anti-HA (Roche), and anti-V5 (Sigma).

Yeast two- and three-hybrid

The primers were designed to clone the ORF corresponding to TPL-N with and without STOP codon (Supplementary Table S1) (Underwood et al., 2006). The entry clones pEN-L4-*GPD*-R1, pEN-R2-*NLS-3xFLAG-6xHis*-L3, and pEN-L1-*NINJA*-L2 were recombined by MultiSite Gateway™ LR reaction with pMG426 as destination vector. Construction of the pGADT7- and pGBKT7-clones, and the Y2H and Y3H were carried out as described (Pauwels et al., 2010) except that transformed yeast cells (strain PJ69-4a) were selected on SD-Ura-Trp-Leu.

REFERENCES

Akbari OS, Oliver D, Eyer K, Pai CY (2009) An Entry/Gateway cloning system for general expression of genes with molecular tags in *Drosophila melanogaster*. BMC cell biology **10:** 8

Alberti S, Gitler AD, Lindquist S (2007) A suite of Gateway cloning vectors for high-throughput genetic analysis in Saccharomyces cerevisiae. Yeast **24:** 913-919

Atanassov, II, Etchells JP, Turner SR (2009) A simple, flexible and efficient PCR-fusion/Gateway cloning procedure for gene fusion, site-directed mutagenesis, short sequence insertion and domain deletions and swaps. Plant methods **5:** 14

ATOME 1 and ATOME 2 http://www-urgv.versailles.inra.fr/atome/index.htm

Benhamed M, Martin-Magniette ML, Taconnat L, Bitton F, Servet C, De Clercq R, De Meyer B, Buysschaert C, Rombauts S, Villarroel R, et al (2008) Genome-scale Arabidopsis promoter array identifies targets of the histone acetyltransferase GCN5. The Plant journal : for cell and molecular biology **56:** 493-504

Brettin T, Altherr MR, Du Y, Mason RM, Friedrich A, Potter L, Langford C, Keller TJ, Jens J, Howie H, et al (2005) Expression capable library for studies of Neisseria gonorrhoeae, version 1.0. BMC microbiology **5:** 50

Burckstummer T, Bennett KL, Preradovic A, Schutze G, Hantschel O, Superti-Furga G, Bauch A (2006) An efficient tandem affinity purification procedure for interaction proteomics in mammalian cells. Nature methods **3:** 1013-1019

Causier B, Ashworth M, Guo W, Davies B (2012) The TOPLESS interactome: a framework for gene repression in Arabidopsis. Plant physiology **158:** 423-438

Cheo DL, Titus SA, Byrd DRN, Hartley JL, Temple GF, Brasch MA (2004) Concerted assembly and cloning of multiple DNA segments using in vitro site-specific recombination: functional analysis of multi-segment expression clones. Genome research **14:** 2111-2120

de Chassey B, Navratil V, Tafforeau L, Hiet MS, Aublin-Gex A, Agaugue S, Meiffren G, Pradezynski F, Faria BF, Chantier T, et al (2008) Hepatitis C virus infection protein network. Molecular systems biology **4:** 230

Deplancke B, Mukhopadhyay A, Ao W, Elewa AM, Grove CA, Martinez NJ, Sequerra R, Doucette-Stamm L, Reece-Hoyes JS, Hope IA, et al (2006) A gene-centered *C. elegans* protein-DNA interaction network. Cell **125:** 1193-1205

Dricot A, Rual JF, Lamesch P, Bertin N, Dupuy D, Hao T, Lambert C, Hallez R, Delroisse JM, Vandenhaute J, et al (2004) Generation of the Brucella melitensis ORFeome version 1.1. Genome research **14:** 2201-2206

Gelperin DM, White MA, Wilkinson ML, Kon Y, Kung LA, Wise KJ, Lopez-Hoyo N, Jiang L, Piccirillo S, Yu H, et al (2005) Biochemical and genetic analysis of the yeast proteome with a movable ORF collection. Genes & development **19:** 2816-2826

Gietz RD, Schiestl RH (2007) High-efficiency yeast transformation using the LiAc/SS carrier DNA/PEG method. Nature protocols **2:** 31-34

Hampton RY, Rine J (1994) Regulated degradation of HMG-CoA reductase, an integral membrane protein of the endoplasmic reticulum, in yeast. The Journal of cell biology **125:** 299-312

Hartley JL, Temple GF, Brasch MA (2000) DNA cloning using in vitro site-specific recombination. Genome research **10:** 1788-1795

Karimi M, Bleys A, Vanderhaeghen R, Hilson P (2007a) Building blocks for plant gene assembly. Plant physiology **145:** 1183-1191

Karimi M, Depicker A, Hilson P (2007b) Recombinational cloning with plant gateway vectors. Plant physiology **145:** 1144-1154

Kwan KM, Fujimoto E, Grabher C, Mangum BD, Hardy ME, Campbell DS, Parant JM, Yost HJ, Kanki JP, Chien CB (2007) The Tol2kit: a multisite gateway-based construction kit for Tol2 transposon transgenesis constructs. Developmental dynamics : an official publication of the American Association of Anatomists **236:** 3088-3099

Labaer J, Qiu Q, Anumanthan A, Mar W, Zuo D, Murthy TV, Taycher H, Halleck A, Hainsworth E, Lory S, et al (2004) The Pseudomonas aeruginosa PA01 gene collection. Genome research **14:** 2190-2200

Lamesch P, Milstein S, Hao T, Rosenberg J, Li N, Sequerra R, Bosak S, Doucette-Stamm L, Vandenhaute J, Hill DE, et al (2004) C. elegans ORFeome version 3.1: increasing the coverage of ORFeome resources with improved gene predictions. Genome research **14:** 2064-2069

Matsuyama A, Arai R, Yashiroda Y, Shirai A, Kamata A, Sekido S, Kobayashi Y, Hashimoto A, Hamamoto M, Hiraoka Y, et al (2006) ORFeome cloning and global analysis of protein localization in the fission yeast Schizosaccharomyces pombe. Nature biotechnology **24:** 841-847

Miller CA, 3rd, Martinat MA, Hyman LE (1998) Assessment of aryl hydrocarbon receptor complex interactions using pBEVY plasmids: expressionvectors with bi-directional promoters for use in Saccharomyces cerevisiae. Nucleic acids research **26:** 3577-3583

The ORFeome Collaboration http://www.orfeomecollaboration.org/

Pathogen Functional Genomics Resource Center http://pfgrc.jcvi.org/

Pauwels L, Barbero GF, Geerinck J, Tilleman S, Grunewald W, Perez AC, Chico JM, Vanden Bossche R, Sewell J, Gil E, et al (2010) NINJA connects the co-repressor TOPLESS to jasmonate signalling. Nature **464:** 788-791

Pauwels L, Goossens A (2011) The JAZ proteins: a crucial interface in the Jasmonate signaling cascade. The Plant cell **23:** 3089-3100

Perehinec TM, Qazi SN, Gaddipati SR, Salisbury V, Rees CE, Hill PJ (2007) Construction and evaluation of multisite recombinatorial (Gateway) cloning vectors for Gram-positive bacteria. BMC molecular biology **8:** 80

Petersen LK, Stowers RS (2011) A Gateway MultiSite recombination cloning toolkit. PloS one **6:** e24531

Rajagopala SV, Yamamoto N, Zweifel AE, Nakamichi T, Huang HK, Mendez-Rios JD, Franca-Koh J, Boorgula MP, Fujita K, Suzuki K, et al (2010) The Escherichia coli K-12 ORFeome: a resource for comparative molecular microbiology. BMC genomics **11:** 470

Reboul J, Vaglio P, Rual JF, Lamesch P, Martinez M, Armstrong CM, Li S, Jacotot L, Bertin N, Janky R, et al (2003) *C. elegans* ORFeome version 1.1: experimental verification of the genome annotation and resource for proteome-scale protein expression. Nature genetics **34:** 35-41

Ro DK, Paradise EM, Ouellet M, Fisher KJ, Newman KL, Ndungu JM, Ho KA, Eachus RA, Ham TS, Kirby J, et al (2006) Production of the antimalarial drug precursor artemisinic acid in engineered yeast. Nature **440:** 940-943

Rual JF, Venkatesan K, Hao T, Hirozane-Kishikawa T, Dricot A, Li N, Berriz GF, Gibbons FD, Dreze M, Ayivi-Guedehoussou N, et al (2005) Towards a proteome-scale map of the human protein-protein interaction network. Nature **437:** 1173-1178

Schroeder BK, House BL, Mortimer MW, Yurgel SN, Maloney SC, Ward KL, Kahn ML (2005) Development of a functional genomics platform for Sinorhizobium meliloti: construction of an ORFeome. Applied and environmental microbiology **71:** 5858-5864

Shyu C, Figueroa P, Depew CL, Cooke TF, Sheard LB, Moreno JE, Katsir L, Zheng N, Browse J, Howe GA (2012) JAZ8 Lacks a Canonical Degron and Has an EAR Motif That Mediates Transcriptional Repression of Jasmonate Responses in Arabidopsis. The Plant cell

Szemenyei H, Hannon M, Long JA (2008) TOPLESS mediates auxin-dependent transcriptional repression during Arabidopsis embryogenesis. Science **319:** 1384-1386

Underwood BA, Vanderhaeghen R, Whitford R, Town CD, Hilson P (2006) Simultaneous high-throughput recombinational cloning of open reading frames in closed and open configurations. Plant biotechnology journal **4:** 317-324

Van Leene J, Stals H, Eeckhout D, Persiau G, Van De Slijke E, Van Isterdael G, De Clercq A, Bonnet E, Laukens K, Remmerie N, et al (2007) A tandem affinity purification-based technology platform to study the cell cycle interactome in Arabidopsis thaliana. Molecular & cellular proteomics : MCP **6:** 1226-1238

Van Leene J, Witters E, Inzé D, De Jaeger G (2008) Boosting tandem affinity purification of plant protein complexes. Trends in plant science **13:** 517-520

von Brunn A, Teepe C, Simpson JC, Pepperkok R, Friedel CC, Zimmer R, Roberts R, Baric R, Haas J (2007) Analysis of intraviral protein-protein interactions of the SARS coronavirus ORFeome. PloS one **2:** e459

Yilmaz A, Nishiyama MY, Jr., Fuentes BG, Souza GM, Janies D, Gray J, Grotewold E (2009) GRASSIUS: a platform for comparative regulatory genomics across the grasses. Plant physiology **149:** 171-180

Chapter 5:
PICOT1 is a target of the E3 ubiquitin ligases RGLG3 and RGLG4

Astrid Nagels Durand[1], Sabrina Iñigo, Andres Ritter, Takayuki Tohge, Elisa Iniesto, Kris Gevaert, Alisdair Fernie, Geert De Jaeger, Laurens Pauwels and Alain Goossens

Manuscript in preparation

[1] Author contributions: cloning and mutagenesis, tandem affinity purifications, yeast two-hybrid analyses, generation of transgenic lines, *in vivo* degradation assays, localization studies, data interpretation and writing.

SUMMARY

Many enzymes depend on iron-sulfur (Fe-S) cofactors for their activity. The human monothiol glutathioredoxin PKCθ-interacting Protein (PICOT/GRX3) is a putative Fe-S carrier protein delivering Fe-S to apo-proteins in the nucleus and cytosol. However, information on regulation of PICOT and its targets is scarce. Here, we identified and characterized *PICOT1/GRXS17*, the ortholog of *PICOT* in the model plant *Arabidopsis thaliana*. PICOT1 was found as a target of RGLG3 and RGLG4, two E3 ubiquitin ligases involved in stress signalling. RGLG3/4 mediated poly-ubiquitination and degradation of PICOT1. Nucleo-cytoplasmic PICOT1 was found to be part of Fe-S assembly complexes and contributed to the maturation of the Fe-S protein XANTHINE DEHYDROGENASE1 (XDH1) that is involved in purine degradation. In contrast to its human ortholog, however, PICOT1 was not essential for the maturation of nuclear and cytoplasmic Fe-S proteins. Instead, the plant ortholog of PICOT was found in a complex with various proteins involved in at least two unrelated processes: purine catabolism and tRNA modification. In accordance with a role in XDH1 maturation, plants with reduced PICOT1 protein levels accumulated purine catabolism intermediaries and showed early onset of senescence. In addition, seedlings with mutations in genes involved in tRNA modifications phenotypically resembled *picot1* knock-out mutants confirming a general role for PICOT1 in this process.

INTRODUCTION

As in any eukaryote, abundance of proteins in plants is often regulated by the ubiquitin (Ub) system. The 76-amino acid polypeptide Ub is covalently attached to target proteins by an enzymatic cascade involving an E1 Ub activating enzyme, a E2 Ub conjugating enzyme and finally an E3 Ub ligase in a process called ubiquitination (Callis, 2014). Ub itself can further be ubiquitinated on one of its lysine residues forming a polyubiquitin chain. Most often in plants this is lysine (K) 48, leading to a signal for degradation by the 26S proteasome. However, other linkages are also possible in plants, leading to different outcomes (Kim et al., 2013). The E2 enzyme constitutes the primary determinant of Ub chain linkage (Ye and Rape, 2009), whereas the specificity of the site of ubiquitination and the target protein is dependent on the E3 ligase (Mattiroli and Sixma, 2014). The most expanded family of plant E3 ligases is characterized by the presence of a RING domain, which mediates interaction of the E3 with the E2∼Ub conjugate by interacting with both the E2 and the donor ubiquitin (Plechanovova et al., 2012). Other domains present in RING E3 ligases or their complexes mediate interaction with target proteins (Deshaies and Joazeiro, 2009).

One subfamily of plant RING-type E3 ligases is the RING DOMAIN LIGASE (RGLG) family that contains five members in the model plant *Arabidopsis thaliana* and is characterized by the presence of a von Willebrand factor type A or copine domain in addition to the characteristic HCa-type RING-domain (Stone et al., 2005; Zhang et al., 2012). *RGLG1* and *RGLG2* function redundantly in Arabidopsis and seedlings with loss-of-function mutations in both genes have severely altered phenotypes such as loss of apical dominance, altered phyllotaxy and leaf shape and increased cell size (Yin et al., 2007). While no ubiquitination targets of RGLG3/4/5 are known presently, two targets of RGLG2 have been identified. First, the auxin transporter PIN2 was shown to be K63 poly-ubiquitinated *in vivo* and this ubiquitination was affected in *rglg1rglg2* double knock-outs (KOs) (Leitner et al., 2012). RGLG1 and RGLG2 were localized predominantly to the plasma membrane, like PIN2 proteins, and this was mediated by a myristoylation site present in their N-terminus (Yin et al., 2007). Second, RGLG1 and RGLG2 were shown to translocate from the plasma membrane to the nucleus under salt stress, where they both target the AP2/ERF family transcription factor ERF53 for proteasomal degradation. ERF53 was shown to be mono-ubiquitinated *in vitro* by RGLG2 and human UbcH5c/UBE2D3 (Cheng et al., 2012).

Two other members of the RGLG family, RGLG3 and RGLG4, have been associated with JA-signalling (Zhang et al., 2012). *RGLG3* and *RGLG4* were shown to function redundantly as double KO *rglg3rglg4* seedlings were less sensitive to JA-mediated root growth inhibition. Alternatively, overexpression of either RGLG3 or RGLG4 led to enhanced sensitivity to JA-mediated root growth inhibition, and this was dependent on COI1 (Zhang et al., 2012). Recently, RGLG3/4 were also reported to regulate the mycotoxin Fumonisin B1 (FB1)-

triggered programmed cell death (PCD) elicited during infection with the fungal pathogen *Fusarium moniliforme* (Zhang et al., 2015). Nothing is known yet on the activity and role of RGLG5.

RGLG1/2, but not RGLG3/4, were found to interact in yeast-two hybrid (Y2H) with the E2 UBC35 (Yin et al., 2007; Zhang et al., 2012). UBC35/UBC13a and UBC36/UBC13b are known to interact with the E2-like proteins UEV1-4 to mediate K63 Ub-chain formation (Michelle et al., 2009; Callis, 2014). Accordingly RGLG2 mediated K63 poly-Ub chain assembly *in vitro* with UBC35 (Yin et al., 2007). In plants, UBC35/36 have been involved in the response to iron-deficiency, together with RGLG1/2 (Pan and Schmidt, 2014).

A large fraction of plant intracellular Fe is incorporated in Fe-S prosthetic groups which are well suited for electron transfer reactions and are often essential for the catalytic function of several enzymes (Balk and Schaedler, 2014). There are three pathways for the assembly of Fe-S clusters in plants: a mitochondrial, a plastidic and a cytosolic pathway. The cytosolic Fe-S assembly (CIA) pathway provides [Fe-S] clusters to cytosolic and nuclear proteins. The three pathways share a common mechanism where the [Fe-S] is pre-assembled on a scaffold protein and then transferred to apo-proteins by carriers or targeting factors (Figure 5-1, Couturier et al., 2013; Balk and Schaedler, 2014).

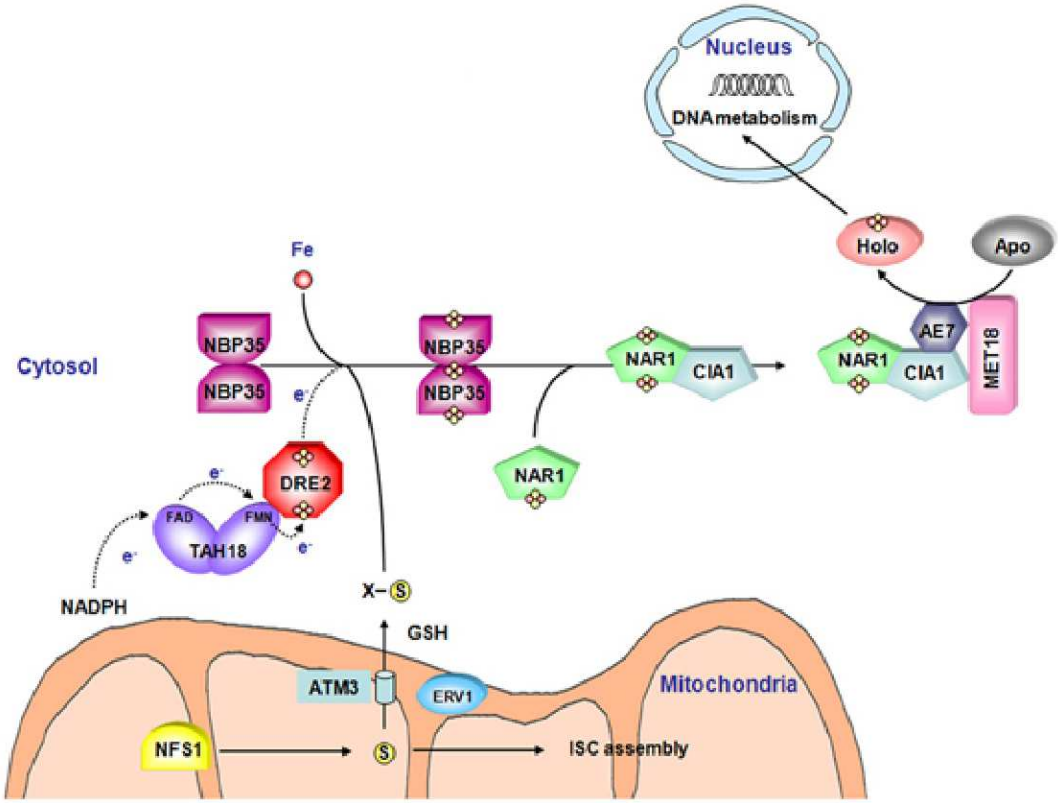

Figure 5-1. Overview of the cytosolic Fe-S assembly (CIA) pathway.

A sulfide compound originating from the mitochondria and iron, whose source is still unclear, are required for the CIA pathway. TAH18 and DRE2 provide the required electrons. The Fe-S cluster is pre-assembled on the scaffold protein NBP35 and then transferred to target apoproteins via a NAR1-CIA1-AE7-MET18 complex. Figure adapted from Couturier et al., 2013.

The yeast proteins ScGrx3/4 have been associated to the CIA pathway. Deletion of ScGrx3/4 leads to defects in cytosolic and mitochondrial Fe-S assembly, de-regulation of Fe-homeostasis and defects in proteins containing di-iron centres. ScGrx3/4 belong to the PICOT protein family and contain one N-terminal thioredoxin (Trx) and one C-terminal glutaredoxin (Grx) domain (Muhlenhoff et al., 2010), also known as PICOT homology domains. The PICOT homology domain is evolutionary conserved and present in a broad array of species including bacteria, yeast, mammalian and plant organisms (Isakov et al., 2000). Like its human and yeast homologs, Arabidposis PICOT1/GRXS17 was shown to bind [2Fe-2S] clusters. *Picot1* KO mutant plants, however, exhibited only a minor decrease in the activity of cytosolic Fe-S enzymes. Instead, Arabidopsis *picot1* plants were hypersensitive to high temperature and long-day photoperiod (Haunhorst et al., 2010; Muhlenhoff et al., 2010; Cheng et al., 2011; Knuesting et al., 2015).

In this chapter, we looked for ubiquitination targets of RGLG3/4 and identified PICOT1 as a RGLG3/4 interacting protein. We show PICOT1 is a ubiquitination target of RGLG3/4 and is degraded in plants in a proteasome-dependent manner. PICOT1 was found to interact with the CIA pathway machinery and with the Fe-S protein Xanthine Dehydrogenase 1 (XDH1) which showed a minor activity decrease in *picot1* KO seedlings. We thus link two extra members of the RGLG-family with one of the major Fe-consuming processes in the cell. In addition, we propose a role for PICOT1 in tRNA modification based on interaction with two known proteins involved in this process and a phenotypic resemblance between *picot1* plants and plants carrying mutations in genes involved in tRNA modification.

RESULTS

RGLG3 and RGLG4 interact with the GRX protein PICOT1

Previously, two members of the RGLG-family (RGLG1 and RGLG2) were localized at the plasma membrane. This was attributed to a myristoylation site present in the N-terminal region of both proteins (Yin et al., 2007). RGLG3 and RGLG4 form a separate clade in the RGLG-family (Figure 5-2A). While the entire N-terminal region is absent in RGLG3, the N-

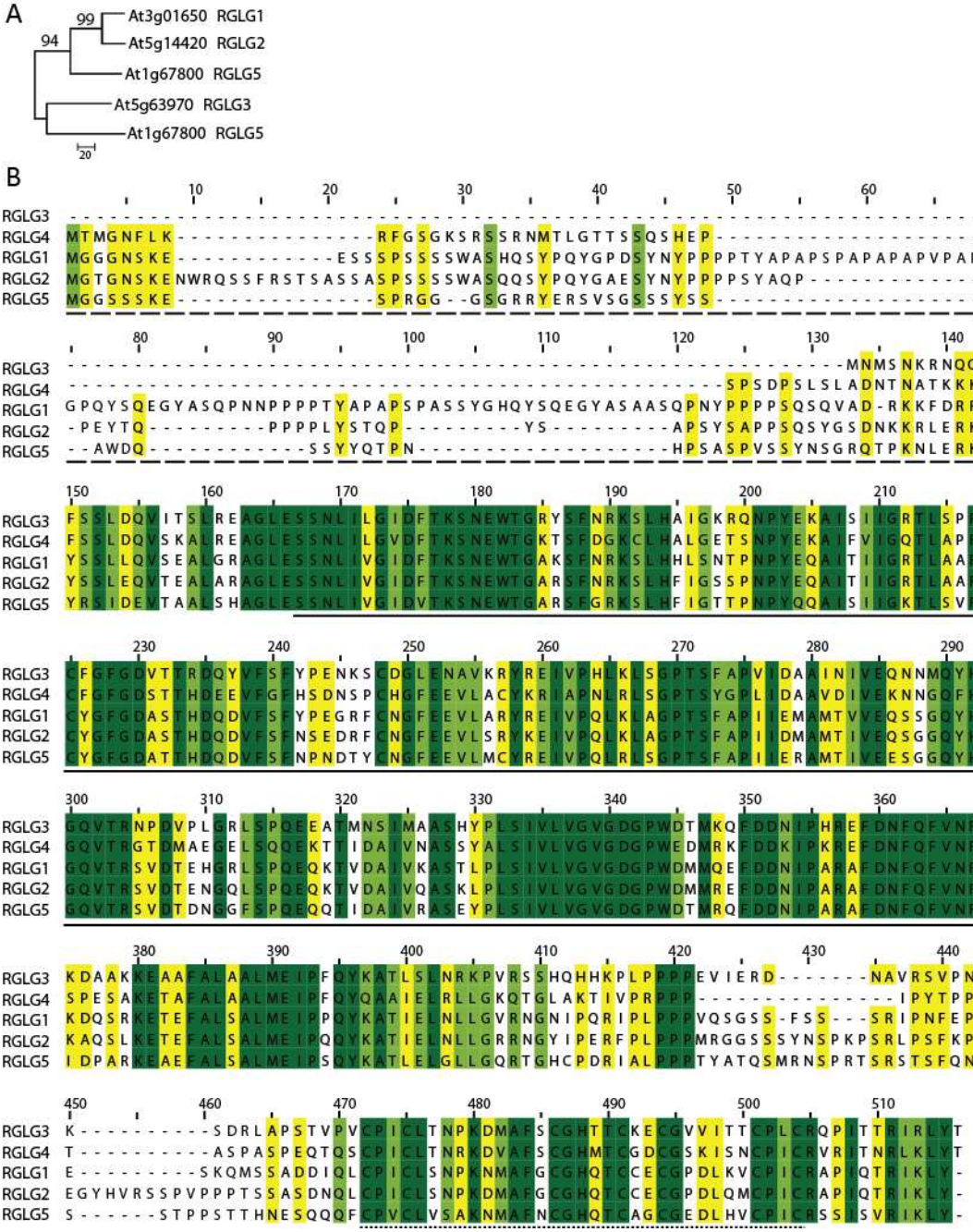

Figure 5-2. RING domain ligase (RGLG) protein family of *Arabidopsis*.

A. Phylogenetic tree of *Arabidopsis* RGLG-proteins, adapted from Zhang et al. (2012). B. Amino acid sequence alignment of RGLG proteins. Yellow to green shading indicate low to high conservation, respectively. Dashed line indicates N-terminal region as determined by Zhang et al., 2012, full line indicates von Willebrand factor type A (vWA) domain and dotted line indicates RING domain.

terminal region of RGLG4 lacks the myristoylation site (Figure 5-2B, Zhang et al., 2012) implying a different subcellular localization for these proteins.

To identify the ubiquitination targets of RGLG3 and RGLG4 we used a "substrate trapping" approach combined with Tandem Affinity Purification (TAP, Harper and Tan, 2012, see Chapter 3). We first introduced mutations in the RING-domain of each of these proteins, known to disrupt correct folding of the RING-domain (Stone et al., 2005). The resulting proteins (named RGLG3mRING and RGLG4mRING) lose interaction with the Ub-charged E2 ligase, but presumably maintain interaction with target proteins. As the targets cannot be ubiquitinated and degraded this may result in enrichment of the interacting target protein during affinity purification. RGLG3mRING and RGLG4mRING were fused carboxy-terminally to a TAP-tag and expressed in *Arabidopsis* cells under a cauliflower mosaic virus (CaMV) 35S promoter.

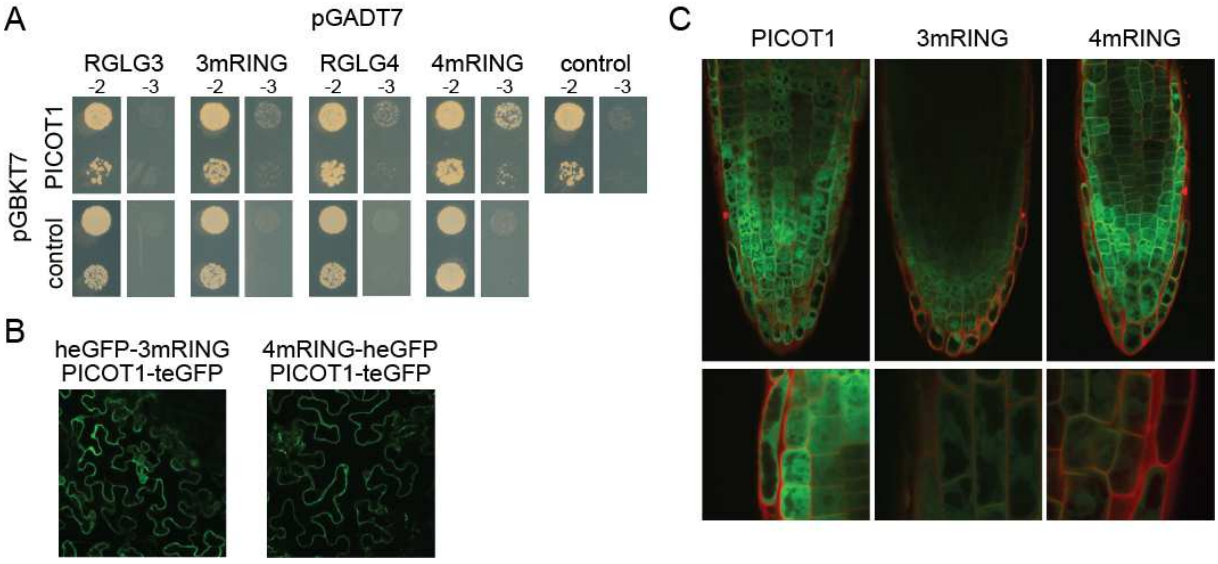

Figure 5-3. PICOT1 interacts with RGLG3 and RGLG4

A. Y2H assay of RGLG3/4 and RGLG3/4mRING with PICOT1. Transformed yeasts were spotted in 10-fold and 100-fold dilutions on control medium (-2) and selective medium (-3). B. RGLG3/4mRING and PICOT1 interaction by BiFC. Head (h) or tail (t) eGFP fusions were transiently expressed in *N. benthamiana*. Controls with unfused eGFP fragments did not result in detectable fluorescent signals (data not shown). C. Confocal root tip images of 4-day-old Arabidopsis seedlings overexpressing PICOT1-GFP, GFP-RGLG3mRING and RGLG4mRING-GFP. Propidium iodide was used to visualize the cell wall.

Using this strategy, we identified the protein PICOT1/GRXS17 as a putative target of RGLG4mRING (Supplementary File S1). PICOT1 was confirmed to interact both with RGLG3mRING and RGLG4mRING in yeast two-hybrid (Y2H) and split-GFP assays (Figure 5-3 A and B). Additionally, both the individual protein fused to GFP as well as the PICOT1/RGLG3mRING and PICOT1/RGLG4mRING pairs were observed to be nucleo-cytoplasmic (Figure 5-3 B and C, Figure 5-4 A). We also observed heterodimerization of RGLG3 and RGLG4 both in TAP and Y2H (Supplementary File S1, Figure 5-4 B).

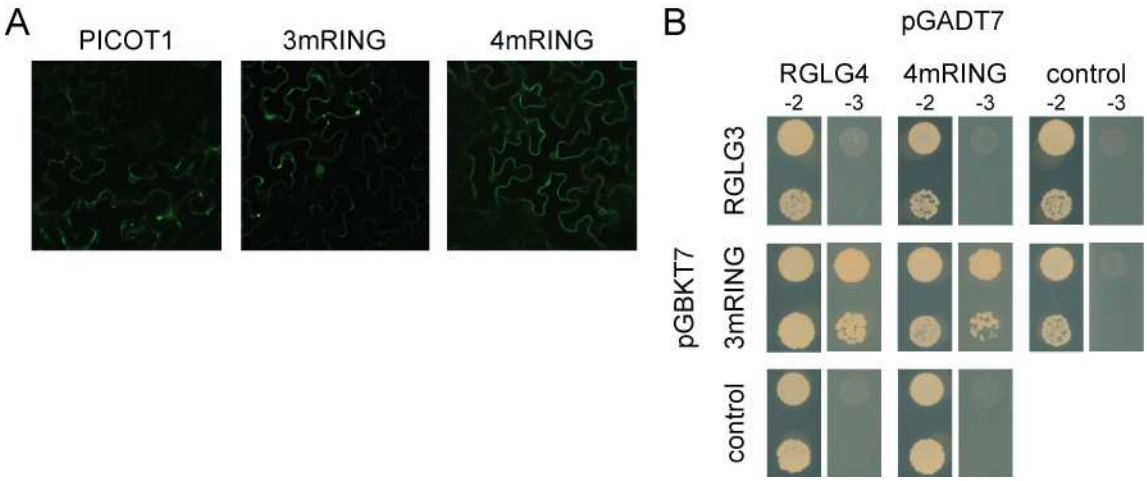

Figure 5-4. Subcellular localization and heterodimerization of RGLG3 and RGLG4.

A. Confocal images of *N. benthamiana* leaves transiently expressing PICOT1-GFP, GFP-RGLG3mRING and GFP-RGLG4mRING. B. Y2H assay of RGLG3/4 and RGLG3/4mRING. Transformed yeasts were spotted in 10-fold and 100-fold dilutions on control medium (-2) and selective medium (-3).

PICOT1 is ubiquitinated by RGLG3 *in vitro*

The Arabidopsis genome encodes 37 different E2 ubiquitin conjugases (AtUBC1 to AtUBC37, Kraft et al., 2005). To determine which E2 works as the ubiquitin donor together with RGLG3 and RGLG4 we screened for interaction of RGLG4 against Arabidopsis E2s by Y2H (Figure 5-5 A). At least one representative of each UBC-group (based on Kraft et al., 2005) was tested, except for group XII. RGLG4 interacted with a subset of *Arabidopsis* E2's consisting of two UBC's belonging to group VI (UBC8 and UBC30) and three UBC's belonging to group VII (UBC15, UBC17 and UBC18), but not with K63-chain forming UBC35 or UBC36 (Figure 5-5) that were reported to interact with RGLG1 and RGLG2 (Yin et al., 2007). RGLG3 interacted with the same subset of E2's and, as anticipated, this interaction was lost with the mRING versions (Figure 5-5 B).

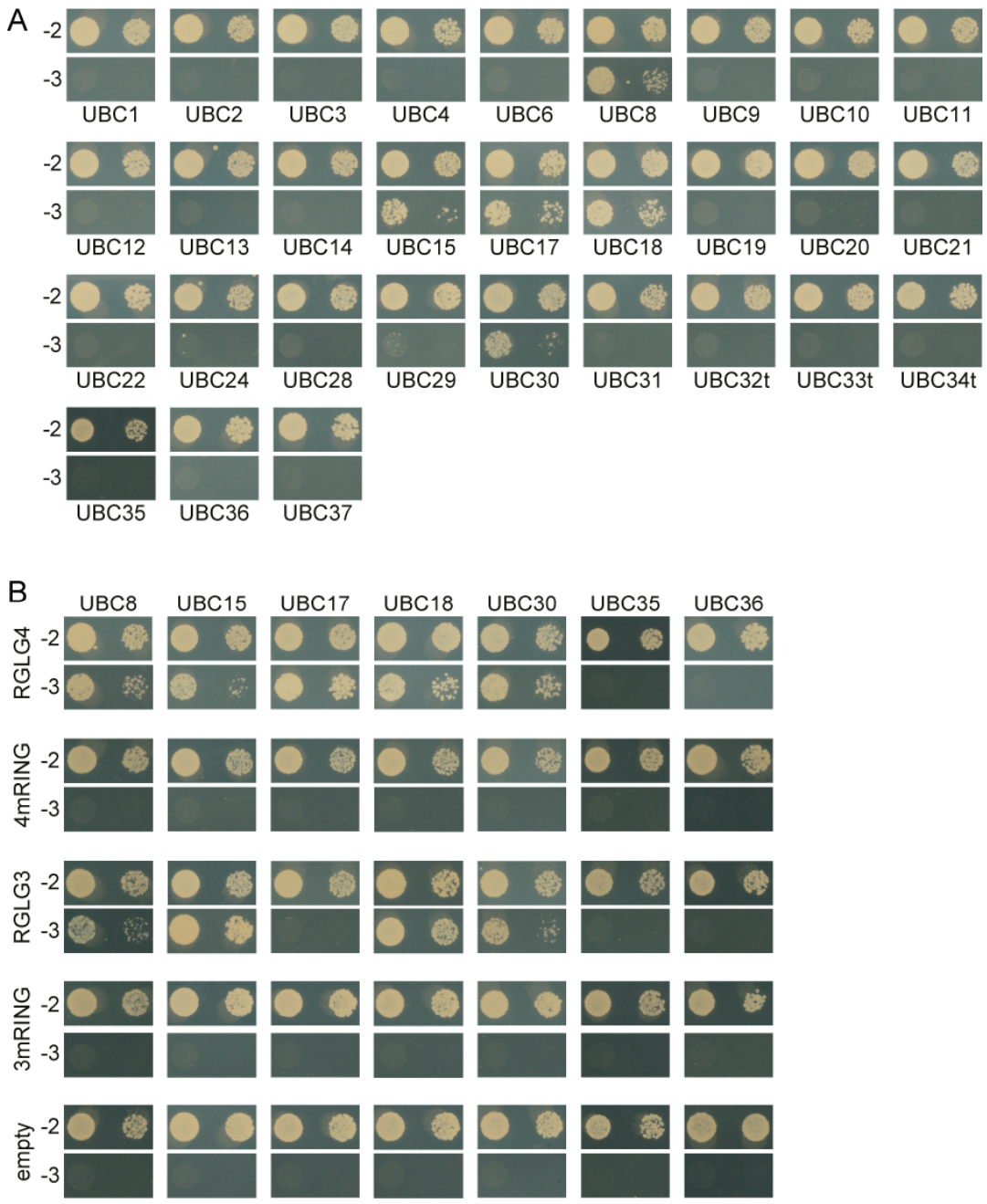

Figure 5-5. RGLG3 and RGLG4 interact with a specific subset of UBC enzymes in Y2H.

A. Y2H assay between RGLG4 and a panel of 30 Arabidopsis E2 ubiquitin conjugases. RGLG4 was fused to the activation domain in pGADT7. The transmembrane domain of group XIV UBC's (UBC32, UBC33 and UBC34) was removed to avoid false negative results (named UBC32t, UBC33t, and UBC34t). B. Validation using RGLG3/4 and mRING variants. Transformed yeasts were spotted in 10-fold and 100-fold dilutions on control medium (-2) and selective medium (-3).

We next re-assessed the E3 ligase activity of RGLG3 and RGLG4 in the presence of the different *Arabidopsis* UBC's identified in Figure 5-5 using *in vitro* ubiquitination assays. Initially, RGLG3 and RGLG4 were expressed in *E. coli* as GST-tagged proteins, unfortunately GST-RGLG3 could not be produced efficiently. GST-RGLG4 auto-ubiquitinated only when UBC30 or its human ortholog HsUbcH5b were included as E2 in the reaction (Figure 5-6). Note that no UBC15~Ub conjugate could be detected, indicating UBC15 was not active in our assay. RGLG4

auto-ubiquitination was dependent on the presence of each critical reaction component (Figure 5-6 B). When we included PICOT1 in the reaction and PICOT1 was visualized specifically on immunoblots, no differential bands were observed in the presence or absence of RGLG4 (Figure 5-6 B).

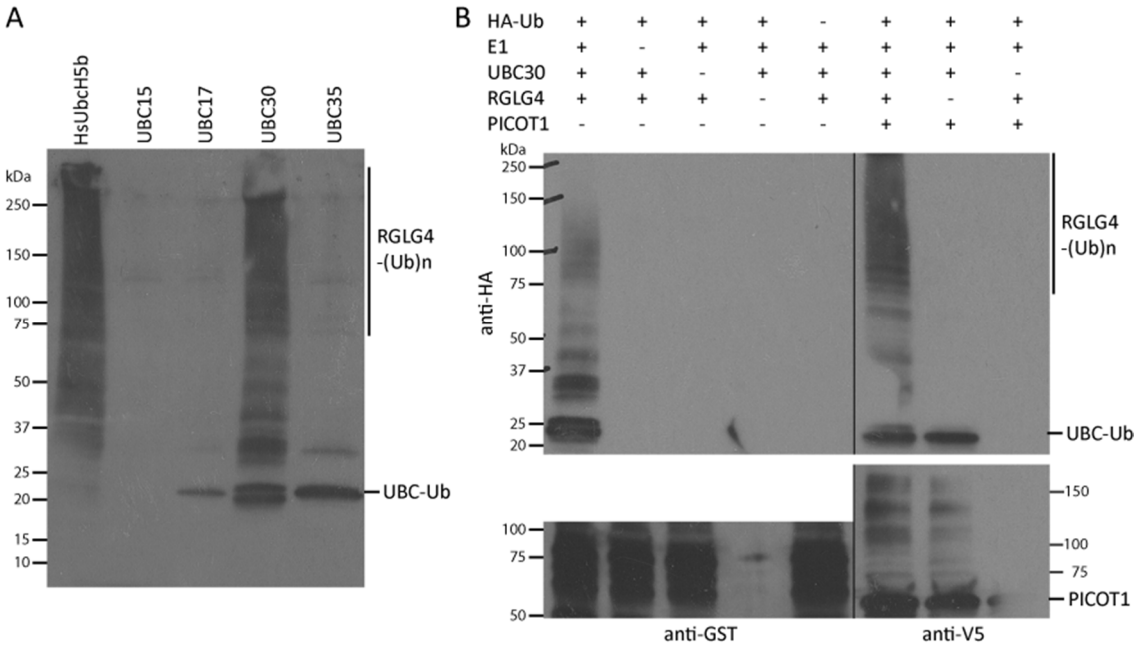

Figure 5-6. PICOT1 *in vitro* ubiquitination assays using GST-RGLG4

A. Auto-ubiquitination assay of GST-RGLG4 (70 kDa) in combination with various *Arabidopsis* E2's and HA-Ub (immunodetection with anti-HA antibodies). B. Extended auto-ubiquitination assay of GST-RGLG4 with UBC30 as E2, in the presence or absence of PICOT1. Note that in lane 4 and lane 8 UBC30-Ub and PICOT1, respectively, are not clearly visible due to a technical issue during blotting (air bubble). Ubiquitinated proteins were detected with anti-HA antibodies (Upper panel). GST-RGLG4 was detected using anti-GST antibodies (left lower panel). PICOT1-V5-HIS (55 kDa) was detected using anti-V5 antibodies (right lower panel).

For the rest of this study, we focused on UBC30, which is probably involved in K48 poly-ubiquitination and which is closely related to human HsUbcH5b that was shown previously to work with RGLG3 and RGLG4 *in vitro* (Zhang et al., 2012). To circumvent GST-RGLG3 insolubility, RGLG3/4 were produced as MBP-fused proteins in *E. coli* and their activity was tested in combination with UBC30 and HsUbcH5b (Figure 5-7). Unfortunately the MBP-RGLG4 yield was very low and this reflected on its E3 ligase activity during *in vitro* assays. We could confirm *in vitro* auto-ubiquitination of RGLG3 using UBC30 in combination with HA-tagged ubiquitin (Figure 5-7 A). When PICOT1 was included in the reaction and specifically visualized on immunoblots, additional higher molecular weight bands could be detected (Figure 5-7B, arrowheads). Remarkably, inclusion of RGLG4 in addition to RGLG3 abolished the formation of higher molecular weight bands of PICOT1. Because RGLG3 and RGLG4 form dimers, RGLG4 can possibly serve as a ubiquitination substrate in addition to PICOT1, making ubiquitination of PICOT1 less abundant in these experiments.

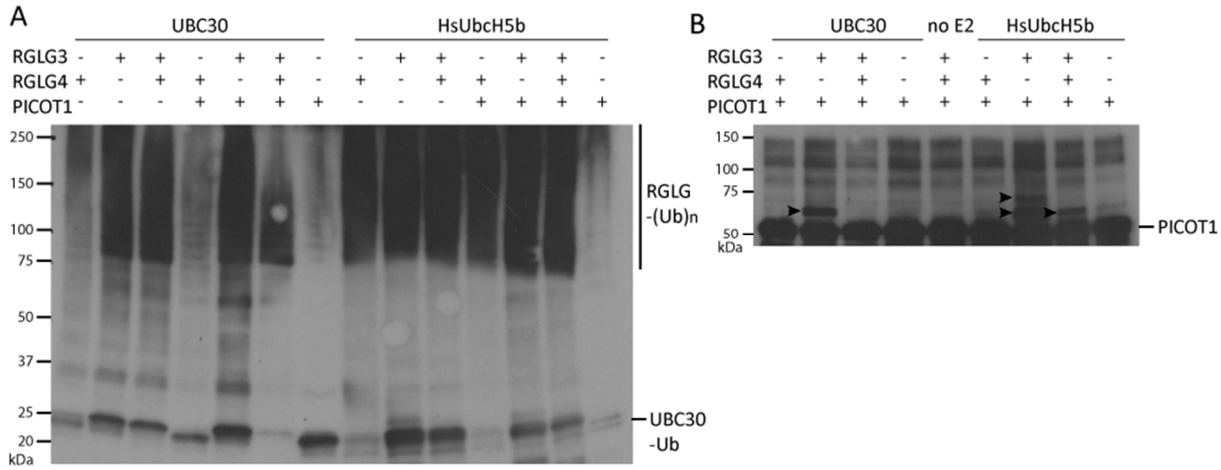

Figure 5-7. PICOT1 *in vitro* ubiquitination assays using MBP-fused RGLG3/4

In vitro PICOT1 ubiquitination assays using MBP-RGLG3 and MBP-RGLG4 in combination with UBC30 or HsUbcH5b. HA-Ub conjugated proteins (A) and PICOT1-V5-HIS (B) were visualized using anti-HA antibodies or anti-V5 antibodies, respectively. Arrowheads indicate higher molecular weight bands originating from PICOT1-V5-HIS modification.

It was remarkable that the expected Ub-ladder resembled a smear rather than individual bands. Particularly when PICOT1 ubiquitination was of interest, we wanted to reduce the amount of auto-ubiquitinating E3 visualized during Ub-immunodetection. We therefore tested lower concentrations of both E2 and E3 in the *in vitro* ubiquitination reaction mix. Based on these assays, we reduced the amounts of enzyme used per reaction five-fold and ten-fold for E2 and E3, respectively (Figure 5-8).

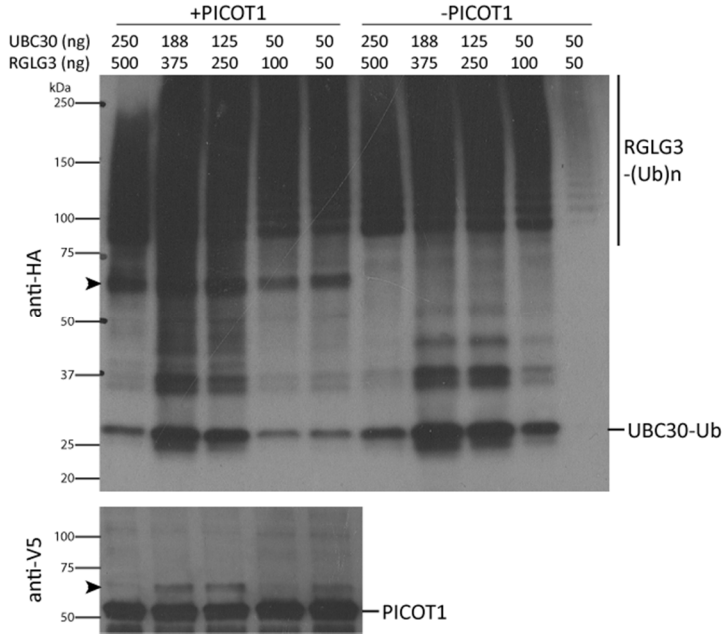

Figure 5-8. Optimalization of the *in vitro* ubiquitination assay.

Different quantities of MBP-RGLG3 and UBC30 were used for optimalization of the i*n vitro* ubiquitination assay, in the presence or absence of PICOT1. HA-Ub conjugates and PICOT1-V5-HIS were visualized on immunoblots using anti-HA antibodies and anti-V5 antibodies, respectively. Arrowheads indicate higher molecular weight bands originating from PICOT1-V5-HIS modification.

Using this optimized assay, we showed that the activity of RGLG3 was dependent on the integrity of the RING-domain (Figure 5-9A). When PICOT1 was included in the assay with functional RGLG3, ubiquitination was now clearly detected at lower molecular weight which could correspond to *in vitro* ubiquitination of PICOT1 by RGLG3 (Figure 5-9B, asterisk). Detection with an anti-V5 antibody indeed identified the lower molecular weight bands as originating from the PICOT1 protein, thus confirming RGLG3-mediated ubiquitination (Figure 5-9C).

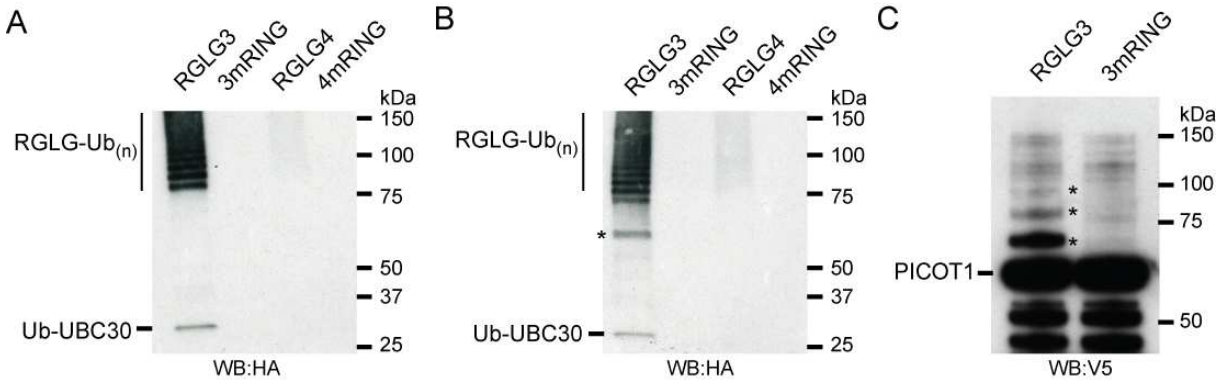

D

```
  1 MSGTVKDIVS KAELDNLRQS GAPVVLHFWA SWCDASKQMD
 41 QVFSHLATDF PRAHFFRVEA EEHPEISEAY SVAAVPYFVF
 81 FKDGKTVDTL EGADPSSLAN KVGKVAGSST SAEPAAPASL
121 GLAAGPTILE TVKENAKASL QDRAQPVSTA DALKSRLEKL
161 TNSHPVMLFM KGIPEEPRCG FSRKVVDILK EVNVDFGSFD
201 ILSDNEVREG LKKFSNWPTF PQLYCNGELL GGADIAIAMH
241 ESGELKDAFK DLGITTVGSK ESQDEAGKGG GVSSGNTGLS
281 ETLRARLEGL VNSKPVMLFM KGRPEEPKCG FSGKVVEILN
321 QEKIEFGSFD ILLDDEVRQG LEVYSNWSSY PQLYVKGELM
361 GGSDIVLEMQ KSGELKKVLT EKGITGEQSL EDRLKALINS
401 SEVMLFMKGS PDEPKCGFSS KVVKALRGEN VSFGSFDILT
441 DEEVRQGIKN FSNWPTFPQL YYKGELIGGC DIIMELSESG
481 DLKATLSE
```

E

	RGLG3		RGLG3mRING	
	-Ub	+Ub	-Ub	+Ub
K11	0	2	0	0
K85	1	2	0	0
K104	0	1	0	0
K137	2	4	0	0
K154	8	3	8	0
K250	1	3	2	0
K260	12	1	9	0
K268	3	6	1	0
K382	0	6	1	0

Figure 5-9. RGLG3 mediated PICOT1 ubiquitination.

A. *In vitro* auto-ubiquitination using recombinant HA-Ub, UBC30 as E2 and MBP-fused RGLG3 or RGLG4 as E3. Ubiquitinated proteins were detected using anti-HA antibodies. B. *In vitro* ubiquitination assay as in A, but including recombinant PICOT1-V5-HIS. C. *In vitro* ubiquitination assay as in B but detection using anti-V5 antibodies. D. PICOT1 protein sequence. Lysines for which a di-glycine rest was detected are highlighted in grey. The thioredoxin domain and the three glutaredoxin domains are shown in blue and orange, respectively. E. Summary of the number of peptides detected with or without a di-glycine modified Lys-residue. Asterisks indicate higher molecular weight bands originating from modified PICOT1-V5-HIS proteins.

Finally, we investigated which Lys-residue(s) in PICOT1 is preferentially targeted by RGLG3 *in vitro*. After separation of the *in vitro* reaction proteins by SDS-PAGE, proteins corresponding to the molecular weight of PICOT1 and higher were isolated, digested with trypsin and analysed using MS. We identified nine Lys-residues in PICOT1 that were specifically ubiquitinated by RGLG3 based on a di-glycine mass shift (Figure 5-9D). In contrast, when RGLG3mRING was used as E3, no ubiquitination sites were found (Figure 5-9E). Remarkably, three additional ubiquitinated Lys-residues were identified as a result of the *in vitro* reaction with RGLG3, two of them in the *att*-site between PICOT1 and the epitope tags, and one in the V5-tag (Supplementary Table S2).

PICOT1 is targeted for degradation by the E3 ligase complex RGLG3/4 *in vivo*

To test if PICOT1 is also *in vivo* ubiquitinated, we generated a stable transformed Arabidopsis line expressing PICOT1-3xHA under control of a constitutive CaMV 35S promoter. Seedling cultures were treated or not with MG132, which had no effect on total PICOT1-HA levels in the corresponding protein extracts (Figure 5-10 A). Using Tandem Ubiquitin Entities (TUbEs, Hjerpe et al., 2009) we successfully isolated poly-ubiquitinated proteins form the total protein extracts (Figure 5-10 B). A high molecular weight smear was detected for PICOT1-HA in TUbE-purified extracts of MG132-treated seedlings, indicating PICOT1-HA poly-ubiquitination (Figure 5-10 C).

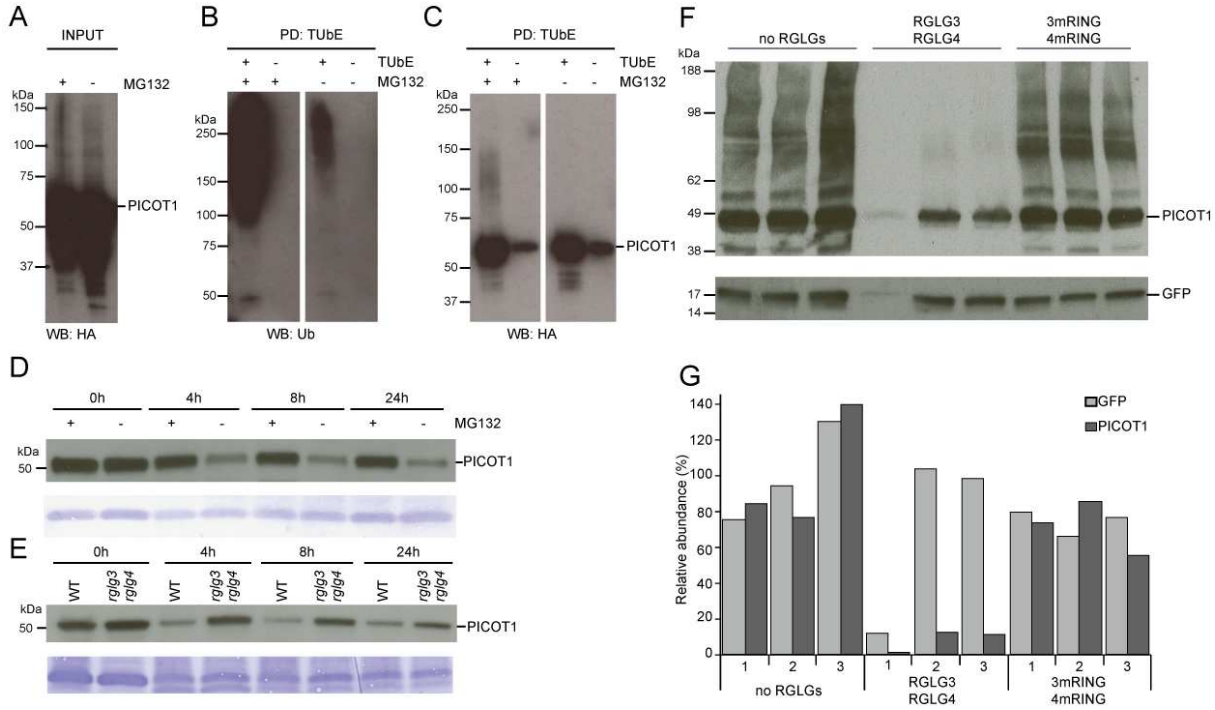

Figure 5-10. PICOT1 is ubiquitinated and degraded by the proteasome in a RGLG3/4 dependent way.

A-C. TUbE assay. A. Immunoblot detecting PICOT1-HA levels in the total protein extracts of seedlings treated overnight with 50 µM MG132 or mock. B. Immunoblot detecting ubiquitinated proteins after isolation of poly-ubiquitinated proteins using TUbE or mock resin. C. Immunoblot detecting PICOT1-HA after TUbE purification. D-E. Cell-free degradation assays. D. Total protein extracts were obtained from 10-day old PICOT1-HA seedlings and incubated for the time indicated with or without 50µM MG132. E. 300 ng PICOT1-V5-HIS recombinant protein was added to total protein extracts that were obtained from 10-day old WT Col-0 or *rglg3rglg4* double mutants and incubated for the time indicated. PICOT1 protein levels were detected by immunoblot with anti-HA or anti-V5 antibodies in D and E, respectively. The coomassie stained membrane is shown as a loading control. F. *In vivo* degradation assay. PICOT1-His was transiently expressed in *N. benthamiana* mesophyll cells, alone or in the presence of RGLG3/RGLG4 or their mRING-versions (3mRING/4mRING). PICOT1 protein levels were detected in total protein extracts prepared from the infiltrated areas by immunoblot with anti-HIS antibodies. GFP was co-transfected as an internal transfection efficiency control and detected by immunoblot using anti-GFP antibodies. Three biological repeats are shown for each condition. G. Quantification of protein levels detected in F.

Using the same PICOT1-HA line, protein stability was visualized over time in the presence or absence of MG132 (Figure 5-10 D) using cell-free degradation assays. When PICOT1-HA was visualized in total protein extracts from 35S::PICOT1-HA seedlings, the protein was degraded over time only in the absence of MG132 confirming PICOT1 degradation is

mediated by the 26S proteasome (Figure 5-10 D). Recombinant PICOT1-V5-His was also degraded over time when incubated in wild-type (WT) cell-free extracts (Figure 5-10 E) but less in extracts derived from the *rglg3rglg4* double mutant (Zhang et al., 2012, see also Figure 6-3). This indicates that 26S proteasome-mediated degradation of PICOT1 is dependent on the presence of functional RGLG3 and/or RGLG4 (Figure 5-10 E).

To further evaluate the effect of RGLG3 and RGLG4 on PICOT1 stability *in planta* we expressed PICOT1 together with RGLG3 and RGLG4 transiently in *N. benthamiana* leaves using agro-infiltration. In the absence of RGLG3 or RGLG4, PICOT1 accumulated as detected in total protein extracts prepared from the infiltrated area. Upon co-expression of PICOT1 with RGLG3 and RGLG4, PICOT1 protein levels were strongly decreased (Figure 5-10 F). Together, these findings indicate that RGLG3 and RGLG4 function together to mediate PICOT1 degradation *in planta.*

PICOT1 interacts with the CIA complex

To get insight into PICOT1 function, we performed TAP on *Arabidopsis* cell cultures and seedlings expressing TAP-tagged PICOT1. Co-purified proteins included nearly all core components of the CIA pathway, two known Fe-S proteins and a number of proteins involved in tRNA metabolism (Table 5-1 and Supplementary File S1).

The CIA pathway is responsible for providing [Fe-S] clusters to respective apo-proteins in the cytosol and the nucleus (Bernard et al., 2013, Figure 5-1). During plant CIA, assembly of the [Fe-S] cluster occurs first on the scaffold protein NBP35 (Bych et al., 2008; Kohbushi et al., 2009). Electrons, which are provided by NADPH oxidation, are mobilized by ATR3 and transferred to NBP35 by DRE2/CIAPIN1 (Bernard et al., 2013). Once the cluster has been assembled on the NBP35 scaffold, it is transferred to apo-proteins by dedicated proteins forming the CIA targeting complex. In *Arabidopsis* this complex is composed of NAR1, CIA1, AE7/CIA2 and MET18 and locates to both the cytoplasm and the nucleus (Luo et al., 2012). MET18 is thought to determine the target-specificity of the complex while CIA1 and CIA2 would facilitate transfer of the Fe-S cluster from NAR1 to the final acceptor proteins (Luo et al., 2012).

Although human and yeast PICOT1 homologs are essential for the maturation of cytosolic and nuclear Fe-S proteins (Muhlenhoff et al., 2010; Haunhorst et al., 2013), *Arabidopsis* PICOT1 was recently shown to play only a minor role in maintaining the activity of two classes of cytosolic Fe-S enzymes (aconitases and aldehyde oxidases, Knuesting et al., 2015). Here, two Fe-S proteins were co-purified with PICOT1 during TAP: XANTHINE DEHYDROGENASE 1 (XDH1) and BolA2. PICOT1 and BolA2 were reported to form [2Fe-2S]-bridged heterodimers in the cytosol and nucleus (Couturier et al., 2014). Interaction between PICOT and XDH1 has not been reported previously.

Table 5-1. Overview of a selection of PICOT1 interacting proteins identified by TAP.

		PICOT1				
		C-GSrh		N-GSrh		
Name	Locus	cells	seedlings	cells	seedlings	Total
PICOT1		**4**	**2**	**2**	**1**	
Cytoplasmic [Fe-S] assembly pathway						
MET18[1,2]	AT5G48120	4	2	2	1	9
CIAPIN / DRE2[1,3]	AT5G18400	4	2	2		8
AE7 / CIA2	AT1G68310	2				2
NAR1	AT4G16440	3				3
CIA1	AT2G26060	2				2
Purine catabolism and salvage						
XDH1 | Xanthine dehydrogenase 1	AT4G34890	3	2	1		6
URH1 | Uridine-ribohydrolase 1	AT2G36310		2		1	3
URH2 | Uridine-ribohydrolase 2	AT1G05620		2		1	3
UREG | Urease accessory protein G	AT2G34470		2			2
tRNA modifications						
CTU1/ROL5 | Cytoplasmic thiouridylase 1	AT2G44270			1		1
CTU2 | Cytoplasmic thiouridylase 2	AT4G35910	1		1		2
2-thiocytidine tRNA biosynthesis protein (TtcA)	AT1G76170	2				2
YbaK/aminoacyl-tRNA synthetase-associated domain	AT1G44835	1				1
Aminoacyl-tRNA ligase[6]	AT1G09620		2		1	3
Other known Fe-S proteins						
AtBolA2[4,5]	AT5G09830	3				3
Radical SAM superfamily protein[7]	AT2G39670		1			1

Proteins identified with LTQ Orbitrap Velos, with at least 2 significant peptides per identification. Only proteins that were identified in at least 2 TAP experiments with the same bait are retained. Background is subtracted. Numbers in columns indicate how many times the protein was identified in 2 TAP experiments per column (except for N-GSrh seedlings: only 1 experiment performed).Interaction was confirmed in yeast ([1]Tarassov et al., 2008), in humans ([2]Stehling et al., 2012, [3]Saito et al., 2011) or in Arabidopsis ([4]Couturier et al., 2014, [5]Braun et al., 2011). [6]Possible background. [7]Found in only 1 TAP experiment.

XDH1 belongs to the family of Xanthine oxidoreductases (XORs) that catalyse the oxidation of hypoxanthine and xanthine to uric acid during purine degradation. XDH1 is active as a homodimer in which each monomer has 3 cofactors: two [2Fe-2S] prosthetic groups, one FAD molecule, and one molybdenum cofactor (Moco), bound to the N-terminal, central and C-terminal part of the protein, respectively (Zarepour et al., 2010). In addition to XDH1, three other proteins involved in purine degradation were also identified in complex with PICOT1: URIDINE RIBOHYDROLASE 1 and 2 (URH1/2) and the UREASE ACCESORY PROTEIN UREG. URH1/2 are nucleoside ribohydrolases with inosine and xanthosine hydrolytic activity, resulting in hypoxanthine and xanthine generation (Riegler et al., 2011; Figure 5-12A). Urease catalyses the hydrolysis of urea to ammonia and carbon dioxide, the final products of purine

degradation. In *Arabidopsis*, Urease activation is mediated by the accessory proteins UreD, UreF and UreG (Witte et al., 2005), only the latter was identified in a complex with PICOT1 (Table 5-1).

Finally, a number of proteins related to tRNA modifications were identified as PICOT1 interacting proteins. CYTOPLASMIC THIOURIDYLASE 1 and 2 (CTU1/2) mediate thiolation of uridine at the wobble position of Glu, Gln and Lys tRNAs (Leidel et al., 2009; Philipp et al., 2014).

PICOT1 regulates XDH1 activity

When we produced recombinant PICOT1 in *E. coli*, the pellet showed a red brownish colour, confirming its capacity to bind [2Fe-2S] clusters (Knuesting et al., 2015). Because XDH1 contains two [2Fe-2S] cofactors that are involved in electron transfer for the reduction of the substrates xanthine and hypoxanthine (Zarepour et al., 2010), we investigated the PICOT1-XDH1 interaction more closely. Direct interaction between XDH1 and PICOT1 was confirmed in a Y2H assay (Figure 5-11 A). To examine the physiological relevance of this interaction, we measured XDH1-activity in Arabidopsis seedlings with altered PICOT1 expression (Figure 5-11 B). We found a reproducible but non-significant minor decrease of XDH1-activity in *picot1* seedlings compared to WT or *rglg3rglg4* double mutant seedlings (Figure 5-11 C). The difference in activity was not due to a difference in XDH1 protein abundance (data not shown). Our findings indicate that PICOT1 contributes to, but is not essential for XDH1 activity, as previously also reported for other cytosolic Fe-S enzymes (Knuesting et al., 2015). In contrast to what is expected, the XDH1 activity was not increased in *rglg3rglg4* seedlings, indicating other E3 ligases might still regulate PICOT1 protein levels in the absence of RGLG3 and RGLG4.

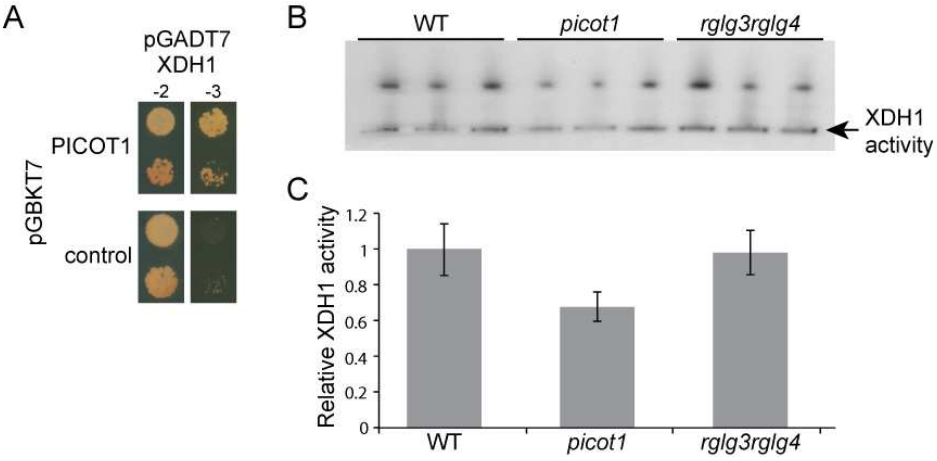

Figure 5-11. PICOT1 interacts with XDH1 and contributes to its activity.

A. Y2H assay between PICOT1 and XDH1. Transformed yeasts were spotted in 10-fold and 100-fold dilutions on control medium (-2) and selective medium (-3). B. XDH1 activity measurements. 100 µg total protein extract obtained from the indicated plant lines was loaded in each lane of a native polyacrylamide gel and subsequently stained using hypoxanthine as substrate. C. Quantification of the XDH1-activity measured in B. Bars represent means ±SEM of three independent biological samples.

The *picot1* mutant differentially accumulates purine catabolism intermediaries

Next to XDH1, that catalyses the rate-limiting step in purine catabolism, three additional enzymes involved in this pathway where identified in a complex with PICOT1 via TAP (Table 5-1, Figure 5-12 A). To evaluate the impact of altered PICOT1 expression on this pathway, we measured the accumulation of uric acid precursors (xanthine and xanthosine) and of ureides (uric acid, allantoin and allantoic acid) in WT, *picot1* and *rglg3rglg4* seedlings (Figure 5-12 B). WT seedlings grown in the presence of the XDH1-inhibitor allopurinol were included to mimic XDH1-deficiency.

The accumulation of xanthine and uric acid showed similar trends between allopurinol treated WT seedlings and *picot1* seedlings. Reduced activity of XDH1 in *picot1* seedlings correlated with enhanced accumulation of xanthine, while unexpectedly, uric acid accumulated in both allopurinol treated WT seedlings and *picot1* seedlings. While xanthosine and allantoic acid accumulated differentially between control and allopurinol treated WT seedlings, no alterations in the accumulation of these compounds was seen in *picot1* seedlings. Finally, the ureide allantoic acid showed opposite accumulation levels in allopurinol treated WT seedlings and *picot1* seedlings. These results suggest that *picot1* seedlings have altered accumulation of purine catabolism intermediaries, of which some can be accounted for by a minor decrease of XDH1 activity in these seedlings. Remarkably, in *rglg3rglg4* double KO seedlings the accumulation of the purine catabolism intermediaries measured here always showed the same trend as in *picot1* seedlings when compared to WT seedlings. This again indicates that RGLG3 and RGLG4 are probably not the only proteins regulating PICOT1 protein levels or activity.

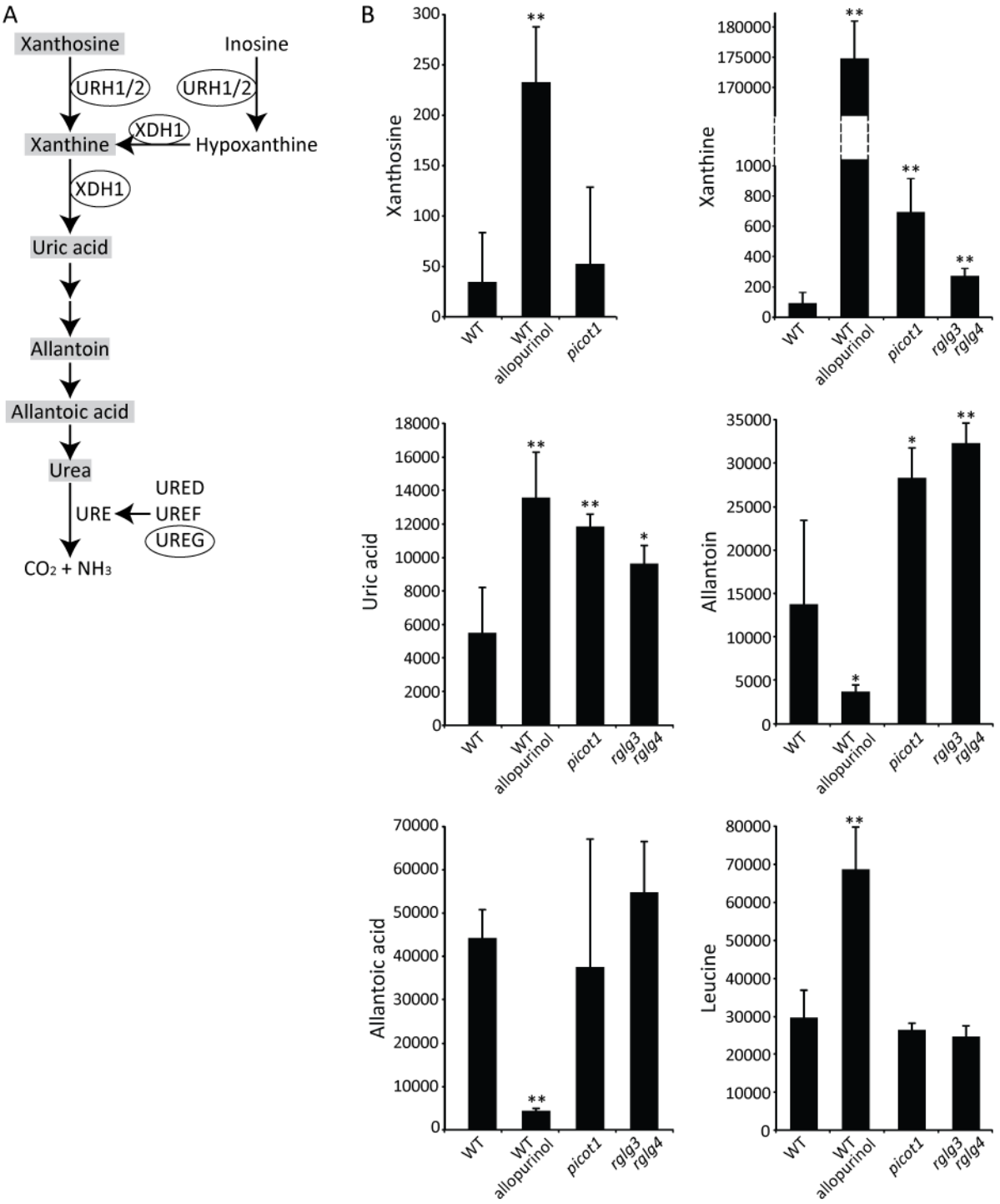

Figure 5-12. Quantification of purine degradation intermediaries.

A. Overview of purine degradation pathway. Enzymes identified in complex with PICOT1 via TAP are encircled. URH1/2, URIDINE HYDROLASE 1/2; URE, UREASE; URED/F/G, UREASE ACCESSORY PROTEIN D/F/G. B. Quantification of purine degradation intermediaries in whole seedlings grown 10 days on MS media supplemented with 1% sucrose and 0.5 mM allopurinol (WT allopurinol) or DMSO (WT, *picot1*, *rglg3rglg4*). Error bars represent mean ±SEM of n=5 (*, p<0.05; **, p<0.01; t-test). Leucine was measured as a control.

RGLG3/4 positively regulate cell death

XDH1-deficient plants have been reported to show earlier onset of age-dependent and dark-induced leaf senescence (Nakagawa et al., 2007; Brychkova et al., 2008). Ureides, like allantoin and allantoate, have been shown to be strong reactive oxygen species (ROS) scavengers, indicating the phenotypes observed in XDH1-deficient plants could also be caused by an excess in ROS due to decreased ROS-scavenging (Brychkova et al., 2008).

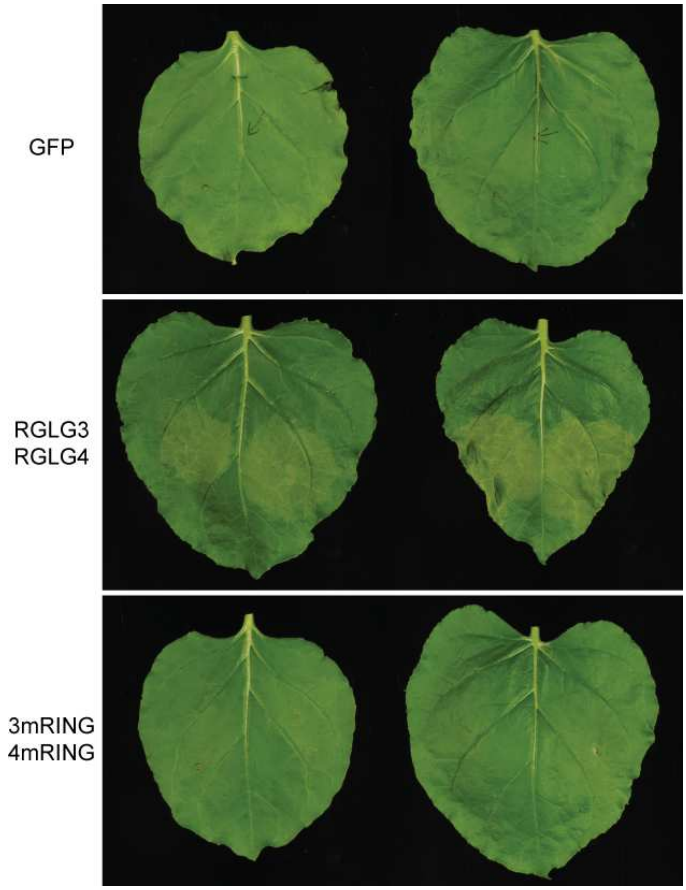

Figure 5-13. PICOT1-degradation leads to early onset of senescence in *N. benthamiana*.

WT or mRING versions of RGLG3 and RGLG4 were transiently co-expressed in *N. benthamiana* mesophyll cells. GFP was used as a negative control. Early onset of senescence is seen as yellowing of the infiltrated areas.

To investigate the role of PICOT1 in XDH1-mediated ROS scavenging, we reasoned PICOT1 depletion could lead to a slight decrease in active XDH1 holo-protein. To mimic PICOT1 depletion, we transiently overexpressed RGLG3 and RGLG4 in *N. benthamiana* leaves. We noticed patches of senescent tissue at the infiltrated areas, but not at the surrounding areas (Figure 5-14). This phenotype was dependent on the integrity of the RING-domain. Together, these results indicate transient overexpression of RGLG3 and RGLG4 in *N. benthamiana* results in early onset of senescence, possibly by depletion of the endogenous PICOT1 protein. This early onset of senescence might result from a disturbance in endogenous XDH1-activity. In addition our results are in accordance to the recently published role for RGLG3 and RGLG4 as positive regulators of programmed cell death induced by the phytotoxin Fumonisin B1 (Zhang et al., 2015).

PICOT1 interacts with tRNA modification enzymes

As mentioned above, two proteins with a known function in tRNA modification were identified as PICOT1 interacting proteins via TAP. CYTOPLASMIC THIOURIDYLASE 1 and 2 (CTU1/ROL5 and CTU2) mediate thiolation of uridine at the wobble position of Glu, Gln and Lys tRNAs. This modification is conserved throughout bacteria and eukaryotes (Leidel et al., 2009; Philipp et al., 2014) and is important for maintaining translational fidelity. To further investigate their interaction with PICOT1, we cloned *CTU1/*2 based on a cDNA template. Notably, two new alternative splicing variants were also picked up, where intron retention leads to introduction of an early stop. We named these splicing variants *CTU1-N* and *CTU2-N*, as they encode mainly the N-terminal part of the protein (Figure 5-14 A). Because *picot1* mutants have been phenotypically associated with *elongata* mutants (Knuesting et al., 2015) and the Elongator complex is essential for mcm^5s^2 tRNA modification, the interaction between PICOT1 and components of the Elongator complex was also investigated using Y2H. We confirmed direct interaction between PICOT1 and both CTU1/2 splicing variants. In addition, ELP4/ELO1 was also able to directly interact with PICOT1 in yeast (Figure 5-14 B). To see if the phenotype of seedlings with loss-of-function mutations in *CTU1/2* resemble *picot1* or *elongata* phenotypes, a KO line for each gene was obtained (*rol5-2* and *ctu2-2*, Leiber et al., 2010; Philipp et al., 2014). As the different subunits of the Elongator complex function non-redundantly and most of the *elo* mutants are in the Ler background, we included the weak *elo3-6* mutant line that has Col-0 background (Nelissen et al., 2010) as a representative member of the *elongata* mutants. At first sight, all mutant lines seem to have strongly elongated leaves when compared to WT plants (Figure 5-14 C). The physical interaction between PICOT1 and CTUs/ELO1 combined with the phenotypic resemblance of KO mutants in the respective genes indicate PICOT1 might be involved in the process of tRNA modification.

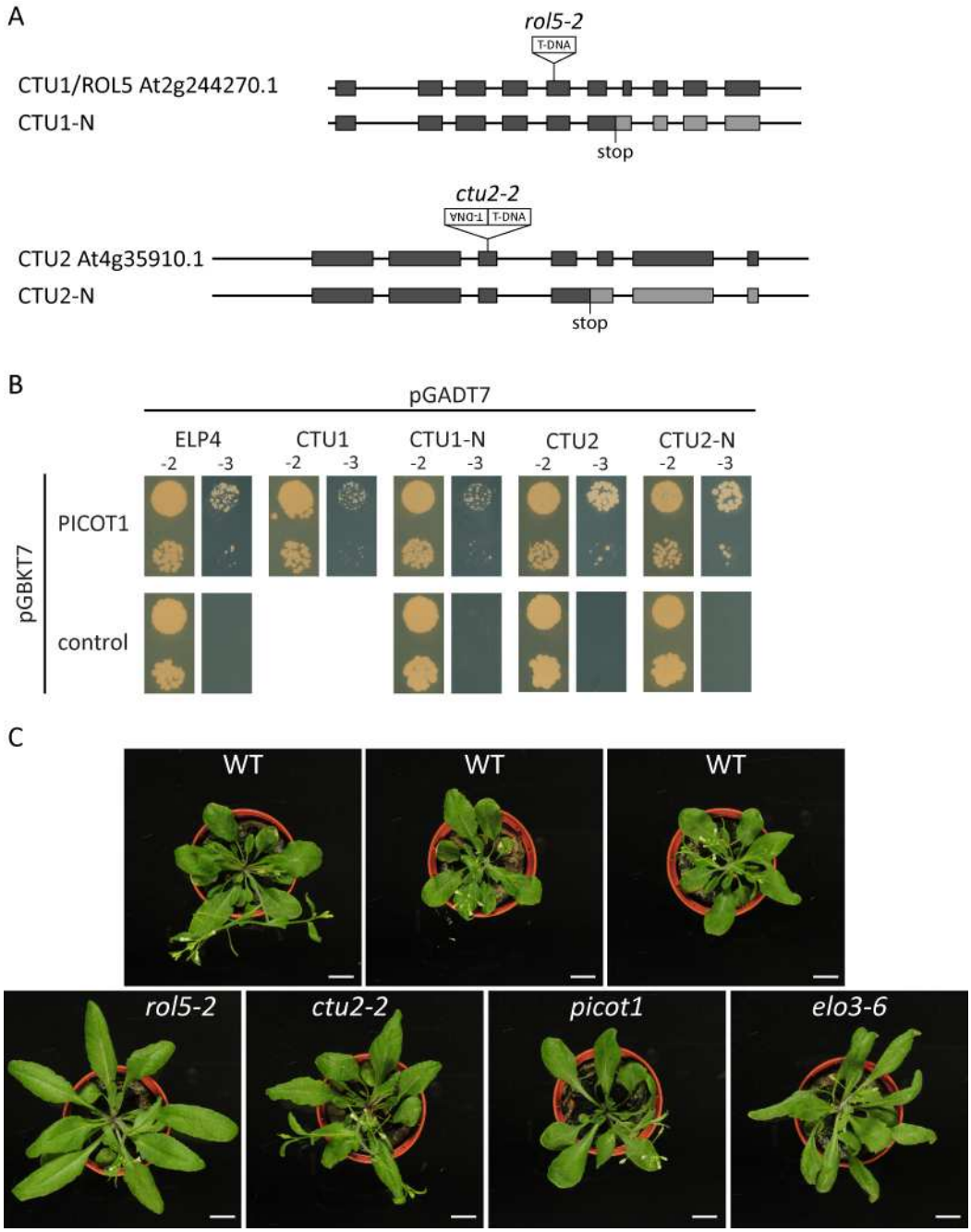

Figure 5-14. PICOT1 interacts directly with proteins involved in tRNA modification.

A. Schematic visualization of *CTU1* and *CTU2* gene structure and T-DNA insertions. Grey boxes represent exons. B. Y2H assay of PICOT1 and different splicing-variants of CTU1/CTU2 and ELP4. Transformed yeasts were spotted in 10-fold and 100-fold dilutions on control medium (-2) and selective medium (-3). C. Photographs were taken 4 weeks after sowing. Plants were grown under long day conditions with 16 h light/8 h dark cycles. WT, wild type Col-0. Scale bar is 13 mm.

DISCUSSION

We have shown here that the E3 ligases RGLG3/4 mediate PICOT1 poly-ubiquitination eventually leading to PICOT1 degradation by the proteasome. We used an optimized *in vitro* ubiquitination assay, where we first identified which *Arabidopsis* E2 can associate with the respective E3's and is thus best appropriate for the *in vitro* reaction. In contrast to RGLG1/2, RGLG3/4 did not interact with K63-specific E2s (UBC35/36). However, since only a truncated version of RGLG2 was able to interact with UBC35 (Yin et al., 2007) and our screen was only performed using full-length RGLG3/4, we cannot exclude that this interaction could take place *in vivo*. Instead, RGLG3/4 interact with two different groups of E2 conjugases, UBC15/17/18 (homologous to HsUbe2w) and UBC8/30 (homologous to HsUbcH5b). While UBC30 characteristically catalyses K48 Ub-chain formation and was functional for *in vitro* poly-ubiquitination of PICOT1 by RGLG3, HsUbe2w has been reported to be an atypical ubiquitin-conjugase that catalyses the attachment of ubiquitin to the N-terminal $–NH_2$ group of the substrate protein (Scaglione et al., 2013). RGLG3/4 auto-ubiquitinating activity was, however, absent in the presence of UBC17. We cannot exclude that the use of N-terminally tagged E3 ligases or absence of additional (unknown) components might be at the basis of the lack of auto-ubiquitination activity, as in general expression of N-terminally tagged PICOT1 constructs was less efficient than that of the C-terminally tagged ones, indicating an intact PICOT1 N-terminus could be important for protein stability.

We found several ubiquitinated Lys-residues resulting from PICOT1 *in vitro* ubiquitination in the presence of RGLG3 and UBC30. This probably reflects the artificial nature of *in vitro* work as we also identified a Ub-modified Lys-residue in the V5 sequence and two additional Ub-modified Lys-residues in the *att*B2 site between the PICOT1 protein and the V5-HIS-tag. Our results emphasize the importance of careful interpretation of results obtained from *in vitro* experiments, as ubiquitination of an epitope tag or att-site can lead to false positive results and the lack of additional factors affecting the specificity of the reaction can, on the other hand, lead to false negative results. Despite the partial artificial nature of the *in vitro* ubiquitination assay, no ubiquitinated peptides of PICOT1 were identified when the assay was performed in the presence of RGLG3mRING emphasizing the reaction reflects an authentic E3-target relationship. In addition, poly-ubiquitination of PICOT1 by RGLG3 in collaboration with the K48-specific UBC30 is in accordance with our findings that *in vivo* PICOT1 protein stability is dependent on proteasomal activity.

PICOT1's domain architecture resembles that of its closest human homolog, HsPicot, which is composed of one Trx domain and two Grx domains (Li et al., 2012). In humans, HsPicot has been shown to be involved in multiple processes including regulation of signalling pathways associated with cancer and cardiac hypertrophy, regulation of intracellular Fe homeostasis and the assembly and trafficking of Fe-S clusters. (Cha et al., 2008; Jeong et al.,

2008; Qu et al., 2011; Haunhorst et al., 2013). The Trx domain of PICOT proteins lacks the dithiol motif in the catalytic centre, and therefore probably functions as a protein-protein interaction platform independent of redox activity (Haunhorst et al., 2010). The Grx domains of PICOT proteins belong to the monothiol class of Grxs, characterized by a CGFS-motif at the redox centre. Monothiol Grxs have not been shown to possess deglutathionylation-activity, instead, they have the possibility to bind [2Fe-2S] clusters (Stroher and Millar, 2012). Four monothiol Grxs are encoded in the *Arabidopsis* genome: GRXS14/CXIP1/GRXCp, GRXS15, GRXS16/CXIP2 and PICOT1. PICOT1 is the only monothiol Grx in Arabidopsis that localizes to the nucleus and cytoplasm, as CXIP1 and CXIP2 localize to plastids and GRXS15 to both plastids and mitochondria (Couturier et al., 2013).

Interactions between PICOT proteins and BolA proteins are conserved in yeast, humans and plants, where it has been demonstrated that the Grx-domain and the BolA-domain are bridged by binding of a [2Fe-2S] cluster (Li et al., 2009; Li et al., 2012; Couturier et al., 2014). In yeast, the PICOT1 homologs ScGrx3/4 are localized in the nucleus where they regulate the nuclear export of ScAft1, a transcription factor that regulates Fe-responsive gene-expression under low Fe conditions (Pujol-Carrion et al., 2006). Heterodimerization of ScGrx3/4 with the BolA-protein ScFra2 leads to nuclear export of ScAft1 (Pujol-Carrion et al., 2006; Li et al., 2009). In plants, BolA2 does not seem to play a role in Fe-homeostasis and the biological outcome of PICOT1-BolA2 interaction remains an unanswered question (Couturier et al., 2014; Roret et al., 2014). In both yeasts and humans, PICOT-homologs play an important role in Fe utilization. ScGrx3/4 deficient yeasts have defects in *de novo* synthesis of [Fe-S] clusters and heme, two of the major Fe-consuming processes in these organisms. Fe-content is not decreased in these yeasts, but the Fe is not bio-available due to deficient Fe-delivery to mitochondria. A similar defect in Fe bio-availability was observed in zebrafish and HeLa cells when HsPicot (or the zebrafish ortholog) was depleted (Muhlenhoff et al., 2010; Haunhorst et al., 2013).

The role of PICOT proteins in the CIA pathway is still not well understood. In yeast, incorporation of [Fe-S] clusters into both cytosolic and mitochondrial proteins is dependent on ScGrx3/4 (Muhlenhoff et al., 2010). We found that in plants, PICOT1 interacts with several components of the CIA, including DRE2, NAR1 and MET18. PICOT1-DRE2 interaction is conserved in yeast and humans where the ortholog of DRE2, Anamorsin, interacts directly with HsPicot. Disturbance of the Anamorsin-Picot interaction has been proposed as a strategy to reduce cell proliferation in solid tumours where Anamorsin expression is enhanced (Tarassov et al., 2008; Saito et al., 2011). The study of the plant ortholog PICOT1 may therefore contribute to research for drug targets. Remarkably, maturation of the yeast Fe-S proteins ScDre2, ScMet18 and ScGrx3/4 itself, is independent of CIA and requires only a functional ISC pathway. In addition, maturation of ScDre2 and ScMet18 is dependent on ScGrx3/4. Despite the fact that PICOT1 interacts with members of the CIA pathway, it does not seem to have an

essential role in *de novo* Fe-S biogenesis as *picot1* plants do not show the embryonic lethal phenotypes associated with core components of the CIA pathway in Arabidopsis. In addition, the absence of PICOT1 was previously shown to have only minor effects on the activity of cytosolic Fe-S proteins like aconitases and aldehyde oxidases (Knuesting et al., 2015).

We identified the [2Fe-2S] containing XDH1 protein as a PICOT1-interacting protein. XDH1 belongs to the family of Xanthine Oxidoreductases (XORs) and is a central player in purine catabolism where it catalyses the oxidation of hypoxanthine and xanthine to uric acid. In mammals, XOR proteins can possess xanthine dehydrogenase (XDH) or xanthine oxidase (XO) activity. In *Arabidopsis* two XOR-genes are present with a strict XDH activity: Xanthine dehydrogenase 1 and 2 (XDH1 and XDH2). Although both genes are located closely to each other on the same chromosome, XDH2 is expressed constitutively at basal levels while XDH1 is differentially expressed upon several stimuli (Hesberg et al., 2004). Like XDHs from other organisms, XDH1 is active as a homodimer where each monomer binds three cofactors: two [2Fe-2S], one FAD, and one molybdenum cofactor (Moco), at respectively the N-terminal, central and C-terminal part of the protein (Zarepour et al., 2010). During purine degradation, xanthine or hypoxanthine are bound by the sulfurated Moco cofactor and subsequently oxidized to uric acid. During this process electrons are transported through the Fe-S clusters to NAD^+ which docks at the FAD-cofactor, producing NADH as a by-product. When NAD^+ concentrations are low, O_2 can replace NAD^+ as the electron acceptor leading to superoxide anion ($O_2^{\cdot-}$) production (Hesberg et al., 2004). We showed here XDH1 activity is only moderately reduced in *picot1* KO plants, in accordance with previous findings (Knuesting et al., 2015). Alternatively, XDH1 also possesses NADH-oxidase activity, which is independent of the Moco cofactor. In this case, NADH functions as the enzyme substrate and O_2 acts as the only electron acceptor, producing NAD^+ and $O_2^{\cdot-}$ (Zarepour et al., 2010). It remains to be determined if PICOT1 also contributes to the NADH oxidase activity of XDH1, or only to the xanthine/hypoxanthine oxidase activity.

Plants deficient in XDH1 are affected in normal growth and development. Seedlings with RNAi-mediated silencing of XDH1 are smaller than WT plants with shorter flowering stems, smaller fruit size and higher sterility rate (Nakagawa et al., 2007). In addition, XDH1-deficient plants also show earlier onset of age-dependent and dark-induced leaf senescence (Nakagawa et al., 2007; Brychkova et al., 2008) and decreased tolerance to drought stress (Watanabe et al., 2010). In accordance with the function of XDH1 in purine catabolism, precursors of uric acid (xanthine and hypoxanthine) are more abundant in XDH1-defficient plants, while downstream products (allantoin and allantoate) are less abundant (Nakagawa et al., 2007; Brychkova et al., 2008). Quantification of these primary metabolites in *picot1* KO plants indicates some of these purine catabolism intermediaries also accumulate differentially in the absence of PICOT1.

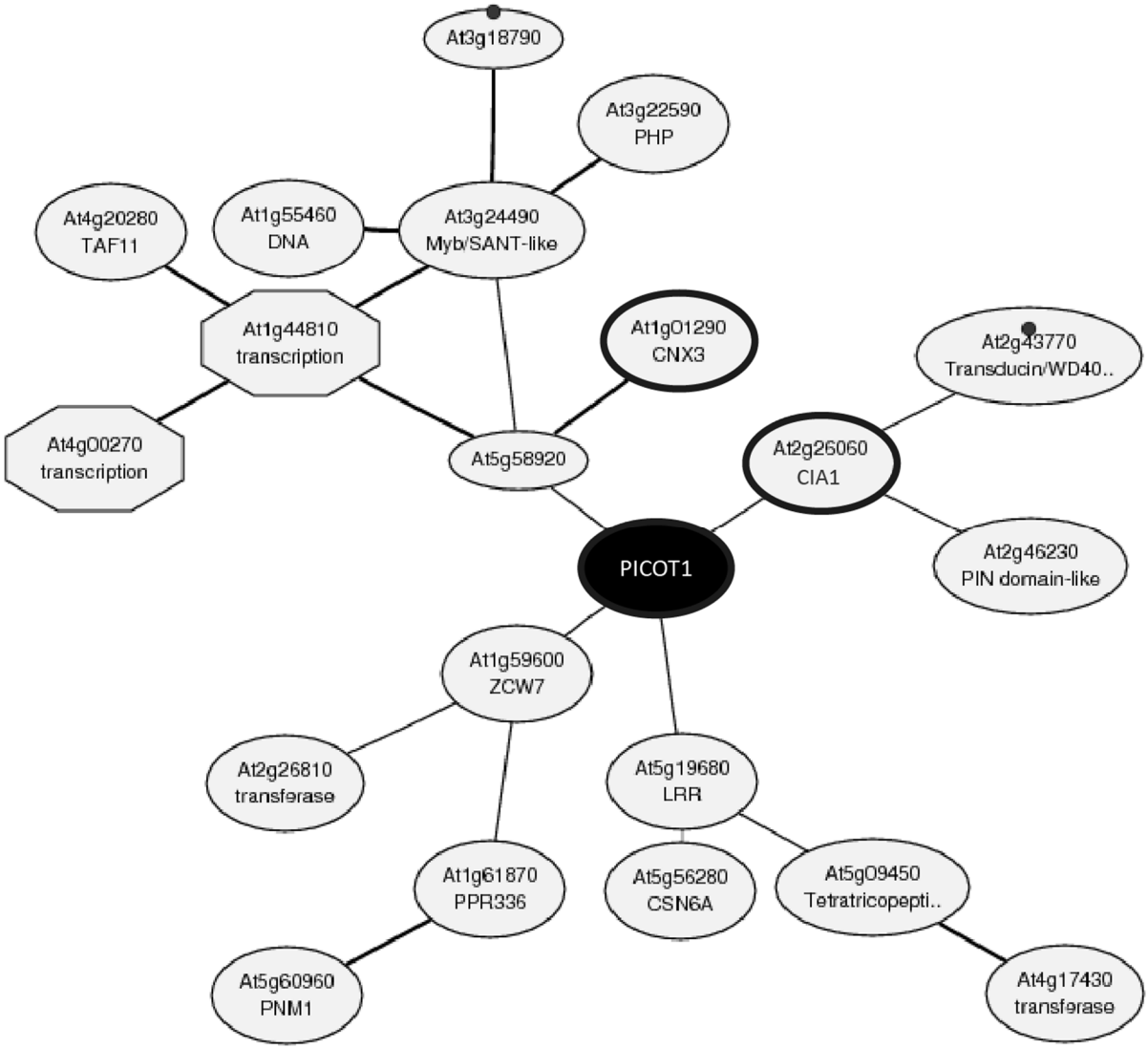

Figure 5-15. *PICOT1* co-expression network.

The co-expressed gene network around *PICOT1* includes CNX3, involved in molybdenum cofactor biosynthesis and *CIA1*, involved in Fe-S cluster maturation. Dots indicate genes encoding spliceosome components. Figure adapted from ATTED-II (Obayashi et al., 2009).

In contrast to mammals, where purine catabolism stops at the level of urea which can be subsequently excreted, nitrogen constitutes a much scarcer molecule for plants. Indeed, plants have evolved a mechanism to recycle the degradation products of purines by further degrading them into products that can be subsequently transported and incorporated again into new molecules. The pleiotropic phenotypic characteristics associated with decreased XDH1 protein levels are thus thought to result from a limitation in nitrogen availability as ureides with high N to C ratio can act as N-transport molecules from source to sink (Werner and Witte, 2011). XDH1 is the rate limiting enzyme in this process and in the light of the upcoming problems due to nitrogen over-fertilization of crops resulting in excess nitrates contaminating the ground water and the health risks associated, understanding the regulation of the purine catabolism pathway could enable the engineering of crops to improve nitrogen utilization and therefore reduce the need for nitrogen-rich fertilizers. Factors regulating

transcription of *XDH1* include the phytohormone abscisic acid and stress triggers like drought, senescence and salinity. As mentioned earlier, xanthine/hypoxanthine oxidizing activity of XDH1 is dependent on the presence of a C-terminal sulfurated Moco (Hesberg et al., 2004; Zarepour et al., 2010). Therefore, Moco cofactor incorporation and sulfuration, constitute two important processes that regulate XDH1 post-translationally and can therefore also influence the purine catabolism pathway. Here, we identified a third mechanism for post-translational regulation of XDH1-activity by PICOT1, possibly involved in the maturation of the [2Fe-2S] cluster on XDH1. Notably, PICOT1 expression is closely co-regulated with CIA1 and CNX3 expression (Figure 5-15, Obayashi et al., 2009), a component of the CIA targeting machinery (Luo et al., 2012) and a protein involved in the first steps of Moco biosynthesis (Teschner et al., 2010), respectively. Thus, the biosynthesis of two different co-factors required for XDH1 activity are co-regulated at the transcriptional level.

Next to XDH1, three additional enzymes involved in purine degradation where identified in a complex with PICOT1: URH1/2 and UREG. URH1/2 catalyse the cleavage of N-glycosidic bonds in inosine and xanthosine, yielding ribose and the respective base (hypoxanthine and xanthine, Riegler et al., 2011). *UreG* encodes a urease accessory protein, necessary for the activation of Urease that catalyses the last step of purine degradation (Witte et al., 2005). Ureides that are produced during purine degradation (e.g. allantoin and allantoate) have been shown to be strong ROS-scavengers. During senescence, ureides accumulate in WT plants but not in XDH1-defficient plants (Brychkova et al., 2008) and this is thought to contribute to the early onset of senescence in these plants. Remarkably, ectopic overexpression of RGLG3/4 in *N. benthamiana* also leads to early onset of senescence in the infiltrated areas. This could be attributed to their ability to target endogenous PICOT1 for degradation thereby disturbing the accumulation of specific purine catabolism intermediaries that can act as ROS scavengers. Indeed, PICOT1 function has been associated with protection against oxidative stress in both *Arabidopsis* and tomato. The authors showed PICOT1 can supress the growth defects of a yeast strain where ScGrx3/4 had been deleted. In addition, expression of PICOT1 in this strain restored the cell survival phenotype under oxidative stress (Cheng et al., 2011; Wu et al., 2012). Heat stress is also known to stimulate the formation of ROS, eventually damaging the cell. Accordingly, *picot1* seedlings have been reported to accumulate higher levels of ROS under heat stress and thermotolerance was compromised in these plants (Cheng et al., 2011).

In addition to a function for PICOT1 in purine catabolism, we have identified a new role for PICOT1 in tRNA modification. Several Fe-S proteins have been associated with RNA modifications, which are necessary for proper RNA function (Kimura and Suzuki, 2015). The best known representative of this category is the Elongator complex, that is required for tRNA wobble uridine modification resulting in 5-methoxycarbonyl-methyluridine (and derivatives) at position 34 (mcm^5U34) of the anticodon. Elongator consists of six proteins (ELP1-6 or ELO1-

6 in plants), of which ELP3/ELO3 is the enzymatic core, containing a radical SAM domain and binding an Fe-S cluster (Mehlgarten et al., 2010). We found that PICOT1 interacts with a component of the Elongator complex, ELP4/ELO1, but not with the known Fe-S protein ELP3/ELO3. A possible link between Elongator and PICOT1 was expected based on phenotypic characteristics of the corresponding mutants. In addition, we identified CTU1 and CTU2, two tRNA thiolating enzymes, as PICOT1 interacting proteins. CTU1/2 catalyse tRNA thiomodification at the wobble uridine (s^2U34, Philipp et al., 2014). Although this modification is thought to be Fe-S independent (Kimura and Suzuki, 2015), we showed here that CTU1/2 interact with PICOT1 thus linking an Fe-S protein to this tRNA modification. In addition, seedlings deficient in CTU1 or CTU2 also show the characteristic elongated leaf phenotype that is also present in *picot1* or *elo3-6* mutants. Furthermore, an uncharacterized protein with homology to bacterial TtcA (two-thio-cytidine) was also identified as a PICOT1 interacting protein. TtcA is responsible for s^2C32 tRNA modification and contains an Fe-S cluster (Bouvier et al., 2014). Although this modification has not been identified in *Arabidopsis* yet (Chen et al., 2010), conservation of the protein in plants and interaction with the Fe-S protein PICOT1 that interacts with several other tRNA modifying proteins indicate it might have a conserved function in plants. tRNA profiling of *picot1* seedlings should allow us to estimate to what extent PICOT1 is necessary for the various modifications described above. Notably, tRNA modifications are important to maintain translational fidelity including accurate decoding of tRNA and maintenance of the reading-frame. *Picot1* seedlings were previously shown to be hypersensitive to high temperature (Cheng et al., 2011; Knuesting et al., 2015), a condition wherein accurate translation is put to the test, indicating the newly identified role of PICOT1 in tRNA modification might contribute to this phenotype.

Finally, it deserves to be mentioned that the evolutionary conservation of the processes described in this chapter is amazing. Both the CIA complex, PICOT-proteins, XOR-proteins and tRNA-modifying enzymes are conserved in plants and humans. Additionally, HsPicot also seems to be regulated by the ubiquitin-proteasome system in human cells, as it has been detected in proteome-wide experiments where ubiquitinated proteins were identified through MS (Kim et al., 2011). Fe-S proteins are thought to be reminiscent of the origin of life, where Fe and S were readily available and which took place under a reducing, anaerobic environment. Metabolic pathways that evolved at these early stages of life became essential to all living organisms and many of them require Fe-S proteins (Sheftel et al., 2010). As Arabidopsis *picot1* seedlings show only mild developmental defects (Cheng et al., 2011; Knuesting et al., 2015) in contrast to the strong developmental defects associated with PICOT-depletion in yeast or animal cells, plants must have evolved alternative proteins or pathways that can take over these evolutionary conserved tasks. It will be interesting in the future to know whether the maturation of other cytosolic or nuclear proteins is also influenced by PICOT1, and if PICOT1-function is restricted to [2Fe-2S] containing proteins or also affects

those that contain other types of Fe-S clusters or Fe-centres. Since we identified PICOT1 as a protein interacting with both early and late-acting factors in CIA, further functional analyses combined with interaction studies will be performed to situate PICOT1 more accurately within this pathway.

EXPERIMENTAL PROCEDURES

Plant material and growth conditions

All mutant lines used in this study were in the Columbia-0 ecotype background. *picot1/grxs17* (SALK_021301), *rglg3rglg4* (SALK_098983, SALK_096022), *rol5-2* (GABI_709D04), *ctu2-2* (GABI_686B10) and *elo3-6* (GABI_555H06) mutants were previously described (Cheng et al., 2011; Zhang et al., 2012; Philipp et al., 2014; Leiber et al., 2010; Nelissen et al., 2010).

Arabidopsis seeds were sterilized by the chlorine gas method and sown on sterile plates containing the corresponding growth media. Plates were kept in the dark at 4°C two days for stratification before being transferred to a growth room with 21°C temperature and a 16 h light / 8 h dark regime, unless mentioned otherwise.

Cloning and site-directed mutagenesis

ORFs were amplified from a cDNA template by PCR using Phusion High-fidelity Polymerase (NEB), with specific primers including *att*B sites and subsequently recombined with pDONR207. For the creation of C-terminal fusions, reverse primers did not include a stop codon. For the construction of mRING variants, corresponding full-length Entry vectors were amplified using Pfu DNA polymerase (Promega) and primers containing the mutations. The PCR product was digested using *Dpn*I before transformation to *E. coli*. Positive colonies were picked and sequence verified. All primers used are listed in Supplementary Table S1. UBC and ELP-entry clones were kindly provided by Judy Callis (UC, Davis) and Mieke Van Lijsebettens (PSB/VIB, UGhent).

Yeast transformation and Yeast two-hybrid

Expression clones for yeast two-hybrid were generated by LR Gateway recombination between respective Entry-clones and pGADT7 or pGBKT7 and co-transformed in competent yeast cells of the *S. cerevisiae* strain PJ69-4A using the LiAc/SS carrier DNA/PEG method (Gietz and Schiestl, 2007). Transformants were selected on SD media lacking Leu and Trp (-2). Dropping was performed as described (Cuéllar Pérez et al., 2013).

Bimolecular Fluorescence Complementation (BiFC)

35S::ORF-tag constructs using the N and C-terminal halves of EGFP (head and tail, respectively) were constructed by triple Gateway reactions using pK7m34GW or pH7m34GW (Karimi et al., 2005) as described in (Boruc et al., 2010). 35S::tag-ORF constructs were generated by double Gateway recombination using pH7m24GW2 or pK7m24GW2 (Boruc et al., 2010). The constructs were co-expressed in *N. benthamiana* using *Agrobacterium*-mediated transient transformation. Interactions were scored by screening the lower epidermal cells for fluorescence using confocal microscopy 3-5 days after transformation using a Leica SP2 confocal microscope.

Agrobacterium-mediated transient transformation of N. benthamiana

WT *N. benthamiana* plants (3–4 weeks old) were used for transient expression of constructs by *Agrobacterium tumefaciens*-mediated transient transformation of lower epidermal leaf cells as previously described (Boruc et al., 2010) using a modified infiltration buffer (10 mM $MgCl_2$, Merck; 10 mM MES pH 5.7, Duchefa; 100 µM Acetosyringone, Sigma-Aldrich) and addition of a P19 expressing *Agrobacterium* strain to boost protein expression (Voinnet et al., 2003). All *Agrobacterium* strains were grown for 2 days, diluted to OD 1 in infiltration buffer and incubated for 2-4 h at room temperature before mixing in a 1:1 ratio with other strains and injecting.

Tandem affinity purification

N or C-terminally tagged TAP constructs (GS or GSrh tag) were generated as described (Van Leene et al., 2015), used for the transformation of Arabidopsis PSB-D cell suspension cultures without callus selection and further grown and subcultured as described (Van Leene et al., 2011). Stably transformed cultures were scaled up and harvested 6 days after subculturing.

Transgenic Arabidopsis seeds were generated by floral dip (Clough and Bent, 1998), using Col-0 as the background ecotype and the same constructs as for cell culture transformation. Transformants were selected as

described (Van Leene et al., 2015). Purifications were performed as described (Van Leene et al., 2015) with the exception that no Benzonase treatment was performed on the cell culture extracts. Expression of TAP-tagged constructs was verified on an aliquot of total protein extract before purification.

Cell-free degradation assays

Total protein extracts were prepared by resuspending ground tissue in cold extraction buffer (25 mM Tris HCl pH 7.5, 10 mM NaCl, 10 mM MgCl2, 4 mM PMSF, 5 mM DTT 5 mM, 10 mM ATP) at a ratio of 1 g tissue per ml extraction buffer and centrifuged at 12000 g for 15 minutes, twice. To test PICOT1 stability, 10-day-old PICOT-HA seedlings were grown under continuous light at 21°C and 50 µM MG132 (Boston Biochem) or 1 % v/v dimethyl sulfoxide as a control was added to the total protein extract. Each reaction was incubated at room temperature and samples were harvested at the indicated time points. To stop the reaction, SDS sample buffer was added, followed by boiling for 10 minutes before gel analysis.

To test protein stability in wild type and mutant background, total protein extraction was performed as above but PMSF, DTT, ATP and 300 ng PICOT1:V5-His were added to 3.5 µg/µl of each protein extract (Bradford, 1976) just before the room temperature incubation.

Localization studies

For generation of transgenic plants with 35S::ORF-GFP or 35S::GFP-ORF expression, entry clones containing PICOT1, RGLG3mRING or RGLG4mRING were recombined with the pFAST-R05 or pFAST-R06, respectively. Transgenic Arabidopsis seeds were generated by floral dip (Clough and Bent, 1998), using Col-0 as the background ecotype. Transformants were selected based on the seed fluorescent marker (RFP) and homozygous T3 plant lines were used in the assays. Localization studies were performed on the roots of 4-day old transgenic seedlings grown vertically on MS plates (10 g/L sucrose and 8 g/L agar), after a brief incubation in propidium iodide (3 mg/L, Sigma) using a Leica SP2 confocal microscope. For localization studies in *N. benthamiana,* leafs were transiently transformed with the same constructs that were used to generate *Arabidopsis* transgenic lines, in addition to a P19 expressing construct. Lower epidermal leaf cells were imaged 3-5 days after infiltration using a Leica SP2 confocal microscope.

Immunodetection

After quantification of the protein content as described by (Bradford, 1976), the indicated protein samples were loaded on a 4–15% TGX gel (Bio-Rad) and ran for 20 min at 300 V. Next, proteins were transferred to 0.2 µm PVDF membranes (Bio-Rad) with the Trans-blot Turbo (Bio-Rad). A 1/1000 dilution of rat monoclonal anti-HA antibodies (clone 3F10, Roche) were used to detect PICOT1-HA or HA-Ub conjugated proteins. A 1/2000 dilution of polyclonal rabbit anti-V5 antibodies (Sigma) were used to detect recombinant PICOT1-V5-HIS. A 1/1000 dilution of monoclonal mouse anti-Ubiquitin antibodies (Millipore, clone FK2) were used to detect mono- and polyubiquitinated proteins. A 1/5000 dilution of HRP-conjugated monoclonal anti-GFP antibodies (Miltenyi Biotech Inc.) were used to detect free GFP. A mixture containing both a 1/2000 dilution of anti-tetra-HIS and a 1/2000 dilution of anti-penta-HIS mouse monoclonal antibodies (Roche) was used to detect PICOT1-HIS. A 1/1000 dilution of polyclonal mouse anti-GST antibodies were used to detect GST-RGLG4. Chemiluminescent detection was performed with Western Bright ECL (Isogen).

Affinity purification of ubiquitinated proteins

Isolation of ubiquitinated proteins was performed as previously described (Manzano et al., 2008) with small modifications. Briefly, 35S::PICOT1-HA seedlings were grown in half-strength liquid MS medium and treated for 24 h with 50 µM MG132 or DMSO before harvesting. Proteins were extracted using buffer BI (50 mM Tris–HCl pH 7.5; 20 mM NaCl; 0.1% NP-40 and 5 mM ATP) plus plant protease inhibitors cocktail (Sigma), 1 mM of PMSF, 50 µM MG132, 10 nM ubiquitin aldehyde and 10 mM N-Ethylmaleimide. Protein extracts were incubated with 40 µL pre-washed TUbE-agarose resin (Hjerpe et al., 2009) or the agarose resin alone at 4°C during 4 h. Afterwards, the beads were washed 2 times with 1 mL BI buffer and once more with 1 mL BII buffer (BI plus 200 mM NaCl) and proteins were eluted by boiling into 50 µL SDS loading buffer. The eluted proteins were separated by SDS-PAGE and analysed by immunoblotting.

In vitro ubiquitination assay

6X-His-E2, His-MBP-E3s, GST-E3s and PICOT1:V5-His fusions were expressed in *Escherichia coli* BL21 and purified according to manufacturer's instructions (Amylose resin, New England Biolabs or Ni-NTA superflow, Qiagen). Proteins were stored in buffer containing 50 mM Tris-HCl pH 7.5, 10 mM $MgCl_2$, 0.2 mM DTT and 20 % v/v glycerol and kept at -80°C until needed. Recombinant 6X-His-HsUbcH5b was obtained from Sigma.

Ubiquitination assays were carried out incubating 50 ng E1 (E-304, Boston Biochem), 50 ng E2, 50 ng E3, 500 ng PICOT-V5-His, 0.1 U CREATINE PHOSPHOKINASE (Sigma, C3755) and 5 µg HA-Ubiquitin (U-110, Boston Biochem) in 1X ubiquitination buffer (50 mM Tris-HCl pH 7.5, 10 mM $MgCl_2$, 0.2 mM DTT, 1 mM ATP and 10 mM phosphocreatine) for 2 hours at 30°C. The reactions were stopped by adding SDS sample buffer and boiling for 10 minutes. Samples were separated on a 4-15% SDS-PAGE gel (Bio-Rad) followed by immunoblotting with anti-HA (Roche) or anti-V5 (Sigma).

Ubiquitinated sites were analysed by Q- Exactive mass spectrometer in LC-MS/MS. Gel samples were prepared for mass spectrometry, 7 slices were cut from Nupage Bis-Tris Gel (4-12%, Invitrogen) and digested with trypsin. The supernatants containing the peptides were separated from the gel pieces by sonication and concentrated by vacuum drying. Every sample was re-dissolved in 20 µl loading solvent for LC-MS/MS. 5 µl of the prepared samples were analysed by the Q-Exactive mass spectrometer in LC-MS/MS mode. The MS/MS data, obtained were presented against the NCBI *E. coli* K12 protein database concatenated with the V5-His-tagged sequence of PICOT1. To identify the proteins, each peptide was linked to a protein by the Mascot algorithm. Each identification was performed with 99% confidence settings.

Metabolites quantification

Metabolite profiling by LC-MS was carried out according to (Tohge and Fernie, 2010).

Enzymatic activity measurement (XDH)

XDH1 activity measurements in plant crude extracts were performed as described in (Hesberg et al., 2004). Briefly, total protein extract was obtained from 10-day-old Arabidopsis seedlings. Plant tissue was grown in liquid nitrogen, resuspended in 2 volumes of extraction buffer (100 mM Tris-HCl pH 7.5, 2.5 mM EDTA, 5 mM DTT) and centrifuged. Supernatants were concentrated using Nanosep centrifugal devices (30K Omega, Pall Life Sciences) and 100 µg of total protein quantified by the method of (Bradford, 1976) were used for activity assays. 4-16% native polyacrylamide gels under non-reducing conditions were run at 4°C, followed by in-gel staining with 1 mM hypoxanthine, 1 mM 3-(4,5-Dimethyl-2-thiazolyl)-2,5-diphenyltetrazolium bromide (MTT) and 0.1 mM phenazine methosulfate in 250 mM Tris-HCl pH 8.5. Bands were quantified using ImageJ software.

REFERENCES

Balk J, Schaedler TA (2014) Iron Cofactor Assembly in Plants. Annual Review of Plant Biology, Vol 65 **65:** 125-+

Bernard DG, Netz DJA, Lagny TJ, Pierik AJ, Balk J (2013) Requirements of the cytosolic iron-sulfur cluster assembly pathway in Arabidopsis. Philos T R Soc B **368**

Boruc J, Van den Daele H, Hollunder J, Rombauts S, Mylle E, Hilson P, Inze D, De Veylder L, Russinova E (2010) Functional Modules in the Arabidopsis Core Cell Cycle Binary Protein-Protein Interaction Network. The Plant cell **22:** 1264-1280

Bouvier D, Labessan N, Clémancey M, Latour J-M, Ravanat J-L, Fontecave M, Atta M (2014) TtcA a new tRNA-thioltransferase with an Fe-S cluster. Nucleic acids research **42:** 7960-7970

Bradford MM (1976) Rapid and Sensitive Method for Quantitation of Microgram Quantities of Protein Utilizing Principle of Protein-Dye Binding. Anal Biochem **72:** 248-254

Braun P, Carvunis AR, Charloteaux B, Dreze M, Ecker JR, Hill DE, Roth FP, Vidal M, Galli M, Balumuri P, et al (2011) Evidence for Network Evolution in an Arabidopsis Interactome Map. Science **333:** 601-607

Brychkova G, Alikulov Z, Fiuhr R, Sagi M (2008) A critical role for ureides in dark and senescence-induced purine remobilization is unmasked in the Atxdh1 Arabidopsis mutant. Plant Journal **54:** 496-509

Bych K, Netz DJA, Vigani G, Bill E, Lill R, Pierik AJ, Balk J (2008) The Essential Cytosolic Iron-Sulfur Protein Nbp35 Acts without Cfd1 Partner in the Green Lineage. Journal of Biological Chemistry **283:** 35797-35804

Callis J (2014) The ubiquitination machinery of the ubiquitin system. The Arabidopsis book / American Society of Plant Biologists **12:** e0174

Cha H, Kim JM, Oh JG, Jeong MH, Park CS, Park J, Jeong HJ, Park BK, Lee YH, Jeong D, et al (2008) PICOT is a critical regulator of cardiac hypertrophy and cardiomyocyte contractility. J Mol Cell Cardiol **45:** 796-803

Chen P, Jager G, Zheng B (2010) Transfer RNA modifications and genes for modifying enzymes in Arabidopsis thaliana. BMC plant biology **10**

Cheng MC, Hsieh EJ, Chen JH, Chen HY, Lin TP (2012) Arabidopsis RGLG2, Functioning as a RING E3 Ligase, Interacts with AtERF53 and Negatively Regulates the Plant Drought Stress Response. Plant physiology **158:** 363-375

Cheng NH, Liu JZ, Liu X, Wu QY, Thompson SM, Lin J, Chang J, Whitham SA, Park S, Cohen JD, et al (2011) Arabidopsis Monothiol Glutaredoxin, AtGRXS17, Is Critical for Temperature-dependent Postembryonic Growth and Development via Modulating Auxin Response. Journal of Biological Chemistry **286:** 20398-20406

Clough SJ, Bent AF (1998) Floral dip: a simplified method for Agrobacterium-mediated transformation of Arabidopsis thaliana. Plant Journal **16:** 735-743

Couturier J, Touraine B, Briat JF, Gaymard F, Rouhier N (2013) The iron-sulfur cluster assembly machineries in plants: current knowledge and open questions. Frontiers in plant science **4**

Couturier J, Wu HC, Dhalleine T, Pegeot H, Sudre D, Gualberto JM, Jacquot JP, Gaymard F, Vignols F, Rouhier N (2014) Monothiol GlutaredoxinBolA Interactions: Redox Control of Arabidopsis thaliana BolA2 and SufE1. Molecular plant **7:** 187-205

Cuéllar Pérez A, Pauwels L, De Clercq R, Goossens A (2013) Yeast two-hybrid analysis of jasmonate signaling proteins. Methods in molecular biology **1011:** 173-185

Deshaies RJ, Joazeiro CAP (2009) RING Domain E3 Ubiquitin Ligases. Annu Rev Biochem **78:** 399-434

Gietz RD, Schiestl RH (2007) High-efficiency yeast transformation using the LiAc/SS carrier DNA/PEG method. Nature protocols **2:** 31-34

Harper JW, Tan MKM (2012) Understanding Cullin-RING E3 Biology through Proteomics-based Substrate Identification. Molecular & Cellular Proteomics **11:** 1541-1550

Haunhorst P, Berndt C, Eitner S, Godoy JR, Lillig CH (2010) Characterization of the human monothiol glutaredoxin 3 (PICOT) as iron-sulfur protein. Biochemical and biophysical research communications **394:** 372-376

Haunhorst P, Hanschmann EM, Brautigam L, Stehling O, Hoffmann B, Muhlenhoff U, Lill R, Berndt C, Lillig CH (2013) Crucial function of vertebrate glutaredoxin 3 (PICOT) in iron homeostasis and hemoglobin maturation. Molecular biology of the cell **24:** 1895-1903

Hesberg C, Hansch R, Mendel RR, Bittner F (2004) Tandem orientation of duplicated xanthine dehydrogenase genes from Arabidopsis thaliana - Differential gene expression and enzyme activities. Journal of Biological Chemistry **279:** 13547-13554

Hjerpe R, Aillet F, Lopitz-Otsoa F, Lang V, England P, Rodriguez MS (2009) Efficient protection and isolation of ubiquitylated proteins using tandem ubiquitin-binding entities. EMBO reports **10:** 1250-1258

Isakov N, Witte S, Altman A (2000) PICOT-HD: a highly conserved protein domain that is often associated with thioredoxin and glutaredoxin modules. Trends Biochem Sci **25:** 537-539

Jeong D, Kim JM, Cha H, Oh JG, Park J, Yun SH, Ju ES, Jeon ES, Hajjar RJ, Park WJ (2008) PICOT attenuates cardiac hypertrophy by disrupting calcineurin - NFAT signaling. Circ Res **102:** 711-719

Karimi M, De Meyer B, Hilson P (2005) Modular cloning in plant cells. Trends in plant science **10:** 103-105

Kim DY, Scalf M, Smith LM, Vierstra RD (2013) Advanced proteomic analyses yield a deep catalog of ubiquitylation targets in Arabidopsis. The Plant cell **25:** 1523-1540

Kim W, Bennett EJ, Huttlin EL, Guo A, Li J, Possemato A, Sowa ME, Rad R, Rush J, Comb MJ, et al (2011) Systematic and Quantitative Assessment of the Ubiquitin-Modified Proteome. Molecular cell **44:** 325-340

Kimura S, Suzuki T (2015) Iron–sulfur proteins responsible for RNA modifications. Biochimica et Biophysica Acta (BBA) - Molecular Cell Research **1853:** 1272-1283

Knuesting J, Riondet C, Maria C, Kruse I, Bécuwe N, König N, Berndt C, Tourrette S, Guilleminot-Montoya J, Herrero E, et al (2015) Arabidopsis Glutaredoxin S17 and Its Partner, the Nuclear Factor Y Subunit C11/Negative Cofactor 2α, Contribute to Maintenance of the Shoot Apical Meristem under Long-Day Photoperiod. Plant physiology **167:** 1643-1658

Kohbushi H, Nakai Y, Kikuchi S, Yabe T, Hori H, Nakai M (2009) Arabidopsis cytosolic Nbp35 homodimer can assemble both [2Fe-2S] and [4Fe-4S] clusters in two distinct domains. Biochemical and biophysical research communications **378:** 810-815

Kraft E, Stone SL, Ma L, Su N, Gao Y, Lau OS, Deng XW, Callis J (2005) Genome analysis and functional characterization of the E2 and RING-type E3 ligase ubiquitination enzymes of Arabidopsis. Plant physiology **139:** 1597-1611

Leiber RM, John F, Verhertbruggen Y, Diet A, Knox JP, Ringli C (2010) The TOR Pathway Modulates the Structure of Cell Walls in Arabidopsis. The Plant cell **22:** 1898-1908

Leidel S, Pedrioli PGA, Bucher T, Brost R, Costanzo M, Schmidt A, Aebersold R, Boone C, Hofmann K, Peter M (2009) Ubiquitin-related modifier Urm1 acts as a sulphur carrier in thiolation of eukaryotic transfer RNA. Nature **458:** 228-U229

Leitner J, Petrasek J, Tomanov K, Retzer K, Parezova M, Korbei B, Bachmair A, Zazimalova E, Luschnig C (2012) Lysine63-linked ubiquitylation of PIN2 auxin carrier protein governs hormonally controlled adaptation of Arabidopsis root growth. Proceedings of the National Academy of Sciences of the United States of America **109:** 8322-8327

Li HR, Mapolelo DT, Dingra NN, Naik SG, Lees NS, Hoffman BM, Riggs-Gelasco PJ, Huynh BH, Johnson MK, Outten CE (2009) The Yeast Iron Regulatory Proteins Grx3/4 and Fra2 Form Heterodimeric Complexes Containing a [2Fe-2S] Cluster with Cysteinyl and Histidyl Ligation. Biochemistry-Us **48:** 9569-9581

Li HR, Mapolelo DT, Randeniya S, Johnson MK, Outten CE (2012) Human Glutaredoxin 3 Forms [2Fe-2S]-Bridged Complexes with Human BolA2. Biochemistry-Us **51:** 1687-1696

Luo DX, Bernard DG, Balk J, Hai H, Cui XF (2012) The DUF59 Family Gene AE7 Acts in the Cytosolic Iron-Sulfur Cluster Assembly Pathway to Maintain Nuclear Genome Integrity in Arabidopsis. The Plant cell **24:** 4135-4148

Manzano C, Abraham Z, Lopez-Torrejon G, Del Pozo JC (2008) Identification of ubiquitinated proteins in Arabidopsis. Plant molecular biology **68:** 145-158

Mattiroli F, Sixma TK (2014) Lysine-targeting specificity in ubiquitin and ubiquitin-like modification pathways. Nat Struct Mol Biol **21:** 308-316

Mehlgarten C, Jablonowski D, Wrackmeyer U, Tschitschmann S, Sondermann D, Jager G, Gong ZZ, Bystrom AS, Schaffrath R, Breunig KD (2010) Elongator function in tRNA wobble uridine modification is conserved between yeast and plants. Mol Microbiol **76:** 1082-1094

Michelle C, Vourc'h P, Mignon L, Andres CR (2009) What Was the Set of Ubiquitin and Ubiquitin-Like Conjugating Enzymes in the Eukaryote Common Ancestor? Journal of molecular evolution **68:** 616-628

Muhlenhoff U, Molik S, Godoy JR, Uzarska MA, Richter N, Seubert A, Zhang Y, Stubbe J, Pierrel F, Herrero E, et al (2010) Cytosolic Monothiol Glutaredoxins Function in Intracellular Iron Sensing and Trafficking via Their Bound Iron-Sulfur Cluster. Cell Metab **12:** 373-385

Nakagawa A, Sakamoto S, Takahashi M, Morikawa H, Sakamoto A (2007) The RNAi-mediated silencing of xanthine dehydrogenase impairs growth and fertility and accelerates leaf senescence in transgenic arabidopsis plants. Plant Cell Physiol **48:** 1484-1495

Nelissen H, De Groeve S, Fleury D, Neyt P, Bruno L, Bitonti MB, Vandenbussche F, Van Der Straeten D, Yamaguchi T, Tsukaya H, et al (2010) Plant Elongator regulates auxin-related genes during RNA polymerase II transcription elongation. Proceedings of the National Academy of Sciences of the United States of America **107:** 1678-1683

Obayashi T, Hayashi S, Saeki M, Ohta H, Kinoshita K (2009) ATTED-II provides coexpressed gene networks for Arabidopsis. Nucleic acids research **37:** D987-D991

Pan IC, Schmidt W (2014) Functional implications of K63-linked ubiquitination in the iron deficiency response of Arabidopsis roots. Frontiers in plant science **4**

Philipp M, John F, Ringli C (2014) The cytosolic thiouridylase CTU2 of Arabidopsis thaliana is essential for posttranscriptional thiolation of tRNAs and influences root development. BMC plant biology **14:** 109

Plechanovova A, Jaffray EG, Tatham MH, Naismith JH, Hay RT (2012) Structure of a RING E3 ligase and ubiquitin-loaded E2 primed for catalysis. Nature **489:** 115-U135

Pujol-Carrion N, Belli G, Herrero E, Nogues A, de la Torre-Ruiz MA (2006) Glutaredoxins Grx3 and Grx4 regulate nuclear localisation of Aft1 and the oxidative stress response in Saccharomyces cerevisiae. J Cell Sci **119:** 4554-4564

Qu Y, Wang JH, Ray PS, Guo H, Huang JA, Shin-Sim M, Bukoye BA, Liu BY, Lee AV, Lin X, et al (2011) Thioredoxin-like 2 regulates human cancer cell growth and metastasis via redox homeostasis and NF-kappa B signaling. J Clin Invest **121:** 212-225

Riegler H, Geserick C, Zrenner R (2011) Arabidopsis thaliana nucleosidase mutants provide new insights into nucleoside degradation. New Phytologist **191:** 349-359

Roret T, Tsan P, Couturier J, Zhang B, Johnson MK, Rouhier N, Didierjean C (2014) Structural and Spectroscopic Insights into BolA-Glutaredoxin Complexes. Journal of Biological Chemistry **289:** 24588-24598

Saito Y, Shibayama H, Tanaka H, Tanimura A, Matsumura I, Kanakura Y (2011) PICOT is a molecule which binds to anamorsin. Biochemical and biophysical research communications **408:** 329-333

Scaglione KM, Basrur V, Ashraf NS, Konen JR, Elenitoba-Johnson KSJ, Todi SV, Paulson HL (2013) The Ubiquitin-conjugating Enzyme (E2) Ube2w Ubiquitinates the N Terminus of Substrates. Journal of Biological Chemistry **288:** 18784-18788

Sheftel A, Stehling O, Lill R (2010) Iron-sulfur proteins in health and disease. Trends Endocrin Met **21:** 302-314

Stehling O, Vashisht AA, Mascarenhas J, Jonsson ZO, Sharma T, Netz DJA, Pierik AJ, Wohlschlegel JA, Lill R (2012) MMS19 Assembles Iron-Sulfur Proteins Required for DNA Metabolism and Genomic Integrity. Science **337:** 195-199

Stone SL, Hauksdottir H, Troy A, Herschleb J, Kraft E, Callis J (2005) Functional analysis of the RING-type ubiquitin ligase family of Arabidopsis. Plant physiology **137:** 13-30

Stroher E, Millar AH (2012) The biological roles of glutaredoxins. Biochem J **446:** 333-348

Tarassov K, Messier V, Landry CR, Radinovic S, Molina MMS, Shames I, Malitskaya Y, Vogel J, Bussey H, Michnick SW (2008) An in vivo map of the yeast protein interactome. Science **320:** 1465-1470

Teschner J, Lachmann N, Schulze J, Geisler M, Selbach K, Santamaria-Araujo J, Balk J, Mendel RR, Bittner F (2010) A Novel Role for Arabidopsis Mitochondrial ABC Transporter ATM3 in Molybdenum Cofactor Biosynthesis. The Plant cell **22:** 468-480

Tohge T, Fernie AR (2010) Combining genetic diversity, informatics and metabolomics to facilitate annotation of plant gene function. Nature protocols **5:** 1210-1227

Van Leene J, Eeckhout D, Cannoot B, De Winne N, Persiau G, Van De Slijke E, Vercruysse L, Dedecker M, Verkest A, Vandepoele K, et al (2015) An improved toolbox to unravel the plant cellular machinery by tandem affinity purification of Arabidopsis protein complexes. Nature protocols **10:** 169-187

Van Leene J, Eeckhout D, Persiau G, Van De Slijke E, Geerinck J, Van Isterdael G, Witters E, De Jaeger G (2011) Isolation of transcription factor complexes from Arabidopsis cell suspension cultures by tandem affinity purification. Methods in molecular biology **754:** 195-218

Voinnet O, Rivas S, Mestre P, Baulcombe D (2003) An enhanced transient expression system in plants based on suppression of gene silencing by the p19 protein of tomato bushy stunt virus. The Plant journal : for cell and molecular biology **33:** 949-956

Watanabe S, Nakagawa A, Izumi S, Shimada H, Sakamoto A (2010) RNA interference-mediated suppression of xanthine dehydrogenase reveals the role of purine metabolism in drought tolerance in Arabidopsis. Febs Lett **584:** 1181-1186

Werner AK, Witte CP (2011) The biochemistry of nitrogen mobilization: purine ring catabolism. Trends in plant science **16:** 381-387

Witte CP, Rosso MG, Romeis T (2005) Identification of three urease accessory proteins that are required for urease activation in Arabidopsis. Plant physiology **139:** 1155-1162

Wu QY, Lin J, Liu JZ, Wang XF, Lim W, Oh M, Park J, Rajashekar CB, Whitham SA, Cheng NH, et al (2012) Ectopic expression of Arabidopsis glutaredoxin AtGRXS17 enhances thermotolerance in tomato. Plant Biotechnol J **10:** 945-955

Ye Y, Rape M (2009) Building ubiquitin chains: E2 enzymes at work. Nature reviews Molecular cell biology **10:** 755-764

Yin XJ, Volk S, Ljung K, Mehlmer N, Dolezal K, Ditengou F, Hanano S, Davis SJ, Schmelzer E, Sandberg G, et al (2007) Ubiquitin lysine 63 chain forming ligases regulate apical dominance in Arabidopsis. The Plant cell **19:** 1898-1911

Zarepour M, Kaspari K, Stagge S, Rethmeier R, Mendel RR, Bittner F (2010) Xanthine dehydrogenase AtXDH1 from Arabidopsis thaliana is a potent producer of superoxide anions via its NADH oxidase activity. Plant molecular biology **72:** 301-310

Zhang X, Wu Q, Cui S, Ren J, Qian W, Yang Y, He S, Chu J, Sun X, Yan C, et al (2015) Hijacking of the jasmonate pathway by the mycotoxin fumonisin B1 (FB1) to initiate programmed cell death in Arabidopsis is modulated by RGLG3 and RGLG4. Journal of experimental botany

Zhang X, Wu Q, Ren J, Qian WQ, He SP, Huang KW, Yu XC, Gao Y, Huang P, An CC (2012) Two Novel RING-Type Ubiquitin Ligases, RGLG3 and RGLG4, Are Essential for Jasmonate-Mediated Responses in Arabidopsis. Plant physiology **160:** 808-822

Chapter 6:
The role of the E3 ligases RGLG3/4 and their candidate targets in jasmonate signalling

Astrid Nagels Durand[1], Sabrina Iñigo, Andres Ritter, Geert De Jaeger, Laurens Pauwels and Alain Goossens

[1] Author contributions: cloning, generation of plant lines, tandem affinity purifications, yeast two-hybrid analyses, JA-sensitivity assays, data interpretation and writing.

SUMMARY

Jasmonates (JAs) are a class of plant hormones that regulate plant development and are involved in the response of plants to both biotic and abiotic stresses. The ubiquitin system is essential for the onset of most hormonal responses by controlling both hormone biosynthesis and signal transduction. In the JA-signalling pathway, the E3 ubiquitin ligase component *COI1* is essential for the perception of the hormone. Two additional E3 ubiquitin ligases *RING LIGASE 3* and *4* (*RGLG3* and *RGLG4*) have been proposed to contribute to JA-signalling, however their precise mode of action during this process is unknown. Here we show that the ubiquitination target of *RGLG3/4*, the glutathioredoxin *PKC*-θ *INTERACTING COUSIN OF THIOREDOXIN-1* (*PICOT1*/*GRXS17*), is a potential regulator of *COI1* function. PICOT1 was found to physically interact with COI1 *in vivo*. Evaluation of the JA-response of *rglg3rglg4* double knock-out seedlings revealed these E3 ligases function in JA-signalling only in the presence of low amounts of JAs. Additionally, *coi1-16*, a temperature sensitive missense allele of *COI1*, could partially complement the *picot1* short-root phenotype. Transcriptome analysis of *picot1*, *coi1-16* and *picot1coi1-16* mutants revealed a set of genes that are upregulated in *coi1-16* in a PICOT1-dependent but JA-independent manner. Our results identify a potential new molecular mechanism for JA-independent COI1 functioning involving RGLG3/4 and PICOT1.

INTRODUCTION

Despite the well-established function of ubiquitination in the control of several hormonal responses in plants (see Chapter 1), only one ubiquitin E3 ligase has been thoroughly characterized in the jasmonate (JA) signalling pathway. The F-box protein COI1 assembles with ASK1/2, RBX1 and CUL1 resulting in a complex E3 ligase. Binding of the bioactive JA hormone JA-Ile, or the analogue chemical Coronatine, enables SCF^{COI1} to bind to JAZ repressors and trigger their ubiquitination and subsequent proteolytic degradation. Together, SCF^{COI1} and JAZ constitute the JA-receptor (Chini et al., 2007; Thines et al., 2007; Sheard et al., 2010). Degradation of JAZ proteins relieves multiple transcription factors of repression, eventually resulting in activation of downstream responses (Pauwels and Goossens, 2011; Kazan and Manners, 2012).

Members of the RING DOMAIN LIGASE (RGLG) family of Arabidopsis have recently been associated with various hormone and stress signalling pathways. The RGLG protein family belongs to a subfamily of plant RING-type E3 ligases and contains five members in *Arabidopsis.* Family members are characterized by the presence of a von Willebrand factor type A or copine domain in addition to the characteristic RING-domain (Whittaker and Hynes, 2002; Stone et al., 2005). *RGLG1* and *RGLG2* were shown to function redundantly and simultaneous loss-of-function mutations in both genes causes severely altered phenotypes including loss of apical dominance, altered phyllotaxy and leaf shape and increased cell size. These phenotypes are at least partially caused by alterations in the directional flow of auxin, which is mediated by PIN-proteins (Yin et al., 2007). Accordingly, RGLG2 was shown to interact with PIN1 and PIN2 (Yin et al., 2007; Leitner et al., 2012). PIN1-type auxin carrier proteins are located at the plasma membrane and are regulated by poly-ubiquitination, amongst others, resulting in endocytosis, vacuolar targeting and finally, proteolytic degradation. Poly-ubiquitination of PIN2 was decreased in *rglg1rglg2* plants, suggesting RGLG1/2 substantially contribute to this process (Leitner et al., 2012).

In addition to a role in polar auxin transport, *RGLG1* and *RGLG2* have also been shown to be involved in the response to abiotic stresses such as drought, salt stress and heat stress by regulating the stability of the abscisic acid-responsive AP2/ERF transcription factor (TF) ERF53. These stress conditions trigger translocation of RGLG1/2 from the plasma membrane to the nucleus, where they both interact with ERF53. Finally, mono-ubiquitination of ERF53 by RGLG2 was confirmed *in vitro* (Cheng et al., 2012; Hsieh et al., 2013).

RGLG3 and RGLG4, two other members of the RGLG family have been associated with JA-signalling (Zhang et al., 2012). JA-mediated root growth inhibition was reported to be decreased in *rglg3rglg4* double knock-out (KO) plants, but not in single KO plants indicating RGLG3 and RGLG4 have redundant functions during JA-signalling. Accordingly, plants overexpressing either RGLG3 or RGLG4 experience enhanced JA-mediated root growth

inhibition. The JA-insensitivity of *rglg3rglg4* seedlings was confirmed on the transcriptional level as induction of JA-responsive genes is decreased when these seedlings are treated with exogenous JA (Zhang et al., 2012).

Although *RGLG3* and *RGLG4* perform redundant functions in JA-signalling, their expression is regulated by JA in different ways. While in mature leafs *RGLG3* is mainly expressed in the veins and its transcription is induced by MeJA treatment, *RGLG4* expression is diffused throughout the tissue and is repressed after MeJA treatment (Zhang et al., 2012). Based on the requirement of functional COI1 for the JA-hypersensitivity phenotypes of RGLG3/4 overexpressing plants, a model was proposed where RGLG3 and RGLG4 function upstream of the known JA core signalling complex (COI1-JAZ-MYC-NINJA). Although experimental confirmation is still needed, the authors speculate RGLG3/4 could be involved in the signal transduction from JA-Ile to COI1 or could influence JA-production through feedback regulation (Zhang et al., 2012).

RGLG3/4 were also reported to function in biotic stress tolerance by regulating Fumonisin B1 (FB1)-triggered programmed cell death (PCD). FB1 is a mycotoxin produced by the fungal pathogen *Fusarium moniliforme* that triggers PCD by inhibiting sphingolipid biosynthesis. In addition to the JA-signalling pathway, FB1-elicited PCD also requires activation of the salicylic acid (SA) signalling pathway. *RGLG3* and *RGLG4* were postulated to regulate the crosstalk between SA and JA in response to *F. moniliforme* infection (Zhang et al., 2015).

In Chapter 5 we showed that RGLG3 and RGLG4 regulate PKC-θ INTERACTING COUSIN OF THIOREDOXIN1 (PICOT1/GRXS17) protein levels by ubiquitination, triggering subsequent proteasomal degradation of the latter. We further also investigated the molecular function of the PICOT1 protein. The glutathioredoxin *PICOT1* is the Arabidopsis ortholog of yeast *GRX3* and human *PICOT*, but the physiological and molecular role of *PICOT1* in plants is not well understood (Couturier et al., 2013). PICOT1 function has been associated with protection against oxidative stress in Arabidopsis and with thermotolerance in Arabidopsis and tomato (Cheng et al., 2011; Wu et al., 2012; Knuesting et al., 2015). *Picot1* loss-of-function plants were hypersensitive to heat stress and this was associated with alterations in polar auxin transport in these mutants (Cheng et al., 2011).

PICOT1 also interacts with and regulates the redox state of BolA2, whose biological function is still unknown in plants. Interaction of PICOT1 with BolA2 is mediated by simultaneous coordination of an iron-sulfur cluster (Fe-S) by both proteins (Couturier et al., 2014; Roret et al., 2014). PICOT1 can also bind Fe-S clusters independent of BolA2 interaction, through the formation of Fe-S bridged homo-dimers, and it can contribute to the activity of cytosolic Fe-S enzymes (Knuesting et al., 2015; see Chapter 5). Finally, PICOT1 has recently been reported to interact with the TF NF-YC11/NC2α and seedlings carrying loss-of-function

mutations in the latter exhibited phenotypes similar to those of the *picot1* mutant (Knuesting et al., 2015).

In this chapter we further characterize the role of RGLG3 and RGLG4 in JA-signalling. We identified more proteins that appear in a complex with RGLG3/4 *in vivo* in the presence or absence of exogenous JA and confirm direct interaction with the hemoglobin GLB3 in addition to PICOT1. While in Chapter 5 we focussed on the molecular interactions between PICOT1 and RGLG3/4, here, we focus on the contribution of RGLG3/4 and PICOT1 to the plant's JA-responses. We demonstrate that PICOT1 interacts with the JA-receptor F-box component COI1 and that the phenotype of *picot1* seedlings can be partially rescued by *coi1-16*, a thermosensitive *COI1*-allele. Finally, the genetic interaction between *COI1* and *PICOT1* was studied in more detail on the transcriptome level and we identified a set of SA-responsive genes that are up-regulated in *coi1-16* in a *PICOT1*-dependent manner in the absence of SA-treatment.

RESULTS

PICOT1 and GLB3 interact with RGLG4

In the previous chapter, Tandem Affinity Purification (TAP) in combination with targeted mutations in RGLG3/RGLG4 were used to identify targets of these E3 ligases. Here, TAP was used to investigate the influence of exogenous JA-treatment on protein interactions mediated by RGLG3 or RGLG4. PSB-D cell cultures expressing TAP-tagged WT or mRING-variants of RGLG3 or RGLG4 were treated with 50 µM JA or 100% ethanol (mock treatment) for 1 minute before harvesting. To increase the sensitivity of the assay, the ultra-sensitive MS device Q-exactive was used to re-analyse the samples of previous TAPs (Table 6-1). We were able to identify additional proteins interacting with RGLG4mRING. However, only two of these proteins have a (predicted) nuclear or cytosolic localization: PICOT1/GRXS17 and HEMOGLOBIN 3 (GLB3). Note that GLB3 was only identified in complex with RGLG4mRING in the JA-treated samples and not in mock-treated samples.

Table 6-1. Summary of RGLG3/4 interacting proteins identified via TAP.

	Bait	RGLG3				RGLG3mRING					RGLG4				RGLG4mRING				
	Detection	Velos				Q-exactive		Velos			Velos				Q-exactive		Velos		
	TAP-tag	C-GS		N-GS		C-GSrh	C-GSrh		N-GSrh		C-GS		N-GS		C-GS	C-GS		N-GS	
	Treatment	JA	mock	JA	mock	mock	JA	mock	JA	mock	JA	mock	JA	mock	mock	JA	mock	JA	mock
Locus	Name																		
AT1G79380	RGLG4		2	2							2	2	2	2	2	2	2	2	2
AT5G63970	RGLG3	2	2	2	2	2	2	2	2	2									
AT4G04950	PICOT1/GRXS17														2		2	2	
AT4G32690	GLB3 | hemoglobin 3															2			
AT2G31810	Small subunit of acetolactate synthase														2				
AT1G32500	NAP6 | SufD homolog														2				

Respecitve baits were fused C or N-terminally to a GS or GS_{rhino} TAP-tag (C/N-GS or C/N-GSrh, respectively) and expressed in Arabidopsis cell cultures. The cultures were treated with 50 µM JA or 100% ethanol (mock) for 1 minute before harvesting. Purified complexes were analysed using mass-spectrometry devices (LTQ Orbitrap Velos or Q-Exactive). Numbers represent the incidence of protein identification out of two experiments. Only proteins that were identified in at least 2 TAP experiments with the same bait are retained. Background is subtracted. Proteins with predicted or experimentally verified localization in chloroplasts or mitochondria are indicated in grey.

The *Arabidopsis* genome encodes three non-symbiotic haemoglobins (Hbs, GLB1-3). In contrast to GLB1 and GLB2 that have a 3-on-3 globin fold, GLB3 is a truncated plant Hb with a 2-on-2 globin fold that is more closely related to bacterial Hbs (Watts et al., 2001). While the biological function of GLB3 is currently unknown, a role for GLB1 and GLB2 has been proposed in shoot organogenesis and NO-scavenging (Wang et al., 2011; Mur et al., 2012). We confirmed the predicted nucleo-cytoplasmic localization of GFP-fused GLB3 by expressing this construct in *N. benthamiana* mesofyll cells (Figure 6-1 A). Based on Y2H assays, we show that

GLB3 can interact directly with RGLGs, as was the case for PICOT1. Remarkably, both RGLG-interacting proteins PICOT1 and GLB3 were able to interact directly, as seen in Y2H assays (Figure 6-1 B).

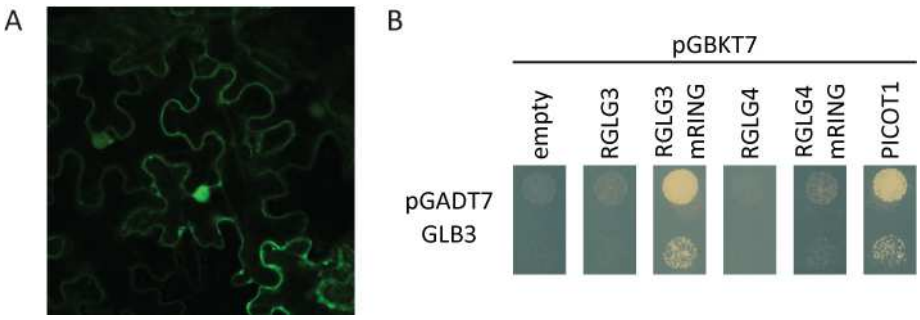

Figure 6-1. GLB3 localization and direct interactions with RGLG3/4.

A. GFP-GLB3 was transiently overexpressed in *N. benthamiana* under control of a CaMV 35S promoter. B. Y2H assay of GLB3 against RGLG3, RGLG4 and PICOT1. Transformed yeasts were spotted in 10-fold and 100-fold dilutions on control medium (not shown) or selective medium.

In previous studies, PICOT1 was reported to migrate from the cytoplasm to the nucleus upon heat stress in *N. benthamiana* (Wu et al., 2012). We therefore also analyzed PICOT1 localization after wounding and after exogenous JA-treatment in stably transformed PICOT1-GFP seedlings. Under these conditions, we did not see any change in PICOT1 subcellular localization. Because ubiquitination could alter the subcellular localization of PICOT1, we visualized PICOT1-GFP in *N. benthamiana* mesophyll cells after co-transfection with WT RGLG3 and RGLG4. No alterations in PICOT1-GFP localization were observed (data not shown).

PICOT1 interacts with the JA-receptor COI1

To determine the role of PICOT1 in the JA-signalling pathway, we investigated the effect of JA-treatment on PICOT1 interacting proteins via TAP (Table 6-2). PSB-D cell cultures and seedlings expressing GSrhino-tagged PICOT1 were generated during previous research (see Chapter 5) and were additionally treated with JA or 100% ethanol (mock treatment) for 1 minute or for 1 hour before harvesting.

Besides components of the cytoplasmic iron-sulfur (Fe-S) assembly complex, several tRNA modifying proteins and known Fe-S proteins (described in detail in previous chapter), several enzymes that catalyse redox reactions, and thus would benefit from the presence of an Fe-S cofactor, were also identified as PICOT1 interacting proteins. However, the most interesting finding was that the JA-receptor COI1 forms a complex with PICOT1, both in cell cultures and in seedlings.

To verify that PICOT1 interacts with COI1 *in planta*, we first confirmed that the two proteins co-localize in the same subcellular compartment. COI1 was N-terminally fused to GFP and expressed under control of a CaMV 35S promoter. Both in stably transformed seedlings

(Figure 6-2A) or transiently transfected *N. benthamiana* mesophyll cells (Figure 6-2B), GFP-COI1 localized exclusively to the nucleus. We subsequently used bimolecular fluorescence complementation (BiFC) combined with transient expression in *N. benthamiana* to show that the interaction between PICOT1 and COI1 is direct and takes place exclusively in the nucleus (Figure 6-2C).

The plant PICOT-protein contains one N-terminal thioredoxin (Trx) domain and three C-terminal glutaredoxin (Grx) domains, also known as PICOT-homology domains (Isakov et al., 2000). To test which protein domain of PICOT1 is required for interaction with COI1 we made an N-terminal and C-terminal truncation of PICOT1 containing either the Trx-domain or the three Grx-domains. The Trx domain of PICOT1 lacks the dithiol motif in the catalytic center, and is therefore thought to function as a protein-protein interaction platform independent of redox activity (Haunhorst et al., 2010). Accordingly, the fragment containing the Trx domain of PICOT1 was sufficient to mediate interaction with COI1 in BiFC experiments (Figure 6-2C) while interaction with COI1 could not be supported by the C-terminal truncation of PICOT1 (data not shown).

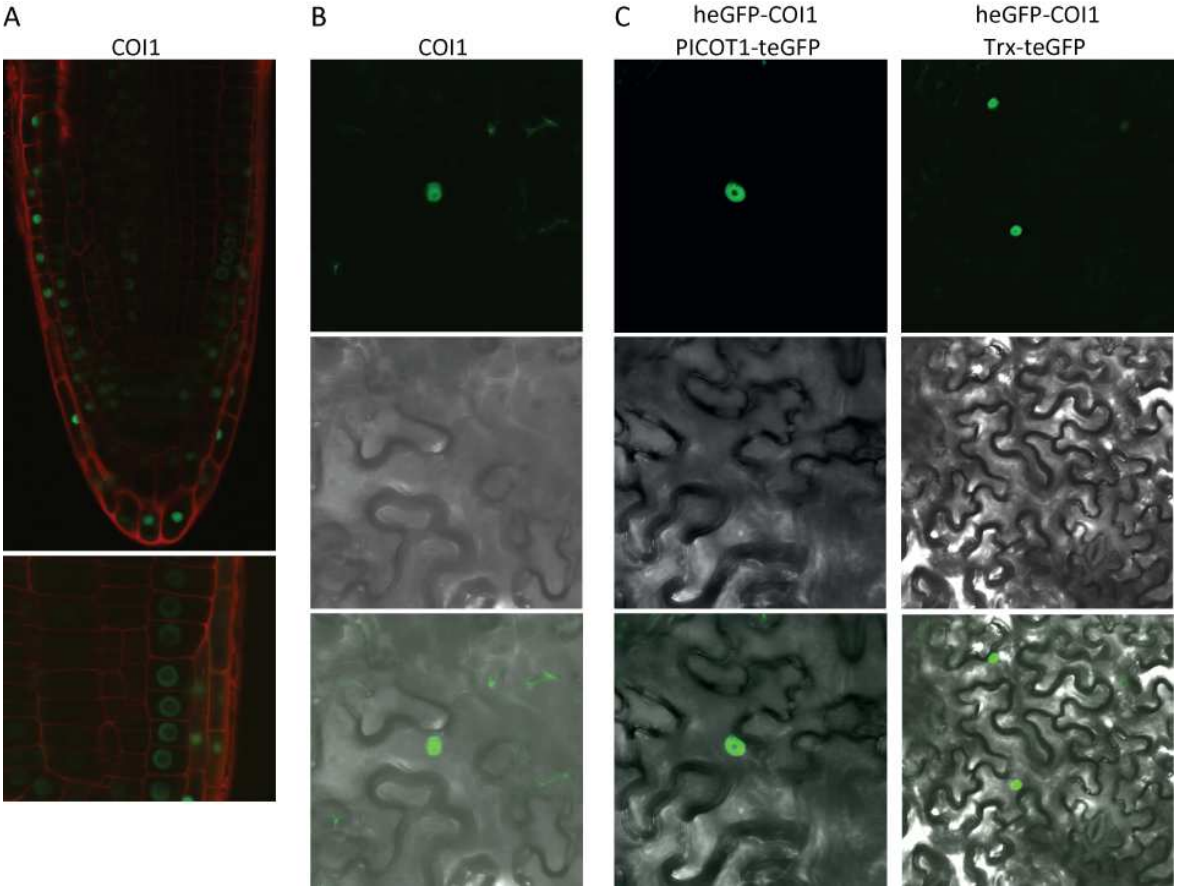

Figure 6-2. PICOT1 interacts with the JA-receptor COI1

Subcellular localization of COI1. A. Confocal root tip images of 4-day-old Arabidopsis seedlings overexpressing GFP-COI1. Propidium iodide was used to visualize the cell wall. B. GFP-COI1 was transiently overexpressed in *N. benthamiana* mesophyll cells. Controls with unfused eGFP fragments did not result in detectable fluorescent signals (data not shown). C. COI1 and PICOT1 interaction by BiFC. Head (h) or tail (t) eGFP fusions of COI1, PICOT1 or Trx-domain of PICOT1 were transiently expressed in *N. benthamiana*.

Table 6-2. PICOT1-GSrh interacting proteins identified using TAP

		PICOT1								
		C-GSrh					N-GSrh			
Name	**Locus**	**1' mock**	**1' JA**	**1h mock**	**1h JA**	**seedling**	**1hJA**	**1h mock**	**seedling**	**Total**
JA-signalling										
COI1	AT2G39940	2	2			2				6
Cytoplasmic [Fe-S] assembly pathway										
MET18	AT5G48120	2	2	2	2	2	2	2	1	15
CIAPIN / DRE2	AT5G18400	2	2	2	2	2	2	2		14
AE7 / CIA2	AT1G68310	2	2		1		2			7
NAR1	AT4G16440	2	2	1	1					6
CIA1	AT2G26060	2	2		1					5
Purine catabolism and salvage										
XDH1 | Xanthine dehydrogenase 1	AT4G34890	2	2	1	1	2	2	1		11
URH1 | Uridine-ribohydrolase 1	AT2G36310					2	1		1	4
URH2 | Uridine-ribohydrolase 2	AT1G05620					2	2		1	5
UREG | Urease accessory protein G	AT2G34470					2				2
tRNA modifications										
CTU1/ROL5 | Cytoplasmic thiouridylase 1	AT2G44270						1	1		2
CTU2 | Cytoplasmic thiouridylase 2	AT4G35910	1	2				1	1		5
2-thiocytidine tRNA biosynthesis protein (TtcA)	AT1G76170	2					1			3
YbaK/aminoacyl-tRNA synthetase-associated	AT1G44835	1	2							3
Aminoacyl-tRNA ligase[1]	AT3G04600		1							1
Aminoacyl-tRNA ligase[2]	AT1G09620					2			1	3
Phenylalanyl-tRNA synthetase	AT3G58140					2				2
Other known Fe-S proteins										
AtBolA2	AT5G09830	2	2	1	2		1			8
Radical SAM superfamily protein[1]	AT2G39670					1				1
NIFS1[2]	AT5G65720					2				2
AtSUFE1	AT4G26500	1	2			1	1	1	1	7
AtBolA1[1]	AT1G55805		1							1
Thioredoxins										
ACHT2 | Atypical Cys /His-rich thioredoxin 2[1]	AT4G29670		1							1
TRXF1 | Thioredoxin F-type 1[1]	AT3G02730					1				1
Kinases and phosphatases										
HXK1 | Hexokinase 1	AT4G29130					2			1	3

Phosphofructokinase family protein	AT1G20950					2			1	3
VTC1 | Vitamin C defective 1[1]	AT2G39770					1				1
Miscellaneous										
AtLARP1a	AT5G21160	2	2							4
XCT | XAP5 family protein	AT2G21150	1	2							3
CA2 | Carbonic anhydrase 2	AT5G14740					2				2
DEA(D/H)-box RNA helicase family protein	AT5G60990					2				2
LON2 |Lon protease 2	AT5G47040					1			1	2
MLP34 | MLP-like protein 34	AT1G70850					1			1	2
CINV1 | Cytosolic invertase 1[1]	AT1G35580					1				1
Adenine nucleotide alpha hydrolases-like[1]	AT3G53990								1	1
Aluminium induced protein	AT3G22850	2	2				1	2		7
Aluminium induced protein[2]	AT5G43830					2				2
RING-protein[1,2]	AT3G54360					1				1
F-box protein[1]	AT1G24800							1		1
Ub interaction motif-containing protein	AT1G43690		2		1					3
unknown protein	AT3G60660	2	1	2	2			1		8
unknown protein	AT5G06590	2	2	1	1					6
unknown protein	AT2G24970			1	1					2
unknown protein	AT2G22660	1	1							2
unknown protein[1]	AT1G18060					1				1
PSAF | Photosystem I subunit F[2]	AT1G31330					2				2
PSAK | Photosystem I subunit K	AT1G30380					2				2
PSAN | Photosystem I reaction center subunit[2]	AT5G64040					2				2
NAI2 | DNA topoisomerase-related[2]	AT3G15950					2				2
CHLI1| Subunit of magnesium chelatase	AT4G18480					2				2
ISE1 | DEAD-box RNA helicase	AT1G12770					2				2
Small subunit of acetolactate synthase	AT2G31810					2				2
FAB1/KAS2 | Fatty acid biosynthesis 1	AT1G74960					2				2
LACS6 | Long-chain acyl-CoA synthetase 6	AT3G05970					2				2
ATPE | ATP synthase ε chain	ATCG00470					2				2
ATP3 | γ subunit of Mt ATP synthase	AT2G33040					1			1	2
ATPC1 | γ subunit of chloroplast ATP syntase[1]	AT4G04640					1				1
GTP-binding family protein	AT3G12080					2				2
NOS1/NOA1/RIF1 | Nitric oxide synthase 1[1]	AT3G47450					1				1
ABA1/ZEP | Zeaxanthin epoxidase[1]	AT5G67030					1				1
ASNAP | α-soluble NSF attachment protein 2[1]	AT3G56190								1	1
trigger factor type chaperone family[1]	AT5G55220								1	1

PICOT1 was fused C or N-terminally to a GSrhino TAP-tag (C-GSrh or N-GSrh, respectively) and expressed in Arabidopsis cell cultures or seedlings under control of a CaMV 35S promoter. The cell cultures were treated with 50µM JA or 100% ethanol (mock) for 1 minute or 1 hour before harvesting. Proteins identified with LTQ Orbitrap Velos, with at least 2 significant peptides per identification. Only proteins that were identified in at least 2 TAP experiments with the same bait are retained. Background is subtracted. Numbers represent the incidence of protein identification out of two experiments or a single experiment (N-GSrh seedlings). Proteins with predicted or experimentally verified localization in chloroplasts or mitochondria are indicated in grey. [1]Found in only 1 TAP experiment. [2]Possible background.

Generation of loss-of-function and overexpression lines

To study the contribution of *RGLG3, RGLG4* and *PICOT1* to JA-signalling, we acquired Arabidopsis lines with T-DNA insertions in the respective genes. In addition to the *RGLG3* and *RGLG4* KO alleles described by (Zhang et al., 2012, renamed *rglg3-1* and *rglg4-1*), we isolated two extra alleles: *rglg3-2* and *rglg4-2*, both in the Col-0 ecotype. The T-DNA insertions were mapped and transcript levels in the respective genes were verified by quantitative Real-time PCR (qRT-PCR, Figure 6-3).

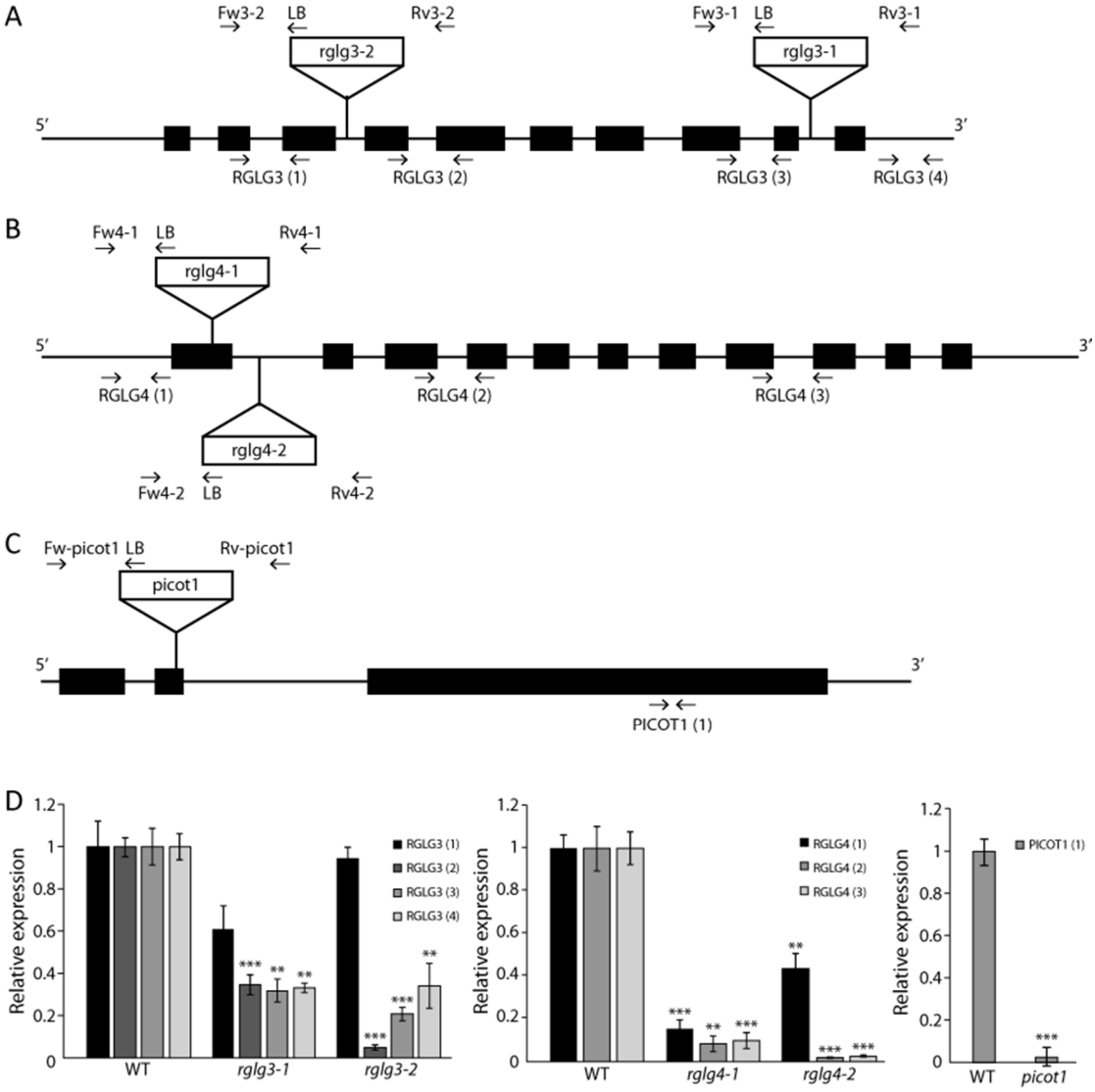

Figure 6-3. Characterization of T-DNA insertional mutants.

Schematic visualization of RGLG3 (A), RGLG4 (B) and PICOT1 (C) gene structure, T-DNA insertions in the corresponding mutants and the primers used for genotyping and for transcript quantifications (D). Black boxes represent exons. Data represent mean ±SEM of three biological replicates (**, p<0.01; ***, p<0.001; t-test). UBC (At5g25760) was used as internal control and expression values were normalized to those of the wild-type (WT).

The genetic interaction between *PICOT1* and *COI1* was investigated in *picot1* (Col-0) lines containing additional mutations in *COI1*. More specifically, we generated *picot1coi1-1*, *picot1coi1-16*, *picot1coi1-21* and *picot1coi1-22* double mutant lines. While *coi1-1* is a male

sterile full KO allele of COI1 introducing an early stop codon (Xie et al., 1998), the three additional *coi1* alleles used are point mutations leading to amino acid substitutions in the LRR-domain of COI1 (Figure 6-4). These alleles are hypo-sensitive to JA-treatment but can still be maintained as homozygous lines at room temperature or at 16°C in the case of the thermo-sensitive *coi1-16* allele (Ellis and Turner, 2002; He et al., 2012).

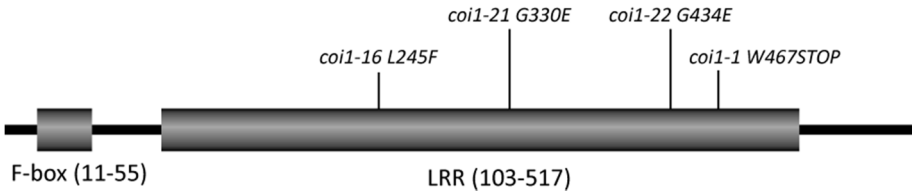

Figure 6-4. *COI1* alleles used in this study

Schematic overview of the COI1 protein structure (592 amino acids) with F-box domain and LRR repeats. The allele designation and associated amino acid change is shown in relation to its linear position. Figure adapted from (He et al., 2012).

Finally, we also generated *Arabidopsis* lines stably expressing PICOT1 fusions to GFP or a hemagglutinin epitope tag (HA) under control of the CaMV 35S promotor. Three independent lines with gradually increasing overexpression were selected for further assays based on immunodetection of the PICOT1 protein levels (Figure 6-5).

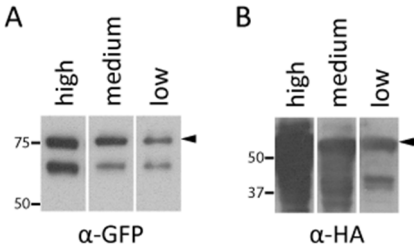

Figure 6-5. PICOT1 overexpression levels.

PICOT1-GFP (81kDa) and PICOT1-HA (58kDa) were stably expressed in Arabidopsis seedlings under control of a pCaMV35S promotor. Three independent lines were selected based on gradually increasing protein levels of PICOT1 detected with on immunoblots with anti-GFP antibody (A) or anti-HA antibody (B). Arrowheads indicate PICOT1.

Phenotypic characterization of seedlings overexpressing *PICOT1*

Seedlings grown in the presence of exogenous JA, characteristically respond with a reduction in growth and a boost in secondary metabolism. These effects can be assessed by measuring the fresh weight, main root length and anthocyanin production of the seedlings. These properties were used to evaluate the JA-sensitivity of different lines with altered expression of *RGLG3, RGLG4* and *PICOT1*.

Both, GFP and HA-tagged PICOT1 lines did not show obvious alterations in JA-responses based on growth parameters (fresh weight and main root length) or the production of secondary metabolites (anthocyanins) when grown on medium containing increasing concentrations MeJA (Figure 6-6). Although some significant alterations in JA-response could

be detected, these did not show a dose-response effect upon increasing MeJA concentrations in the medium nor increasing PICOT1 expression levels and are therefore not considered relevant alterations.

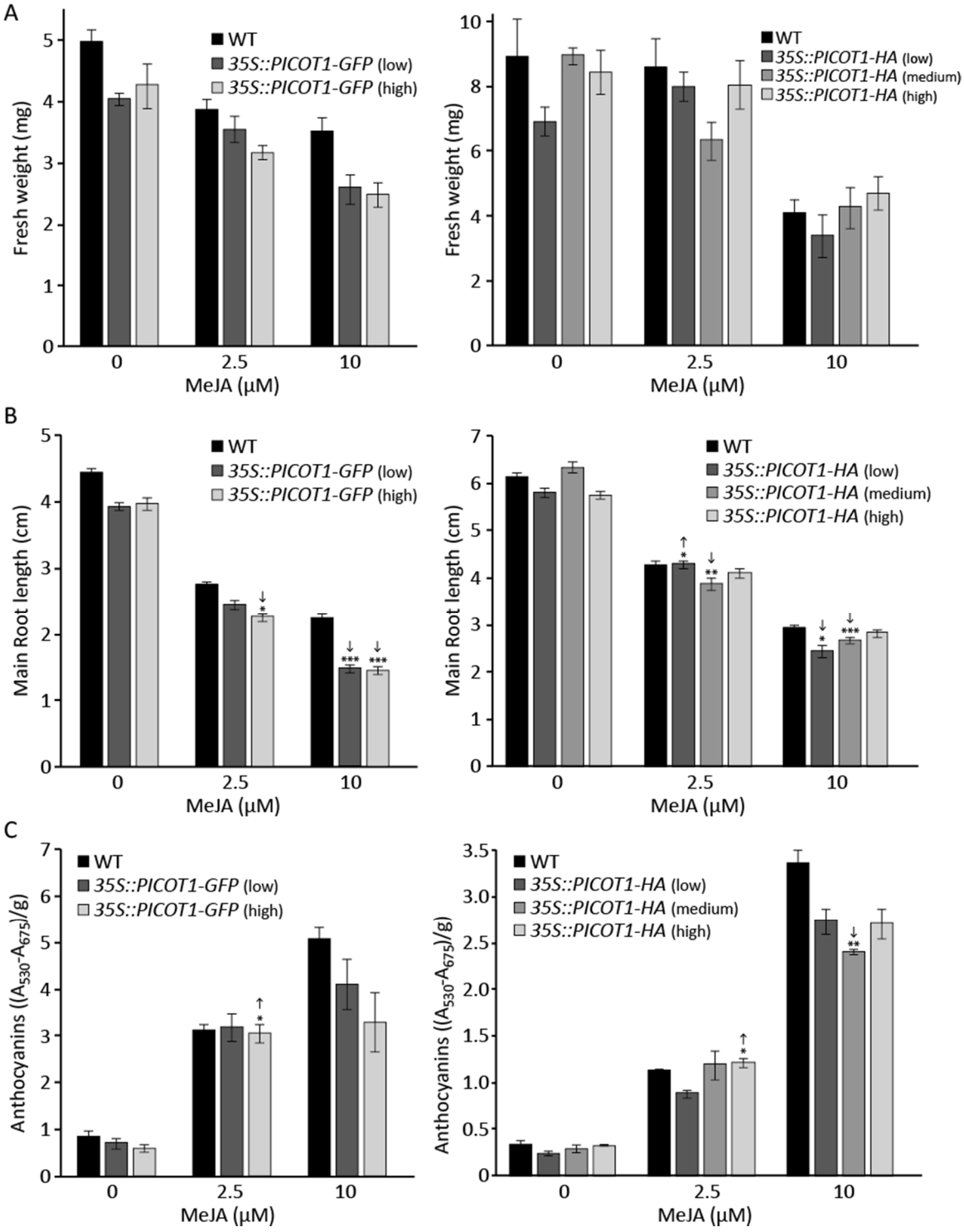

Figure 6-6. JA-responses of *PICOT1* overexpression lines.

Seedlings expressing different levels of GFP or HA-tagged PICOT1 were grown on MS supplemented with 0 µM, 2.5 µM or 10 µM MeJA. A. Fresh weight per seedling of 14 day-old seedlings. B. Main root length of 11 day-old seedlings. C. Anthocyanin accumulation was determined in the same seedlings as (A). Data represent mean ±SEM of n=4 (A,C) or n>16 (B) (*, p<0.05; **, p<0.01; ***, p<0.001; t-test; ↑ or ↓, value significantly larger or smaller than expected, respectively).

rglg3 rglg4 seedlings are not hyposensitive to JA

We next evaluated the JA-response of *rglg3* and *rglg4* KO seedlings. *Rglg3* or *rglg4* single KO seedlings were smaller than WT in control conditions. Although measurement of the fresh weight, main root length and anthocyanin content (Figure 6-7 A, B) sometimes indicated an altered sensitivity to JA, significant alterations did not correlate with increasing MeJA concentration in the medium, were only seen in one of the two KO mutants of each gene or were contradictory depending on the parameter measured. These results confirm that *rglg3* and *rglg4* single KO mutants do not respond differentially to JA, as was reported previously (Zhang et al., 2012).

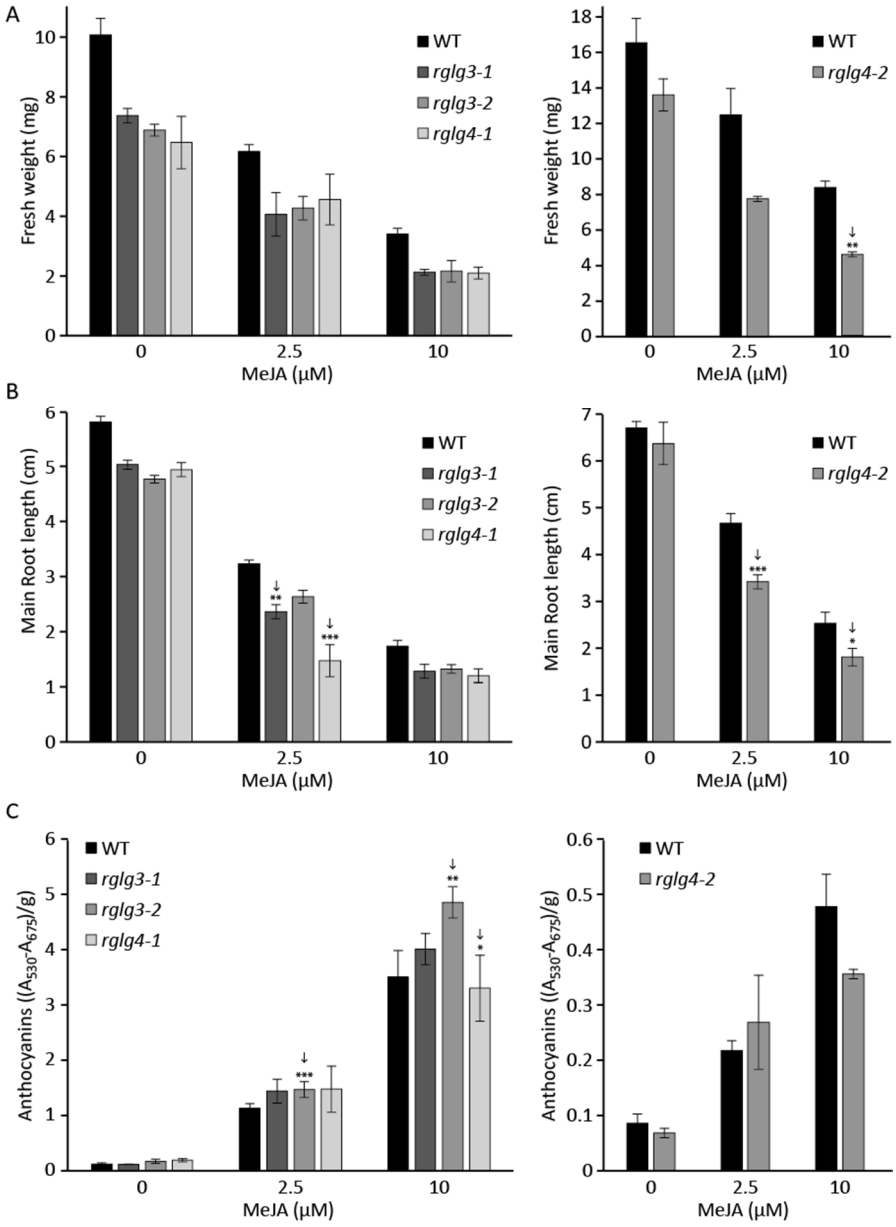

Figure 6-7. JA-mediated growth inhibition and anthocyanin accumulation in *rglg* single KO lines.

Seedlings were grown for 14 days on solid (A,B) or liquid (C) MS with 0 µM, 2.5 µM or 10 µM MeJA. A. The fresh weight per seedling was measured at 14 days. B. The main root length was measured at 11 days. C. Anthocyanins per gram fresh weight were measured at 14 days. Error bars represent ±SEM of n=3 (A,B) or n=4 (C) (*, p<0.05; **, p<0.01; ***, p<0.001; t-test; ↑ or ↓, value significantly larger or smaller than expected, respectively).

We subsequently investigated the JA-sensitivity of *rglg3rglg4* double mutant lines (Figure 6-8). Similar to single *rglg* mutant seedlings, double mutants were smaller than WT seedlings under control conditions. This defect was however more pronounced in double mutants than in single mutants, based on their fresh weight. This could indicate that *RGLG3* and *RGLG4* might have non-redundant functions in addition to their redundant role in JA-signalling. Strikingly, *rglg3rglg4* double mutant seedlings did not show the severe JA-insensitive phenotype published earlier (Zhang et al., 2012), but rather presented a minor but significant decrease in JA-sensitivity when grown in the presence of low amounts of MeJA (2.5 µM). This effect was almost completely lost when seedlings were grown in the presence of higher MeJA concentrations.

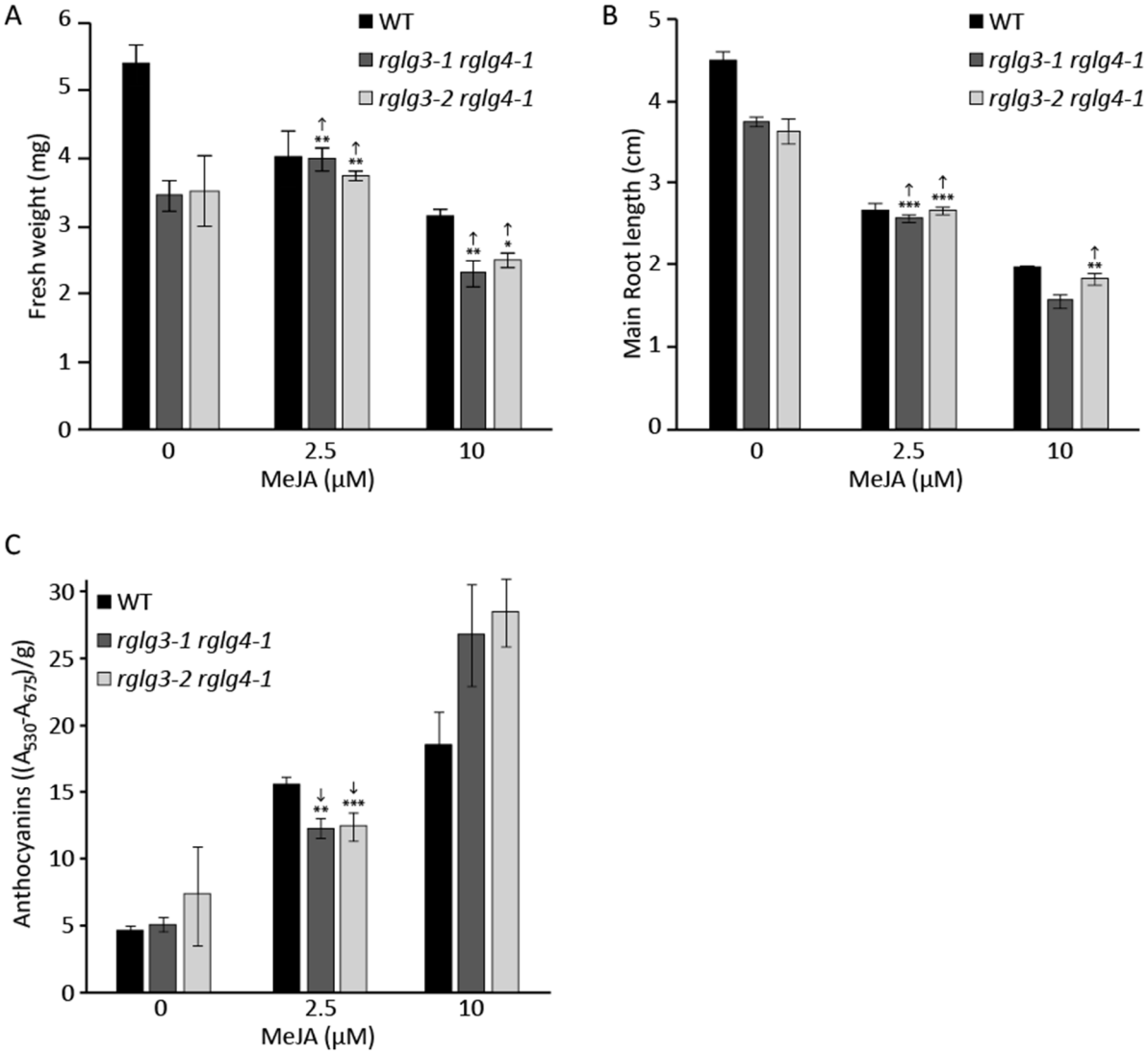

Figure 6-8. JA-mediated growth inhibition and anthocyanin accumulation in *rglg3rglg4* double mutant lines.

Seedlings were grown for 14 days on solid MS with 0 µM, 2.5 µM or 10 µM MeJA. A. The fresh weight per seedling was measured at 14 days. B. The main root length was measured at 11 days. C. Anthocyanins per gram fresh weight were measured at 14 days. Error bars represent ±SEM of n=4 (A,C) or n>22 (B) (*, p<0.05; **, p<0.01; ***, p<0.001; t-test; ↑ or ↓, value significantly larger or smaller than expected, respectively).

To further assess the JA-sensitivity of *rglg3rglg4* seedlings, we repeated the experiment with the exact same conditions as described in Zhang et al. (2012). Main root length measurement did not reveal an altered JA-sensitivity as both KO lines showed contradicting phenotypes (Figure 6-9 A). These seedlings were then used to inspect the expression of two JA-marker genes (*VSP2* and *PDF1.2*). Zhang et al reported negligible induction of *PDF1.2* and around 4-fold lower induction of *VSP2* by JA-treatment in *rglg3-1rglg4-1* seedlings. However, our expression analyses did not reveal significant alterations in response to JA-treatment when compared to WT seedlings (Figure 6-9B), indicating both *rglg3rglg4* KO lines behave as WT when grown in the presence of high (> 2.5 µM) MeJA concentrations.

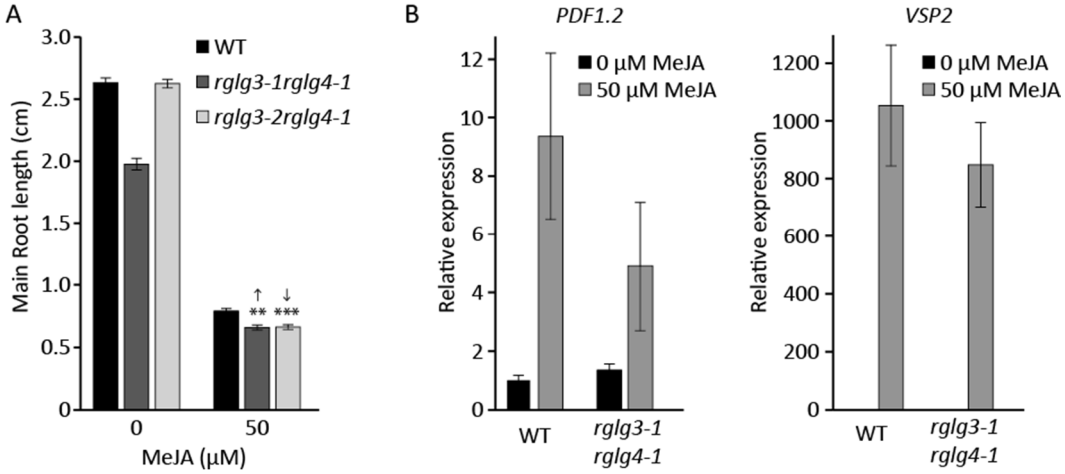

Figure 6-9. JA-mediated root growth inhibition and gene induction in *rglg3rglg4* seedlings

Seedlings were grown for 9 days on MS with or without 50 µM MeJA. A. The main root length was measured at day 9, error bars represent ±SEM (n>40). B. qRT-PCR analysis of JA-responsive expression of PDF1.2 and VSP2 in the seedlings used in A. Data represent mean ±SEM of three biological replicates (*, p<0.05; **, p<0.01; ***, p<0.001; t-test; ↑ or ↓, value significantly larger or smaller than expected, respectively). UBC (At5g25760) was used as internal control and expression values were normalized to those of the wild-type after mock treatment.

Genetic interaction between *PICOT1* and *COI1*

To investigate the relationship between *PICOT1* and *COI1*, we first assessed the JA-response of *picot1* KO seedlings and of *picot1coi1* double mutants. As reported previously, *picot1* grown under standard conditions (long-day photoperiod, 21°C) already had a shorter root in the absence of exogenous hormone treatment (Knuesting et al., 2015; Figure 6-10A). Root growth of *picot1* seedlings was further reduced upon MeJA treatment, although to a lower extent than in WT seedlings (Figure 6-10B).

Next, we evaluated the genetic interaction between *PICOT1* and *COI1* by assessing the JA-responses of *picot1coi1* double mutant lines. In the absence of exogenous MeJA, we observed partial rescue of the *picot1* short-root phenotype by *coi1-16* (Figure 6-11 A-C). This partial rescue of *picot1* phenotype was even stronger when *coi1-21picot1* was studied (Figure 6-11 D-E).

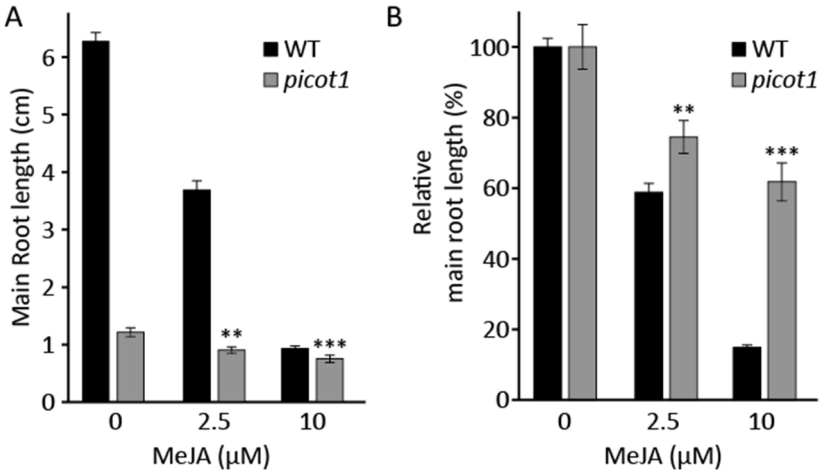

Figure 6-10. Root length elongation of *picot1* seedlings in the presence of MeJA.

The main root length was measured of 11 day-old seedlings that were grown on MS in the presence of 0 µM, 2.5 µM or 10 µM MeJA, shown as absolute measurements (A) or relative measurements (B) where the root length at 0 µM was used to normalize measurements and corresponds to 100%. Data represent mean ±SEM of n>14 (*, p<0.05; **, p<0.01; ***, p<0.001; t-test).

Surprisingly, introduction of the *coi1-22* allele did not rescue the *picot1* short-root phenotype (Figure 6-12). In contrast to other *coi1* lines tested here, single mutant *coi1-22* seedlings were already smaller than WT in the absence of exogenous JA (Figure 6-12 A, Figure 6-13 A), similar to *picot1* seedlings. Compared to WT seedlings, *coi1-22* seedlings were only slightly hyposensitive to JA. In addition, *coi1-22picot1* double mutant seedlings were even smaller than either of the single mutant seedlings. Moreover, double mutants were chlorotic, prompting us to investigate chlorophyll levels in these lines (Figure 6-13). Although *picot1* or *coi1-22* single mutant seedlings had more or similar chlorophyll content as WT plants, *picot1coi1-22* double mutants showed a strong decrease in chlorophyll b content (Figure 6-13 B). Finally, *picot1coi1-22* seedlings also contained less carotenoids than WT or the single mutants (Figure 6-13 C). Taken together, our results indicate that some *coi1* mutant alleles can partially rescue the *picot1* short-root phenotype, whereas others, like *coi1-22,* aggravate or create other phenotypes when combined with *picot1,* including phenotypes that were not obvious in either of the single mutant lines.

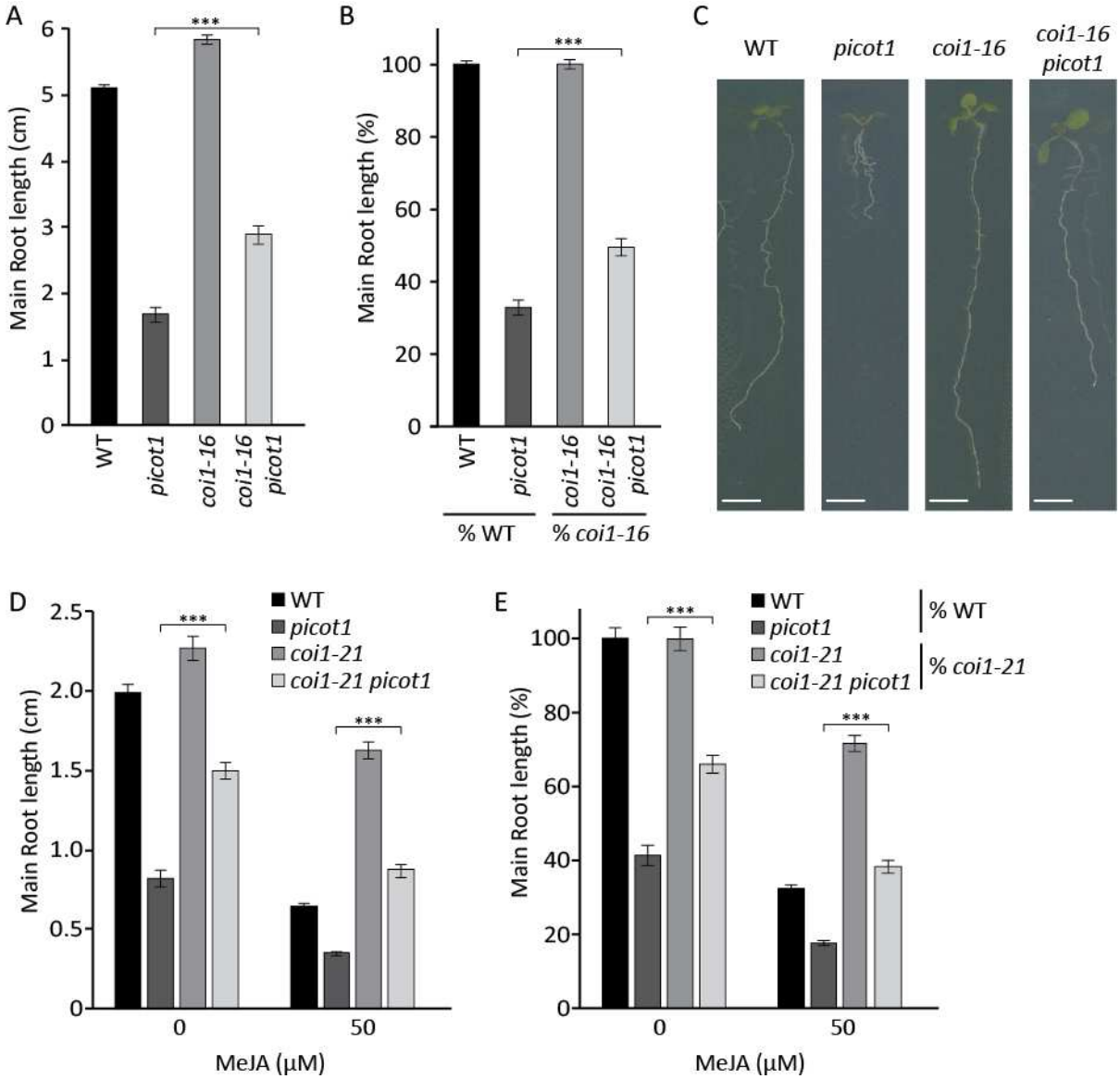

Figure 6-11. The short-root phenotype of *picot1* is partially rescued by *coi1-16* and *coi1-21.*

The main root length of 11 day-old (A-C) or 7 day-old (D-E) seedlings grown on MS with or without MeJA was measured. Root lengths are indicated as absolute measurements (A,D) or relative to the WT and *coi1* background at 0 µM MeJA for *picot1* and *picot1coi1,* respectively (B,E). Representative seedlings are shown in C, scale bar corresponds to 5 mm. Data represent mean ±SEM of n>28 (A-C), or n>10 (D,E) (*, p<0.05; **, p<0.01; ***, p<0.001; t-test).

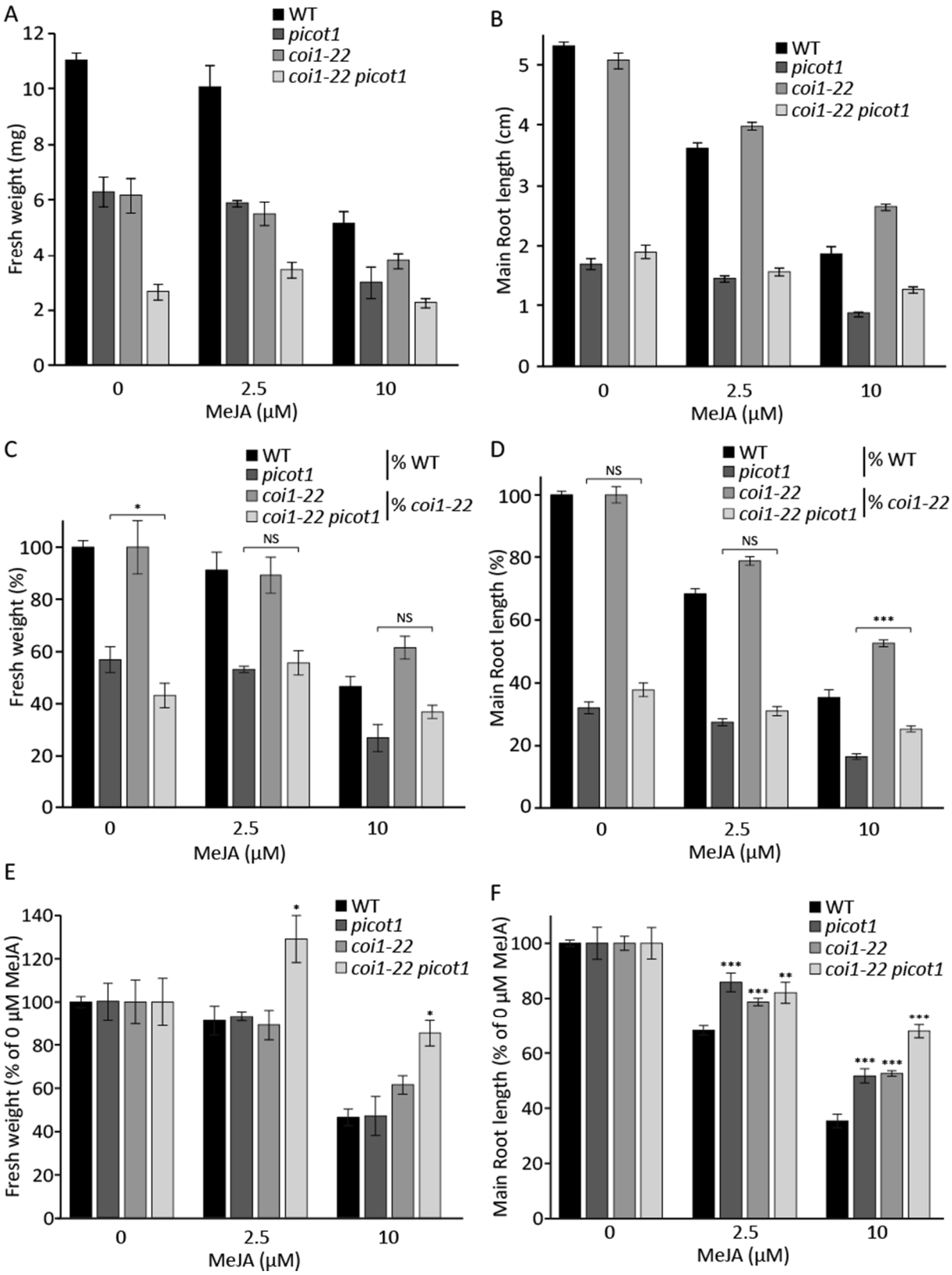

Figure 6-12. JA-mediated growth inhibition in *picot1coi1-22* double mutants.

Seedlings were grown on MS with or without MeJA. A-B. Fresh weight of 14 day-old *coi1-21picot1* seedlings. C-D. Main root length of 11 day old-seedlings. Measurements are expressed as absolute values (A,C) or as relative percentages of WT or *coi1-22* at 0 µM MeJA for *picot1* or *picot1coi1-22,* respectively. Data represent mean ±SEM of n=4 (A-B) or n>18 (C-D) (NS, non-significant; *, p<0.05; **, p<0.01; ***, p<0.001; t-test).

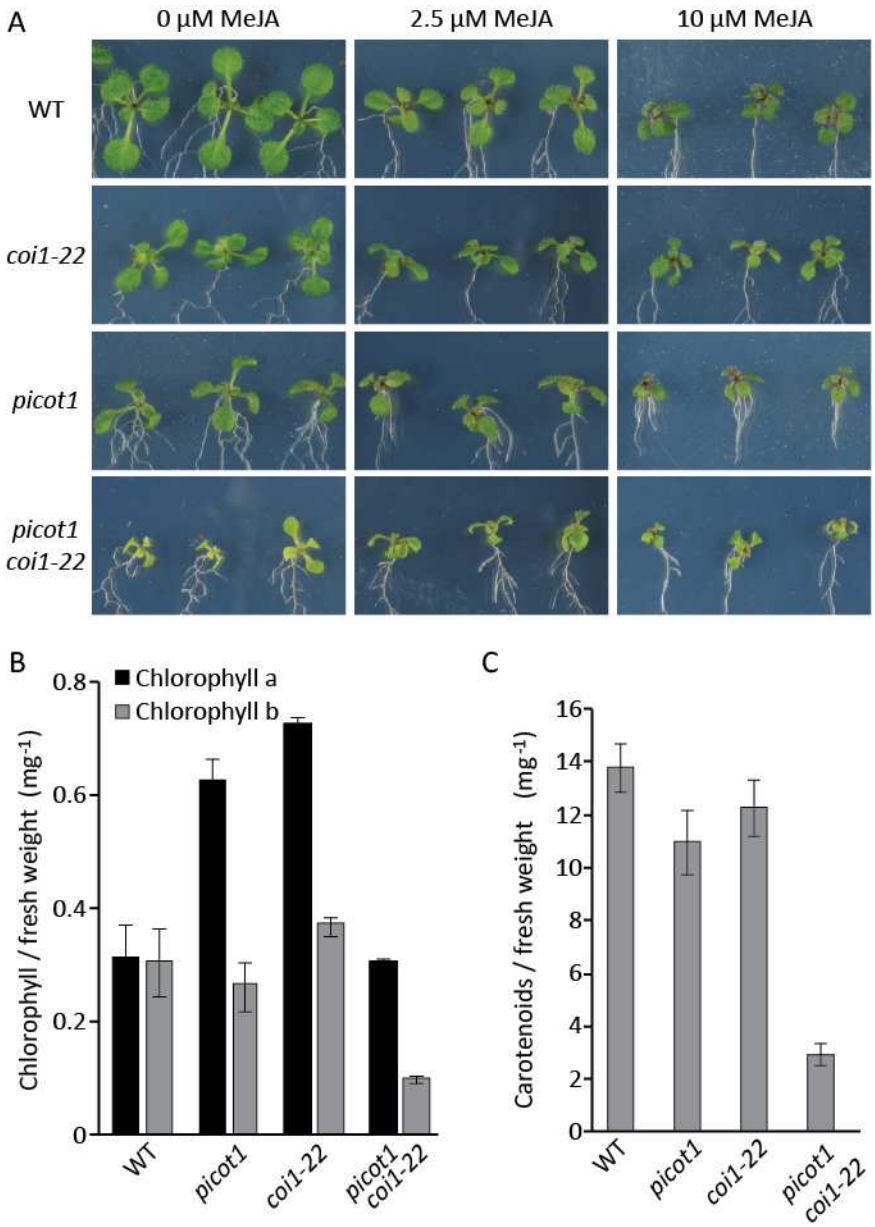

Figure 6-13. *Picot1coi1-22* double KO seedlings are chlorotic.

Seedlings were grown on MS supplemented with 0 µM, 2.5 µM or 10 µM MeJA for 14 days. A. Representative seedlings of each line and treatment, 14 days old. Chlorophyll (B) and carotenoid (C) accumulation was measured in the different lines. Data represent mean ±SEM of n=4.

Transcript profiling of *picot1* and *coi1-16picot1*

The phenotypic characterization of seedlings with altered expression of *PICOT1* did not reveal a clear role for *PICOT1* in JA-signalling. Nevertheless, *coi1-16* and *coi1-21* could successfully rescue part of the short-root phenotype seen in *picot1* KO lines. To further elucidate the function of *PICOT1,* we analysed the transcriptome of *picot1, coi1-16* and *picot1coi1-16* double mutant by performing RNA-seq (see Supplementary Tables S3-5).

Because *coi1-16* could partially rescue the *picot1* short root phenotype, we looked for genes that were up-regulated in *picot1* and whose up-regulation was lost in the *coi1-16picot1* cross. These included a small number of genes involved in JA-biosynthesis or signalling (Figure 6-14 A). The starting product for the biosynthesis of JAs is α-linolenic acid, present in chloroplast membranes. Consecutive action of three enzymes – a 13-LIPOXYGENASE (LOX), a 13-ALLENE OXIDE SYNTHASE (AOS) and a ALLENE OXIDE CYCLASE (AOC) – yields the JA-precursor cis-12-oxophytodienoic acid (OPDA). Four genes in Arabidopsis encode AOCs (*AOC1-4*) and 13-LOXs (*LOX1-4*). *AOCs* have organ-specific expression patterns with *AOC1* and *AOC2* expressed in fully developed leaves but not in roots or vasculature bundles (Stenzel et al., 2012). While two 13-LOXs (*LOX3* and *LOX4*) are essential for JA-biosynthesis during flower development (Caldelari et al., 2011), *LOX2* is involved in senescence-related and wound-induced JA-production (Glauser et al., 2009; Seltmann et al., 2010). *ETHYLENE RESPONSE FACTOR*s (*ERFs*) TFs are members of the APETALA2 (AP2)-TF family that bind to the GCC-box motif present in promotors of several ethylene and JA-inducible genes as well as pathogenesis-related genes. Expression of *AtERF2* was shown to be induced by JA or by infection with the necrotrophic fungus *Fusarium oxysporum*. AtERF2 functions as a positive regulator of JA-responsive defence genes and concomitant resistance to *F. oxysporum.* In addition, AtERF2 also enhances JA-induced root growth inhibition (McGrath et al., 2005).

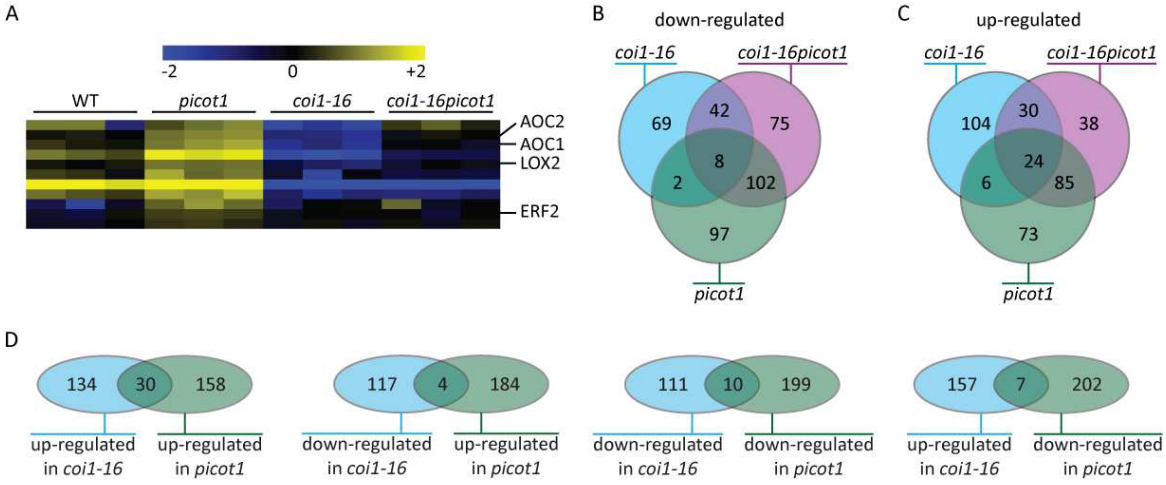

Figure 6-14. General outcome of transcript profiling of *picot1, coi1-16* and *coi1-16picot1*

A. Gene cluster comprising JA-biosynthesis that are upregulated in *picot1*. B-C. Number of genes differentially down-regulated (B) or upregulated (C) in the different mutant lines when compared to wild type (WT). D. Number of overlapping genes that are differentially up or down regulated in the different mutant lines when compared to WT.

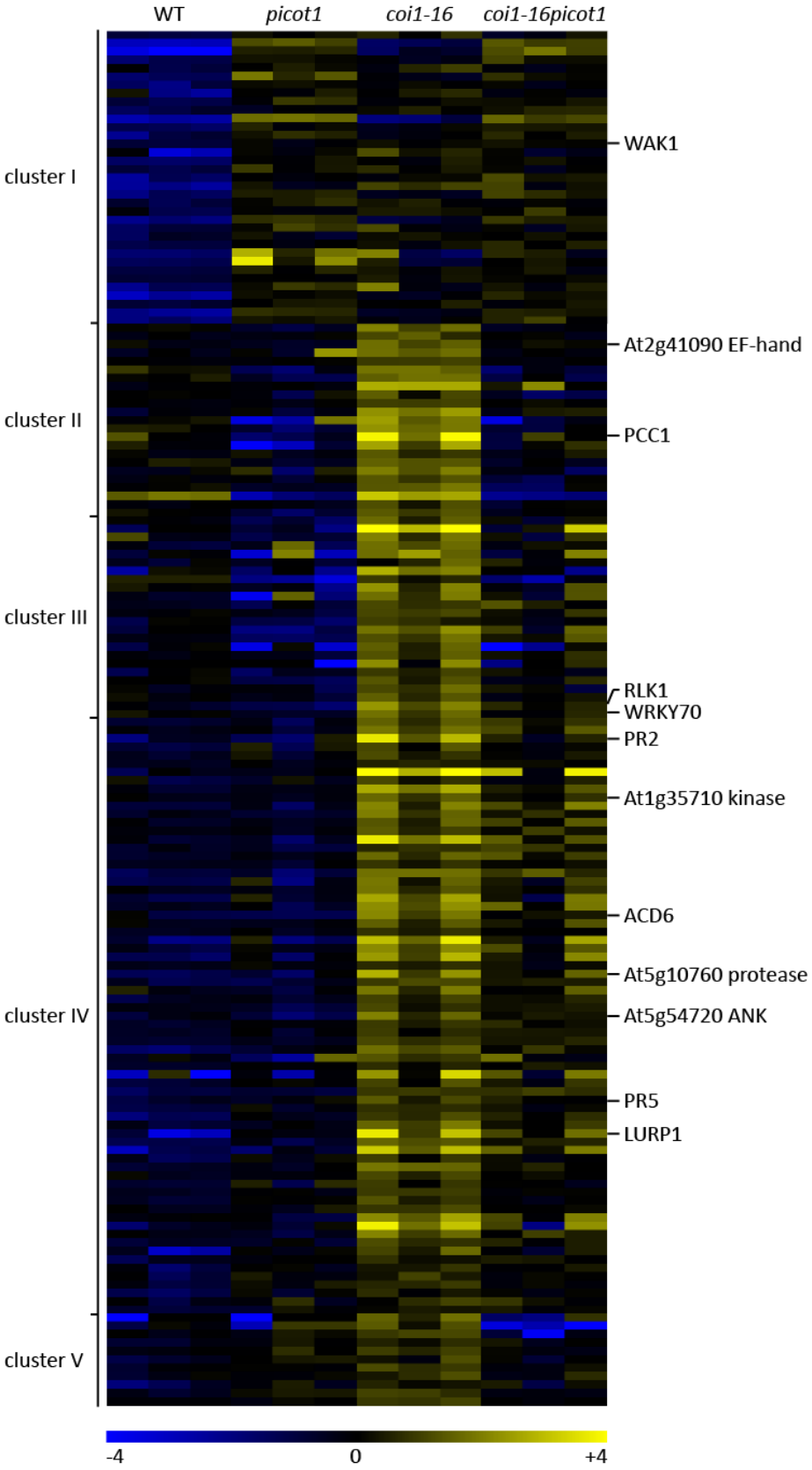

Figure 6-15. Up-regulated genes in *coi1-16* are less up-regulated in *coi1-16picot1*.

Up-regulated genes in *coi1-16* seedlings could be grouped in five clusters. Cluster I contains genes that are similarly up-regulated in all mutant lines. Clusters II-V contain genes whose up-regulation is counteracted in *coi1-16picot1* seedlings. Genes belonging to the LURP (late upregulated in response to *Hyaloperonospera parasitica*) regulon are indicated.

In total, 209 genes were significantly down-regulated and 188 genes were significantly up-regulated at least two-fold in *picot1* when compared to WT. Inspection of the overlap between differentially regulated genes between the *picot1* and the *coi1-16* line indicated the major overlap was seen between up-regulated genes in both lines (Figure 6-14 D). A major trend that caught our attention was that a great number of genes (164) are up-regulated in untreated *coi1-16* seedlings, indicating functional COI1 is required to negatively regulate these genes in the absence of JA. Remarkably, 129 of these genes are less up-regulated in the *coi1-16picot1* line compared to the *coi1-16* single mutant line (Figure 6-15), indicating functional PICOT1 protein is necessary for the induction of these genes. Several of these genes belong to the LURP (late upregulated in response to *Hyaloperonospora parasitica, Hp*, now known as *H. arabidopsidis*) regulon (Figure 6-16), a group of genes that are co-ordinately up-regulated in response to the pathogen (Eulgem et al., 2004; Knoth et al., 2007). The LURP regulon representative gene *LURP1*, was shown to be an important component of the plant immune system and to function in SA-dependent defence pathways mediating R-protein-triggered and basal resistance to *Hp* (Knoth and Eulgem, 2008).

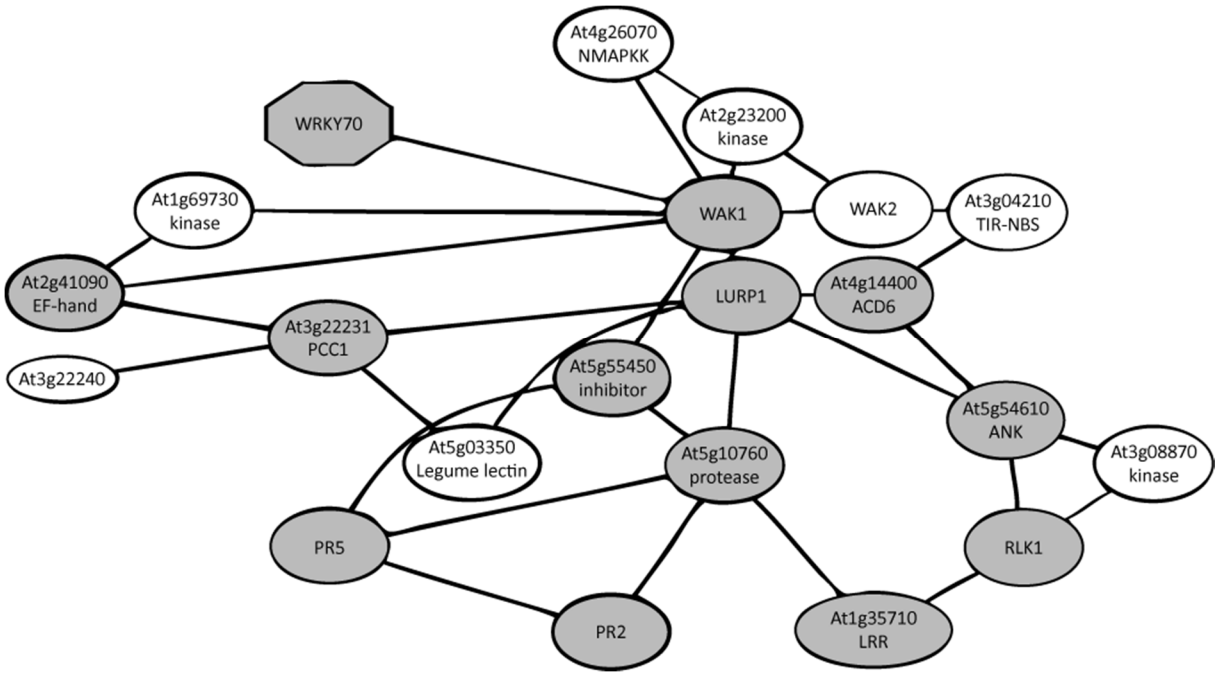

Figure 6-16. *Coi1-16* affects expression of genes belonging to the LURP regulon.

Co-expressed gene network of LURP1 (late upregulated in response to *Hyaloperonospera parasitica-1*), representative gene of the LURP-regulon. Genes that were up-regulated in *coi1-16* are highlighted. Figure adapted from ATTED-II (Obayashi et al., 2009).

DISCUSSION

RGLG3 and *RGLG4* positively regulate JA-signalling at low hormone concentrations

Since the identification of SCF^{COI1} as an essential E3 ligase in JA-signalling, only two other E3 ligases have been proposed to function in this pathway: the RING-type E3-ligases RGLG3 and RGLG4. RGLG3/4 were proposed to function redundantly as positive regulators of JA-signalling, and to function upstream of *COI1* (Zhang et al., 2012). Surprisingly, in our assays, *rglg3rglg4* seedlings grown in the presence of exogenous JA had WT-like phenotypes. However, when grown in the presence of low JA concentrations (2.5µM) *rglg3rglg4* double KO seedlings became slightly insensitive to JA-treatment. We can therefore state that RGLG3/4 contribute to the induction of JA-responses only in response to low JA concentrations.

PICOT1 binds to iron-sulfur proteins

Although RGLG3/4 have been proposed to function upstream of COI1, no molecular basis for their function is known yet. We have identified two proteins that interact directly with RGLG3 and RGLG4, and have focussed our research on elucidating the function of one of them: the glutathioredoxin PICOT1, which is a ubiquitination target of RGLG3/4 (described in Chapter 5). PICOT1 interacts with a large number of proteins *in vivo*. While some of the PICOT1-interacting proteins are involved in specific pathways (i.e. cytosolic Fe-S cluster assembly, purine catabolism and tRNA modification) others are seemingly unrelated. PICOT1 is known to bind Fe-S clusters (Couturier et al., 2014; Knuesting et al., 2015), and several of the identified PICOT1-interacting proteins are Fe-S proteins.

Remarkably, PICOT1 interacted with a large number of enzymes. Because Fe-S prosthetic groups have the ability to transfer electrons or stabilize reaction intermediaries, they are essential for the catalytic function of several enzymes (Balk and Schaedler, 2014). PICOT1 contains an N-terminal Trx domain, in addition to three C-terminal Grx domains that are responsible for Fe-S cluster binding. Because the Trx domain of PICOT proteins lacks the dithiol motif in the catalytic centre, this domain probably functions as a protein-protein interaction platform independent of redox activity (Haunhorst et al., 2010; Hoffmann et al., 2011). We therefore speculate that our results reflect a mix of a number of proteins that interact specifically with PICOT1, probably through its Trx domain, while many other proteins interact with PICOT1 through one of its Fe-S clusters. Distinction between these two groups of PICOT1-interacting proteins could be made in the future by performing new TAP experiments with solely the N-terminal part of PICOT1 containing the Trx domain as bait.

PICOT1 regulates the JA-receptor COI1

Besides the JAZ proteins, COI1 has only been shown to physically interact with two components of SCF-complexes, SKP1 and CULLIN1, and with the histone deacetylase HDA6/RPD3b (Dai et al., 2002; Devoto et al., 2002; Chini et al., 2007; Thines et al., 2007). Here, we show that PICOT1 interacts directly with COI1 *in planta*. This interaction is mediated only by the Trx-domain of PICOT1, in accordance with the fact that COI1 has not been reported to bind an Fe-S cluster and does not have signature motifs corresponding to Fe-S binding sites.

A reducing environment has been reported to positively influence the interaction between COI1 and JAZ proteins, in the presence of JA-Ile or the analogue chemical coronatine (Yan et al., 2009). It is therefore tempting to speculate that PICOT1 could influence COI1 function by altering its redox status. However, phenotypic analysis of seedlings with altered *PICOT1* expression did not point to alterations in the JA-response. In addition, transcriptome analysis of *picot1* seedlings did not reveal major changes in the expression of JA-responsive genes, indicating PICOT1 does not play a significant role in JA-signalling.

Seedlings with deficient *PICOT1* expression showed strongly impaired root growth when grown under normal conditions even in the absence of exogenous JA. This short-root phenotype was partially rescued by introduction of specific *COI1* mutant alleles in the *picot1* background. Partial rescue was visible in *coi1-16picot1* and *coi1-21picot1* seedlings, but not in *coi1-22picot1* seedlings. The *picot1* short-root phenotype thus appears to be COI1-dependent in a JA-independent manner.

JA-independent functions of COI1 have been reported previously. Infection of *Arabidopsis* plants with the soil-borne fungal pathogen *Verticillium longisporum* causes reduced shoot growth and induces early senescence. COI1 was shown to be required for plant susceptibility to this vascular pathogen, independent of JA-Ile or any JA-Ile mimic (Ralhan et al., 2012). Alternatively, phytoprostanes inhibit root growth and induce the production of secondary metabolites similarly to JA. The inhibition of root growth by phytoprostanes was shown to be COI1-dependent but JA-independent (Stotz et al., 2013). When transcript profiling of *picot1*, *coi1-16* and *coi1-16picot1* seedlings was performed, we noticed a large set of genes was differentially up-regulated in *coi1-16* in the absence of exogenous JA-treatment. The majority of this genes was less up-regulated in *coi1-16picot1* seedlings, suggesting their expression is dependent on *PICOT1*.

***Coi1-16* is an atypical *coi1* allele**

Coi1-16 is a conditional fertile *coi1*-allele that is almost completely sterile when grown at room temperature but becomes fertile when grown at 16°C (Ellis and Turner, 2002), it therefore seems probable that this mutation differs from other *coi1* mutations. COI1 protein

levels have been evaluated in the different *coi1* alleles and cannot account for these differences. While *coi1-1* is a true null allele, low coi1 protein levels could be detected in *coi1-16* and *coi1-21* plants, and *coi1-22* accumulated the highest level of coi1 protein, which was still much lower than the COI1-level in WT plants (He et al., 2012).

Coi1-16 contains a point mutation leading to incorporation of a phenylalanine residue instead of a leucine residue at position 245 in the protein (Ellis and Turner, 2002). The crystal structure of COI1 has been determined, making it possible to map this mutation onto the structure. The LRR repeats of COI1 form a barrel-like structure where the top surface has three long loops that are involved in substrate binding (Sheard et al., 2010). A fourth loop formed by LRR-8 protrudes both at the top and at the side of the barrel (red loop in Figure 6-17). The Leu residue at position 245 (blue spheres in Figure 6-17) is located at the base of LRR-7, in close proximity to the base of LRR-8. In *coi1-16* this Leu is substituted by a Phe and, although Leu and Phe are both considered hydrophobic amino acids, the aromatic benzyl side chain of Phe is larger than the isobutyl side chain of Leu. This amino acid substitution might therefore disturb the formation or positioning of the LRR-8 loop.

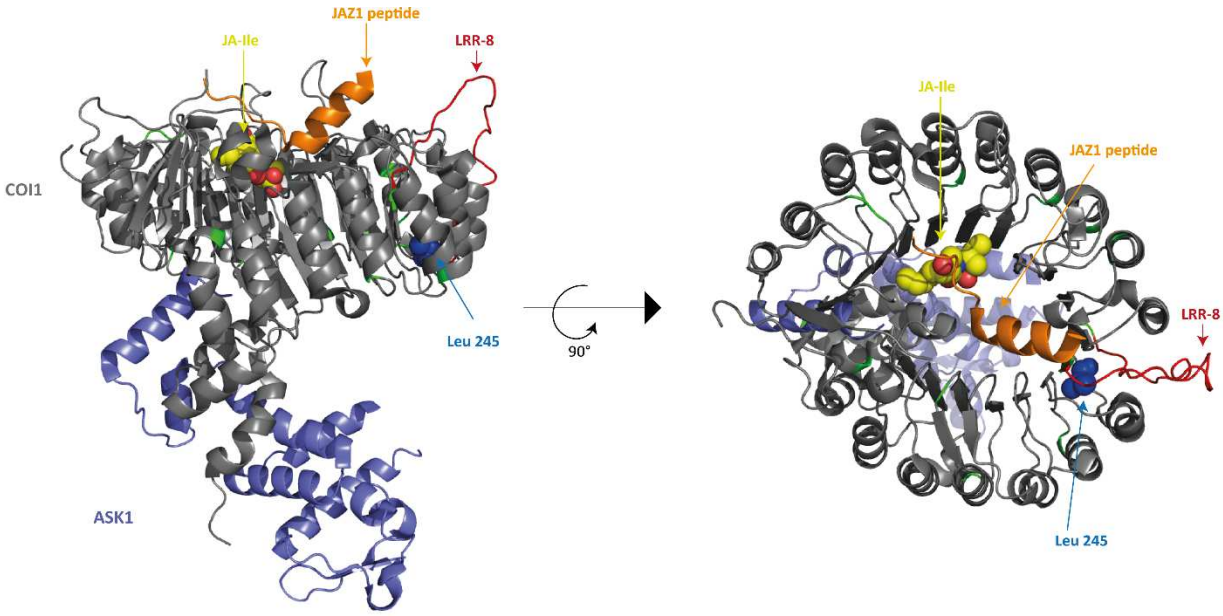

Figure 6-17. Crystal structure of COI1 in complex with ASK1, JA-Ile and the JAZ degron.

COI1–ASK1 (grey and purple ribbons, respectively) with the JAZ degron peptide (responsible for interaction of JAZ with COI1 and JA-Ile, orange ribbon) and JA-Ile (yellow space-fill representation). The conserved Cys residues of COI1 are shown as green ribbons. The residue mutated in the *coi1-16* allele is shown in blue space-fill representation. The loop formed by LRR-8 is highlighted as a red ribbon. Figure adapted from (Sheard et al., 2010).

The up-regulation of JA-independent gene transcription in *coi1-16* indicates a JA-independent function of COI1 is altered in this mutant, which could be caused by alteration of LRR-8 loop formation or positioning. Comparison between the transcriptome analysis of *coi1-16* and *coi1-16picot1* indicates this JA-independent function of COI1 is, at least partially, dependent on PICOT1.

Based on phenotypic and transcriptomic data obtained during this research we propose a possible model for *PICOT1* function during COI1-dependent signalling (Figure 6-18). We propose that the protein COI1 functions in two distinct pathways: one involves JA-perception leading to the initiation of JA-responses, while the other is JA-independent. Given the fact that not all *coi1*-alleles rescue the *picot1* phenotype, we propose that COI1 exists in two different states, determining in which pathway the protein will function. Consistent with our results, we propose that *coi1-16* encodes a protein that is trapped in one state, which is involved in the regulation of JA-independent gene expression. In this model PICOT1 functions as a positive regulator of JA-independent COI1 function.

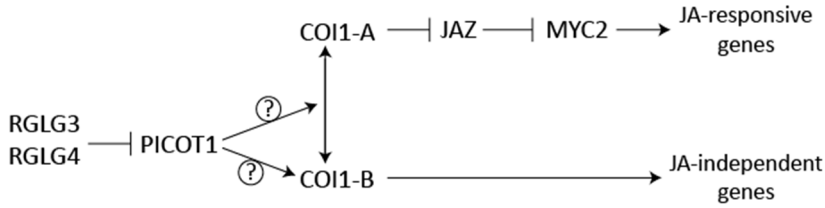

Figure 6-18. Possible mode of action of RGLGs and PICOT1 during COI1-dependent signalling.

Model where *COI1* functions downstream of *PICOT1*. RGLG3/4 control PICOT1 protein stability. COI1 exists in two states (COI1-A and COI1-B). PICOT1 interacts with COI1-A or COI1-B and either regulates transition to COI1-B state or stimulates the activity of COI1-B to activate the expression of JA-independent genes.

Among the genes that were upregulated in *coi1-16* seedlings, members of a set of co-regulated genes referred to as the LURP (late upregulated in response to *Hyaloperonospora parasitica*) regulon (Eulgem et al., 2004) were overrepresented. Members of the LURP-regulon are involved in the defence response against this biotrophic pathogen that is responsible for causing downy mildew disease (Knoth et al., 2007). Their induction is dependent on SA-signalling (Knoth and Eulgem, 2008). Our results indicate that in *coi1-16* seedlings, induction of the LURP-regulon is independent of pathogen infection pointing to a role for the JA-receptor in mediating transcription of SA-dependent genes in the absence of SA.

Taken together, we have provided a molecular link between the E3 ubiquitin ligases RGLG3/4 and the core JA-signalling pathway. This link is constituted by the ubiquitination target of RGLG3/4 that interacts directly with COI1. PICOT1 regulates a JA-independent function of COI1. It is well recognized that there is extensive cross-talk between JA-signalling and SA-signalling and in most cases it concerns antagonistic interactions (Caarls et al., 2015). Our results indicate a JA-independent role for COI1 in the induction of SA-dependent gene expression in the absence of SA.

EXPERIMENTAL PROCEDURES

Plant material and growth conditions

All mutant lines used in this study were in the Columbia-0 ecotype background, except *coi1-16* that was generated by EMS mutagenesis of *Col-gl1* plants homozygous for *VSP1::luciferase* as described (Ellis and Turner, 2002). *Coi1-21* and *coi1-22* were obtained in a *rar1-21* suppressor screen through EMS-mutagenesis (Hubert et al., 2009) and have been described in (He et al., 2012). *Picot1/grxs17* (SALK_021301), *rglg3-1* (SALK_098983), *rglg4-1* (SALK_096022) mutants were previously described (Cheng et al., 2011; Zhang et al., 2012). Additional T-DNA insertion mutants were obtained from the GABI-Kat T-DNA collection (Kleinboelting et al., 2012) or the SALK T-DNA collection: *rglg3-2* (GABI_577A04) and *rglg4-2* (SALK_042504). In the case of T-DNA insertion mutants, homozygous plants were selected by PCR screening with the appropriate primers (Supplementary Table S1). For *coi1-16, coi1-21* and *coi1-22* homozygous plants were selected in *picot1* background with PCR-based dCAP markers (Supplementary Table S1).

Arabidopsis seeds were sterilized by the chlorine gas method and sown on sterile plates containing the corresponding growth media. Plates were kept in the dark at 4°C two days for stratification before being transferred to a growth room with 21°C temperature and a 16 h light / 8 h dark regime, unless mentioned otherwise.

Generation of PICOT1 overexpression lines

35S::PICOT1-GFP construct was generated by LR Gateway recombination between PICOT1 Entry clone and pFAST-R05. The 35S::PICOT1-HA construct was generated by MultiSite Gateway recombination between Entry clones encoding the cauliflower 35S promoter, PICOT1 and the HA-tag and pK8m34GW-FAST. Transgenic Arabidopsis seeds were generated by floral dip (Clough and Bent, 1998), using Col-0 as the background ecotype Transgenic seeds were selected based on the seed-fluorescent marker (Shimada et al., 2010; Vanholme et al., 2013).

Cloning and site-directed mutagenesis

ORFs were amplified from a cDNA template by PCR using Phusion High-fidelity Polymerase (NEB), with specific primers including *att*B sites and subsequently recombined with pDONR207. For the creation of C-terminal fusions, reverse primers did not include a stop codon. For the construction of mRING variants, corresponding full-length Entry vectors were amplified using Pfu DNA polymerase (Promega) and primers containing the mutations. The PCR product was digested using *Dpn*I before transformation to *E. coli*. Positive colonies were picked and sequence verified. PICOT1 N-terminal domain (amino acids 1-135) and C-terminal domain (amino acids 138-488) were cloned using specific primers including *att*-sites and a new stop or start codon, respectively. All primers used are listed in Supplementary Table S1.

Yeast transformation and Yeast two-hybrid

Expression clones for yeast two-hybrid were generated by LR Gateway recombination between respective Entry-clones and pGADT7 or pGBKT7 and co-transformed in competent yeast cells of the *S. cerevisiae* strain PJ69-4A using the LiAc/SS carrier DNA/PEG method (Gietz and Schiestl, 2007). Transformants were selected on SD media lacking Leu and Trp (-2). Dropping was performed as described (Cuéllar Pérez et al., 2013).

Bimolecular Fluorescence Complementation (BiFC)

35S::ORF-tag constructs using the N and C-terminal halves of eGFP (head and tail, respectively) were constructed by triple Gateway reactions using pK7m34GW or pH7m34GW (Karimi et al., 2005) as described in (Boruc et al., 2010). 35S::tag-ORF constructs were generated by double Gateway recombination using pH7m24GW2 or pK7m24GW2 (Boruc et al., 2010). The constructs were co-expressed in *N. benthamiana* using *Agrobacterium*-mediated transient transformation. Interactions were scored by screening the lower epidermal cells for fluorescence using confocal microscopy 3-5 days after transformation using a Leica SP2 upright confocal microscope.

Agrobacterium-mediated transient transformation of N. benthamiana

WT *N. benthamiana* plants (3–4 weeks old) were used for transient expression of constructs by *Agrobacterium tumefaciens*-mediated transient transformation of lower epidermal leaf cells as previously described (Boruc et al., 2010) using a modified infiltration buffer (10 mM $MgCl_2$, Merck; 10 mM MES pH 5.7, Duchefa; 100 µM Acetosyringone, Sigma-Aldrich) and addition of a P19 expressing *Agrobacterium* strain to boost protein expression (Voinnet et al., 2003). All *Agrobacterium* strains were grown for 2 days, diluted to OD 1 in infiltration buffer and incubated for 2-4 h at room temperature before mixing in a 1:1 ratio with other strains and injecting.

Tandem affinity purification

N or C-terminally tagged TAP constructs (GS or GSrh tag) were generated as described (Van Leene et al., 2015), used for the transformation of Arabidopsis PSB-D cell suspension cultures without callus selection and further grown and subcultured as described (Van Leene et al., 2011). Stably transformed cultures were scaled up and harvested 6 days after subculturing. Cells were treated with 50 µM JA (Duchefa) for 1 min before harvesting. Expression of TAP-tagged constructs in stably transformed Arabidopsis PSB-D cultures was verified on an aliquot of total protein extract before purification.

Transgenic Arabidopsis seeds were generated by floral dip (Clough and Bent, 1998), using Col-0 as the background ecotype and the same constructs as for cell culture transformation. Transformants were selected as described (Van Leene et al., 2015). Purifications were performed as described (Van Leene et al., 2015) with the exception that no Benzonase treatment was performed on the cell extracts.

Localization studies

Entry clones containing GLB3 or COI1 were recombined with pFAST-R06, generating 35S::GFP-ORF expression vectors. *N. benthamiana* leafs were transiently transformed with these constructs, in addition to a P19 expressing construct. Lower epidermal leaf cells were imaged 3-5 days after infiltration using a Leica SP2 upright confocal microscope.

Immunodetection

Total protein extracts were obtained from 14 day-old seedlings grown on MS media supplemented with 1% sucrose using HB-buffer as described in (Van Leene et al., 2015). After quantification of the protein content using the Bradford assay (Bio-Rad), the indicated protein samples were loaded on a 4–15% TGX gel (Bio-Rad) and ran for 20 min at 300 V. Next, proteins were transferred to 0.2 µm PVDF membranes (Bio-Rad) with the Trans-blot Turbo (Bio-Rad). A 1/1000 dilution of rat monoclonal anti-HA antibodies (clone 3F10, Roche) were used to detect PICOT1-HA. A 1/5000 dilution of HRP-conjugated monoclonal anti-GFP antibodies (Miltenyi Biotech Inc.) were used to detect PICOT1-GFP. Chemiluminescent detection was performed with Western Bright ECL (Isogen).

qRT-PCR

Seedlings were grown on MS (1% sucrose) with agar, horizontally, for 14 days. Total RNA was extracted with an RNeasy plant mini kit (Qiagen) from whole seedlings. For cDNA synthesis, 500 ng to 1µg of RNA was used with the iScript cDNA Synthesis Kit (Bio-Rad) according to the instructions of the manufacturer. The primer sequences used in the qRT-PCR experiments are listed in Supplementary Table S1. Relative expression levels were determined with the Light-Cycler 480 Real-TimeSYBR green PCR System (Roche). The data were first normalized to the expression level of the housekeeping genes for each RNA sample.

RNA-seq analysis

Seedlings were grown on MS (1% sucrose) with agar, vertically, for 14 days. Three biological replicates were harvested for each line. RNA was isolated using the RNeasy Plant Mini Kit (Qiagen) and DNase I treated (Promega). RNA samples were processed by first preparing a Trueseq RNA-Seq library (Illumina) and then sequenced at 50bp single read using Illumina HiSeq 2000 technology at GATC Biotech Ltd - Germany. Read quality control, filtering, mapping to the TAIR10 Arabidopsis genome and read counting were carried out using the Galaxy portal running on an internal server (http://galaxyproject.org/). Sequences were filtered and trimmed,

respectively with the Filter FASTQ v1 and FASTQ Quality Trimmer v1 tools with default settings (http://www.bioinformatics.babraham.ac.uk/projects/fastqc/). Reads were subsequently mapped to the TAIR10 version of the Arabidopsis genome using GSNAPv2 (Wu and Nacu, 2010) allowing a maximum of 5 mismatches. The concordantly paired reads that uniquely map to the genome where used for quantification on the gene level with HTSeq-count from the HTSeq python package (Anders et al., 2015). Data was normalized using TMM, implemented in edgeR (Robinson et al., 2010) and common dispersion was then estimated using the conditional maximum likelihood method (Robinson and Smyth, 2008). Differentially expressed genes were defined by a 2-fold difference between mutant lines and the wild-type control with P-value<0.05. The false discovery rate (FDR) was limited to 5% according to Benjamini and Hochberg (1995).

Root measurements

The indicated plant lines were germinated and grown vertically on MS media supplemented with 1% sucrose for 11 days. The main root length was determined using ImageJ software (http://imagej.nih.gov/ij/).

Anthocyanin quantification

Anthocyanin content was measured of whole seedlings grown on MS supplemented with 1% sucrose for 14 days as described in (Vanderauwera et al., 2005). Briefly, chlorophylls and anthocyanins were extracted in MeOH HCl 1%. Back-extraction of the chlorophylls was performed using chloroform. The supernatant was transferred to a 96-well plate and absorbance at wavelengths 663nm and 646nm were measured using a microplate spectrophotometer. The anthocyanin concentration per sample is expressed as (A_{530}-A_{657}) per gram fresh weight.

Chlorophyll and carotenoid quantification

Chlorophyll content was determined using spectrophotometry as described in (Wellburn et al., 1983). Chlorophyll was extracted from ground frozen plant material by incubation in 80% aqueous acetone during 1 hour at 4°C. Remaining cellular debris was separated from chlorophylls by centrifugation. The supernatant was transferred to a 96-well plate and absorbance at wavelengths 663nm and 646nm were measured using a microplate spectrophotometer (Molecular Devices, US).

Chlorophyll a/b content was calculated as: $C_a = 12.21 \times A_{663} - 2.81 \times A_{646}$ or $C_b = 20.13 \times A_{646} - 5.03 \times A_{663}$. Carotenoid content (xanthophylls and carotenes) was calculated as: Carotenoids = $(1000 \times A_{470} - 3.27 \times C_a - 104 \times C_b)/227$. Results are expressed as C_a / C_b / carotenoids per miligram fresh weight.

REFERENCES

Anders S, Pyl PT, Huber W (2015) HTSeq-a Python framework to work with high-throughput sequencing data. Bioinformatics **31:** 166-169

Balk J, Schaedler TA (2014) Iron Cofactor Assembly in Plants. Annual Review of Plant Biology, Vol 65 **65:** 125-+

Benjamini Y, Hochberg Y (1995) Controlling the false discovery rate - a practical and powerful approach to multiple testing. J R Stat Soc Ser B - Methodol **57**: 289 - 300

Boruc J, Van den Daele H, Hollunder J, Rombauts S, Mylle E, Hilson P, Inze D, De Veylder L, Russinova E (2010) Functional Modules in the Arabidopsis Core Cell Cycle Binary Protein-Protein Interaction Network. The Plant cell **22:** 1264-1280

Caarls L, Pieterse CMJ, Van Wees SCM (2015) How salicylic acid takes transcriptional control over jasmonic acid signaling. Frontiers in plant science **6**

Caldelari D, Wang GG, Farmer EE, Dong XN (2011) Arabidopsis lox3 lox4 double mutants are male sterile and defective in global proliferative arrest. Plant molecular biology **75:** 25-33

Cheng MC, Hsieh EJ, Chen JH, Chen HY, Lin TP (2012) Arabidopsis RGLG2, Functioning as a RING E3 Ligase, Interacts with AtERF53 and Negatively Regulates the Plant Drought Stress Response. Plant physiology **158:** 363-375

Cheng NH, Liu JZ, Liu X, Wu QY, Thompson SM, Lin J, Chang J, Whitham SA, Park S, Cohen JD, et al (2011) Arabidopsis Monothiol Glutaredoxin, AtGRXS17, Is Critical for Temperature-dependent Postembryonic Growth and Development via Modulating Auxin Response. Journal of Biological Chemistry **286:** 20398-20406

Chini A, Fonseca S, Fernandez G, Adie B, Chico JM, Lorenzo O, Garcia-Casado G, Lopez-Vidriero I, Lozano FM, Ponce MR, et al (2007) The JAZ family of repressors is the missing link in jasmonate signalling. Nature **448:** 666-671

Clough SJ, Bent AF (1998) Floral dip: a simplified method for Agrobacterium-mediated transformation of Arabidopsis thaliana. Plant Journal **16:** 735-743

Couturier J, Touraine B, Briat JF, Gaymard F, Rouhier N (2013) The iron-sulfur cluster assembly machineries in plants: current knowledge and open questions. Frontiers in plant science **4**

Couturier J, Wu HC, Dhalleine T, Pegeot H, Sudre D, Gualberto JM, Jacquot JP, Gaymard F, Vignols F, Rouhier N (2014) Monothiol GlutaredoxinBolA Interactions: Redox Control of Arabidopsis thaliana BolA2 and SufE1. Molecular plant **7:** 187-205

Cuéllar Pérez A, Pauwels L, De Clercq R, Goossens A (2013) Yeast two-hybrid analysis of jasmonate signaling proteins. Methods in molecular biology **1011:** 173-185

Dai L, Xu L, Huang D, Li X, Luo K, Guan C (2002) ASK1 physically interacts with COI1 and is required for male fertility in Arabidopsis. Science in China Series C, Life sciences / Chinese Academy of Sciences **45:** 631-636

Devoto A, Nieto-Rostro M, Xie DX, Ellis C, Harmston R, Patrick E, Davis J, Sherratt L, Coleman M, Turner JG (2002) COI1 links jasmonate signalling and fertility to the SCF ubiquitin-ligase complex in Arabidopsis. Plant Journal **32:** 457-466

Ellis C, Turner JG (2002) A conditionally fertile coi1 allele indicates cross-talk between plant hormone signalling pathways in Arabidopsis thaliana seeds and young seedlings. Planta **215:** 549-556

Eulgem T, Weigman VJ, Chang HS, McDowell JM, Holub EB, Glazebrook J, Zhu T, Dangl JL (2004) Gene expression signatures from three genetically separable resistance gene signaling pathways for downy mildew resistance. Plant physiology **135:** 1129-1144

Gietz RD, Schiestl RH (2007) High-efficiency yeast transformation using the LiAc/SS carrier DNA/PEG method. Nature protocols **2:** 31-34

Glauser G, Dubugnon L, Mousavi SAR, Rudaz S, Wolfender JL, Farmer EE (2009) Velocity Estimates for Signal Propagation Leading to Systemic Jasmonic Acid Accumulation in Wounded Arabidopsis. Journal of Biological Chemistry **284:** 34506-34513

Haunhorst P, Berndt C, Eitner S, Godoy JR, Lillig CH (2010) Characterization of the human monothiol glutaredoxin 3 (PICOT) as iron-sulfur protein. Biochemical and biophysical research communications **394:** 372-376

He YJ, Chung EH, Hubert DA, Tornero P, Dangl JL (2012) Specific Missense Alleles of the Arabidopsis Jasmonic Acid Co-Receptor COI1 Regulate Innate Immune Receptor Accumulation and Function. Plos Genet **8**

Hoffmann B, Uzarska MA, Berndt C, Godoy JR, Haunhorst P, Lillig CH, Lill R, Muhlenhoff U (2011) The Multidomain Thioredoxin-Monothiol Glutaredoxins Represent a Distinct Functional Group. Antioxid Redox Sign **15:** 19-30

Hsieh EJ, Cheng MC, Lin TP (2013) Functional characterization of an abiotic stress-inducible transcription factor AtERF53 in Arabidopsis thaliana. Plant molecular biology **82:** 223-237

Hubert DA, He YJ, McNulty BC, Tornero P, Dangl JL (2009) Specific Arabidopsis HSP90.2 alleles recapitulate RAR1 cochaperone function in plant NB-LRR disease resistance protein regulation. Proceedings of the National Academy of Sciences of the United States of America **106:** 9556-9563

Isakov N, Witte S, Altman A (2000) PICOT-HD: a highly conserved protein domain that is often associated with thioredoxin and glutaredoxin modules. Trends Biochem Sci **25:** 537-539

Karimi M, De Meyer B, Hilson P (2005) Modular cloning in plant cells. Trends in plant science **10:** 103-105

Kazan K, Manners JM (2012) JAZ repressors and the orchestration of phytohormone crosstalk. Trends in plant science **17:** 22-31

Kleinboelting N, Huep G, Kloetgen A, Viehoever P, Weisshaar B (2012) GABI-Kat SimpleSearch: new features of the Arabidopsis thaliana T-DNA mutant database. Nucleic acids research **40:** D1211-D1215

Knoth C, Eulgem T (2008) The oomycete response gene LURP1 is required for defense against Hyaloperonospora parasitica in Arabidopsis thaliana. Plant Journal **55:** 53-64

Knoth C, Ringler J, Dangl JL, Eulgem T (2007) ArabidopsisWRKY70 is required for full RPP4-mediated disease resistance and basal defense against Hyaloperonospora parasitica. Mol Plant Microbe In **20:** 120-128

Knuesting J, Riondet C, Maria C, Kruse I, Bécuwe N, König N, Berndt C, Tourrette S, Guilleminot-Montoya J, Herrero E, et al (2015) Arabidopsis Glutaredoxin S17 and Its Partner, the Nuclear Factor Y Subunit C11/Negative Cofactor 2α, Contribute to Maintenance of the Shoot Apical Meristem under Long-Day Photoperiod. Plant physiology **167:** 1643-1658

Leitner J, Petrasek J, Tomanov K, Retzer K, Parezova M, Korbei B, Bachmair A, Zazimalova E, Luschnig C (2012) Lysine63-linked ubiquitylation of PIN2 auxin carrier protein governs hormonally controlled adaptation of Arabidopsis root growth. Proceedings of the National Academy of Sciences of the United States of America **109:** 8322-8327

McGrath KC, Dombrecht B, Manners JM, Schenk PM, Edgar CI, Maclean DJ, Scheible WR, Udvardi MK, Kazan K (2005) Repressor- and activator-type ethylene response factors functioning in jasmonate signaling and disease resistance identified via a genome-wide screen of Arabidopsis transcription factor gene expression. Plant physiology **139:** 949-959

Mur LAJ, Sivakumaran A, Mandon J, Cristescu SM, Harren FJM, Hebelstrup KH (2012) Haemoglobin modulates salicylate and jasmonate/ethylene-mediated resistance mechanisms against pathogens. Journal of experimental botany **63:** 4375-4387

Obayashi T, Hayashi S, Saeki M, Ohta H, Kinoshita K (2009) ATTED-II provides coexpressed gene networks for Arabidopsis. Nucleic acids research **37:** D987-D991

Pauwels L, Goossens A (2011) The JAZ proteins: a crucial interface in the jasmonate signaling cascade. The Plant cell **23:** 3089-3100

Ralhan A, Schottle S, Thurow C, Iven T, Feussner I, Polle A, Gatz C (2012) The Vascular Pathogen Verticillium longisporum Requires a Jasmonic Acid-Independent COI1 Function in Roots to Elicit Disease Symptoms in Arabidopsis Shoots. Plant physiology **159:** 1192-1203

Robinson MD, McCarthy DJ, Smyth GK (2010) edgeR: a Bioconductor package for differential expression analysis of digital gene expression data. Bioinformatics **26:** 139-140

Robinson MD, Smyth GK (2008) Small-sample estimation of negative binomial dispersion, with applications to SAGE data. Biostatistics **9:** 321-332

Roret T, Tsan P, Couturier J, Zhang B, Johnson MK, Rouhier N, Didierjean C (2014) Structural and Spectroscopic Insights into BolA-Glutaredoxin Complexes. Journal of Biological Chemistry **289:** 24588-24598

Seltmann MA, Stingl NE, Lautenschlaeger JK, Krischke M, Mueller MJ, Berger S (2010) Differential Impact of Lipoxygenase 2 and Jasmonates on Natural and Stress-Induced Senescence in Arabidopsis. Plant physiology **152:** 1940-1950

Sheard LB, Tan X, Mao H, Withers J, Ben-Nissan G, Hinds TR, Kobayashi Y, Hsu FF, Sharon M, Browse J, et al (2010) Jasmonate perception by inositol-phosphate-potentiated COI1-JAZ co-receptor. Nature **468:** 400-405

Shimada TL, Shimada T, Hara-Nishimura I (2010) A rapid and non-destructive screenable marker, FAST, for identifying transformed seeds of Arabidopsis thaliana. Plant Journal **61:** 519-528

Stenzel I, Otto M, Delker C, Kirmse N, Schmidt D, Miersch O, Hause B, Wasternack C (2012) ALLENE OXIDE CYCLASE (AOC) gene family members of Arabidopsis thaliana: tissue- and organ-specific promoter activities and in vivo heteromerization. Journal of experimental botany **63:** 6125-6138

Stone SL, Hauksdottir H, Troy A, Herschleb J, Kraft E, Callis J (2005) Functional analysis of the RING-type ubiquitin ligase family of Arabidopsis. Plant physiology **137:** 13-30

Stotz HU, Mueller S, Zoeller M, Mueller MJ, Berger S (2013) TGA transcription factors and jasmonate-independent COI1 signalling regulate specific plant responses to reactive oxylipins. Journal of experimental botany **64:** 963-975

Thines B, Katsir L, Melotto M, Niu Y, Mandaokar A, Liu G, Nomura K, He SY, Howe GA, Browse J (2007) JAZ repressor proteins are targets of the SCF(COI1) complex during jasmonate signalling. Nature **448:** 661-665

Van Leene J, Eeckhout D, Cannoot B, De Winne N, Persiau G, Van De Slijke E, Vercruysse L, Dedecker M, Verkest A, Vandepoele K, et al (2015) An improved toolbox to unravel the plant cellular machinery by tandem affinity purification of Arabidopsis protein complexes. Nature protocols **10:** 169-187

Van Leene J, Eeckhout D, Persiau G, Van De Slijke E, Geerinck J, Van Isterdael G, Witters E, De Jaeger G (2011) Isolation of transcription factor complexes from Arabidopsis cell suspension cultures by tandem affinity purification. Methods in molecular biology **754:** 195-218

Vanderauwera S, Zimmermann P, Rombauts S, Vandenabeele S, Langebartels C, Gruissem W, Inze D, Van Breusegem F (2005) Genome-wide analysis of hydrogen peroxide-regulated gene expression in Arabidopsis reveals a high light-induced transcriptional cluster involved in anthocyanin biosynthesis. Plant physiology **139:** 806-821

Vanholme R, Cesarino I, Rataj K, Xiao YG, Sundin L, Goeminne G, Kim H, Cross J, Morreel K, Araujo P, et al (2013) Caffeoyl Shikimate Esterase (CSE) Is an Enzyme in the Lignin Biosynthetic Pathway in Arabidopsis. Science **341:** 1103-1106

Voinnet O, Rivas S, Mestre P, Baulcombe D (2003) An enhanced transient expression system in plants based on suppression of gene silencing by the p19 protein of tomato bushy stunt virus. The Plant journal : for cell and molecular biology **33:** 949-956

Wang YP, Elhiti M, Hebelstrup KH, Hill RD, Stasolla C (2011) Manipulation of hemoglobin expression affects Arabidopsis shoot organogenesis. Plant Physiol Bioch **49:** 1108-1116

Wellburn AR, Gounaris I, Fassler L, Lichtenthaler HK (1983) Changes in Plastid Ultrastructure and Fluctuations of Cellular Isoprenoid and Carbohydrate Compounds during Continued Etiolation of Dark-Grown Oat Seedlings. Physiol Plantarum **59:** 347-354

Whittaker CA, Hynes RO (2002) Distribution and evolution of von Willebrand/integrin A domains: widely dispersed domains with roles in cell adhesion and elsewhere. Molecular biology of the cell **13:** 3369-3387

Wu QY, Lin J, Liu JZ, Wang XF, Lim W, Oh M, Park J, Rajashekar CB, Whitham SA, Cheng NH, et al (2012) Ectopic expression of Arabidopsis glutaredoxin AtGRXS17 enhances thermotolerance in tomato. Plant Biotechnol J **10:** 945-955

Wu TD, Nacu S (2010) Fast and SNP-tolerant detection of complex variants and splicing in short reads. Bioinformatics **26:** 873-881

Xie DX, Feys BF, James S, Nieto-Rostro M, Turner JG (1998) COI1: an Arabidopsis gene required for jasmonate-regulated defense and fertility. Science **280:** 1091-1094

Yan J, Zhang C, Gu M, Bai Z, Zhang W, Qi T, Cheng Z, Peng W, Luo H, Nan F, et al (2009) The Arabidopsis CORONATINE INSENSITIVE1 protein is a jasmonate receptor. The Plant cell **21:** 2220-2236

Yin XJ, Volk S, Ljung K, Mehlmer N, Dolezal K, Ditengou F, Hanano S, Davis SJ, Schmelzer E, Sandberg G, et al (2007) Ubiquitin lysine 63 chain forming ligases regulate apical dominance in Arabidopsis. The Plant cell **19:** 1898-1911

Zhang X, Wu Q, Cui S, Ren J, Qian W, Yang Y, He S, Chu J, Sun X, Yan C, et al (2015) Hijacking of the jasmonate pathway by the mycotoxin fumonisin B1 (FB1) to initiate programmed cell death in Arabidopsis is modulated by RGLG3 and RGLG4. Journal of experimental botany

Zhang X, Wu Q, Ren J, Qian WQ, He SP, Huang KW, Yu XC, Gao Y, Huang P, An CC (2012) Two Novel RING-Type Ubiquitin Ligases, RGLG3 and RGLG4, Are Essential for Jasmonate-Mediated Responses in Arabidopsis. Plant physiology **160:** 808-822

Chapter 7:
Conclusions and perspectives

Astrid Nagels Durand

During the course of this research we aimed at extending the knowledge on the relationship between the ubiquitin (Ub) system and the jasmonate (JA) signalling pathway, by identifying and characterizing additional E3s functioning in the latter pathway. Here, we provide an overview on the conclusions that can be drawn based on the findings described in previous chapters. Characteristic to scientific research, new findings lead to new questions. Accordingly, open questions that have risen from our findings will be discussed, and approaches to address some of this issues will be proposed.

The Ubiquitin system and Jasmonate signalling

At the time this research started, SCF^{COI1} was the only E3 Ub ligase known to function in JA-signalling. In 2012, Zhang and colleges reported two RING LIGASE family members (*RGLG3* and *RGLG4*) also participate in JA-signalling. We have further expanded the list of candidate E3 ligases involved in JA-signalling, based on available transcriptomic data, and identified candidate targets for a number of these E3s. My research further focussed on the characterization of two E3-target couples (BRIZ1/2-LARP6b and RGLG3/4-PICOT1), while AE31-SRPK4, ATL23-RD21A and RGLG3/4-GLB3 were further characterized in our group by Dr. Andres Ritter, Dr. Patricia Fernández-Calvo and Dr. Sabrina Iñigo, respectively. Though we could not identify putative targets for the rest of the candidate E3s, further phenotypic characterization of the JA-response of mutants with altered expression of the corresponding genes should allow verification of their involvement in JA-signalling.

Methods to identify E3 ligase targets

During this research, targets of E3 ligases were identified based on the combination of two protein-protein interaction techniques. First, a customized Tandem Affinity Purification (TAP; Van Leene et al., 2015) assay was employed to identify all proteins that appear as a complex with the E3 of choice. The TAP platform was developed in the lab of Prof. Dr. Geert De Jaeger and allows screening for protein interactions in cell cultures, without the need for generation of transgenic lines. Customization concerned the introduction of specific mutations in the E3 ligases used as baits. Next, yeast two-hybrid was employed to differentiate between direct and indirect interactions with the E3 ligase. Both experiments can be performed in a relatively small time-frame, and, as demonstrated in the previous chapters, are efficient for the identification of plant E3 ligase targets.

For the study of *in vivo* ubiquitination of Arabidopsis proteins in yeast (*Saccharomyces cerevisiae*), we generated a set of Multisite Gateway destination vectors for expression of (plant) proteins in yeast (Nagels Durand et al., 2012). These vectors have a broader purpose, as expression of heterologous proteins in yeast is often performed to characterize the function

of the gene, complementation of yeast mutations by heterologous orthologs being the most straight-forward example. These vectors have indeed proven to be useful, for example, in yeast three-hybrid assays (Cuéllar Pérez et al., 2014).

The "Heterologous Ubiquitination Assay" (HUbA) in yeast did not achieve the expected results (yet). Nevertheless, modification of LARP6b, candidate target of the heterodimeric E3 ligase BRIZ1/2, was dependent on co-expression of both BRIZ1 and BRIZ2 in yeast. However, we could not detect the modified LARP6b as being a ubiquitinated protein. In other words, we succeeded in molecularly re-assembling the modification reaction of LARP6b in yeast, but we were not able to detect and correctly interpret this modification.

Some general aspects of the HUbA could still be improved in order to succeed in our intention to use this platform as an *in vivo* ubiquitination assay. First, production of an active plant E3 ligase in yeast should be evaluated as a pre-requisite for target modification. It is generally believed that E3 ligases have the ability to auto-ubiquitinate, and this property should be exploited to select for yeast strains that express active E3 ligase. Why heterologous E3 ligases are sometimes not active in yeast is still not clear. One possibility is that epitope tagging of the E3 could interfere with correct folding of the protein or disturb interaction with the endogenous E2. Another possibility could be that high expression of the heterologous proteins interferes with their production in yeast. HUbA assays described in this thesis were performed using high copy-number plasmids and constitutive promotors. A second point of action would thus be to reduce expression levels of the heterologous proteins by using low copy-number plasmids (e.g. centromeric or integrative plasmids, available as Multisite Gateway compatible destination vectors) or by expressing the constructs under control of inducible promotors (which were also cloned as Multisite Gateway compatible building blocks during this research). Especially when the post-translational modification machinery of the host is needed, expression levels of the heterologous proteins should not exceed the endogenous capacity of the host to modify these proteins. In the particular case of BRIZ1/2, detection of the modified LARP6b should be repeated using anti-Nedd8 antibodies, as the closely related human protein BRAP2 has been linked to Nedd8-modification (Takashima et al., 2013).

PICOT1 constitutes a ubiquitination target of the E3 ligases RGLG3 and RGLG4

Using the customized TAP strategy, we were able to identify two putative targets of RGLG3 and RGLG4: PICOT1 and GLB3. Subsequent research showed PICOT1 is ubiquitinated by RGLG3/4, eventually leading to degradation of the protein by the proteasome. The research described in this thesis focussed on PICOT1, while GLB3 is currently the research topic of Dr. Sabrina Iñigo, a member of our group.

The human and yeast orthologs of PICOT1 function in the regulation of iron (Fe) homeostasis (Muhlenhoff et al., 2010; Haunhorst et al., 2013). RGLG1 and RGLG2, were shown to associate with UBC35 (Yin et al., 2007) to mediate K63 poly-ubiquitination of PIN2, thereby regulating directional auxin flow (Leitner et al., 2012). Intriguingly, both *rglg1rglg2* and *ubc35* mutants have altered Fe-responses (Li and Schmidt, 2010; Pan and Schmidt, 2014) while polar auxin transport is affected in *picot1* mutants (Cheng et al., 2011). These subtle connections encourage future investigation on PICOT1 protein stability in *rglg1rglg2* plants and, conversely, investigation of Fe-responses of *picot1* seedlings. From the results presented in this thesis, it cannot be excluded that other RGLG-proteins could target ubiquitination of PICOT1.

In addition to K48-forming E2 Ub conjugases, our research showed RGLG3/4 can interact with E2s that typically catalyse attachment of Ub to the N-terminus of target proteins. Because N-terminal tagging of PICOT1 often lead to inefficient expression of the construct, we can speculate on a requirement of PICOT1 N-terminal ubiquitination for protein stability. This phenomenon could be investigated in first instance by expression of a translational fusion construct Ub-PICOT1. Evaluation of protein stability, protein-protein interactions or phenotypic characteristics should highlight the impact of PICOT1 N-terminal ubiquitination.

PICOT1 associates with Fe-S proteins

PICOT1 has been reported to form Fe-S bridged homo or hetero-dimers (Couturier et al., 2014; Knuesting et al., 2015). TAP experiments using PICOT1 as bait revealed PICOT1 binding to Fe-S proteins is a general feature of this protein. The number of cytosolic or nuclear proteins that are known to bind Fe-S clusters in Arabidopsis is low (<20 confirmed Fe-S proteins; Balk and Pilon, 2011). In addition, pathways leading to the assembly of Fe-S clusters in plants are still poorly characterized, with most knowledge being extrapolated from other organisms based on the conservation of orthologous genes. Remarkably, almost the entire cytosolic Fe-S assembly complex was isolated from Arabidopsis cell cultures using PICOT1 as a bait during TAP assays. As the glutaredoxin (Grx) domains of PICOT1 account for its ability to bind Fe-S clusters, these domains could be used as baits to further inventarize Fe-S proteins and the Fe-S assembly machinery in Arabidopsis, given that our results bring TAP forward as a suitable platform for the investigation of this pathway.

PICOT1 is involved in tRNA modification

A useful tool to study transfer RNA (tRNA) modifications at the third anti-codon position uridine (Wobble uridine) in yeast is zymocin. Zymocin is a killer toxin produced by the yeast *Kluyveromyces lactis*, that cleaves tRNAs that carry modified wobble uridine bases in *S. cerevisiae*. Screen for mutants with increased resistance to zymocin identified all Elongator complex subunits, the yeast orthologs of CTU1 and CTU2, the gene encoding the Ub-like URM1 and the yeast URM E1 (Jablonowski et al., 2001). In a different screen, elevated expression of one of the yeast orthologs of PICOT1 (ScGrx3) was shown to decrease the sensitivity of the organism for the toxin (Jablonowski et al., 2001). Based on the results presented in this thesis, one would expect mutations in ScGrx3 would also lead to zymocin resistance. However, ScGrx3 and ScGrx4 (both PICOT1 orthologs) function redundantly in yeast (Pujol-Carrion et al., 2006), indicating mutation of both genes would be necessary to reveal a potential function in zymocin resistance. Why overexpression of ScGrx3 leads to zymocin resistance remains unclear, but nevertheless points to a conserved function of PICOT1 orthologs in tRNA modification. We have set up a collaboration with the group of Prof. Dr. Raffael Schaffrath, to investigate the effect of overexpression of Arabidopsis PICOT1 on zymocin resistance in yeast. Further tRNA profiling of Arabidopsis WT and *picot1* seedlings should contribute to clarify the role of PICOT1 in tRNA modification.

PICOT1 as a potential regulator of COI1 JA-independent function.

During this research we identified interaction between *COI1* and *PICOT1* at three different levels. First, at the protein level, COI1 and PICOT1 interact directly with each other in the nucleus. Second, *COI1* and *PICOT1* genes interact genetically since *coi1-16* can rescue the short root phenotype of *picot1* in the *coi1-16picot1* mutant. Finally, *PICOT1* and *COI1* interact on the transcript level as the majority of genes that are upregulated in *coi1-16* are partially dependent on *PICOT1* for their upregulation and thus are less upregulated in *coi1-16picot1* plants. Remarkably, we did not identify alterations in the JA-response of *picot1* seedlings.

Based on the above mentioned observations we have proposed a possible model for PICOT1-mediated regulation of COI1 function, independent of JA-Ile perception. In this model, COI1 exists in two states where one state (COI1-A) is involved in JA-Ile perception and the activation of JA-responses through degradation of JAZs, and the other state (COI1-B) is involved in the transcription of a different set of (JA-independent) genes.

It is not clear at this moment if PICOT1 functions to promote transition of COI1-A to COI1-B or stimulates the activity of COI1-B once it has reached this state. Another unanswered question would be what this “state” differences are. Structural differences in COI1 might alter its function and these could be mediated by PICOT1. PICOT1 is known to form dimers where

the active site of each Grx domain of one monomer is bridged by a [2Fe-2S] cluster to a Grx domain in the other monomer. Because PICOT1 interacts with COI1 through its thioredoxin (Trx) domain, COI1 binding can be mediated either by PICOT1 monomer or dimer. In the case where a PICOT1 monomer is able to mediate COI1 interaction, it could still form homodimers through its Grx domains, thus binding two COI1 proteins simultaneously. This could be a mechanism to stabilize COI1-dimers that, in turn, might function in a process unrelated to JA-Ile perception. The occurrence of COI1 or PICOT1 dimers *in vivo* could be verified by preparing and separating protein extracts under native conditions (native-PAGE) followed by detection of the proteins on immunoblots.

The absence of up-regulated JA-responsive genes in the transcriptome analysis of *coi1-16* further indicates the upregulated genes in this line are not regulated by TFs known to play a role in JA-signalling. Because COI1 has not been shown to bind DNA, transcription of these genes must thus be mediated by yet unknown factors. Based on our hypothesis that in *coi1-16* plants, $COI1^{L245F}$ protein is trapped in the COI1-B state, a possible approach to identify additional factors with a role in the pathway regulated by COI1-B could be to use of $COI1^{L245F}$ as a bait in TAP experiments, provided that we could overexpress this protein to an acceptable level in Arabidopsis cell cultures.

PICOT1 was recently found to interact with TF NF-YC11/NC2α (Knuesting et al., 2015). Because the phenotype of *picot1* seedlings resembles that of *nf-yc11* seedlings, NF-YC11 is a candidate TF that could regulate COI1-B dependent gene expression. The expression levels of COI1-B-dependent genes in the *nf-yc11* mutant should be measured to test this hypothesis. Because COI1 is an F-box protein and PICOT1 can interact with both COI1 and with NF-YC11, NF-YC11 protein levels could be regulated by COI1. This hypothesis could easily be tested in the *picot1* background (vs WT) or using transient expression of the respective proteins in *N. benthamiana*. Another possibility to identify proteins involved in the regulation of COI1-B dependent gene expression would be to use the data generated during transcriptome analysis of *coi1-16* to search for overrepresentation of transcription binding sites in the promotors of differentially upregulated genes based on bio-informatics approaches.

The mutant phenotype of the aerial parts of *picot1* seedlings has been shown to be affected by photoperiod in a temperature dependent manner (Knuesting et al., 2015). Accordingly, the authors describe *picot1* seedlings behave like WT when grown at 15°C. It will therefore be interesting to test if the short-root phenotype of *picot1* seedlings is also affected in a temperature dependent manner and to test the different lines generated during the time-course of this PhD at different conditions: long-day vs short-day photoperiod, high-light condition and elevated as well as decreased temperatures (28°C, 21°C and 15°C). In addition, lines overexpressing RGLG3 or RGLG4 are being generated, and these lines will contribute to the investigation of the role of PICOT1 *in planta.*

REFERENCES

Balk J, Pilon M (2011) Ancient and essential: the assembly of iron-sulfur clusters in plants. Trends in plant science **16:** 218-226

Cheng NH, Liu JZ, Liu X, Wu QY, Thompson SM, Lin J, Chang J, Whitham SA, Park S, Cohen JD, et al (2011) Arabidopsis Monothiol Glutaredoxin, AtGRXS17, Is Critical for Temperature-dependent Postembryonic Growth and Development via Modulating Auxin Response. Journal of Biological Chemistry **286:** 20398-20406

Couturier J, Wu HC, Dhalleine T, Pegeot H, Sudre D, Gualberto JM, Jacquot JP, Gaymard F, Vignols F, Rouhier N (2014) Monothiol GlutaredoxinBolA Interactions: Redox Control of Arabidopsis thaliana BolA2 and SufE1. Molecular plant **7:** 187-205

Cuéllar Pérez A, Nagels Durand A, Vanden Bossche R, De Clercq R, Persiau G, Van Wees SCM, Pieterse CMJ, Gevaert K, De Jaeger G, Goossens A, et al (2014) The Non-JAZ TIFY Protein TIFY8 from Arabidopsis thaliana Is a Transcriptional Repressor. PloS one **9**

Haunhorst P, Hanschmann EM, Brautigam L, Stehling O, Hoffmann B, Muhlenhoff U, Lill R, Berndt C, Lillig CH (2013) Crucial function of vertebrate glutaredoxin 3 (PICOT) in iron homeostasis and hemoglobin maturation. Molecular biology of the cell **24:** 1895-1903

Jablonowski D, Butler AR, Fichtner L, Gardiner D, Schaffrath R, Stark MJR (2001) Sit4p protein phosphatase is required for sensitivity of Saccharomyces cerevisiae to Kluyveromyces lactis zymocin. Genetics **159:** 1479-1489

Knuesting J, Riondet C, Maria C, Kruse I, Bécuwe N, König N, Berndt C, Tourrette S, Guilleminot-Montoya J, Herrero E, et al (2015) Arabidopsis Glutaredoxin S17 and Its Partner, the Nuclear Factor Y Subunit C11/Negative Cofactor 2α, Contribute to Maintenance of the Shoot Apical Meristem under Long-Day Photoperiod. Plant physiology **167:** 1643-1658

Leitner J, Petrasek J, Tomanov K, Retzer K, Parezova M, Korbei B, Bachmair A, Zazimalova E, Luschnig C (2012) Lysine63-linked ubiquitylation of PIN2 auxin carrier protein governs hormonally controlled adaptation of Arabidopsis root growth. Proceedings of the National Academy of Sciences of the United States of America **109:** 8322-8327

Li W, Schmidt W (2010) A lysine-63-linked ubiquitin chain-forming conjugase, UBC13, promotes the developmental responses to iron deficiency in Arabidopsis roots. The Plant journal : for cell and molecular biology **62:** 330-343

Muhlenhoff U, Molik S, Godoy JR, Uzarska MA, Richter N, Seubert A, Zhang Y, Stubbe J, Pierrel F, Herrero E, et al (2010) Cytosolic Monothiol Glutaredoxins Function in Intracellular Iron Sensing and Trafficking via Their Bound Iron-Sulfur Cluster. Cell Metab **12:** 373-385

Nagels Durand A, Moses T, De Clercq R, Goossens A, Pauwels L (2012) A MultiSite Gateway vector set for the functional analysis of genes in the model Saccharomyces cerevisiae. BMC molecular biology **13:** 30

Pan IC, Schmidt W (2014) Functional implications of K63-linked ubiquitination in the iron deficiency response of Arabidopsis roots. Frontiers in plant science **4**

Pujol-Carrion N, Belli G, Herrero E, Nogues A, de la Torre-Ruiz MA (2006) Glutaredoxins Grx3 and Grx4 regulate nuclear localisation of Aft1 and the oxidative stress response in Saccharomyces cerevisiae. J Cell Sci **119:** 4554-4564

Takashima O, Tsuruta F, Kigoshi Y, Nakamura S, Kim J, Katoh MC, Fukuda T, Irie K, Chiba T (2013) Brap2 regulates temporal control of NF-kappaB localization mediated by inflammatory response. PloS one **8:** e58911

Van Leene J, Eeckhout D, Cannoot B, De Winne N, Persiau G, Van De Slijke E, Vercruysse L, Dedecker M, Verkest A, Vandepoele K, et al (2015) An improved toolbox to unravel the plant cellular machinery by tandem affinity purification of Arabidopsis protein complexes. Nature protocols **10:** 169-187

Yin XJ, Volk S, Ljung K, Mehlmer N, Dolezal K, Ditengou F, Hanano S, Davis SJ, Schmelzer E, Sandberg G, et al (2007) Ubiquitin lysine 63 chain forming ligases regulate apical dominance in Arabidopsis. The Plant cell **19:** 1898-1911

Zhang X, Wu Q, Ren J, Qian WQ, He SP, Huang KW, Yu XC, Gao Y, Huang P, An CC (2012) Two Novel RING-Type Ubiquitin Ligases, RGLG3 and RGLG4, Are Essential for Jasmonate-Mediated Responses in Arabidopsis. Plant physiology **160:** 808-822

Acknowledgements
Dankwoord

First of all, I would like to thank my promotors Alain and Laurens. Thanks Alain for believing in me after I did my master thesis in the lab and giving me the opportunity to stay for a PhD in the metabol-group. Laurens, I couldn't have wished for a better supervisor than you. You are incredibly smart and still manage to be cool as well! I really enjoyed working with you the past years, the endless discussions where one theme leads to another and one eventually gets lost in science, the coffee breaks and of course the friendship. The metabol group actually has the perfect blend of science and diversion, where very good scientific practice and team-work is combined with a friendly and relaxed atmosphere where the members actually do feel like a team, I was very lucky to be part of this team.

Amparo, you held my hand during my first steps into science and you showed me how sociable end fun scientists can actually be, I really enjoyed spending time with you in the lab and outside the lab as well, and also thanks for saving my spanish from decay! You and Robin took care of me when I first arrived in the lab and made me feel part of the group immediately! And after Amparo left, Robin took over and became my coffee-break buddy. Robin, I am very thankful for the fact that you know how to not do work-talk during a break ;-) and also because you listened without (almost) any complaints to all my cat-stories!! Your friendship means a lot to me and I hope to keep in touch with you and Els after I fly out of the metabol-nest. Of course I also want to thank you for helping me at work, some of your tips and tricks are priceless!

Related to the scientific achievements reached during this PhD, there are some people I need to thank in particular since we actually worked together on this project. Of course I already mentioned Laurens, but I certainly also have to mention Rebecca, who helped me throughout my PhD and Sabrina. When I started this project, no one else was really working on ubiquitination, and when I heard she was joining our lab to work on this topic I was very glad! We could suddenly do twice the amount of work at the same time and this reflected in the great results we got. I enjoyed working with you Sabrina, and all my prejudices about Argentinians are now gone thanks to you ;-) Not to get me started on how well Peruvians and Chileans normally get along, but how could someone not get along with the super friendly Andres?! Together we expanded the south American clan of the metabol group, later also joined by Jennifer, Bianca and Gabriela… We reached ¼ of the group, nice!!

Of course in addition to the people who work together with you because it's their job, there are also those that have no other choice: the master students. They don't always realize it but they are much appreciated, and so I want to thank Jana, Sofie and Jonas for the hard work. Sofie, I especially enjoyed the year you spent in our lab, always in a good mood, always ready to have fun, very sociable, and hilariously clumsy ;-) Jonas, you were my guinea-pig-student so I probably made quite some mistakes with you, however I am relieved to see that

you turned out fine anyway! Thanks for the help during that year, and also afterwards, for making our desk-corner a cosy prank-safe place.

I also want to thank the rest of the (ex) metabol girls (Marie-Laure, Gwen, Janine, Piti, Tessa, Adeline) and boys (Phill, Fabian, Karel, Alex, Jacob, Yuechen, Jan, Michele, Michiel and Nathan), for making our work environment a place worth working in and for all the fun we had over the last 4 years! In the beginning of my PhD, however, I also spent a lot of time in the functional interactomics group, where Jelle and Geert P taught me all about the TAP technique and Eveline, Nancy, Dominique and Geert DJ always made me feel welcome. A special thanks to Geert P and Dominique for helping me with the post-purification and post-detection parts!!! Of course this collaboration took a new dimension when Jelle became my Jelleke… to you thanks for being there for me whenever I needed support, for making the best out of the PhD holidays, of course also for your scientific advice from time to time, and for making this PhD journey even more fun!

Quisiera también agradecer a mi familia: papi, mami y Marquito ya que estuvieron siempre listos para apoyarme y nunca han dejado de creer en mi. También quiero agradecer a mi familia en Perú, que desde lejos me hacen saber que están tan orgullosos de mi, y eso me da mucha alegría. Ook de Belgische kant van de familie moet bedankt worden want ook zij hebben telkens hun steun en trots uitgedrukt en hebben er mee voor gezorgd dat ik deze uitdaging aandurfde.

Finally, I also want to thank all my friends who were there during the last four years to support me and to provide great quality entertainment during the non-working hours, especially Lotte, Tess, Karlien, Els en Joris: merci dat jullie zo ‘n goeie vrienden zijn en dat jullie altijd voor mij klaar staan als ik jullie nodig heb!

Astrid

Additional scientific publications

Cuéllar Pérez *et al.* (2014). The non-JAZ TIFY protein TIFY8 from Arabidopsis thaliana is a transcriptional repressor. *PloS one* **9** (1): e84891.

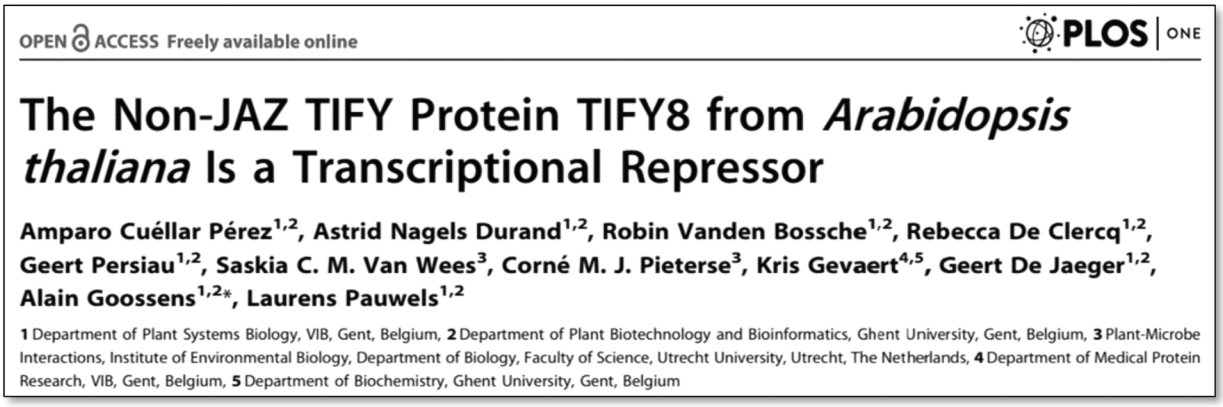

OPEN ACCESS Freely available online

PLOS | ONE

The Non-JAZ TIFY Protein TIFY8 from *Arabidopsis thaliana* Is a Transcriptional Repressor

Amparo Cuéllar Pérez[1,2], Astrid Nagels Durand[1,2], Robin Vanden Bossche[1,2], Rebecca De Clercq[1,2], Geert Persiau[1,2], Saskia C. M. Van Wees[3], Corné M. J. Pieterse[3], Kris Gevaert[4,5], Geert De Jaeger[1,2], Alain Goossens[1,2]*, Laurens Pauwels[1,2]

1 Department of Plant Systems Biology, VIB, Gent, Belgium, **2** Department of Plant Biotechnology and Bioinformatics, Ghent University, Gent, Belgium, **3** Plant-Microbe Interactions, Institute of Environmental Biology, Department of Biology, Faculty of Science, Utrecht University, Utrecht, The Netherlands, **4** Department of Medical Protein Research, VIB, Gent, Belgium, **5** Department of Biochemistry, Ghent University, Gent, Belgium

ABSTRACT

Jasmonate (JA) signalling is mediated by the JASMONATE-ZIM DOMAIN (JAZ) repressor proteins, which are degraded upon JA perception to release downstream responses. The ZIM protein domain is characteristic of the larger TIFY protein family. It is currently unknown if the atypical member TIFY8 is involved in JA signalling. Here we show that the TIFY8 ZIM domain is functional and mediated interaction with PEAPOD proteins and NINJA. TIFY8 interacted with TOPLESS through NINJA and accordingly acted as a transcriptional repressor. *TIFY8* expression was inversely correlated with JAZ expression during development and after infection with *Pseudomonas syringae*. Nevertheless, transgenic lines with altered TIFY8 expression did not show changes in JA sensitivity. Despite the functional ZIM domain, no interaction with JAZ proteins could be found. In contrast, TIFY8 was found in protein complexes involved in regulation of dephosphorylation, deubiquitination and O-linked N-acetylglucosamine modification suggesting an important role in nuclear signal transduction.

Author contribution: Generation of TIFY8-GS expressing Arabidopsis cell cultures and tandem affinity purification of TIFY8 interacting proteins.

Gonzalez *et al*. (2015). A Repressor Protein Complex Regulating Leaf Growth in the Dicot Arabidopsis. *Plant Cell.* In press.

A Repressor Protein Complex Regulating Leaf Growth in the Dicot Arabidopsis

Nathalie Gonzalez°, Laurens Pauwels°, Alexandra Baekelandt°, Liesbeth De Milde, Jelle Van Leene, Nienke Besbrugge, Ken S Heyndrickx, Amparo Cuéllar Pérez, Astrid Nagels Durand, Rebecca De Clercq, Eveline Van De Slijke, Robin Vanden Bossche, Dominique Eeckhout, Kris Gevaert, Klaas Vandepoele, Geert De Jaeger, Alain Goossens, and Dirk Inzé*

ABSTRACT

Cell number is an important determinant of final organ size. In the leaf, a large proportion of cells are derived from the stomatal lineage. Meristemoids undergo asymmetric divisions, generating several pavement cells next to the two guard cells. However, the mechanism controlling the asymmetric divisions of these stem cells before they differentiate is not well understood. Here, we characterized PEAPOD (PPD) proteins, the only transcriptional regulators known to negatively regulate meristemoid division. PPD proteins interact with KIX8 and KIX9, which act as adaptor proteins for the co-repressor TOPLESS. D3-type cyclin encoding genes were identified among direct targets of PPD2, being negatively regulated by PPDs and KIX8/9. Accordingly, kix8-kix9 mutants phenocopied PPD loss-of-function producing larger leaves resulting from increased meristemoid amplifying divisions. The identified conserved complex might be specific for leaf growth in the second dimension, since it is not present in Poaceae (grasses), which also lack the developmental program it controls.

Author contribution: Generation of GS-tagged KIX8 expressing Arabidopsis cell cultures and tandem affinity purification of KIX8 and PPD2 interacting proteins.

Curriculum vitae

PERSONAL DETAILS

Astrid Nagels Durand
°02-01-1986, Huaraz, Peru
+32 497 74 78 89
astrid.nagelsdurand@gmail.com

EDUCATION

2011-2015 PhD student (sciences: biotechnology) at Ghent University
Thesis: "Identification and characterization of E3 ubiquitin ligases involved in jasmonate signalling"
Promotors: Prof. Dr. Alain Goossens and Dr. Laurens Pauwels

2007-2010 Master in Biochemistry and Biotechnology (distinction)
Dissertation: "Phenotypic screen of plants with modulated expression of candidate jasmonate signalling proteins"
Promotor: Prof. Dr. Alain Goossens and Prof. Dr. Dirk Inzé.

2004-2008 Bachelor in Biochemistry and Biotechnology

RESEARCH EXPERIENCE

2011-2015 Predoctoral fellow at the department of Plant Biotechnology and Bio-informatics of Ghent University and the department of Plant Systems Biology of the Flanders Institute of Biotechnology (VIB)

PUBLICATIONS

Pauwels L, Ritter A, Nagels Durand A, Goossens J, Liu H, Gu Y, Geerinck J, Boter M, Vanden Bossche R, De Clercq R, Van Leene J, Gevaert K, De Jaeger G, Solano R, Stone S, Innes R, Callis J and Goossens A. **The RING E3 ligase KEEP ON GOING modulates JAZ12 stability**. Submitted to Plant Physiology.

Gonzalez N, Pauwels L, Baekelandt A, De Milde L, Cuéllar Pérez A, Nagels Durand A, De Clercq R, Van De Slijke E, Vanden Bossche R, Van Leene J, Heyndrickx K, Eeckhout D, Gevaert K, Vandepoele K, De Jaeger G, Goossens A and Inzé D. **A Repressor Protein Complex Regulating Leaf Growth in the Dicot Arabidopsis**. Accepted by The Plant Cell.

Cuéllar Pérez A, Nagels Durand A, Vanden Bossche R, De Clercq R, Persiau G, Van Wees SCM, Pieterse CMJ, Gevaert K, De Jaeger G, Goossens A and Pauwels L. (2014) **The Non-JAZ TIFY Protein TIFY8 from Arabidopsis thaliana Is a Transcriptional Repressor**. *PloS one* 9

Nagels Durand A, Moses T, De Clercq R, Goossens A, Pauwels L (2012) **A MultiSite Gateway vector set for the functional analysis of genes in the model Saccharomyces cerevisiae**. *BMC molecular biology* 13: 30

OTHER SCIENTIFIC COMMUNICATIONS

Nagels Durand A, Pauwels L and Goossens A. **Specific identification of E3 ligase targets in Arabidopsis thaliana.** Poster presented at The Ubiquitin Family, Cold Spring Harbor (USA). 14-18th of May, 2013.

Nagels Durand A, Pauwels L, Geerinck J, De Jaeger G and Goossens A. **Specific identification of E3 ubiquitin-ligase targets**. Poster presented at the Belgian Plant Biotechnology Association Symposium. Louvain-la-Neuve (Belgium), November 2011.

Nagels Durand A, Pauwels L, Geerinck J, De Jaeger G and Goossens A. **Specific identification of E3 ubiquitin-ligase targets**. Presentation at Utrecht Summer School on Environmental Signalling, Utrecht (The Netherlands). 22-24th of August, 2011.

ATTENDED MEETINGS AND COURSES

- Transferable skills workshops: Communication skills
  Basic course. UGhent, February 2012.
  Scientific writing. UGhent, June 2014.
- Mass Spectrometry Data Processing. BioInformatics Training and Services (BITS, VIB), Ghent, March 2013
- Transferable skills workshops: Leadership & Personal efficiency
  Meeting skills. UGhent, March 2012.
  Personal effectiveness. UGhent, April-May, 2012
- Transferable skills workshop: Career management
  Networking skills. UGhent, March, 2012.
- The Ubiquitin Family, Cold Spring Harbor (USA). May, 2013.
- Belgian Plant Biotechnology Association Symposium. Louvain-la-Neuve (Belgium), November, 2011.
- Utrecht Summer School on Environmental Signalling, Utrecht (The Netherlands). August, 2011.
- Science Ethics I. VIB Research Training Course (VRTC), Ghent, March 2011.

SUPERVISION OF UNDERGRADUATE STUDENTS

2013-2014 Jana Wyckmans (Master in Biochemistry and Biotechnology, UGhent)
Dissertation: *"Identification and characterization of putative targets of E3 ubiquitin ligases involved in jasmonate signalling".*

2012-2013 Sofie Aesaert (Master in Biochemistry and Biotechnology, UGhent)
Dissertation: *"Identification and characterization of targets of E3 ubiquitin ligases involved in hormone signalling".*

2011-2012 Jonas Goossens (Master in Biochemistry and Biotechnology, UGhent)
Dissertation: *"Investigation of JAZ12 as a potential target of ubiquitin ligases SCF^{COI1} and KEG in the jasmonate signalling pathway".*

Supplementary data

Supplementary Table 1. Primer pairs used in this research.

Name	Sequence	Strand	Application	Target	Remarks
#1171	GGGGACAAGTTTGTACAAAAAAGCAGGCTCCATGGAGAACCCGAACAACTTG	Rv	Cloning	AE31	attB1-AE31
#1172	GGGGACCACTTTGTACAAGAAAGCTGGGTCTCMGCTTTGCTCTCCACGAC	Fw	Cloning	AE31	AE31-attB2
#1173	AAACAGGATTGCCCCTTTAGCCAGAACTCAG	Rv	Mutagenesis	AE31	AE31mRING
#1174	AATCCTGTTTCCGTGTTTGACGTTGGAG	Fw	Mutagenesis	AE31	AE31mRING
#1159	GGGGACAAGTTTGTACAAAAAAGCAGGCTCCATGCACTACACACGCATCTC	Fw	Cloning	ATL23	attB1-ATL23
#1160	GGGGACCACTTTGTACAAGAAAGCTGGGTCTCMACATGGACTTTGATTTTC	Rv	Cloning	ATL23	ATL23-attB2
#1167	ATCAACGGAAGCTGCTGTTGCCCTTGAAGAT	Fw	Mutagenesis	ATL23	ATL23mRING
#1168	TTCCGTTGATCTAGCTATTACGGCTAGC	Rv	Mutagenesis	ATL23	ATL23mRING
#1338	GGGGACAAGTTTGTACAAAAAAGCAGGCTCCATGTGCTCCACACGGCGTCG	Fw	Cloning	ATL23	attB1-ATG-ATL23dTM
#1100	GGGGACAAGTTTGTACAAAAAAGCAGGCTCCATGGCTGTTCAAGCTCATCA	Fw	Cloning	BOI	attB1-BOI
#1101	GGGGACCACTTTGTACAAGAAAGCTGGGTCTCMAGAAGACATGTTAACATGC	Rv	Cloning	BOI	BOI1-attB2
#1102	TTTGTGTTTGGCTACGGTTGCTGGTGGTTCG	Fw	Mutagenesis	BOI	BOI1mRING
#1103	CAAACACAAATGACGACATGGTAACACC	Rv	Mutagenesis	BOI	BOI1mRING
#1406	CACAACCATGGCCAATGCTTCCTTCCATTG	Fw	Mutagenesis	BRIZ2	BRIZ2mRING
#1407	CATGGTTGTGAGAATGCCACCTGTGTCTTG	Rv	Mutagenesis	BRIZ2	BRIZ2mRING
#1739	AGGATGGTAAGTGGCTTCATGA	FwP	Genotyping	COI1	coi1-16 dCAPS primer, XbaI cuts WT (224 vs 200bp)
#1740	CAAGGAGCCACCACAAAATTCTTCTA	RvP	Genotyping	COI1	coi1-16 dCAPS primer, XbaI cuts WT (224 vs 200bp)
#1707	GTTTTTCTTCAGACAAGGAATGTAACCG	FwP	Genotyping	COI1	coi1-21 dCAPS primer, HpaII cuts WT (190 vs 212bp)
#1708	GTTATATCTGAGACATACACCGCCATGTAT	RvP	Genotyping	COI1	coi1-21 dCAPS primer, HpaII cuts WT (190 vs 212bp)
#1709	CTTTGGCTCAGGGCTGCC	FwP	Genotyping	COI1	coi1-22 dCAPS primer, BamHI cuts WT (190 vs 210bp)
#1710	GCAAATCGTCTGAGTTTCTTGGAT	RvP	Genotyping	COI1	coi1-22 dCAPS primer, BamHI cuts WT (190 vs 210bp)
#2096	GGGGACAAGTTTGTACAAAAAAGCAGGCTCCATGGAGGCCAAGAAC	Fw	Cloning	CTU1	attB1-ROL5
#2097	GGGGACCACTTTGTACAAGAAAGCTGGGTCTCMGAAATCCAGAGATCC	Rv	Cloning	CTU1	ROL5-attB2
#2104	TCGTCGGAGTTGGATCAATAG	Fw	Genotyping	CTU1	GABI_709D04 rol5-2
#2105	TGGAGAAGTAATCCAGCTTCTTG	Rv	Genotyping	CTU1	GABI_709D04 rol5-2
#2098	CTTCGACGATGGAAGATTCTG	Fw	Genotyping	CTU2	GABI_686B10 ctu2-2
#2099	TCGAAGTGGAAGTACAATGGG	Rv	Genotyping	CTU2	GABI_686B10 ctu2-2
#2163	GGGGACAAGTTTGTACAAAAAAGCAGGCTCCATGGCTTGTAATTCCTC	Fw	Cloning	CTU2	attB1-CTU2
#2164	GGGGACCACTTTGTACAAGAAAGCTGGGTCTCMGACAACCTCTTCATC	Rv	Cloning	CTU2	CTU2-attB2
#1408	GGGGACAAGTTTGTACAAAAAAGCAGGCTCCATGCAATCGCTGCAAGATAAG	Fw	Cloning	GLB3	attB1-GLB3
#1409	GGGGACCACTTTGTACAAGAAAGCTGGGTCTCMTTCTTCTGCTGGTTTATTG	Rv	Cloning	GLB3	GLB3-attB2
#1493	GATAATGGCTTGGAATTGCAG	Fw	Genotyping	GLB3	SALK_060213 glb3-1
#1494	TGCTATTGCAAATTTGCAGTG	Rv	Genotyping	GLB3	SALK_060213 glb3-1
#992	GGGGACAAGTTTGTACAAAAAAGCAGGCTCCATGGCTGATCAACAAACCCTAG	Fw	Cloning	LARP6b	attB1-LARP6b
#993	GGGGACCACTTTGTACAAGAAAGCTGGGTCTCMCTCTGCCTGAACCATAACCG	Rv	Cloning	LARP6b	LARP6b-attB2
pGPD-Fw	ATAGAAAAGTTGTTGGATCCGTCGAAACTAAG	Fw	Cloning	pBEVY-A	attB4-pGPD
pGPD-Rv	TGTACAAACTTGTACTGCCATTTCAAAGAATACG	Rv	Cloning	pBEVY-A	pGPD-attB1R
pGAL1-Fw	AGAAAAGTTGAACAACTTCTTTTC	Fw	Cloning	pBEVY-GL	attB4-pGAL1
pGAL1-Rv	GTACAAACTTGTAGTTGATTGTAT	Rv	Cloning	pBEVY-GL	pGAL1-attB1R
#1021	GGTGATGATATTAAGAAACATTTTCG	Fw	Genotyping	PDR5	pdr5 verification primer
#1022	GTCATTCAATAATCGTTGGTCGACTTC	Rv	Genotyping	PDR5	pdr5 verification primer
pADH1-Fw	ATAGAAAAGTTGTTACGGATTAGAAGCCGCC	Fw	Cloning	pGAD424	attB4-pADH1
pADH1-Rv	TGTACAAACTTGTGGTTTTTTCTCCTTGACGTTA	Rv	Cloning	pGAD424	pADH1-attB1R

#1402	GGGGACAAGTTTGTACAAAAAAGCAGGCTCCATGAGCGGTACGGTGAAG	Fw	Cloning	PICOT1	attB1-PICOT1
#1403	GGGGACCACTTTGTACAAGAAAGCTGGGTCTCMCTCGGATAGAGTTGCTTTG	Rv	Cloning	PICOT1	PICOT1-attB2
#1415	CTTTCGCATTCTCCTTCACAG	Fw	Genotyping	PICOT1	SALK_021301 picot1
#1416	CCTTCTCCCTCTTCGAAGATG	Rv	Genotyping	PICOT1	SALK_021301 picot1
#1472	CGCCAAGGCCTTAAAGTGTA	Fw	qPCR	PICOT1	PICOT1(1)
#1473	CATAAGCTCGCCTTTCACG	Rv	qPCR	PICOT1	PICOT1(1)
#1537	GGGGACAAGTTTGTACAAAAAAGCAGGCTCCATGGCTTCTTTACAAGACCGAGC	Fw	Cloning	PICOT1-Grx	attB1-ATG-3xGrx(PICOT1)
#1536	GGGGACCACTTTGTACAAGAAAGCTGGGTCTCAATTCTCCTTCACAGTTTCAAG	Rv	Cloning	PICOT1-Trx	Trx(PICOT1)-attB2 (+stop)
#1549	GGGGACCACTTTGTACAAGAAAGCTGGGTCTCCATTCTCCTTCACAGTTTCAAG	Rv	Cloning	PICOT1-Trx	Trx(PICOT1)-attB2 (-stop)
XhoI-attR4	GCAGTACGGAGCTCCAACTTTGTATAGAAAAGTTG	Fw	Cloning	pKm43GW	XhoI-attR4
SacI-attR3	GATAGTGTCTCGAGCAACTATGTATAATAAAGTTG	Rv	Cloning	pKm43GW	SacI-attR3
#1019	CTTTTAAGTTTTCGTATCCGCTCGTTCGAAAGACTTTAGACAAAACAGCTGAAGCTTCG	Fw	Mutagenesis	pUG6	PDR5 disruption cassette
#1020	GTCCATCTTGGTAAGTTTCTTTTCTTAACCAAATTCAAAATTCTAGCATAGGCCACTAGTGGATCTG	Rv	Mutagenesis	pUG6	PDR5 disruption cassette
#1146	GGGGACAAGTTTGTACAAAAAAGCAGGCTCCATGAACATGAGCAATAAACG	Fw	Cloning	RGLG3	attB1-RGLG3
#1147	GGGGACCACTTTGTACAAGAAAGCTGGGTCTCMAGTGTACAGCCTTATCC	Rv	Cloning	RGLG3	RGLG3-attB2
#1153	TCACACGACAGCCAAGGAAGCCGGAGTTGTTA	Fw	Mutagenesis	RGLG3	RGLG3mRING
#1154	TGTCGTGTGACCGCAGCTAAAAGCCATGTC	Rv	Mutagenesis	RGLG3	RGLG3mRING
#1282	TGGAGTAGGAGATGGACCATG	Fw	Genotyping	RGLG3	SALK_098983 rglg3-1
#1283	TTTTTCCATTGGTATCGTTGC	Rv	Genotyping	RGLG3	SALK_098983 rglg3-1
#1284	GTTTCATTGTGTCCCATGGTC	Fw	Genotyping	RGLG3	GABI_577A04 rglg3-2
#1285	TTCTGAAGGTTCTTGTGCTGC	Rv	Genotyping	RGLG3	GABI_577A04 rglg3-2
#1286	ATGGGAGAACTTTCCACAACC	Fw	Genotyping	RGLG3	GABI_577A04 rglg3-2
#1287	AGTCTCGGTCATACACATCCG	RvP	Genotyping	RGLG3	GABI_577A04 rglg3-2
#1462	GTCCCACATTTGAAGTTGTCC	Fw	qPCR	RGLG3	RGLG3(2)
#1463	GGTATTGCATATTGTTCTGCTCA	Rv	qPCR	RGLG3	RGLG3(2)
#1464	CAGATGACAGAAACTGCAGAGAA	Fw	qPCR	RGLG3	RGLG3(3)
#1465	GTCAAGCAAATCGGGCATAC	Rv	qPCR	RGLG3	RGLG3(3)
#1822	TTACCAAGAGCAATGAGTGGACA	Fw	qPCR	RGLG3	RGLG3(1)
#1823	TGGATTCTGTCTTTTACCAATGGC	Rv	qPCR	RGLG3	RGLG3(1)
#1824	AGAACATTGTACAGTCCAAGCAGA	Fw	qPCR	RGLG3	RGLG3(4)
#1825	CGCATATCTCCTTGTTTCGGC	Rv	qPCR	RGLG3	RGLG3(4)
#1148	GGGGACAAGTTTGTACAAAAAAGCAGGCTCCATGACTATGGGGAATTTCTTAAAG	Fw	Cloning	RGLG4	attB1-RGLG4
#1149	GGGGACCACTTTGTACAAGAAAGCTGGGTCTCMTGTGTAAAGCTTTAGCCG	Rv	Cloning	RGLG4	RGLG4-attB2
#1155	CACATGACTGCTGGAGATGCCGGATCCA	Fw	Mutagenesis	RGLG4	RGLG4mRING
#1156	AGTCATGTGGCCACAGCTGAAAGCCACG	Rv	Mutagenesis	RGLG4	RGLG4mRING
#1274	AAGCCATGACATGGAGAATTG	Fw	Genotyping	RGLG4	SALK_096022 rglg4-1
#1275	ATGTTTAAGTCCCCATCTGGC	Rv	Genotyping	RGLG4	SALK_096022 rglg4-1
#1278	AAGCCATGACATGGAGAATTG	Fw	Genotyping	RGLG4	SALK_096022 rglg4-1
#1279	GTAATGATTGTTGCCGCGTAG	Rv	Genotyping	RGLG4	SALK_096022 rglg4-1
#1466	ATCAAGCAGCCATCGAACTC	Fw	qPCR	RGLG4	RGLG4(3)
#1467	TGGCCTCGGAACTATTGTCT	Rv	qPCR	RGLG4	RGLG4(3)
#1468	ATCCCTTGTTTCGGCTTTG	Fw	qPCR	RGLG4	RGLG4(2)
#1469	TGGAGAATTGTCGCTATGGA	Rv	qPCR	RGLG4	RGLG4(2)
#1820	TCCTTGGCGTCTTGAAGAGT	Fw	qPCR	RGLG4	RGLG4(1)
#1821	TTCGAATTGGAATTCAGATTTTT	Rv	qPCR	RGLG4	RGLG4(1)
#1157	GGGGACAAGTTTGTACAAAAAAGCAGGCTCCATGGCGTTTAATCACAGAAAAATG	Fw	Cloning	RING1	attB1-RING1

#1158	GGGGACCACTTTGTACAAGAAAGCTGGGTCTCMACTGGTGTTACCAGTTAC	Rv	Cloning	RING1	RING1-attB2
#1165	CGGCACAGAAGCCTCTGTCGCCTTAAACGAG	Fw	Mutagenesis	RING1	RING1mRING
#1166	TTCTGTGCCGTCGATTATCCCTTCTCCC	Rv	Mutagenesis	RING1	RING1mRING
#1339	GGGGACAAGTTTGTACAAAAAAGCAGGCTCCATGTACCTCCACATCACGCAAC	Fw	Cloning	RING1	attB1-ATG-RING1dTM
#1175	GGGGACAAGTTTGTACAAAAAAGCAGGCTCCATGGCGATGAGAGGTGTCG	Rv	Cloning	SIS3	attB1-SIS3
#1176	GGGGACCACTTTGTACAAGAAAGCTGGGTCTCMTCTCCGAGATGGAGATAG	Fw	Cloning	SIS3	SIS3-attB2
#1177	CCATAATTTCGCTGTGGAGGCCATAGACCAG	Rv	Cloning	SIS3	SIS3mRING
#1178	GAAATTATGGGCGCAAGGTAAACCTC	Fw	Cloning	SIS3	SIS3mRING
#669	ATTTTGCCGATTTCGGAAC		Genotyping	T-DNA	SALK T-DNA primer
#1041	CCCATTTGGACGTGAATGTAGACAC		Genotyping	T-DNA	Gabi-Kat T-DNA primer
TPL-N-Fw	GGGGACAAGTTTGTACAAAAAAGCAGGCTCCATGTCTTCTCTTAGTAGAGAG	Fw	Cloning	TPL	attB1-TPL-N
TPL-N-Rv	GGGGACCACTTTGTACAAGAAAGCTGGGTCTCMATTTTTACAAAGCTGGTGTTG	Rv	Cloning	TPL	TPL-N-attB2
#1644	GGGGACAAGTTTGTACAAAAAAGCAGGCTCCATGGGTTCACTGAAAAAGG	FwP	Cloning	XDH1	attB1-XDH1
#1645	GGGGACCACTTTGTACAAGAAAGCTGGGTCTCMAACACTAAGATTAGGGTAGAAATC	RvP	Cloning	XDH1	XDH1-attB2
M13-Fw	GTAAAACGACGGCCAGT	Fw	PCR		M13-Fw
M13-Rv	CCAGGAAACAGCTATGACCAT	Rv	PCR		M13-Rv

Supplementary Table 2. Overview of PICOT1 peptides identified by MS after *in vitro* ubiquitination assays.

				Spectral count															
modified sequence	start	end	Modified Lys in PICOT1	Band 13	Band 3	Band 4	Band 5	Band 6	Band 2	Band 1	Band 14	Band 12	Band 11	Band 10	Band 9	Band 8	Band 7	Total WT E3	Total mutant E3
NH2-DIVSK<GGe>AELDNLR-COOH	7	18	11									1	1					2	0
NH2-QMDQVFSHLATDFPR-COOH	38	52		33	3	6	6	6	2	0	37	9	9	8	5	2	1	71	56
NH2-VEAEEHPEISEAYSVAAVPYFVFFK-COOH	58	82		11	1	1	0	0	0	0	14	2	0	2	1	0	1	20	13
NH2-DGK<GGe>TVDTLEGADPSSLANK-COOH	83	101	85									1		1				2	0
NH2-DGKTVDTLEGADPSSLANK-COOH	83	101									1							1	0
NH2-TVDTLEGADPSSLANK-COOH	86	101		11	0	1	1	2	1	0	11	3	3	3	1	0	0	21	16
NH2-VGK<GGe>VAGSSTSAEPAAPASLGLAAGPTILETVK-COOH	102	133	104									1						1	0
NH2-VAGSSTSAEPAAPASLGLAAGPTILETVK-COOH	105	133		5		1					5	2	2					9	6
NH2-VAGSSTSAEPAAPASLGLAAGPTILETVKENAK-COOH	105	137									2							2	0
NH2-ENAK<GGe>ASLQDR-COOH	134	143	137									2		1	1			4	0
NH2-AQPVSTADALK-COOH	144	154		4	1	1	1		1		4	1			1	1		7	8
NH2-AQPVSTADALK<GGe>SR-COOH	144	156	154											1	1	1		3	0
NH2-AQPVSTADALKSR-COOH	144	156									1							1	0
NH2-LTNSHPVMLFMK-COOH	160	171		6	0	0	1	0	0	0	4	3	0	0	0	0	0	7	7
NH2-EVNVDFGSFDILSDNEVR-COOH	191	208		0	0	2	2	1	0	0	11	1	1	1	1	0	1	16	5
NH2-FSNWPTFPQLYC<Prp>NGELLGGADIAIAM<Mox>HESGELK-COOH	214	246		1														0	1
NH2-DAFK<GGe>DLGITTVGSK-COOH	247	260	250								1	2						3	0
NH2-DAFKDLGITTVGSK-COOH	247	260		2							1							1	2
NH2-DLGITTVGSK-COOH	251	260		3	0	0	1	1	1	1	6	1	1	1	0	0	1	10	7
NH2-DLGITTVGSK<GGe>ESQDEAGK-COOH	251	268	260												1			1	0
NH2-DLGITTVGSKESQDEAGK-COOH	251	268									1							1	0
NH2-ESQDEAGK<GGe>GGGVSSGNTGLSETLR-COOH	261	284	268								1	1	1	1	1		1	6	0
NH2-ESQDEAGKGGGVSSGNTGLSETLR-COOH	261	284		1							1							1	1
NH2-GGGVSSGNTGLSETLR-COOH	269	284		6	1	2	1	3	1	1	8	3	1	1	1	1	1	16	15
NH2-ARLEGLVNSK-COOH	285	294		1														0	1
NH2-ARLEGLVNSKPVM<Mox>LFM<Mox>K-COOH	285	301		4	0	0	0	0	0	0	3	0	0	0	0	0	0	3	4
NH2-LEGLVNSK-COOH	287	294		2	1	1	1	1			2	1	1	1	1	1	1	8	6
NH2-LEGLVNSKPVMLFMK-COOH	287	301		6	0	0	0	0	0	0	6	0	2	1	0	0	0	9	6
NH2-VVEILNQEK-COOH	315	323		2	1	1	1				2	1	1			1		5	5
NH2-IEFGSFDILLDDEVR-COOH	324	338		23	0	2	3	2	1	1	18	17	13	5	4	3	2	62	32

NH2-VYSNWSSYPQLYVK-COOH	343	356		5	1	1	1				7	2	1	1	1	1	1	14	8
NH2-GELMGGSDIVLEMQK-COOH	357	371		73	1	4	4	4	3	2	76	29	12	6	4	2	4	133	91
NH2-VLTEK<GGe>GITGEQSLEDR-COOH	378	393	382									1	1	2	1	1		6	0
NH2-VLTEKGITGEQSLEDR-COOH	378	393		1														0	1
NH2-GITGEQSLEDR-COOH	383	393		7	1	1	1		1		6	2	1	1	1	1		12	11
NH2-GITGEQSLEDRLK-COOH	383	395									2							2	0
NH2-ALINSSEVMLFMK-COOH	396	408		26	3	2	5	3	0	0	17	7	5	6	3	2	1	41	39
NH2-GENVSFGSFDILTDEEVR-COOH	428	445		34	1	3	4	1	2	1	41	19	5	4	3	2	2	76	46
NH2-NFSNWPTFPQLYYK-COOH	450	463		4	0	1	2	1	0	0	6	2	2	1	1	1	0	13	8
NH2-GELIGGCDIIMELSESGDLK-COOH	464	483		7	0	0	0	0	0	0	8	1	0	0	0	0	0	9	7
Tag/att-site:																			
NH2-ATLSEGDPAFLYK-COOH	484	496									6							6	0
NH2-ATLSEGDPAFLYK-COOH	484	496										2						2	0
NH2-ATLSEGDPAFLYK-COOH	484	496		5														0	5
NH2-ATLSEGDPAFLYK-COOH	484	496			1	1	1	1	1				1	1	1	1	1	5	5
NH2-ATLSEGDPAFLYK<GGe>VVINSK-COOH	484	502	496									1						1	0
NH2-ATLSEGDPAFLYKVVINSK-COOH	484	502		1							1							1	1
NH2-VVINSK<GGe>LEGK-COOH	497	506	502								1	2						3	0
NH2-LEGK<GGe>PIPNPLLGLDSTR-COOH	503	519	506									1	1	1				3	0
NH2-LEGKPIPNPLLGLDSTR-COOH	503	519		6							4	2	2					8	6
NH2-PIPNPLLGLDSTR-COOH	507	519									14							14	0
NH2-PIPNPLLGLDSTR-COOH	507	519		8														0	8
NH2-PIPNPLLGLDSTR-COOH	507	519			1	1	2	1	1			3	1	2	2	2	1	11	6

Bands indicate gel-fragments isolated after separation of the proteins used in *in vitro* ubiquitination assays. Bands 14 -12 -11 - 10 - 9 - 8 - 7: originated from in vitro assay using WT E3 ligase. Band 14 corresponds to the molecular weight of unmodified PICOT1, 12-7: fragments with increasing molecular weight. Bands 13 -6 - 5 - 4 - 3 - 2 - 1: originated from in vitro assay using mutant E3 ligase. Band 13 corresponds to the molecular weight of unmodified PICOT1, 6-1: fragments with increasing molecular weight.

Supplementary Table S3. Differentially expressed genes obtained by RNA-Sequencing analysis of the *picot1* line.

Locus	logFC	logCPM	PValue	FDR	Short description
AT2G03130	7.8431	-0.9583	1.64E-23	4.36E-21	Ribosomal protein L12/ ATP-dependent Clp protease adaptor protein ClpS family protein
AT2G24255	7.5244	-1.2068	1.41E-19	2.61E-17	Protein of unknown function (DUF295)
AT1G30170	6.7259	0.9718	2.32E-73	5.05E-70	Protein of unknown function (DUF295)
AT4G17710	5.9496	-0.9566	2.33E-23	5.94E-21	homeodomain GLABROUS 4 (HDG4)
AT5G53230	5.1691	1.1845	5.76E-80	1.41E-76	Protein of unknown function (DUF295)
AT5G14490	4.9533	-0.6570	2.03E-24	5.85E-22	NAC domain containing protein 85 (NAC085)
AT5G55270	4.7198	-0.0076	2.91E-33	1.78E-30	Protein of unknown function (DUF295)
AT5G59390	4.6879	-0.2682	3.65E-30	1.66E-27	XH/XS domain-containing protein
AT5G54560	4.6639	-1.3435	1.14E-15	1.52E-13	Protein of unknown function (DUF295)
AT5G53240	4.6525	-0.9294	2.67E-19	4.80E-17	Protein of unknown function (DUF295)
AT3G01345	4.4126	0.2226	1.98E-40	1.62E-37	Expressed protein
AT4G05380	4.3607	0.0290	1.26E-33	8.00E-31	P-loop containing nucleoside triphosphate hydrolases superfamily protein
AT5G60250	4.3006	2.8474	1.98E-145	1.29E-141	zinc finger (C3HC4-type RING finger) family protein
AT4G05370	4.2930	-0.6389	1.14E-21	2.66E-19	BCS1 AAA-type ATPase
AT2G20800	4.1930	2.0061	2.66E-91	8.69E-88	NAD(P)H dehydrogenase B4 (NDB4)
AT4G22470	3.9753	2.9779	4.65E-13	4.16E-11	protease inhibitor/seed storage/lipid transfer protein (LTP) family protein
AT3G01600	3.7631	3.0316	7.30E-144	3.58E-140	NAC domain containing protein 44 (NAC044)
AT2G18720	3.6950	-0.4126	1.82E-23	4.76E-21	Translation elongation factor EF1A/initiation factor IF2gamma family protein
AT2G39030	3.6676	0.4972	4.77E-08	1.93E-06	Acyl-CoA N-acyltransferases (NAT) superfamily protein
AT4G12490	3.6453	3.2611	3.06E-20	6.18E-18	Bifunctional inhibitor/lipid-transfer protein/seed storage 2S albumin superfamily protein
AT3G22860	3.0983	-0.7617	4.34E-14	4.45E-12	eukaryotic translation initiation factor 3 subunit C2 (TIF3C2)
AT5G47000	3.0965	-0.0307	1.80E-21	4.11E-19	Peroxidase superfamily protein
AT4G32510	3.0591	-1.4097	3.57E-10	2.11E-08	HCO3- transporter family
AT5G20240	3.0528	-0.8197	1.06E-14	1.19E-12	PISTILLATA (PI)
AT4G12480	2.9736	6.9036	1.06E-57	1.57E-54	pEARLI 1
AT5G58610	2.9158	1.6751	9.47E-58	1.55E-54	PHD finger transcription factor, putative
AT5G13210	2.8400	3.3197	2.04E-87	5.73E-84	Uncharacterised conserved protein UCP015417, vWA
AT3G54530	2.8270	-0.3893	4.72E-16	6.61E-14	unknown protein
AT4G12470	2.8266	4.8391	1.06E-28	4.17E-26	azelaic acid induced 1 (AZI1)
AT5G24280	2.8123	4.1506	1.02E-127	4.00E-124	GAMMA-IRRADIATION AND MITOMYCIN C INDUCED 1 (GMI1)
AT3G18610	2.7156	1.9487	1.12E-57	1.57E-54	nucleolin like 2 (NUC-L2)
AT5G64060	2.6805	1.8069	7.69E-54	9.42E-51	NAC domain containing protein 103 (NAC103)
AT1G36180	2.6310	5.8323	6.22E-167	6.10E-163	acetyl-CoA carboxylase 2 (ACC2)
AT1G03710	2.5470	-0.9329	1.63E-10	1.02E-08	Cystatin/monellin superfamily protein
AT4G21680	2.4794	1.2493	6.10E-20	1.17E-17	NITRATE TRANSPORTER 1.8 (NRT1.8)
AT1G17960	2.4753	2.4977	1.75E-66	3.43E-63	Threonyl-tRNA synthetase

AT1G11070	2.4537	2.2998	5.34E-51	5.81E-48	Similar to Hydroxyproline-rich glycoprotein family protein
AT1G30160	2.4404	0.8004	6.13E-29	2.50E-26	Protein of unknown function (DUF295)
AT1G49570	2.4232	3.1231	6.18E-57	8.07E-54	Peroxidase superfamily protein
AT5G24640	2.3760	0.4693	3.29E-21	7.19E-19	unknown protein
AT5G09570	2.3161	1.7229	1.58E-39	1.24E-36	Cox19-like CHCH family protein
AT1G05490	2.2963	0.7971	1.71E-25	5.25E-23	chromatin remodeling 31 (chr31)
AT2G18190	2.2698	-0.5504	1.49E-11	1.10E-09	P-loop containing nucleoside triphosphate hydrolases superfamily protein
AT5G44575	2.2674	0.1789	2.43E-11	1.72E-09	unknown protein
AT5G07200	2.1916	0.0057	1.44E-15	1.88E-13	gibberellin 20-oxidase 3 (GA20OX3)
AT5G12030	2.1478	-0.4739	4.01E-11	2.72E-09	heat shock protein 17.6A (HSP17.6A)
AT3G58270	2.1348	2.4710	4.66E-51	5.37E-48	Arabidopsis phospholipase-like protein (PEARLI 4) with TRAF-like domain
AT2G47520	2.1346	-0.1203	8.29E-15	9.52E-13	HYPOXIA RESPONSIVE ERF (ETHYLENE RESPONSE FACTOR) 2 (HRE2)
AT5G58840	2.1010	-0.7230	2.76E-09	1.42E-07	Subtilase family protein
AT2G18193	2.0929	4.6821	3.26E-38	2.46E-35	P-loop containing nucleoside triphosphate hydrolases superfamily protein
AT1G20350	2.0614	-0.6479	3.49E-10	2.08E-08	translocase inner membrane subunit 17-1 (TIM17-1)
AT1G76470	2.0370	-0.6079	1.02E-09	5.65E-08	NAD(P)-binding Rossmann-fold superfamily protein
AT1G70260	2.0312	2.0482	5.53E-33	3.29E-30	nodulin MtN21 /EamA-like transporter family protein
AT1G30660	2.0098	-0.9147	8.56E-08	3.25E-06	
AT3G27620	1.9986	-0.0357	1.32E-12	1.13E-10	alternative oxidase 1C (AOX1C)
AT2G38340	1.9289	0.0990	8.10E-14	8.10E-12	Integrase-type DNA-binding superfamily protein
AT4G12735	1.9024	-0.2646	1.12E-09	6.14E-08	unknown protein
AT3G09950	1.8924	-0.4923	1.03E-09	5.70E-08	unknown protein
AT5G51440	1.8907	2.9705	4.93E-46	5.09E-43	HSP20-like chaperones superfamily protein
AT2G21450	1.8832	-0.6898	1.61E-08	7.23E-07	chromatin remodeling 34 (CHR34)
AT1G18100	1.8678	2.3204	1.17E-24	3.48E-22	E12A11
AT2G21640	1.8663	2.4958	2.10E-30	9.79E-28	unknown protein
AT4G15350	1.8526	-0.7776	8.00E-08	3.06E-06	cytochrome P450, family 705, subfamily A, polypeptide 2 (CYP705A2)
AT2G41730	1.8312	2.7400	1.39E-36	9.41E-34	unknown protein
AT1G65570	1.8228	0.6566	1.68E-17	2.72E-15	Pectin lyase-like superfamily protein
AT1G53540	1.7874	-0.5366	6.84E-08	2.66E-06	HSP20-like chaperones superfamily protein
AT4G16590	1.7828	-0.6030	4.41E-08	1.80E-06	cellulose synthase-like A01 (CSLA01)
AT1G70440	1.7752	0.8400	4.33E-18	7.20E-16	similar to RCD one 3 (SRO3)
AT1G20400	1.7694	0.7318	6.06E-15	7.11E-13	FUNCTIONS IN: molecular_function unknown
AT2G38250	1.7461	1.0757	2.73E-20	5.57E-18	Homeodomain-like superfamily protein
AT3G46230	1.7274	0.7771	2.46E-13	2.31E-11	heat shock protein 17.4 (HSP17.4)
AT5G19470	1.7022	2.7655	5.44E-09	2.65E-07	nudix hydrolase homolog 24 (NUDT24)
AT3G28580	1.6985	1.3791	1.19E-11	8.96E-10	P-loop containing nucleoside triphosphate hydrolases superfamily protein
AT1G49920	1.6932	-0.8888	1.97E-06	5.28E-05	MuDR family transposase
AT1G61255	1.6724	-0.8046	6.06E-07	1.86E-05	Similar to glycine-rich protein

AT1G67760	1.6513	0.6887	4.77E-15	5.84E-13	TCP-1/cpn60 chaperonin family protein
AT5G11410	1.6440	0.7932	1.66E-14	1.81E-12	Protein kinase superfamily protein
AT2G04050	1.6328	3.8197	1.93E-14	2.06E-12	MATE efflux family protein
AT1G65500	1.6113	1.4600	3.21E-13	2.97E-11	unknown protein
AT5G67060	1.6049	-0.2688	1.73E-08	7.72E-07	HECATE 1 (HEC1)
AT5G25230	1.5970	0.9286	4.52E-16	6.38E-14	Ribosomal protein S5/Elongation factor G/III/V family protein
AT1G52120	1.5967	3.2178	1.04E-28	4.17E-26	Mannose-binding lectin superfamily protein
AT4G36570	1.5946	0.9778	2.13E-12	1.75E-10	RAD-like 3 (RL3)
AT2G42430	1.5888	1.0904	3.22E-17	4.96E-15	lateral organ boundaries-domain 16 (LBD16)
AT1G18835	1.5868	-0.8893	5.81E-06	1.35E-04	MINI ZINC FINGER 3 (MIF3)
AT4G30250	1.5855	0.7416	2.27E-05	4.44E-04	P-loop containing nucleoside triphosphate hydrolases superfamily protein
AT1G53130	1.5774	0.6593	3.27E-13	3.01E-11	GRIM REAPER (GRI)
AT3G45730	1.5712	2.2311	2.70E-24	7.67E-22	unknown protein
AT3G47030	1.5694	-0.0415	4.69E-09	2.31E-07	F-box and associated interaction domains-containing protein
AT1G54890	1.5664	0.8721	3.84E-14	3.98E-12	Late embryogenesis abundant (LEA) protein-related
AT5G19700	1.5645	1.4530	1.95E-18	3.30E-16	MATE efflux family protein
AT4G20690	1.5636	-0.3952	7.10E-08	2.75E-06	unknown protein
AT4G15210	1.5388	2.4580	1.74E-15	2.23E-13	beta-amylase 5 (BAM5)
AT2G44570	1.5291	0.8942	7.31E-15	8.49E-13	glycosyl hydrolase 9B12 (GH9B12)
AT3G21720	1.4924	2.1238	4.06E-13	3.67E-11	isocitrate lyase (ICL)
AT5G67430	1.4863	2.8286	5.21E-20	1.02E-17	Acyl-CoA N-acyltransferases (NAT) superfamily protein
AT1G66920	1.4782	0.6856	1.04E-10	6.75E-09	Protein kinase superfamily protein
AT5G37490	1.4712	-0.8576	5.53E-05	9.57E-04	ARM repeat superfamily protein
AT3G59930	1.4592	-0.7282	1.06E-05	2.28E-04	FUNCTIONS IN: molecular_function unknown
AT1G19380	1.4538	1.0789	3.89E-08	1.60E-06	Protein of unknown function (DUF1195)
AT2G23170	1.4324	3.1675	1.62E-31	8.61E-29	GH3.3
AT5G44574	1.4300	-0.6117	7.97E-06	1.78E-04	unknown protein
AT5G46050	1.4238	0.0951	1.71E-06	4.66E-05	peptide transporter 3 (PTR3)
AT1G52060	1.4216	3.9461	9.97E-38	7.24E-35	Mannose-binding lectin superfamily protein
AT4G33970	1.4064	-0.6773	1.76E-05	3.58E-04	Leucine-rich repeat (LRR) family protein
AT1G64160	1.4019	0.1512	3.73E-08	1.54E-06	Disease resistance-responsive (dirigent-like protein) family protein
AT4G02700	1.3892	1.3765	5.50E-15	6.57E-13	
AT4G15160	1.3807	6.5393	2.11E-15	2.69E-13	Bifunctional inhibitor/lipid-transfer protein/seed storage 2S albumin superfamily protein
AT3G11260	1.3767	-0.7107	2.10E-05	4.15E-04	WUSCHEL related homeobox 5 (WOX5)
AT3G48520	1.3548	1.7855	5.27E-16	7.28E-14	cytochrome P450, family 94, subfamily B, polypeptide 3 (CYP94B3)
AT4G22960	1.3530	0.4665	1.31E-08	5.97E-07	Protein of unknown function (DUF544)
AT4G11720	1.3369	-0.7358	4.02E-05	7.33E-04	HAPLESS 2 (HAP2)
AT3G14060	1.3310	2.7325	6.70E-16	9.12E-14	unknown protein
AT3G20710	1.3242	-0.3587	3.46E-05	6.43E-04	F-box family protein

AT1G52070	1.3060	4.9117	2.99E-26	9.93E-24	Mannose-binding lectin superfamily protein
AT1G61800	1.3046	1.7120	4.32E-16	6.13E-14	glucose-6-phosphate/phosphate translocator 2 (GPT2)
AT2G32830	1.3018	-0.8245	6.91E-05	1.16E-03	Encodes Pht1
AT3G08860	1.2867	4.8593	1.75E-42	1.49E-39	PYRIMIDINE 4 (PYD4)
AT2G04070	1.2790	0.2872	1.21E-07	4.42E-06	MATE efflux family protein
AT3G22142	1.2738	6.1850	1.37E-21	3.16E-19	Bifunctional inhibitor/lipid-transfer protein/seed storage 2S albumin superfamily protein
AT3G24780	1.2735	1.2546	8.11E-13	7.10E-11	Uncharacterised conserved protein UCP015417, vWA
AT5G55110	1.2731	0.4314	7.67E-07	2.29E-05	Stigma-specific Stig1 family protein
AT1G76930	1.2718	8.2336	2.02E-24	5.85E-22	extensin 4 (EXT4)
AT2G34340	1.2705	0.8270	1.31E-10	8.38E-09	Protein of unknown function, DUF584
AT1G52040	1.2676	5.2807	4.34E-21	9.35E-19	myrosinase-binding protein 1 (MBP1)
AT3G13130	1.2666	-0.7931	1.42E-04	2.11E-03	unknown protein
AT3G04320	1.2614	1.4747	4.93E-14	5.01E-12	Kunitz family trypsin and protease inhibitor protein
AT3G52780	1.2561	-0.6598	4.49E-05	8.04E-04	PAP20
AT4G38340	1.2488	0.0141	1.41E-06	3.96E-05	Plant regulator RWP-RK family protein
AT4G30140	1.2473	5.6542	1.19E-25	3.75E-23	CUTICLE DESTRUCTING FACTOR 1 (CDEF1)
AT2G38823	1.2451	1.0749	2.01E-09	1.06E-07	unknown protein
AT3G45060	1.2406	-0.4820	1.77E-05	3.60E-04	high affinity nitrate transporter 2.6 (NRT2.6)
AT3G13080	1.2397	6.2305	9.98E-44	9.31E-41	multidrug resistance-associated protein 3 (MRP3)
AT4G06746	1.2280	-0.0902	3.52E-06	8.77E-05	related to AP2 9 (RAP2.9)
AT3G58190	1.2241	-0.9177	8.01E-04	8.61E-03	lateral organ boundaries-domain 29 (LBD29)
AT3G21520	1.2209	0.5942	6.23E-09	3.00E-07	DUF679 domain membrane protein 1 (DMP1)
AT1G68480	1.2169	-0.2766	4.98E-06	1.19E-04	JAGGED (JAG)
AT3G14700	1.2141	-0.5033	6.55E-05	1.11E-03	SART-1 family
AT5G61740	1.2083	0.3148	1.01E-07	3.72E-06	ABC2 homolog 14 (ATH14)
AT4G01985	1.2070	1.7042	1.27E-05	2.68E-04	unknown protein
AT5G58390	1.1941	3.0264	7.78E-09	3.66E-07	Peroxidase superfamily protein
AT3G48700	1.1923	1.5956	1.43E-12	1.22E-10	carboxyesterase 13 (CXE13)
AT1G34460	1.1906	-0.9363	6.62E-04	7.46E-03	B1 type cyclin
AT1G27020	1.1844	2.0929	1.49E-04	2.20E-03	unknown protein
AT5G48850	1.1749	3.6637	5.39E-19	9.44E-17	SULPHUR DEFICIENCY-INDUCED 1 (ATSDI1)
AT2G27550	1.1703	2.9705	3.96E-18	6.63E-16	centroradialis (ATC)
AT5G12330	1.1676	3.2921	2.95E-11	2.05E-09	LATERAL ROOT PRIMORDIUM 1 (LRP1)
AT5G38700	1.1664	-0.1246	2.05E-05	4.06E-04	unknown protein
AT3G19200	1.1633	0.1635	7.24E-07	2.18E-05	unknown protein
AT1G24260	1.1613	0.0822	1.76E-06	4.78E-05	SEPALLATA3 (SEP3)
AT5G44568	1.1566	-0.1104	1.25E-05	2.64E-04	unknown protein
AT2G43590	1.1538	6.2958	1.68E-13	1.61E-11	Chitinase family protein
AT4G13680	1.1516	-0.0465	9.14E-06	2.00E-04	Protein of unknown function (DUF295)

AT5G63090	1.1422	0.7759	2.46E-07	8.38E-06	LATERAL ORGAN BOUNDARIES (LOB)
AT5G60520	1.1360	2.5943	9.96E-16	1.33E-13	Late embryogenesis abundant (LEA) protein-related
AT1G13330	1.1330	1.0768	1.18E-09	6.45E-08	Arabidopsis Hop2 homolog (AHP2)
AT1G03660	1.1276	-0.4460	6.79E-05	1.14E-03	Ankyrin-repeat containing protein
AT3G62270	1.1246	5.8965	2.87E-11	2.01E-09	HCO3- transporter family
AT1G52770	1.1192	0.4271	4.09E-07	1.31E-05	Phototropic-responsive NPH3 family protein
AT1G24095	1.1189	2.1256	6.03E-15	7.11E-13	Putative thiol-disulphide oxidoreductase DCC
AT1G43910	1.1135	2.4765	3.53E-15	4.38E-13	P-loop containing nucleoside triphosphate hydrolases superfamily protein
AT1G19630	1.0978	0.4228	5.04E-07	1.58E-05	cytochrome P450, family 722, subfamily A, polypeptide 1 (CYP722A1)
AT4G16240	1.0960	-0.2926	1.02E-04	1.62E-03	unknown protein
AT3G49580	1.0863	4.2018	1.16E-13	1.14E-11	RESPONSE TO LOW SULFUR 1 (LSU1)
AT4G16563	1.0837	3.0586	3.32E-14	3.46E-12	Eukaryotic aspartyl protease family protein
AT1G69310	1.0802	3.6718	2.17E-22	5.25E-20	WRKY DNA-binding protein 57 (WRKY57)
AT5G20820	1.0797	0.2187	2.89E-06	7.37E-05	SAUR-like auxin-responsive protein family
AT3G27630	1.0785	-0.8287	1.23E-03	1.20E-02	unknown protein
AT3G15720	1.0762	1.5566	2.73E-11	1.92E-09	Pectin lyase-like superfamily protein
AT4G14780	1.0761	0.2935	7.71E-06	1.73E-04	Protein kinase superfamily protein
AT4G16600	1.0748	0.2866	3.06E-06	7.75E-05	Nucleotide-diphospho-sugar transferases superfamily protein
AT4G23130	1.0697	-0.4296	5.99E-04	6.88E-03	cysteine-rich RLK (RECEPTOR-like protein kinase) 5 (CRK5)
AT2G18600	1.0673	1.6474	2.32E-11	1.64E-09	Ubiquitin-conjugating enzyme family protein
AT5G13330	1.0615	2.6651	4.88E-16	6.79E-14	related to AP2 6l (Rap2.6L)
AT3G62460	1.0506	3.4776	2.44E-12	1.99E-10	Putative endonuclease or glycosyl hydrolase
AT3G13210	1.0443	-0.3164	1.62E-04	2.37E-03	crooked neck protein, putative / cell cycle protein, putative
AT3G61630	1.0412	3.6366	2.21E-20	4.61E-18	cytokinin response factor 6 (CRF6)
AT5G39580	1.0361	2.8709	1.74E-13	1.65E-11	Peroxidase superfamily protein
AT5G18180	1.0347	-0.6141	5.93E-04	6.82E-03	H/ACA ribonucleoprotein complex, subunit Gar1/Naf1 protein
AT3G28500	1.0311	-0.4333	2.18E-04	3.03E-03	60S acidic ribosomal protein family
AT3G05660	1.0295	0.9974	5.07E-08	2.04E-06	receptor like protein 33 (RLP33)
AT5G60040	1.0288	4.3056	4.74E-27	1.66E-24	nuclear RNA polymerase C1 (NRPC1)
AT3G44300	1.0195	6.4975	2.95E-26	9.93E-24	nitrilase 2 (NIT2)
AT5G19880	1.0158	0.1457	7.14E-05	1.19E-03	Peroxidase superfamily protein
AT4G22710	1.0111	0.7508	7.39E-07	2.22E-05	cytochrome P450, family 706, subfamily A, polypeptide 2 (CYP706A2)
AT1G20620	1.0100	10.4325	4.03E-24	1.11E-21	catalase 3 (CAT3)
AT2G36270	1.0057	0.3976	4.88E-06	1.17E-04	ABA INSENSITIVE 5 (ABI5)
AT5G52940	1.0028	0.8410	3.51E-07	1.15E-05	Protein of unknown function (DUF295)
AT4G20235	-1.0020	-0.8017	1.91E-03	1.69E-02	cytochrome P450, family 71, subfamily A, polypeptide 28 (CYP71A28)
AT5G53380	-1.0025	-0.8501	2.19E-03	1.89E-02	O-acyltransferase (WSD1-like) family protein
AT4G04700	-1.0048	1.3951	6.54E-09	3.13E-07	calcium-dependent protein kinase 27 (CPK27)
AT1G24130	-1.0048	-0.0500	2.61E-04	3.54E-03	Transducin/WD40 repeat-like superfamily protein

AT1G12570	-1.0092	2.2742	7.33E-11	4.85E-09	Glucose-methanol-choline (GMC) oxidoreductase family protein
AT1G14220	-1.0100	0.3891	4.83E-06	1.16E-04	Ribonuclease T2 family protein
AT5G38710	-1.0203	1.8201	1.42E-11	1.06E-09	Methylenetetrahydrofolate reductase family protein
AT3G29630	-1.0206	1.5082	1.25E-09	6.78E-08	UDP-Glycosyltransferase superfamily protein
AT4G12520	-1.0207	2.5350	2.07E-12	1.71E-10	Bifunctional inhibitor/lipid-transfer protein/seed storage 2S albumin superfamily protein
AT3G12460	-1.0216	-0.6949	1.64E-03	1.51E-02	Polynucleotidyl transferase, ribonuclease H-like superfamily protein
AT3G13610	-1.0229	5.8197	2.13E-23	5.49E-21	2-oxoglutarate (2OG) and Fe(II)-dependent oxygenase superfamily protein
AT5G67090	-1.0235	0.3223	5.45E-06	1.28E-04	Subtilisin-like serine endopeptidase family protein
AT3G45430	-1.0283	1.3272	9.13E-10	5.13E-08	Concanavalin A-like lectin protein kinase family protein
AT5G59360	-1.0294	0.7129	3.15E-07	1.03E-05	unknown protein
AT5G65030	-1.0298	-0.0636	1.20E-04	1.84E-03	unknown protein
AT5G45960	-1.0312	1.1336	1.12E-08	5.14E-07	GDSL-like Lipase/Acylhydrolase superfamily protein
AT3G05155	-1.0320	0.0818	1.38E-05	2.89E-04	Major facilitator superfamily protein
AT5G10946	-1.0328	0.7462	4.04E-07	1.30E-05	unknown protein
AT5G53250	-1.0341	3.3419	2.62E-13	2.44E-11	arabinogalactan protein 22 (AGP22)
AT5G18050	-1.0344	0.9515	1.41E-07	5.08E-06	SAUR-like auxin-responsive protein family
AT3G09960	-1.0387	0.3340	3.35E-06	8.38E-05	Calcineurin-like metallo-phosphoesterase superfamily protein
AT5G62340	-1.0392	2.5366	7.04E-12	5.47E-10	Plant invertase/pectin methylesterase inhibitor superfamily protein
AT5G39110	-1.0473	-0.8864	1.68E-03	1.54E-02	RmlC-like cupins superfamily protein
AT2G43440	-1.0510	-0.1713	3.59E-05	6.63E-04	F-box and associated interaction domains-containing protein
AT5G40990	-1.0515	-0.5197	3.79E-04	4.76E-03	GDSL lipase 1 (GLIP1)
AT2G18800	-1.0536	1.7143	8.47E-12	6.49E-10	xyloglucan endotransglucosylase/hydrolase 21 (XTH21)
AT4G04760	-1.0573	-0.7666	1.62E-03	1.50E-02	Major facilitator superfamily protein
AT3G09400	-1.0574	0.1178	2.78E-05	5.29E-04	pol-like 3 (PLL3)
AT5G46900	-1.0582	4.0158	7.05E-25	2.13E-22	Bifunctional inhibitor/lipid-transfer protein/seed storage 2S albumin superfamily protein
AT5G42510	-1.0587	1.2436	7.50E-08	2.89E-06	Disease resistance-responsive (dirigent-like protein) family protein
AT2G41480	-1.0594	2.4384	9.87E-15	1.11E-12	Peroxidase superfamily protein
AT1G18970	-1.0594	3.4860	2.47E-22	5.90E-20	germin-like protein 4 (GLP4)
AT2G24310	-1.0649	-0.5752	8.13E-04	8.72E-03	unknown protein
AT3G55900	-1.0673	-0.6467	5.24E-04	6.19E-03	F-box family protein
AT1G16530	-1.0693	1.6295	3.67E-11	2.52E-09	ASYMMETRIC LEAVES 2-like 9 (ASL9)
AT3G47220	-1.0705	0.9287	1.45E-08	6.59E-07	phosphatidylinositol-speciwc phospholipase C9 (PLC9)
AT5G63140	-1.0714	2.3215	5.80E-14	5.86E-12	purple acid phosphatase 29 (PAP29)
AT2G38995	-1.0746	2.4936	1.88E-14	2.03E-12	O-acyltransferase (WSD1-like) family protein
AT2G04800	-1.0777	1.4511	4.48E-10	2.64E-08	unknown protein
ATCG00810	-1.0798	-0.6254	3.88E-04	4.85E-03	ribosomal protein L22 (RPL22)
AT3G52770	-1.0801	-0.1099	5.67E-05	9.76E-04	LITTLE ZIPPER 3 (ZPR3)
AT2G40960	-1.0811	3.1766	2.81E-21	6.32E-19	Single-stranded nucleic acid binding R3H protein
AT1G63520	-1.0821	0.2984	8.90E-06	1.96E-04	Protein of unknown function (DUF3527)

AT1G17147	-1.0842	1.5033	1.37E-11	1.02E-09	VQ motif-containing protein
AT5G49780	-1.0851	0.9635	7.15E-09	3.39E-07	Leucine-rich repeat protein kinase family protein
AT3G29430	-1.0854	-0.4161	1.31E-04	1.98E-03	Terpenoid synthases superfamily protein
AT2G18470	-1.0917	1.3664	2.85E-10	1.74E-08	roline-rich extensin-like receptor kinase 4 (PERK4)
AT5G43230	-1.0967	0.2060	3.16E-06	7.94E-05	unknown protein
AT5G42600	-1.1031	4.0057	1.20E-25	3.75E-23	marneral synthase (MRN1)
AT2G18690	-1.1115	2.5207	3.30E-11	2.28E-09	unknown protein
AT1G52890	-1.1122	-0.1563	5.44E-05	9.45E-04	NAC domain containing protein 19 (NAC019)
AT1G28480	-1.1153	-0.0084	1.06E-05	2.28E-04	GRX480
AT5G57010	-1.1195	1.2466	1.58E-10	9.93E-09	calmodulin-binding family protein
AT5G65690	-1.1237	1.1879	7.40E-10	4.20E-08	phosphoenolpyruvate carboxykinase 2 (PCK2)
AT1G66090	-1.1266	0.0648	2.24E-05	4.38E-04	Disease resistance protein (TIR-NBS class)
AT2G30432	-1.1268	0.0545	5.20E-06	1.23E-04	TRICHOMELESS1 (TCL1)
AT3G48940	-1.1283	-1.0066	2.29E-03	1.95E-02	Remorin family protein
AT3G19615	-1.1319	-0.7102	1.54E-04	2.27E-03	unknown protein
AT1G10340	-1.1382	0.1564	4.20E-06	1.03E-04	Ankyrin repeat family protein
AT5G56970	-1.1425	-1.0816	3.63E-03	2.76E-02	cytokinin oxidase 3 (CKX3)
AT1G66270	-1.1439	6.4364	1.49E-37	1.04E-34	BGLU21
AT1G26380	-1.1446	2.2712	2.99E-14	3.16E-12	FAD-binding Berberine family protein
AT3G22910	-1.1472	-0.0154	5.63E-06	1.31E-04	ATPase E1-E2 type family protein / haloacid dehalogenase-like hydrolase family protein
AT4G36880	-1.1490	2.0825	7.32E-15	8.49E-13	cysteine proteinase1 (CP1)
AT1G13550	-1.1502	-1.1018	1.95E-03	1.72E-02	Protein of unknown function (DUF1262)
AT4G23493	-1.1506	0.4891	1.65E-07	5.79E-06	unknown protein
AT5G49770	-1.1506	0.1634	1.87E-06	5.03E-05	Leucine-rich repeat protein kinase family protein
AT2G01520	-1.1556	7.6398	3.15E-21	7.01E-19	owering.
AT5G51470	-1.1582	-0.5327	1.68E-04	2.44E-03	Auxin-responsive GH3 family protein
AT2G38600	-1.1589	-0.0932	4.35E-06	1.06E-04	HAD superfamily, subfamily IIIB acid phosphatase
AT3G01260	-1.1596	3.5702	2.53E-28	9.74E-26	Galactose mutarotase-like superfamily protein
ATCG00800	-1.1698	0.0952	1.64E-06	4.50E-05	RESISTANCE TO PSEUDOMONAS SYRINGAE 3 (RPS3)
AT1G62280	-1.1709	1.8365	6.13E-12	4.81E-10	SLAC1 homologue 1 (SLAH1)
AT5G38970	-1.1790	0.1946	1.60E-06	4.42E-05	brassinosteroid-6-oxidase 1 (BR6OX1)
AT1G15050	-1.1829	-0.8399	5.01E-04	5.96E-03	indole-3-acetic acid inducible 34 (IAA34)
AT5G23030	-1.1839	-0.3150	9.72E-06	2.11E-04	tetraspanin12 (TET12)
AT1G63295	-1.1839	1.2409	1.44E-10	9.16E-09	Remorin family protein
AT4G24340	-1.1846	1.9909	1.19E-14	1.32E-12	Phosphorylase superfamily protein
AT1G21550	-1.1850	0.0975	2.76E-06	7.06E-05	Calcium-binding EF-hand family protein
AT5G47450	-1.1934	3.6940	8.37E-12	6.43E-10	TONOPLAST INTRINSIC PROTEIN 2;3 (TIP2;3)
AT1G29270	-1.1950	-0.2486	2.03E-05	4.02E-04	unknown protein
AT3G45860	-1.1950	0.7122	6.80E-09	3.24E-07	cysteine-rich RLK (RECEPTOR-like protein kinase) 4 (CRK4)

AT4G15480	-1.1951	0.5771	2.52E-08	1.08E-06	UGT84A1
AT5G59680	-1.2039	1.7169	1.47E-14	1.61E-12	Leucine-rich repeat protein kinase family protein
AT4G01895	-1.2077	-0.6976	1.77E-04	2.54E-03	systemic acquired resistance (SAR) regulator protein NIMIN-1-related
AT3G55890	-1.2153	0.7965	3.44E-09	1.74E-07	Yippee family putative zinc-binding protein
AT5G13320	-1.2206	2.2826	1.53E-16	2.24E-14	AVRPPHB SUSCEPTIBLE 3 (PBS3)
AT5G25250	-1.2219	1.7383	5.69E-15	6.76E-13	SPFH/Band 7/PHB domain-containing membrane-associated protein family
AT1G66020	-1.2270	0.4517	2.04E-08	8.94E-07	Terpenoid cyclases/Protein prenyltransferases superfamily protein
AT4G37060	-1.2279	-1.0030	4.70E-04	5.66E-03	PATATIN-like protein 5 (PLP5)
AT1G19510	-1.2371	-1.0787	1.69E-03	1.55E-02	RAD-like 5 (RL5)
AT4G40020	-1.2437	-0.0582	1.63E-06	4.49E-05	Myosin heavy chain-related protein
AT4G26320	-1.2468	2.8844	1.31E-09	7.09E-08	arabinogalactan protein 13 (AGP13)
AT1G05650	-1.2481	1.2816	5.89E-11	3.94E-09	Pectin lyase-like superfamily protein
AT2G24850	-1.2561	-0.3611	4.37E-06	1.06E-04	tyrosine aminotransferase 3 (TAT3)
AT1G65680	-1.2579	-1.0713	1.70E-03	1.56E-02	expansin B2 (EXPB2)
AT1G53625	-1.2616	1.9558	3.32E-13	3.04E-11	unknown protein
AT2G31083	-1.2649	-0.2696	4.02E-06	9.85E-05	CLAVATA3/ESR-RELATED 5 (CLE5)
AT5G02540	-1.2678	2.3772	4.36E-20	8.64E-18	NAD(P)-binding Rossmann-fold superfamily protein
AT1G73330	-1.2697	8.5723	1.56E-27	5.56E-25	drought-repressed 4 (DR4)
AT4G21380	-1.2715	1.8533	3.47E-15	4.36E-13	receptor kinase 3 (RK3)
AT5G39120	-1.2834	-0.2125	1.51E-06	4.23E-05	RmlC-like cupins superfamily protein
AT5G14470	-1.2859	-0.8977	2.59E-04	3.52E-03	GHMP kinase family protein
AT4G12545	-1.2905	3.2621	3.12E-26	1.02E-23	Bifunctional inhibitor/lipid-transfer protein/seed storage 2S albumin superfamily protein
AT1G52800	-1.2947	1.0146	1.83E-11	1.33E-09	2-oxoglutarate (2OG) and Fe(II)-dependent oxygenase superfamily protein
AT5G23990	-1.2987	3.5405	8.78E-31	4.41E-28	ferric reduction oxidase 5 (FRO5)
AT1G67980	-1.2987	-0.2667	1.88E-05	3.80E-04	caffeoyl-CoA 3-O-methyltransferase (CCOAMT)
AT5G65600	-1.2997	-0.2630	1.40E-06	3.95E-05	Concanavalin A-like lectin protein kinase family protein
AT4G22212	-1.3105	2.2161	1.21E-18	2.08E-16	Arabidopsis defensin-like protein
AT5G23830	-1.3109	4.0591	1.28E-27	4.75E-25	MD-2-related lipid recognition domain-containing protein
AT2G15220	-1.3116	4.1452	2.29E-29	9.96E-27	Plant basic secretory protein (BSP) family protein
AT1G63450	-1.3137	0.4091	4.06E-09	2.02E-07	root hair specific 8 (RHS8)
AT5G65340	-1.3171	-0.7314	6.60E-05	1.12E-03	Protein of unknown function, DUF617
AT5G35480	-1.3264	0.4694	6.73E-10	3.84E-08	unknown protein
AT4G25510	-1.3361	-0.9906	7.72E-05	1.28E-03	unknown protein
ATCG01020	-1.3397	-0.6836	6.41E-06	1.47E-04	ribosomal protein L32 (RPL32)
AT1G01380	-1.3410	0.0404	4.77E-08	1.93E-06	ENHANCER OF TRY AND CPC 1 (ETC1)
AT2G19500	-1.3413	0.3691	1.16E-08	5.30E-07	cytokinin oxidase 2 (CKX2)
AT4G12550	-1.3504	4.0289	3.15E-29	1.32E-26	Auxin-Induced in Root cultures 1 (AIR1)
AT3G21800	-1.3519	-0.7510	6.08E-05	1.04E-03	UDP-glucosyl transferase 71B8 (UGT71B8)
AT4G07960	-1.3583	0.7383	2.13E-11	1.53E-09	Cellulose-synthase-like C12 (CSLC12)

AT5G09730	-1.3663	0.4021	5.80E-09	2.80E-07	beta-xylosidase 3 (BXL3)
AT3G47480	-1.3676	0.6708	7.87E-11	5.19E-09	Calcium-binding EF-hand family protein
AT2G16230	-1.3677	-0.3527	4.97E-06	1.19E-04	O-Glycosyl hydrolases family 17 protein
AT5G35940	-1.3693	0.2423	3.80E-08	1.56E-06	Mannose-binding lectin superfamily protein
AT3G19320	-1.3708	0.1317	1.67E-08	7.48E-07	Leucine-rich repeat (LRR) family protein
AT1G13510	-1.3778	1.0620	1.76E-13	1.67E-11	Protein of unknown function (DUF1262)
AT2G46495	-1.3789	1.4571	7.31E-16	9.81E-14	RING/U-box superfamily protein
AT5G46890	-1.3834	3.9260	5.00E-30	2.23E-27	Bifunctional inhibitor/lipid-transfer protein/seed storage 2S albumin superfamily protein
AT2G28210	-1.3864	0.3070	1.23E-09	6.71E-08	alpha carbonic anhydrase 2 (ACA2)
AT5G02170	-1.3902	1.4776	6.93E-17	1.05E-14	Transmembrane amino acid transporter family protein
AT2G02300	-1.3947	-0.9436	1.21E-04	1.86E-03	phloem protein 2-B5 (PP2-B5)
AT3G55910	-1.3987	-0.5078	5.61E-06	1.31E-04	unknown protein
AT1G77520	-1.4010	3.6112	1.36E-27	4.94E-25	O-methyltransferase family protein
AT5G39000	-1.4076	-0.7000	1.38E-05	2.88E-04	Malectin/receptor-like protein kinase family protein
AT5G39670	-1.4121	1.2667	1.45E-15	1.88E-13	Calcium-binding EF-hand family protein
AT1G27140	-1.4190	2.4551	6.80E-24	1.85E-21	glutathione S-transferase tau 14 (GSTU14)
AT3G27940	-1.4210	-0.8901	4.57E-05	8.16E-04	LOB domain-containing protein 26 (LBD26)
AT1G18990	-1.4400	-0.6674	7.09E-06	1.62E-04	Protein of unknown function, DUF593
AT3G02850	-1.4428	1.4973	2.53E-17	4.00E-15	SKOR, a member of Shaker family potassium ion (K+) channel
AT5G53200	-1.4535	0.5258	8.40E-10	4.73E-08	TRIPTYCHON (TRY)
AT1G36622	-1.4614	0.6185	2.05E-11	1.48E-09	unknown protein
AT3G62760	-1.4667	1.1924	4.58E-13	4.12E-11	GSTF13
AT1G09240	-1.4684	0.1296	4.40E-09	2.17E-07	nicotianamine synthase 3 (NAS3)
AT3G13784	-1.4757	2.5095	3.79E-26	1.22E-23	cell wall invertase 5 (CWINV5)
AT5G23780	-1.4811	-0.7783	4.47E-05	8.01E-04	DOMAIN OF UNKNOWN FUNCTION 724 9 (DUF9)
AT4G10310	-1.4845	2.5781	2.00E-19	3.67E-17	high-affinity K+ transporter 1 (HKT1)
AT1G13520	-1.4874	2.4387	2.26E-20	4.67E-18	Protein of unknown function (DUF1262)
AT2G24720	-1.4973	0.5066	9.47E-11	6.19E-09	glutamate receptor 2.2 (GLR2.2)
AT1G74080	-1.5010	-0.6139	3.15E-06	7.94E-05	myb domain protein 122 (MYB122)
AT3G12240	-1.5059	-0.5085	2.38E-06	6.24E-05	serine carboxypeptidase-like 15 (SCPL15)
AT5G45000	-1.5101	-0.1424	9.74E-08	3.63E-06	Disease resistance protein (TIR-NBS-LRR class) family
AT4G12510	-1.5108	1.7979	3.30E-21	7.19E-19	Bifunctional inhibitor/lipid-transfer protein/seed storage 2S albumin superfamily protein
AT3G26610	-1.5109	1.6467	2.13E-19	3.88E-17	Pectin lyase-like superfamily protein
AT3G46300	-1.5112	-0.7070	3.32E-06	8.30E-05	unknown protein
AT5G26920	-1.5170	3.0398	7.13E-17	1.07E-14	CAM-BINDING PROTEIN 60-LIKE G (CBP60G)
AT1G60470	-1.5171	2.8804	8.62E-20	1.63E-17	galactinol synthase 4 (GolS4)
AT5G37478	-1.5176	-0.7532	8.32E-06	1.84E-04	TPX2 (targeting protein for Xklp2) protein family
AT5G25260	-1.5268	1.2281	1.36E-13	1.32E-11	SPFH/Band 7/PHB domain-containing membrane-associated protein family
AT5G54190	-1.5335	3.6517	2.09E-32	1.17E-29	protochlorophyllide oxidoreductase A (PORA)

AT1G06310	-1.5358	-0.5068	8.85E-07	2.60E-05	acyl-CoA oxidase 6 (ACX6)
AT3G55710	-1.5371	3.5858	7.01E-43	6.24E-40	UDP-Glycosyltransferase superfamily protein
AT1G04660	-1.5396	0.0637	2.17E-08	9.47E-07	glycine-rich protein
AT2G29130	-1.5398	1.4243	3.01E-19	5.36E-17	laccase 2 (LAC2)
AT1G08090	-1.5427	2.3119	1.27E-14	1.41E-12	nitrate transporter 2:1 (NRT2:1)
AT3G17520	-1.5442	-0.6028	2.57E-06	6.65E-05	Late embryogenesis abundant protein (LEA) family protein
AT4G04990	-1.5648	1.9176	1.85E-16	2.69E-14	Protein of unknown function (DUF761)
AT5G44120	-1.5685	-0.3150	1.62E-03	1.50E-02	CRUCIFERINA (CRA1)
AT2G30750	-1.6009	5.6456	1.80E-34	1.18E-31	cytochrome P450, family 71, subfamily A, polypeptide 12 (CYP71A12)
AT2G23270	-1.6354	-0.6232	1.19E-06	3.41E-05	unknown protein
AT5G62420	-1.6677	0.0531	3.12E-10	1.87E-08	NAD(P)-linked oxidoreductase superfamily protein
AT5G23840	-1.6721	1.8956	2.35E-26	8.09E-24	MD-2-related lipid recognition domain-containing protein
AT5G48430	-1.6750	2.5495	1.58E-22	3.87E-20	Eukaryotic aspartyl protease family protein
AT1G47890	-1.6858	-0.4473	1.97E-08	8.67E-07	receptor like protein 7 (RLP7)
AT1G06923	-1.6951	-0.9855	3.28E-06	8.22E-05	Similar to: ovate family protein 17
AT3G16670	-1.6985	4.2932	1.63E-31	8.61E-29	Pollen Ole e 1 allergen and extensin family protein
AT1G26410	-1.7207	1.7210	8.40E-13	7.32E-11	FAD-binding Berberine family protein
AT4G14630	-1.7369	3.4311	1.06E-23	2.84E-21	germin-like protein 9 (GLP9)
AT5G48400	-1.8203	0.3353	9.70E-15	1.11E-12	ATGLR1.2
AT3G62950	-1.8204	0.7386	5.07E-17	7.70E-15	Thioredoxin superfamily protein
AT2G35980	-1.8565	1.8498	2.88E-31	1.48E-28	YELLOW-LEAF-SPECIFIC GENE 9 (YLS9)
AT3G61390	-1.8581	0.5484	6.52E-16	8.94E-14	RING/U-box superfamily protein
AT4G33120	-1.8585	1.7435	2.41E-29	1.03E-26	S-adenosyl-L-methionine-dependent methyltransferases superfamily protein
AT3G06220	-1.8836	-0.9115	2.95E-07	9.74E-06	AP2/B3-like transcriptional factor family protein
AT4G31970	-1.8911	2.3145	1.26E-10	8.07E-09	cytochrome P450, family 82, subfamily C, polypeptide 2 (CYP82C2)
AT1G52790	-1.8948	-0.9856	6.69E-07	2.02E-05	contains PF03171 2OG-Fe(II) oxygenase superfamily domain
AT1G53610	-1.9288	-1.1991	3.89E-06	9.58E-05	unknown protein
AT3G21660	-1.9314	-0.4035	5.29E-10	3.08E-08	UBX domain-containing protein
AT1G49030	-1.9358	-0.7558	1.05E-08	4.81E-07	PLAC8 family protein
AT4G22214	-2.0124	1.4553	2.08E-30	9.79E-28	Defensin-like (DEFL) family protein
AT5G49870	-2.0173	-1.0526	8.32E-08	3.17E-06	Mannose-binding lectin superfamily protein
AT3G01175	-2.0224	-0.9018	2.24E-08	9.73E-07	Protein of unknown function (DUF1666)
AT4G33720	-2.0302	0.3790	3.36E-04	4.33E-03	CAP (Cysteine-rich secretory proteins, Antigen 5, and Pathogenesis-related 1 protein)
AT1G50930	-2.0389	-1.2092	1.08E-06	3.14E-05	unknown protein
AT4G11170	-2.0556	0.5013	1.34E-18	2.28E-16	Disease resistance protein (TIR-NBS-LRR class) family
AT2G19060	-2.0879	0.6011	1.15E-19	2.15E-17	SGNH hydrolase-type esterase superfamily protein
AT1G13500	-2.1453	-1.2325	6.64E-07	2.01E-05	Protein of unknown function (DUF1262)
AT4G15990	-2.1715	-0.3416	2.85E-12	2.30E-10	unknown protein
AT1G77530	-2.2366	2.6955	1.52E-60	2.72E-57	O-methyltransferase family protein

AT1G26390	-2.3131	3.7957	1.33E-17	2.17E-15	FAD-binding Berberine family protein
AT1G52820	-2.3279	2.9611	1.72E-32	9.92E-30	2-oxoglutarate (2OG) and Fe(II)-dependent oxygenase superfamily protein
AT3G21460	-2.4625	0.0957	8.27E-19	1.43E-16	Glutaredoxin family protein
AT5G38910	-2.6048	2.0703	7.04E-44	6.91E-41	RmlC-like cupins superfamily protein
AT1G58320	-2.6543	0.7670	1.15E-30	5.62E-28	PLAC8 family protein
AT1G05880	-2.6857	-1.1877	7.95E-09	3.71E-07	ARIADNE 12 (ARI12)
AT5G06900	-3.6295	-0.5686	6.05E-20	1.17E-17	cytochrome P450, family 93, subfamily D, polypeptide 1 (CYP93D1)
AT4G27570	-3.6929	-0.8894	3.07E-17	4.77E-15	UDP-Glycosyltransferase superfamily protein
AT3G05950	-3.7672	-1.3139	2.96E-13	2.75E-11	RmlC-like cupins superfamily protein
AT4G04950	-7.8621	4.2847	0.00E+00	0.00E+00	PICOT1

FC, fold change; CPM, counts per million; FDR, false discovery rate

Supplementary Table S4. Differentially expressed genes obtained by RNA-Sequencing analysis of the *coi1-16* line.

Locus	logFC	logCPM	PValue	FDR	Short description
AT4G04500	9.9652	0.8849	3.55E-26	1.08E-23	cysteine-rich RLK (RECEPTOR-like protein kinase) 37 (CRK37)
AT5G55150	8.3031	-0.6530	1.19E-30	4.34E-28	Protein of unknown function (DUF295)
AT1G13470	7.5525	0.5473	4.38E-45	2.97E-42	Protein of unknown function (DUF1262)
AT1G33960	6.2681	0.9408	2.91E-16	3.95E-14	AVRRPT2-INDUCED GENE 1 (AIG1)
AT1G21240	4.9667	0.8382	1.03E-20	2.08E-18	wall associated kinase 3 (WAK3)
AT2G14560	4.7646	1.1353	1.13E-15	1.41E-13	LATE UPREGULATED IN RESPONSE TO HYALOPERONOSPORA PARASITICA (LURP1)
AT5G52760	4.5195	0.2640	3.79E-24	1.04E-21	Copper transport protein family
AT4G23210	4.3403	0.7977	1.93E-19	3.43E-17	cysteine-rich RLK (RECEPTOR-like protein kinase) 13 (CRK13)
AT2G18660	4.3197	0.6285	4.54E-22	1.03E-19	PLANT NATRIURETIC PEPTIDE A (PNP-A)
AT4G23140	3.9441	0.7534	1.95E-18	3.19E-16	cysteine-rich RLK (RECEPTOR-like protein kinase) 6 (CRK6)
AT3G57260	3.7758	2.2335	3.85E-15	4.52E-13	beta-1,3-glucanase 2 (BGL2)
AT4G38560	3.6313	0.7998	3.56E-19	6.09E-17	Arabidopsis phospholipase-like protein (PEARLI 4) family
AT5G10760	3.4986	1.9842	2.20E-20	4.21E-18	Eukaryotic aspartyl protease family protein
AT2G32680	3.4618	0.5675	8.15E-18	1.27E-15	receptor like protein 23 (RLP23)
AT2G18190	3.2717	0.3521	1.17E-34	5.00E-32	P-loop containing nucleoside triphosphate hydrolases superfamily protein
AT4G11890	3.2395	0.5607	2.71E-19	4.72E-17	Protein kinase superfamily protein
AT3G01345	3.0515	-0.8581	1.05E-14	1.17E-12	Expressed protein
AT1G21250	2.9781	3.4643	6.58E-39	3.16E-36	cell wall-associated kinase (WAK1)
AT1G11785	2.9037	-0.8441	2.86E-14	2.98E-12	unknown protein
AT3G22231	2.8970	1.8937	2.74E-10	1.62E-08	PATHOGEN AND CIRCADIAN CONTROLLED 1 (PCC1)
AT5G26270	2.8638	3.2136	8.05E-133	2.64E-129	unknown protein
AT3G30720	2.8482	2.6632	5.57E-103	1.22E-99	QUA-QUINE STARCH (QQS)
AT2G45550	2.6667	-1.0164	1.04E-10	6.62E-09	cytochrome P450, family 76, subfamily C, polypeptide 4 (CYP76C4)
AT2G18180	2.6222	-0.7411	2.82E-13	2.57E-11	Sec14p-like phosphatidylinositol transfer family protein
AT2G15042	2.5982	1.2988	1.62E-44	1.03E-41	Leucine-rich repeat (LRR) family protein
AT1G73805	2.5959	0.5783	8.48E-14	8.20E-12	Calmodulin binding protein-like
AT4G23220	2.5346	0.8378	8.00E-19	1.33E-16	cysteine-rich RLK (RECEPTOR-like protein kinase) 14 (CRK14)
AT3G50480	2.5238	2.5512	1.82E-16	2.51E-14	homolog of RPW8 4 (HR4)
AT1G05675	2.5054	-0.7659	6.05E-13	5.23E-11	UDP-Glycosyltransferase superfamily protein
AT2G04070	2.4707	1.2448	7.68E-34	3.09E-31	MATE efflux family protein
AT4G14365	2.4685	1.9156	9.35E-24	2.46E-21	XB3 ortholog 4 in Arabidopsis thaliana (XBAT34)
AT5G12030	2.4598	-0.1591	1.19E-05	2.44E-04	heat shock protein 17.6A (HSP17.6A)
AT4G12490	2.3762	2.1785	7.41E-04	7.59E-03	Bifunctional inhibitor/lipid-transfer protein/seed storage 2S albumin superfamily protein
AT2G34655	2.3410	0.6134	7.86E-27	2.50E-24	unknown protein
AT5G13210	2.3253	2.9275	3.11E-46	2.27E-43	Uncharacterised conserved protein UCP015417, vWA
AT4G14400	2.3245	3.7050	1.83E-14	1.94E-12	ACCELERATED CELL DEATH 6 (ACD6)

AT5G60900	2.2963	0.6806	9.63E-18	1.49E-15	receptor-like protein kinase 1 (RLK1)
AT2G03821	2.2588	-0.5869	5.45E-12	4.25E-10	unknown protein
AT4G04490	2.2503	1.1674	3.27E-18	5.33E-16	cysteine-rich RLK (RECEPTOR-like protein kinase) 36 (CRK36)
AT2G04450	2.1810	0.7690	5.45E-20	1.03E-17	nudix hydrolase homolog 6 (NUDT6)
AT2G32140	2.1786	-0.0478	1.11E-14	1.22E-12	transmembrane receptors
AT1G65790	2.1277	-0.5827	7.76E-12	5.90E-10	receptor kinase 1 (RK1)
AT3G22235	2.1017	0.3017	6.14E-10	3.43E-08	unknown Similar to:pathogen and circadian controlled 1
AT1G01680	2.0556	-0.4611	1.62E-11	1.21E-09	plant U-box 54 (PUB54)
AT2G17040	2.0212	1.3012	1.10E-20	2.22E-18	NAC domain containing protein 36 (NAC036)
AT4G11460	2.0173	0.1466	4.89E-16	6.33E-14	cysteine-rich RLK (RECEPTOR-like protein kinase) 30 (CRK30)
AT1G53490	2.0172	2.3071	5.81E-50	4.40E-47	RING/U-box superfamily protein
AT3G09922	2.0014	-0.5415	1.29E-10	8.05E-09	INDUCED BY PHOSPHATE STARVATION1 (IPS1)
AT2G41100	1.9921	4.7519	7.56E-21	1.57E-18	TOUCH 3 (TCH3)
AT5G54610	1.9731	0.7269	3.91E-11	2.73E-09	ankyrin (ANK)
AT2G13810	1.9649	1.1287	1.13E-14	1.24E-12	AGD2-like defense response protein 1 (ALD1)
AT2G29220	1.8855	-0.3141	6.79E-11	4.58E-09	Concanavalin A-like lectin protein kinase family protein
AT5G37450	1.8847	-0.6376	1.01E-09	5.40E-08	Leucine-rich repeat protein kinase family protein
AT5G42530	1.8498	6.1899	9.75E-18	1.50E-15	unknown protein
AT4G23130	1.8484	0.1822	6.65E-11	4.50E-09	cysteine-rich RLK (RECEPTOR-like protein kinase) 5 (CRK5)
AT2G46400	1.8453	1.0557	3.65E-16	4.89E-14	Group III
AT1G23840	1.8386	-0.8097	4.26E-09	2.02E-07	unknown protein
AT5G58610	1.7803	0.8057	1.98E-20	3.83E-18	PHD finger transcription factor, putative
AT2G04050	1.7328	3.9272	1.26E-16	1.76E-14	MATE efflux family protein
AT1G75040	1.7294	2.5521	4.98E-14	5.06E-12	pathogenesis-related gene 5 (PR5)
AT1G35230	1.7247	0.8949	1.92E-10	1.17E-08	arabinogalactan protein 5 (AGP5)
AT1G49920	1.7103	-0.8250	1.98E-07	6.44E-06	MuDR family transposase
AT2G20800	1.7097	-0.0515	1.34E-11	1.00E-09	NAD(P)H dehydrogenase B4 (NDB4)
AT2G04040	1.6914	1.6100	6.44E-29	2.19E-26	TX1
AT1G01560	1.6745	1.0963	2.02E-07	6.58E-06	MAP kinase 11 (MPK11)
AT3G56710	1.6367	1.6666	4.36E-11	3.01E-09	SIGMA FACTOR BINDING PROTEIN 1 (SIB1)
AT2G36710	1.6308	-0.9985	3.33E-06	8.07E-05	Pectin lyase-like superfamily protein
AT5G58840	1.6268	-1.0006	4.73E-06	1.10E-04	Subtilase family protein
AT5G59670	1.6115	0.8204	1.82E-17	2.72E-15	Leucine-rich repeat protein kinase family protein
AT3G52970	1.6093	0.6390	3.52E-09	1.70E-07	cytochrome P450, family 76, subfamily G, polypeptide 1 (CYP76G1)
AT3G22910	1.6012	1.4396	8.96E-14	8.61E-12	ATPase E1-E2 type family protein / haloacid dehalogenase-like hydrolase family protein
AT2G20142	1.5963	0.4663	1.45E-10	8.99E-09	Toll-Interleukin-Resistance (TIR) domain family protein
AT1G35710	1.5758	3.9213	6.05E-16	7.79E-14	Protein kinase family protein with leucine-rich repeat domain
AT5G44568	1.5726	0.2439	7.11E-12	5.42E-10	unknown protein
AT2G41090	1.5596	6.1766	1.67E-19	2.99E-17	Calcium-binding EF-hand family protein

AT3G44260	1.5588	2.0659	1.14E-15	1.41E-13	Polynucleotidyl transferase, ribonuclease H-like superfamily protein
AT2G24600	1.5580	1.1452	2.21E-11	1.61E-09	Ankyrin repeat family protein
AT5G51190	1.5562	0.6202	6.94E-14	6.80E-12	Integrase-type DNA-binding superfamily protein
AT1G19250	1.5442	2.0108	4.77E-14	4.86E-12	flavin-dependent monooxygenase 1 (FMO1)
AT5G42380	1.5152	-0.1397	2.34E-08	9.47E-07	calmodulin like 37 (CML37)
AT5G52750	1.5109	0.8851	9.66E-13	8.12E-11	Heavy metal transport/detoxification superfamily protein
AT4G34400	1.5065	0.0298	7.85E-10	4.23E-08	AP2/B3-like transcriptional factor family protein
AT4G16240	1.5009	0.0110	1.25E-09	6.55E-08	unknown protein
AT3G29430	1.4733	0.9234	3.95E-16	5.22E-14	Terpenoid synthases superfamily protein
AT3G46230	1.4609	0.6300	1.36E-05	2.75E-04	heat shock protein 17.4 (HSP17.4)
AT1G24260	1.4469	0.3238	1.15E-10	7.25E-09	SEPALLATA3 (SEP3)
AT4G18250	1.4414	0.5065	4.44E-10	2.53E-08	receptor serine/threonine kinase, putative
AT1G15540	1.4356	-0.1908	3.30E-07	1.03E-05	2-oxoglutarate (2OG) and Fe(II)-dependent oxygenase superfamily protein
AT3G16650	1.4266	1.5234	1.67E-21	3.61E-19	Transducin/WD40 repeat-like superfamily protein
AT3G16530	1.4188	3.4177	2.55E-13	2.34E-11	Legume lectin family protein
AT5G35525	1.3965	-0.4731	1.07E-06	3.02E-05	PLAC8 family protein
AT4G20690	1.3691	-0.4728	1.07E-06	3.02E-05	unknown protein
AT1G78030	1.3670	-0.5809	3.30E-06	8.00E-05	unknown protein
AT1G23110	1.3664	1.0231	7.92E-15	8.87E-13	unknown protein
AT1G10340	1.3657	1.4330	1.32E-08	5.71E-07	Ankyrin repeat family protein
AT5G54710	1.3561	2.3868	1.23E-20	2.45E-18	Ankyrin repeat family protein
AT3G56400	1.3556	3.5210	4.47E-11	3.08E-09	WRKY DNA-BINDING PROTEIN 70 (WRKY70)
AT4G15680	1.3467	0.2671	2.39E-09	1.20E-07	Thioredoxin superfamily protein
AT1G66920	1.3415	0.6551	1.91E-11	1.41E-09	Protein kinase superfamily protein
AT5G56810	1.3390	-0.6156	3.28E-06	7.99E-05	F-box/RNI-like/FBD-like domains-containing protein
AT5G08760	1.3226	1.7277	2.29E-12	1.86E-10	unknown protein
AT3G60420	1.3208	2.4023	1.11E-10	7.02E-09	Phosphoglycerate mutase family protein
AT1G78750	1.2983	0.0115	1.98E-08	8.23E-07	F-box/RNI-like superfamily protein
AT1G15125	1.2967	0.6703	1.83E-05	3.53E-04	S-adenosyl-L-methionine-dependent methyltransferases superfamily protein
AT2G25510	1.2908	5.4645	1.72E-13	1.61E-11	unknown protein
AT2G14580	1.2595	1.1878	1.40E-04	1.93E-03	basic pathogenesis-related protein 1 (PRB1)
AT2G36750	1.2589	0.3908	3.99E-09	1.91E-07	UDP-glucosyl transferase 73C1 (UGT73C1)
AT5G09470	1.2584	-0.8934	1.22E-04	1.72E-03	dicarboxylate carrier 3 (DIC3)
AT1G80840	1.2494	0.5234	1.41E-09	7.30E-08	WRKY DNA-binding protein 40 (WRKY40)
AT4G00970	1.2446	1.4273	5.45E-15	6.28E-13	cysteine-rich RLK (RECEPTOR-like protein kinase) 41 (CRK41)
AT1G17710	1.2326	-0.2332	3.06E-06	7.54E-05	Pyridoxal phosphate phosphatase-related protein
AT3G18610	1.2291	0.8352	2.93E-10	1.72E-08	nucleolin like 2 (NUC-L2)
AT1G56150	1.2186	0.1413	3.40E-08	1.33E-06	SAUR-like auxin-responsive protein family
AT2G46440	1.1856	1.3682	1.19E-10	7.49E-09	cyclic nucleotide-gated channels (CNGC11)

AT5G67060	1.1771	-0.4966	2.27E-05	4.24E-04	HECATE 1 (HEC1)
AT1G57630	1.1758	-0.0750	4.64E-05	7.65E-04	Toll-Interleukin-Resistance (TIR) domain family protein
AT4G23170	1.1748	1.7632	2.39E-15	2.85E-13	EP1
AT5G54720	1.1721	0.6490	3.49E-08	1.36E-06	Ankyrin repeat family protein
AT5G55450	1.1651	2.4319	1.60E-09	8.29E-08	Bifunctional inhibitor/lipid-transfer protein/seed storage 2S albumin superfamily protein
AT3G27940	1.1571	0.3011	3.13E-08	1.24E-06	LOB domain-containing protein 26 (LBD26)
AT3G50930	1.1547	3.2089	4.84E-16	6.31E-14	cytochrome BC1 synthesis (BCS1)
AT2G18193	1.1496	4.0049	5.06E-14	5.11E-12	P-loop containing nucleoside triphosphate hydrolases superfamily protein
AT1G29110	1.1445	-0.7885	2.25E-04	2.84E-03	Cysteine proteinases superfamily protein
AT4G33970	1.1443	-0.7922	2.28E-04	2.87E-03	Leucine-rich repeat (LRR) family protein
AT1G28370	1.1366	-0.3929	5.61E-05	8.98E-04	ERF domain protein 11 (ERF11)
AT5G20710	1.1348	0.9632	8.48E-08	3.03E-06	beta-galactosidase 7 (BGAL7)
AT5G55460	1.1307	-0.0643	2.80E-06	6.96E-05	Bifunctional inhibitor/lipid-transfer protein/seed storage 2S albumin superfamily protein
AT3G49110	1.1236	2.4987	5.88E-05	9.33E-04	peroxidase CA (PRXCA)
AT2G32830	1.1178	-0.8959	3.63E-04	4.26E-03	Encodes Pht1
AT1G78970	1.1177	4.6326	9.86E-41	5.12E-38	ARABIDOPSIS THALIANA LUPEOL SYNTHASE 1 (LUP1)
AT1G19960	1.1166	4.0161	3.32E-14	3.44E-12	unknown Similar to:transmembrane receptors
AT4G15670	1.1156	-0.5706	7.93E-05	1.21E-03	Thioredoxin superfamily protein
AT3G29410	1.1146	3.5647	1.04E-18	1.72E-16	Terpenoid cyclases/Protein prenyltransferases superfamily protein
AT5G20790	1.1145	2.8994	1.37E-05	2.76E-04	unknown protein
AT5G39110	1.1093	0.1605	6.08E-07	1.81E-05	RmlC-like cupins superfamily protein
AT4G12470	1.1075	3.5123	1.88E-15	2.27E-13	azelaic acid induced 1 (AZI1)
AT2G02010	1.1061	1.2512	7.57E-07	2.20E-05	glutamate decarboxylase 4 (GAD4)
AT1G65110	1.1049	-0.8227	2.82E-04	3.44E-03	Ubiquitin carboxyl-terminal hydrolase-related protein
AT3G11010	1.0998	2.1408	5.80E-13	5.05E-11	receptor like protein 34 (RLP34)
AT5G60250	1.0987	0.2286	7.60E-06	1.65E-04	zinc finger (C3HC4-type RING finger) family protein
AT3G23120	1.0887	-0.2011	1.40E-05	2.81E-04	receptor like protein 38 (RLP38)
AT5G06900	1.0851	0.9005	2.16E-08	8.86E-07	cytochrome P450, family 93, subfamily D, polypeptide 1 (CYP93D1)
AT1G20400	1.0806	0.2803	2.36E-06	5.98E-05	FUNCTIONS IN: molecular_function unknown
AT3G47100	1.0715	-1.0105	1.84E-03	1.56E-02	unknown protein
AT2G44460	1.0704	1.9807	5.38E-08	2.01E-06	beta glucosidase 28 (BGLU28)
AT4G36570	1.0677	0.6435	2.02E-08	8.34E-07	RAD-like 3 (RL3)
AT4G29610	1.0631	1.2926	7.31E-11	4.88E-09	Cytidine/deoxycytidylate deaminase family protein
AT4G24570	1.0590	2.1024	5.66E-11	3.87E-09	dicarboxylate carrier 2 (DIC2)
AT5G54490	1.0583	0.9280	1.01E-07	3.53E-06	pinoid-binding protein 1 (PBP1)
AT3G20440	1.0514	4.6220	1.96E-35	8.56E-33	EMBRYO DEFECTIVE 2729 (EMB2729)
AT3G45730	1.0330	1.8904	3.69E-11	2.60E-09	unknown protein
AT3G14900	1.0309	4.5835	7.44E-30	2.62E-27	unknown protein
AT1G30190	1.0297	-0.7969	1.85E-03	1.57E-02	unknown protein

AT4G14819	1.0273	0.4819	1.90E-07	6.22E-06	Protein of unknown function (DUF1677)
AT5G01540	1.0206	1.9083	1.07E-13	1.02E-11	LecRKA4.2 At5g01550
AT4G23340	1.0155	-0.7834	3.80E-04	4.41E-03	2-oxoglutarate (2OG) and Fe(II)-dependent oxygenase superfamily protein
AT4G22470	1.0147	0.5808	6.10E-04	6.49E-03	protease inhibitor/seed storage/lipid transfer protein (LTP) family protein
AT4G37370	1.0105	3.4308	1.03E-11	7.70E-10	cytochrome P450, family 81, subfamily D, polypeptide 8 (CYP81D8)
AT5G25250	1.0104	2.8319	5.74E-07	1.71E-05	SPFH/Band 7/PHB domain-containing membrane-associated protein family
AT5G44585	1.0091	-0.0618	6.13E-05	9.70E-04	unknown protein
AT1G21520	1.0064	1.3839	5.40E-11	3.71E-09	unknown protein
AT5G47600	1.0060	-0.4501	2.11E-04	2.70E-03	HSP20-like chaperones superfamily protein
AT5G16980	1.0043	2.7873	1.46E-20	2.84E-18	Zinc-binding dehydrogenase family protein
AT5G18180	1.0011	-0.6099	4.93E-04	5.45E-03	H/ACA ribonucleoprotein complex, subunit Gar1/Naf1 protein
AT2G34010	-1.0028	-0.1767	2.71E-05	4.92E-04	unknown protein
AT3G02480	-1.0083	2.4558	1.07E-04	1.55E-03	Late embryogenesis abundant protein (LEA) family protein
AT2G23348	-1.0092	-0.8237	1.68E-03	1.46E-02	unknown protein
AT5G44120	-1.0097	-0.1895	6.02E-03	3.89E-02	CRUCIFERINA (CRA1)
AT3G12900	-1.0111	4.6611	8.48E-07	2.44E-05	2-oxoglutarate (2OG) and Fe(II)-dependent oxygenase superfamily protein
AT2G21510	-1.0121	-0.9398	1.34E-03	1.22E-02	DNAJ heat shock N-terminal domain-containing protein
AT1G24147	-1.0121	1.2556	6.97E-09	3.16E-07	unknown protein
AT4G13800	-1.0141	2.4659	3.14E-13	2.84E-11	Protein of unknown function (DUF803)
AT2G28700	-1.0145	-0.5645	1.62E-04	2.18E-03	AGAMOUS-like 46 (AGL46)
AT3G47340	-1.0198	4.5466	1.12E-12	9.28E-11	glutamine-dependent asparagine synthase 1 (ASN1)
AT2G32290	-1.0210	1.9749	3.05E-15	3.62E-13	beta-amylase 6 (BAM6)
AT4G31940	-1.0234	7.3241	9.65E-07	2.76E-05	cytochrome P450, family 82, subfamily C, polypeptide 4 (CYP82C4)
AT4G08870	-1.0250	6.1942	6.29E-30	2.25E-27	Arginase/deacetylase superfamily protein
AT1G33055	-1.0341	-0.7649	4.19E-04	4.77E-03	unknown protein
AT3G21620	-1.0525	-0.4970	5.73E-05	9.13E-04	ERD (early-responsive to dehydration stress) family protein
AT1G18990	-1.0525	-0.5875	1.45E-04	1.99E-03	Protein of unknown function, DUF593
AT1G28530	-1.0531	2.8037	1.31E-22	3.08E-20	unknown protein
AT5G03210	-1.0671	-0.7165	1.28E-04	1.79E-03	unknown protein
AT2G23010	-1.0728	2.4086	8.79E-12	6.66E-10	serine carboxypeptidase-like 9 (SCPL9)
AT5G62040	-1.0752	1.0278	2.04E-10	1.23E-08	PEBP (phosphatidylethanolamine-binding protein) family protein
AT1G22590	-1.0758	2.8848	1.14E-23	2.95E-21	AGAMOUS-like 87 (AGL87)
AT5G15500	-1.0773	2.3148	1.10E-12	9.20E-11	Ankyrin repeat family protein
AT5G38420	-1.0773	10.7362	3.62E-33	1.42E-30	Ribulose bisphosphate carboxylase (small chain) family protein
AT5G25640	-1.0788	-1.0118	6.60E-04	6.95E-03	Rhomboid-related intramembrane serine protease family protein
AT5G25880	-1.0879	1.1502	6.24E-12	4.80E-10	NADP-malic enzyme 3 (NADP-ME3)
AT5G42650	-1.0888	6.6993	2.52E-27	8.14E-25	allene oxide synthase (AOS)
AT5G17220	-1.0926	3.5892	3.82E-08	1.48E-06	glutathione S-transferase phi 12 (GSTF12)
AT1G09180	-1.0949	0.4794	1.93E-08	8.02E-07	secretion-associated RAS super family 1 (SARA1A)

AT2G37260	-1.0985	1.2802	9.69E-13	8.12E-11	TRANSPARENT TESTA GLABRA 2 (TTG2/WRKY44)
AT1G52120	-1.0995	1.8018	8.23E-09	3.66E-07	Mannose-binding lectin superfamily protein
AT5G42580	-1.1059	2.9352	7.22E-24	1.95E-21	cytochrome P450, family 705, subfamily A, polypeptide 12 (CYP705A12)
AT4G13410	-1.1076	0.2661	7.47E-08	2.72E-06	ATCSLA15
AT4G15440	-1.1144	2.3570	6.13E-21	1.29E-18	hydroperoxide lyase 1 (HPL1)
AT3G59710	-1.1288	0.6938	1.11E-09	5.86E-08	NAD(P)-binding Rossmann-fold superfamily protein
AT4G25510	-1.1291	-0.9744	3.57E-04	4.19E-03	unknown protein
AT2G34810	-1.1443	3.5864	1.33E-14	1.45E-12	FAD-binding Berberine family protein
AT5G09720	-1.1516	-1.0687	3.04E-04	3.66E-03	Magnesium transporter CorA-like family protein
AT2G43530	-1.1571	3.1764	1.65E-22	3.78E-20	Scorpion toxin-like knottin superfamily protein
AT3G03341	-1.1683	0.1225	1.60E-07	5.35E-06	unknown protein
AT4G34550	-1.1701	0.0366	5.51E-07	1.65E-05	unknown Similar to:F-box family protein
AT1G17380	-1.1781	-0.2371	1.38E-06	3.75E-05	jasmonate-zim-domain protein 5 (JAZ5)
AT5G40790	-1.1819	-0.7423	5.11E-05	8.29E-04	unknown protein
AT5G23840	-1.1828	2.0400	1.22E-19	2.20E-17	MD-2-related lipid recognition domain-containing protein
AT5G44050	-1.1864	2.4182	1.58E-22	3.65E-20	MATE efflux family protein
AT1G25450	-1.1941	4.3039	4.13E-52	3.39E-49	3-ketoacyl-CoA synthase 5 (KCS5)
AT3G20340	-1.1946	0.6569	8.91E-11	5.79E-09	FUNCTIONS IN: molecular_function unknown
AT4G38730	-1.2052	2.4657	2.33E-24	6.54E-22	Protein of unknown function (DUF803)
AT5G57123	-1.2068	0.6667	8.11E-11	5.36E-09	unknown protein
AT1G11112	-1.2105	-0.3849	1.34E-06	3.66E-05	unknown protein
AT1G79840	-1.2289	3.2651	2.02E-23	5.09E-21	GLABRA 2 (GL2)
AT3G29590	-1.2364	2.6249	1.95E-09	9.92E-08	AT5MAT
AT1G18830	-1.2582	-0.2745	6.75E-07	1.98E-05	Transducin/WD40 repeat-like superfamily protein
AT1G74650	-1.2618	0.1447	4.31E-09	2.04E-07	myb domain protein 31 (MYB31)
AT4G22880	-1.2653	4.1288	1.37E-07	4.63E-06	leucoanthocyanidin dioxygenase (LDOX)
AT3G25770	-1.2671	5.9072	2.80E-42	1.58E-39	allene oxide cyclase 2 (AOC2)
AT4G23600	-1.2988	5.6803	6.43E-10	3.55E-08	CORONATINE INDUCED 1 (CORI3)
AT1G13650	-1.3009	5.6307	1.39E-76	1.71E-73	unknown Similar to:18S pre-ribosomal assembly protein gar2-related
AT3G55500	-1.3273	3.1294	4.93E-15	5.71E-13	expansin A16 (EXPA16)
AT5G10946	-1.3307	0.6544	1.37E-12	1.13E-10	unknown protein
AT3G25830	-1.3567	-1.0219	3.26E-05	5.76E-04	terpene synthase-like sequence-1,8-cineole (TPS-CIN)
AT1G70700	-1.3600	3.5629	2.96E-51	2.33E-48	TIFY7
AT1G45616	-1.3698	-0.0469	7.63E-09	3.41E-07	receptor like protein 6 (RLP6)
AT5G42800	-1.3836	4.3597	2.07E-07	6.71E-06	dihydroflavonol 4-reductase (DFR)
AT2G33850	-1.3917	5.7182	1.61E-52	1.38E-49	unknown protein
AT1G66100	-1.3972	5.8987	5.34E-36	2.50E-33	Plant thionin
AT5G54060	-1.3976	2.7554	3.29E-08	1.29E-06	UDP-glucose:flavonoid 3-o-glucosyltransferase (UF3GT)
AT2G33380	-1.4126	3.6553	2.23E-27	7.31E-25	RESPONSIVE TO DESSICATION 20 (RD20)

AT1G01600	-1.4323	2.9463	8.89E-33	3.43E-30	cytochrome P450, family 86, subfamily A, polypeptide 4 (CYP86A4)
AT1G10657	-1.4356	2.1380	1.58E-29	5.45E-27	Plant protein 1589 of unknown function
AT3G55240	-1.4790	3.1566	6.83E-20	1.28E-17	FUNCTIONS IN: molecular_function unknown
AT2G21140	-1.5176	4.9770	4.23E-87	6.41E-84	proline-rich protein 2 (PRP2)
AT1G48470	-1.5203	-0.8974	1.41E-06	3.83E-05	Encodes cytosolic glutamine synthase isozyme. Expression of mRNA is not detectable in roots.
AT3G25760	-1.5543	3.5368	3.76E-46	2.65E-43	allene oxide cyclase 1 (AOC1)
AT1G64160	-1.5596	-1.2024	7.15E-06	1.56E-04	Disease resistance-responsive (dirigent-like protein) family protein
AT2G27550	-1.6092	1.7076	5.71E-25	1.68E-22	centroradialis (ATC)
AT3G27920	-1.6120	-0.5301	3.04E-09	1.49E-07	myb domain protein 0 (MYB0)
AT1G52890	-1.6135	-0.3154	1.79E-09	9.16E-08	NAC domain containing protein 19 (NAC019)
AT5G65070	-1.6171	-0.4077	1.35E-09	7.02E-08	MADS AFFECTING FLOWERING 4 (MAF4)
AT5G05340	-1.6583	0.5918	2.22E-08	9.03E-07	Peroxidase superfamily protein
AT1G52400	-1.7564	7.3563	2.18E-39	1.10E-36	beta glucosidase 18 (BGLU18)
AT1G02065	-1.8264	0.7592	2.32E-15	2.78E-13	squamosa promoter binding protein-like 8 (SPL8)
AT1G12570	-1.8684	2.0497	8.32E-41	4.55E-38	Glucose-methanol-choline (GMC) oxidoreductase family protein
AT4G13570	-1.8935	0.5649	6.12E-22	1.35E-19	histone H2A 4 (HTA4)
AT1G18710	-1.8975	3.1336	1.96E-68	2.15E-65	myb domain protein 47 (MYB47)
AT1G56650	-1.9531	1.4544	1.33E-21	2.91E-19	production of anthocyanin pigment 1 (PAP1)
AT5G39520	-1.9734	-0.2560	3.13E-07	9.79E-06	Protein of unknown function (DUF1997)
AT4G13560	-1.9866	0.4807	4.71E-22	1.05E-19	unfertilized embryo sac 15 (UNE15)
AT3G28270	-2.0180	4.0495	9.88E-41	5.12E-38	Protein of unknown function (DUF677)
AT4G13572	-2.0534	1.2375	5.68E-36	2.60E-33	unknown protein
AT5G64667	-2.0673	-1.1665	1.46E-08	6.25E-07	inflorescence deficient in abscission (IDA)-like 2 (IDL2)
AT3G52550	-2.1274	-0.1118	3.47E-17	5.07E-15	unknown Similar to:ovate family protein 18
AT1G73325	-2.1410	-0.5551	3.65E-13	3.26E-11	Kunitz family trypsin and protease inhibitor protein
AT5G40330	-2.1912	1.0369	1.50E-34	6.30E-32	myb domain protein 23 (MYB23)
AT2G43440	-2.1994	-0.4826	3.44E-15	4.06E-13	F-box and associated interaction domains-containing protein
AT4G27435	-2.2026	1.9863	7.22E-59	6.47E-56	Protein of unknown function (DUF1218)
AT2G24850	-2.4168	-0.6618	1.11E-15	1.39E-13	tyrosine aminotransferase 3 (TAT3)
AT2G28210	-2.4665	0.0554	1.99E-23	5.08E-21	alpha carbonic anhydrase 2 (ACA2)
AT2G39330	-2.5220	1.9532	5.53E-63	5.18E-60	jacalin-related lectin 23 (JAL23)
AT1G27940	-2.5530	1.0133	1.60E-43	9.86E-41	P-glycoprotein 13 (PGP13)
AT4G13575	-2.5536	3.3265	6.30E-91	1.03E-87	unknown protein
AT5G24770	-2.5934	7.2913	3.15E-235	2.07E-231	vegetative storage protein 2 (VSP2)
AT1G14250	-2.6188	4.6968	3.39E-73	3.93E-70	GDA1/CD39 nucleoside phosphatase family protein
AT3G61840	-2.6385	-1.0314	3.14E-13	2.84E-11	Protein of unknown function (DUF688)
AT3G59010	-2.6886	2.5049	4.13E-96	8.13E-93	pectin methylesterase 61 (PME61)
AT1G52000	-2.7118	5.7300	1.10E-126	3.10E-123	Mannose-binding lectin superfamily protein
AT3G28220	-2.7129	5.7672	2.18E-93	3.90E-90	TRAF-like family protein

AT1G63710	-2.7312	0.8388	2.54E-43	1.51E-40	cytochrome P450, family 86, subfamily A, polypeptide 7 (CYP86A7)
AT1G52030	-2.8024	1.9539	5.45E-68	5.64E-65	myrosinase-binding protein 2 (MBP2)
AT5G11190	-2.8109	-0.9724	8.68E-16	1.11E-13	shine3 (SHN3)
AT2G20870	-3.0503	-0.9517	4.39E-17	6.36E-15	cell wall protein precursor, putative
AT3G44860	-3.1195	0.5698	1.68E-42	9.72E-40	farnesoic acid carboxyl-O-methyltransferase (FAMT)
AT5G24780	-3.3470	4.5954	6.55E-159	2.58E-155	vegetative storage protein 1 (VSP1)
AT4G17470	-3.5482	1.3699	6.79E-77	9.56E-74	alpha/beta-Hydrolases superfamily protein
AT5G55720	-4.5980	-0.0932	1.38E-44	9.03E-42	Pectin lyase-like superfamily protein
AT5G33370	-5.3220	2.8650	1.59E-184	7.83E-181	GDSL-like Lipase/Acylhydrolase superfamily protein
AT1G52040	-5.8173	3.5560	4.36E-245	4.30E-241	myrosinase-binding protein 1 (MBP1)
AT2G38540	-6.3760	9.0168	0.00E+00	0.00E+00	lipid transfer protein 1 (LP1)
AT1G06100	-6.4194	0.8777	2.96E-67	2.91E-64	Fatty acid desaturase family protein
AT1G65450	-6.5960	1.2969	1.71E-123	4.21E-120	HXXXD-type acyl-transferase family protein
AT3G13540	-7.9834	-1.1813	1.76E-24	5.04E-22	myb domain protein 5 (MYB5)
AT2G04032	-9.8319	0.6410	8.46E-77	1.11E-73	zinc transporter 7 precursor (ZIP7)

FC, fold change; CPM, counts per million; FDR, false discovery rate

Supplementary Table S5. Differentially expressed genes obtained by RNA-Sequencing analysis of the *coi1-16picot1* line.

Locus	logFC	logCPM	PValue	FDR	Short description
AT1G30170	6.1922	0.5012	3.82E-28	9.13E-26	Protein of unknown function (DUF295)
AT3G01345	5.2932	1.0514	2.56E-57	2.39E-54	Expressed protein
AT5G53230	4.9445	0.9866	1.96E-67	2.40E-64	Protein of unknown function (DUF295)
AT5G53240	4.8660	-0.7295	4.25E-23	7.45E-21	Protein of unknown function (DUF295)
AT2G20800	4.0891	1.9020	1.26E-90	3.10E-87	NAD(P)H dehydrogenase B4 (NDB4)
AT5G59390	4.0363	-0.8310	2.31E-19	2.85E-17	XH/XS domain-containing protein
AT5G55270	4.0059	-0.6352	7.52E-22	1.21E-19	Protein of unknown function (DUF295)
AT5G60250	3.8351	2.4100	1.52E-76	2.30E-73	zinc finger (C3HC4-type RING finger) family protein
AT4G05380	3.8130	-0.4292	1.39E-22	2.33E-20	P-loop containing nucleoside triphosphate hydrolases superfamily protein
AT5G44120	3.5612	2.7694	7.77E-07	1.62E-05	CRUCIFERINA (CRA1)
AT3G01600	3.4787	2.7633	1.21E-84	2.64E-81	NAC domain containing protein 44 (NAC044)
AT2G18720	3.4193	-0.6189	3.31E-19	4.00E-17	Translation elongation factor EF1A/initiation factor IF2gamma family protein
AT5G20240	3.2208	-0.6612	1.35E-18	1.58E-16	PISTILLATA (PI)
AT5G65080	3.0209	1.1303	5.30E-48	3.15E-45	MADS AFFECTING FLOWERING 5 (MAF5)
AT5G13210	3.0179	3.4750	6.02E-80	1.18E-76	Uncharacterised conserved protein UCP015417, vWA
AT2G14560	2.8452	-0.5441	1.86E-15	1.51E-13	LATE UPREGULATED IN RESPONSE TO HYALOPERONOSPORA PARASITICA (LURP1)
AT2G18190	2.7908	-0.1089	1.00E-17	1.06E-15	P-loop containing nucleoside triphosphate hydrolases superfamily protein
AT3G22860	2.7360	-1.0251	5.98E-11	2.83E-09	eukaryotic translation initiation factor 3 subunit C2 (TIF3C2)
AT5G24240	2.6883	2.4294	3.42E-10	1.44E-08	
AT5G58610	2.6818	1.4782	2.56E-53	2.09E-50	PHD finger transcription factor, putative
AT3G18610	2.6105	1.8529	7.99E-50	5.22E-47	nucleolin like 2 (NUC-L2)
AT5G24280	2.5722	3.9336	1.24E-71	1.74E-68	GAMMA-IRRADIATION AND MITOMYCIN C INDUCED 1 (GMI1)
AT1G49570	2.5329	3.2141	1.16E-40	4.86E-38	Peroxidase superfamily protein
AT5G47000	2.4154	-0.5567	1.10E-13	7.53E-12	Peroxidase superfamily protein
AT5G09570	2.3859	1.7763	3.74E-53	2.93E-50	Cox19-like CHCH family protein
AT5G58840	2.3778	-0.5060	1.77E-13	1.19E-11	Subtilase family protein
AT5G64060	2.3565	1.5326	6.54E-46	3.47E-43	NAC domain containing protein 103 (NAC103)
AT2G04050	2.3531	4.3865	2.54E-18	2.84E-16	MATE efflux family protein
AT1G17960	2.3454	2.3854	5.44E-43	2.54E-40	Threonyl-tRNA synthetase
AT2G18193	2.3169	4.8584	9.50E-30	2.55E-27	P-loop containing nucleoside triphosphate hydrolases superfamily protein
AT1G30160	2.2967	0.6928	3.36E-27	7.33E-25	Protein of unknown function (DUF295)
AT1G36180	2.2349	5.4874	3.30E-126	1.29E-122	acetyl-CoA carboxylase 2 (ACC2)
AT5G19470	2.2324	3.1797	9.56E-08	2.46E-06	nudix hydrolase homolog 24 (NUDT24)
AT3G54530	2.1973	-0.8452	1.06E-09	4.11E-08	unknown protein
AT1G73805	2.1851	0.1900	6.61E-11	3.11E-09	Calmodulin binding protein-like
AT5G24640	2.1573	0.3255	5.41E-20	7.32E-18	unknown protein

AT3G21720	2.1455	2.6172	1.45E-21	2.23E-19	isocitrate lyase (ICL)
AT1G71280	2.1384	-1.1660	3.24E-08	9.18E-07	DEA(D/H)-box RNA helicase family protein
AT4G12480	2.0979	6.1458	1.28E-48	8.09E-46	pEARLI 1
AT3G30720	2.0973	2.0030	1.22E-23	2.26E-21	QUA-QUINE STARCH (QQS)
AT5G10760	2.0462	0.7022	6.53E-10	2.64E-08	Eukaryotic aspartyl protease family protein
AT4G12735	1.9974	-0.1727	1.49E-12	8.93E-11	unknown protein
AT1G53490	1.9949	2.2435	5.17E-43	2.47E-40	RING/U-box superfamily protein
AT3G27620	1.9938	-0.0182	1.74E-14	1.31E-12	alternative oxidase 1C (AOX1C)
AT1G70260	1.9738	1.9908	7.93E-41	3.38E-38	nodulin MtN21 /EamA-like transporter family protein
AT2G04070	1.9640	0.7982	4.27E-20	5.90E-18	MATE efflux family protein
AT4G12490	1.9439	1.7856	1.00E-17	1.06E-15	Bifunctional inhibitor/lipid-transfer protein/seed storage 2S albumin superfamily protein
AT2G47520	1.8994	-0.2862	3.89E-12	2.22E-10	HYPOXIA RESPONSIVE ERF (ETHYLENE RESPONSE FACTOR) 2 (HRE2)
AT4G21680	1.8918	0.8078	3.87E-20	5.38E-18	NITRATE TRANSPORTER 1.8 (NRT1.8)
AT3G45730	1.8741	2.4654	3.07E-16	2.75E-14	unknown protein
AT3G53040	1.8734	-0.1856	3.22E-09	1.13E-07	late embryogenesis abundant protein, putative / LEA protein, putative
AT5G51440	1.8707	2.9516	1.17E-42	5.34E-40	HSP20-like chaperones superfamily protein
AT2G41730	1.8496	2.7505	1.45E-36	5.18E-34	unknown protein
AT4G14365	1.8469	1.3729	2.97E-08	8.44E-07	XB3 ortholog 4 in Arabidopsis thaliana (XBAT34)
AT1G05490	1.8285	0.4471	6.47E-17	6.32E-15	chromatin remodeling 31 (chr31)
AT3G15670	1.8224	0.4290	9.34E-06	1.41E-04	Late embryogenesis abundant protein (LEA) family protein
AT4G12470	1.8151	3.9871	1.88E-26	3.80E-24	azelaic acid induced 1 (AZI1)
AT5G12030	1.7801	-0.7478	6.29E-08	1.67E-06	heat shock protein 17.6A (HSP17.6A)
AT3G58270	1.7727	2.1887	2.15E-42	9.58E-40	Arabidopsis phospholipase-like protein (PEARLI 4) with TRAF-like domain
AT1G30660	1.7559	-1.0933	4.71E-06	7.91E-05	
AT5G25230	1.7333	1.0243	9.24E-22	1.47E-19	Ribosomal protein S5/Elongation factor G/III/V family protein
AT5G19700	1.7232	1.5829	3.19E-14	2.33E-12	MATE efflux family protein
AT2G35300	1.6907	-0.5506	1.71E-08	5.16E-07	Late embryogenesis abundant protein, group 1 protein
AT5G67060	1.6901	-0.1854	7.43E-11	3.47E-09	HECATE 1 (HEC1)
AT1G49920	1.6768	-0.8925	7.28E-07	1.53E-05	MuDR family transposase
AT1G20400	1.6731	0.6490	4.45E-14	3.17E-12	FUNCTIONS IN: molecular_function unknown
AT5G10140	1.6433	0.2429	1.99E-13	1.32E-11	FLOWERING LOCUS C (FLC)
AT2G38250	1.6393	1.0049	1.55E-20	2.22E-18	Homeodomain-like superfamily protein
AT2G45135	1.6336	-1.0024	2.00E-06	3.75E-05	RING/U-box superfamily protein
AT3G13130	1.6242	-0.5495	6.84E-08	1.81E-06	unknown protein
AT2G38340	1.6200	-0.1334	2.88E-10	1.23E-08	Integrase-type DNA-binding superfamily protein
AT1G18100	1.6192	2.1226	4.99E-27	1.06E-24	E12A11
AT2G15042	1.6174	0.4854	1.32E-14	1.01E-12	Leucine-rich repeat (LRR) family protein
AT3G28580	1.5992	1.2909	4.64E-21	6.79E-19	P-loop containing nucleoside triphosphate hydrolases superfamily protein
AT4G23220	1.5990	0.0657	1.09E-08	3.44E-07	cysteine-rich RLK (RECEPTOR-like protein kinase) 14 (CRK14)

AT1G70440	1.5746	0.7015	7.38E-16	6.35E-14	similar to RCD one 3 (SRO3)
AT1G34460	1.5616	-0.6972	4.62E-07	1.02E-05	B1 type cyclin
AT3G50480	1.5604	1.7409	4.23E-08	1.17E-06	homolog of RPW8 4 (HR4)
AT4G38340	1.5578	0.2284	1.33E-11	6.93E-10	Plant regulator RWP-RK family protein
AT5G07200	1.5511	-0.4841	1.03E-07	2.63E-06	gibberellin 20-oxidase 3 (GA20OX3)
AT2G23170	1.5391	3.2407	1.17E-19	1.51E-17	GH3.3
AT2G41100	1.5278	4.3533	5.47E-12	3.02E-10	TOUCH 3 (TCH3)
AT5G09470	1.5009	-0.7806	4.23E-06	7.19E-05	dicarboxylate carrier 3 (DIC3)
AT5G19890	1.4858	-0.1140	2.23E-08	6.52E-07	Peroxidase superfamily protein
AT2G44570	1.4501	0.8377	8.34E-15	6.47E-13	glycosyl hydrolase 9B12 (GH9B12)
AT3G50930	1.4402	3.3704	1.92E-21	2.90E-19	cytochrome BC1 synthesis (BCS1)
AT1G65570	1.4379	0.3822	5.24E-11	2.50E-09	Pectin lyase-like superfamily protein
AT4G22470	1.4275	0.8139	3.78E-14	2.73E-12	protease inhibitor/seed storage/lipid transfer protein (LTP) family protein
AT2G43590	1.4176	6.4706	8.65E-20	1.13E-17	Chitinase family protein
AT2G17040	1.4163	0.8019	6.52E-13	4.08E-11	NAC domain containing protein 36 (NAC036)
AT3G13080	1.3813	6.3200	1.34E-37	5.04E-35	multidrug resistance-associated protein 3 (MRP3)
AT2G21640	1.3737	2.1219	4.87E-23	8.46E-21	unknown protein
AT1G43910	1.3704	2.6502	3.42E-27	7.36E-25	P-loop containing nucleoside triphosphate hydrolases superfamily protein
AT5G67430	1.3699	2.7364	1.48E-16	1.39E-14	Acyl-CoA N-acyltransferases (NAT) superfamily protein
AT3G61630	1.3609	3.8496	1.22E-16	1.16E-14	cytokinin response factor 6 (CRF6)
AT4G04490	1.3564	0.4445	9.91E-05	1.05E-03	cysteine-rich RLK (RECEPTOR-like protein kinase) 36 (CRK36)
AT1G67760	1.3521	0.4723	2.78E-11	1.40E-09	TCP-1/cpn60 chaperonin family protein
AT4G30140	1.3446	5.7121	2.03E-25	3.99E-23	CUTICLE DESTRUCTING FACTOR 1 (CDEF1)
AT1G21890	1.3438	-0.5452	2.55E-06	4.60E-05	nodulin MtN21 /EamA-like transporter family protein
AT2G47770	1.3386	-0.2472	3.62E-04	3.03E-03	TSPO(outer membrane tryptophan-rich sensory protein)-related (TSPO)
AT5G26270	1.3309	1.9620	1.08E-03	7.26E-03	unknown protein
AT3G09950	1.3202	-0.8633	5.19E-05	6.09E-04	unknown protein
AT3G48700	1.3178	1.6602	2.97E-19	3.64E-17	carboxyesterase 13 (CXE13)
AT2G36750	1.3084	0.3678	6.52E-09	2.13E-07	UDP-glucosyl transferase 73C1 (UGT73C1)
AT1G11070	1.3073	1.4119	3.05E-13	1.98E-11	unkonwn protein
AT4G13680	1.3071	0.0465	8.87E-08	2.29E-06	Protein of unknown function (DUF295)
AT4G20690	1.2990	-0.5725	5.21E-06	8.61E-05	unknown protein
AT2G42430	1.2964	0.8697	1.96E-12	1.16E-10	lateral organ boundaries-domain 16 (LBD16)
AT2G20142	1.2926	0.2125	1.89E-07	4.64E-06	Toll-Interleukin-Resistance (TIR) domain family protein
AT1G03660	1.2895	-0.3584	9.11E-07	1.85E-05	Ankyrin-repeat containing protein
AT4G13420	1.2816	2.8688	2.21E-09	8.04E-08	high affinity K+ transporter 5 (HAK5)
AT2G33070	1.2678	0.3340	5.95E-03	2.80E-02	nitrile specifier protein 2 (NSP2)
AT4G11720	1.2664	-0.8013	8.52E-05	9.30E-04	HAPLESS 2 (HAP2)
AT1G52770	1.2645	0.5182	5.05E-10	2.08E-08	Phototropic-responsive NPH3 family protein

AT3G24780	1.2613	1.2382	2.45E-10	1.06E-08	Uncharacterised conserved protein UCP015417, vWA
AT1G21250	1.2611	2.0443	6.64E-07	1.41E-05	cell wall-associated kinase (WAK1)
AT1G52120	1.2609	2.9683	1.01E-27	2.37E-25	Mannose-binding lectin superfamily protein
AT4G36570	1.2565	0.7345	1.47E-11	7.61E-10	RAD-like 3 (RL3)
AT1G33280	1.2468	0.0150	1.29E-07	3.23E-06	NAC domain containing protein 15 (NAC015)
AT1G53130	1.2351	0.4006	7.29E-09	2.36E-07	GRIM REAPER (GRI)
AT5G37450	1.2189	-1.1426	5.41E-04	4.22E-03	Leucine-rich repeat protein kinase family protein
AT2G46400	1.2177	0.5578	4.62E-07	1.02E-05	Group III
AT4G32810	1.2120	0.5590	9.40E-10	3.70E-08	carotenoid cleavage dioxygenase 8 (CCD8)
AT4G37390	1.1958	3.1048	1.32E-12	7.92E-11	BRU6
AT1G19630	1.1902	0.4905	2.11E-09	7.69E-08	cytochrome P450, family 722, subfamily A, polypeptide 1 (CYP722A1)
AT1G35230	1.1875	0.4690	1.97E-07	4.80E-06	arabinogalactan protein 5 (AGP5)
AT2G38210	1.1870	0.6456	1.29E-09	4.92E-08	putative PDX1-like protein 4 (PDX1L4)
AT4G01985	1.1773	1.6867	1.18E-12	7.15E-11	unknown protein
AT3G22142	1.1730	6.1021	5.91E-19	7.06E-17	Bifunctional inhibitor/lipid-transfer protein/seed storage 2S albumin superfamily protein
AT3G57260	1.1705	0.0336	1.87E-05	2.56E-04	beta-1,3-glucanase 2 (BGL2)
AT2G34340	1.1663	0.7432	3.35E-10	1.42E-08	Protein of unknown function, DUF584
AT5G44568	1.1609	-0.0875	1.71E-06	3.28E-05	unknown protein
AT3G21520	1.1576	0.5400	2.97E-09	1.06E-07	DUF679 domain membrane protein 1 (DMP1)
AT5G19650	1.1500	-0.2205	1.98E-06	3.71E-05	ovate family protein 8 (OFP8)
AT1G23110	1.1488	0.8230	8.83E-06	1.34E-04	unknown protein
AT4G16240	1.1487	-0.2761	7.45E-05	8.32E-04	unknown protein
AT4G24110	1.1481	0.2612	2.28E-07	5.47E-06	unknown protein
AT5G52300	1.1452	1.4803	1.00E-06	2.03E-05	LOW-TEMPERATURE-INDUCED 65 (LTI65)
AT4G14780	1.1388	0.3364	2.87E-07	6.75E-06	Protein kinase superfamily protein
AT4G30250	1.1369	0.4619	3.36E-06	5.86E-05	P-loop containing nucleoside triphosphate hydrolases superfamily protein
AT4G25010	1.1200	-0.8432	6.45E-04	4.83E-03	Nodulin MtN3 family protein
AT2G39510	1.1185	3.3818	1.65E-07	4.08E-06	nodulin MtN21 /EamA-like transporter family protein
AT1G21460	1.1155	3.3743	1.44E-17	1.51E-15	Nodulin MtN3 family protein
AT1G09380	1.1129	0.2709	3.65E-07	8.23E-06	nodulin MtN21 /EamA-like transporter family protein
AT1G09080	1.1125	1.3673	1.53E-11	7.92E-10	BIP3
AT2G44460	1.1119	1.9541	7.43E-05	8.31E-04	beta glucosidase 28 (BGLU28)
AT5G65980	1.1105	0.3571	1.35E-07	3.38E-06	Auxin efflux carrier family protein
AT1G05680	1.1059	4.8227	2.00E-08	5.97E-07	Uridine diphosphate glycosyltransferase 74E2 (UGT74E2)
AT5G59670	1.1037	0.4224	6.71E-08	1.78E-06	Leucine-rich repeat protein kinase family protein
AT3G48520	1.0949	1.6014	1.86E-11	9.54E-10	cytochrome P450, family 94, subfamily B, polypeptide 3 (CYP94B3)
AT1G69720	1.0920	-0.9048	1.38E-03	8.77E-03	heme oxygenase 3 (HO3)
AT5G52390	1.0916	1.2167	4.88E-10	2.02E-08	PAR1 protein
AT5G17760	1.0861	3.6094	3.65E-32	1.07E-29	P-loop containing nucleoside triphosphate hydrolases superfamily protein

AT5G48850	1.0805	3.5834	3.95E-05	4.85E-04	SULPHUR DEFICIENCY-INDUCED 1 (ATSDI1)
AT1G08430	1.0779	2.8263	6.33E-09	2.08E-07	aluminum-activated malate transporter 1 (ALMT1)
AT4G24150	1.0774	0.1019	5.55E-06	9.10E-05	growth-regulating factor 8 (GRF8)
AT3G20710	1.0740	-0.5046	2.86E-04	2.49E-03	F-box family protein
AT2G04040	1.0723	1.1239	1.02E-09	3.99E-08	TX1
AT3G46230	1.0718	0.3067	2.09E-06	3.89E-05	heat shock protein 17.4 (HSP17.4)
AT1G65500	1.0691	1.0795	1.70E-09	6.29E-08	unknown protein
AT4G15160	1.0679	6.3080	6.37E-09	2.09E-07	Bifunctional inhibitor/lipid-transfer protein/seed storage 2S albumin superfamily protein
AT1G21520	1.0561	1.3713	1.03E-11	5.45E-10	unknown protein
AT3G62460	1.0524	3.4628	2.27E-23	4.05E-21	Putative endonuclease or glycosyl hydrolase
AT2G21350	1.0366	0.6850	5.19E-08	1.41E-06	RNA-binding CRS1 / YhbY (CRM) domain protein
AT4G33040	1.0283	2.4920	1.57E-16	1.46E-14	Thioredoxin superfamily protein
AT2G04450	1.0244	-0.0980	1.80E-05	2.47E-04	nudix hydrolase homolog 6 (NUDT6)
ATMG00030	1.0220	2.4321	3.25E-08	9.19E-07	unknown protein.
AT1G61800	1.0213	1.5180	1.11E-06	2.23E-05	glucose-6-phosphate/phosphate translocator 2 (GPT2)
AT5G56990	1.0194	1.1003	6.12E-10	2.49E-08	unknown protein
AT3G14700	1.0131	-0.6369	6.75E-04	5.01E-03	SART-1 family
AT4G02700	1.0108	1.1084	7.01E-10	2.82E-08	
AT1G28370	1.0069	-0.5293	6.28E-04	4.74E-03	ERF domain protein 11 (ERF11)
AT5G12330	1.0063	3.1694	2.35E-13	1.54E-11	LATERAL ROOT PRIMORDIUM 1 (LRP1)
AT1G23940	1.0036	1.8592	9.90E-14	6.83E-12	ARM repeat superfamily protein
AT3G14060	1.0029	2.4971	3.06E-09	1.08E-07	unknown protein
AT1G69310	1.0028	3.6114	2.47E-28	6.07E-26	WRKY DNA-binding protein 57 (WRKY57)
AT5G51190	1.0015	0.1899	9.95E-06	1.49E-04	Integrase-type DNA-binding superfamily protein
AT3G13784	-1.0055	2.6240	1.50E-10	6.70E-09	cell wall invertase 5 (CWINV5)
AT2G25130	-1.0057	-0.9474	1.59E-03	9.83E-03	ARM repeat superfamily protein
AT1G06310	-1.0136	-0.4118	1.71E-04	1.65E-03	acyl-CoA oxidase 6 (ACX6)
AT3G45280	-1.0138	-1.0563	1.43E-03	9.00E-03	syntaxin of plants 72 (SYP72)
AT2G43510	-1.0149	3.9776	3.40E-25	6.61E-23	trypsin inhibitor protein 1 (TI1)
AT5G36140	-1.0162	2.6771	1.19E-12	7.16E-11	cytochrome P450, family 716, subfamily A, polypeptide 2 (CYP716A2)
AT5G19110	-1.0213	1.2892	4.36E-11	2.12E-09	Eukaryotic aspartyl protease family protein
AT3G06160	-1.0224	1.1399	9.73E-10	3.82E-08	AP2/B3-like transcriptional factor family protein
AT1G13520	-1.0245	2.5527	2.75E-14	2.02E-12	Protein of unknown function (DUF1262)
AT1G52800	-1.0301	1.0738	5.01E-09	1.69E-07	2-oxoglutarate (2OG) and Fe(II)-dependent oxygenase superfamily protein
AT5G47450	-1.0325	3.7270	3.60E-08	1.01E-06	TONOPLAST INTRINSIC PROTEIN 2;3 (TIP2;3)
AT4G22610	-1.0330	0.7314	2.40E-08	6.98E-07	Bifunctional inhibitor/lipid-transfer protein/seed storage 2S albumin superfamily protein
AT5G04150	-1.0338	2.1567	1.48E-03	9.25E-03	BHLH101
AT5G57810	-1.0371	-0.7399	4.09E-04	3.35E-03	tetraspanin15 (TET15)
AT1G53660	-1.0410	-0.8508	6.54E-04	4.88E-03	nodulin MtN21 /EamA-like transporter family protein

AT3G51450	-1.0419	2.2806	2.30E-18	2.59E-16	Calcium-dependent phosphotriesterase superfamily protein
AT4G37060	-1.0434	-0.9903	1.40E-03	8.83E-03	PATATIN-like protein 5 (PLP5)
AT5G49780	-1.0434	0.9575	4.53E-09	1.55E-07	Leucine-rich repeat protein kinase family protein
AT3G21180	-1.0471	2.0056	1.82E-13	1.22E-11	autoinhibited Ca(2+)-ATPase 9 (ACA9)
AT1G22340	-1.0479	-0.9470	1.20E-03	7.88E-03	UDP-glucosyl transferase 85A7 (UGT85A7)
AT5G39520	-1.0488	-0.0271	4.62E-03	2.29E-02	Protein of unknown function (DUF1997)
AT3G26610	-1.0504	1.7532	2.13E-13	1.40E-11	Pectin lyase-like superfamily protein
AT1G73330	-1.0508	8.6273	4.23E-55	3.60E-52	drought-repressed 4 (DR4)
AT1G52410	-1.0510	4.8274	3.43E-16	3.03E-14	TSK-associating protein 1 (TSA1)
AT1G56160	-1.0514	-0.1841	3.46E-05	4.35E-04	myb domain protein 72 (MYB72)
AT1G52890	-1.0538	-0.1620	5.23E-05	6.14E-04	NAC domain containing protein 19 (NAC019)
AT4G37940	-1.0566	1.4217	1.11E-11	5.85E-10	AGAMOUS-like 21 (AGL21)
AT5G24420	-1.0567	4.1361	9.88E-36	3.40E-33	6-phosphogluconolactonase 5 (PGL5)
AT1G74080	-1.0577	-0.5427	2.12E-04	1.98E-03	myb domain protein 122 (MYB122)
AT2G19800	-1.0609	2.9707	3.06E-17	3.06E-15	myo-inositol oxygenase 2 (MIOX2)
AT1G25450	-1.0679	4.3059	1.48E-26	3.06E-24	3-ketoacyl-CoA synthase 5 (KCS5)
AT5G04370	-1.0700	0.7743	4.52E-09	1.55E-07	NAMT1
AT5G40590	-1.0703	0.9818	5.16E-10	2.12E-08	Cysteine/Histidine-rich C1 domain family protein
AT5G24410	-1.0721	0.7805	4.65E-09	1.58E-07	6-phosphogluconolactonase 4 (PGL4)
AT2G31180	-1.0742	-0.0970	1.28E-05	1.84E-04	myb domain protein 14 (MYB14)
AT4G04840	-1.0760	4.5228	1.17E-26	2.46E-24	methionine sulfoxide reductase B6 (MSRB6)
AT1G16120	-1.0771	0.4514	8.12E-08	2.11E-06	wall associated kinase-like 1 (WAKL1)
AT3G55890	-1.0775	0.8064	2.12E-09	7.72E-08	Yippee family putative zinc-binding protein
AT4G37700	-1.0796	0.1218	2.62E-06	4.70E-05	unknown protein
ATCG00810	-1.0797	-0.6563	2.22E-04	2.05E-03	ribosomal protein L22 (RPL22)
AT2G34810	-1.0804	3.5698	3.37E-21	5.01E-19	FAD-binding Berberine family protein
AT1G77520	-1.0816	3.6932	1.79E-11	9.21E-10	O-methyltransferase family protein
AT2G24310	-1.0826	-0.6289	1.88E-04	1.79E-03	unknown protein
AT4G14630	-1.0831	3.5923	3.61E-07	8.17E-06	germin-like protein 9 (GLP9)
AT1G29270	-1.0832	-0.2513	3.17E-05	4.05E-04	unknown protein
AT1G19510	-1.0842	-1.1115	1.08E-03	7.25E-03	RAD-like 5 (RL5)
AT2G21510	-1.0868	-0.9673	1.64E-03	1.00E-02	DNAJ heat shock N-terminal domain-containing protein
AT4G39950	-1.0928	6.5636	3.04E-41	1.32E-38	cytochrome P450, family 79, subfamily B, polypeptide 2 (CYP79B2)
ATCG00740	-1.0938	-0.2052	9.73E-06	1.46E-04	RNA polymerase subunit alpha (RPOA)
AT4G01630	-1.0938	2.5582	1.94E-19	2.42E-17	expansin A17 (EXPA17)
AT5G05600	-1.0966	3.5183	1.63E-27	3.67E-25	2-oxoglutarate (2OG) and Fe(II)-dependent oxygenase superfamily protein
AT4G23600	-1.0999	5.7013	4.45E-43	2.18E-40	CORONATINE INDUCED 1 (CORI3)
AT5G18050	-1.1017	0.9086	1.53E-09	5.73E-08	SAUR-like auxin-responsive protein family
AT2G43440	-1.1102	-0.2164	5.87E-06	9.53E-05	F-box and associated interaction domains-containing protein

AT3G25830	-1.1145	-0.9539	7.60E-04	5.50E-03	terpene synthase-like sequence-1,8-cineole (TPS-CIN)
AT4G36880	-1.1162	2.0669	3.22E-18	3.55E-16	cysteine proteinase1 (CP1)
AT4G21830	-1.1182	2.0173	5.87E-18	6.36E-16	methionine sulfoxide reductase B7 (MSRB7)
AT1G47395	-1.1204	4.1999	1.19E-03	7.83E-03	unknown protein
AT5G47240	-1.1244	2.3533	3.21E-18	3.55E-16	nudix hydrolase homolog 8 (NUDT8)
AT5G56550	-1.1248	0.7747	1.79E-09	6.59E-08	involved in tolerance to heavy metals and oxidative stress.
AT2G15220	-1.1260	4.1833	1.03E-38	3.96E-36	Plant basic secretory protein (BSP) family protein
AT2G31083	-1.1309	-0.2826	4.15E-06	7.09E-05	CLAVATA3/ESR-RELATED 5 (CLE5)
AT1G66800	-1.1317	2.8650	1.31E-22	2.21E-20	NOT a cinnamyl-alcohol dehydrogenase.
AT1G66270	-1.1382	6.4264	3.63E-35	1.23E-32	BGLU21
AT1G54095	-1.1398	-0.8494	3.69E-04	3.07E-03	Protein of unknown function (DUF1677)
AT1G60470	-1.1422	2.9650	2.26E-17	2.32E-15	galactinol synthase 4 (GolS4)
AT5G25880	-1.1455	1.1066	5.88E-12	3.23E-10	NADP-malic enzyme 3 (NADP-ME3)
AT3G26040	-1.1455	-0.2242	3.58E-06	6.20E-05	HXXXD-type acyl-transferase family protein
AT5G44050	-1.1462	2.3924	6.46E-22	1.06E-19	MATE efflux family protein
AT4G26320	-1.1581	2.8883	1.15E-11	6.01E-10	arabinogalactan protein 13 (AGP13)
AT2G33850	-1.1608	5.7470	1.03E-27	2.37E-25	unknown protein
AT3G59340	-1.1622	1.0595	1.27E-10	5.71E-09	Eukaryotic protein of unknown function (DUF914)
AT1G47400	-1.1625	3.4391	2.87E-04	2.49E-03	unknown protein
AT3G01260	-1.1705	3.5500	4.17E-36	1.46E-33	Galactose mutarotase-like superfamily protein
AT2G01880	-1.1712	2.3285	3.63E-18	3.97E-16	purple acid phosphatase 7 (PAP7)
AT4G21780	-1.1742	-0.6214	4.38E-05	5.32E-04	unknown protein
AT3G55910	-1.1779	-0.4965	2.36E-05	3.14E-04	unknown protein
AT1G50930	-1.1814	-1.0717	6.65E-04	4.95E-03	unknown protein
AT4G13410	-1.1859	0.2235	3.36E-08	9.48E-07	ATCSLA15
AT3G09940	-1.1874	2.9686	2.14E-29	5.67E-27	monodehydroascorbate reductase (MDHAR)
AT1G66280	-1.1904	5.7803	9.57E-33	2.93E-30	BGLU22
AT1G21550	-1.1937	0.0532	3.35E-07	7.68E-06	Calcium-binding EF-hand family protein
AT1G22890	-1.1950	1.6245	1.01E-14	7.75E-13	unknown protein
AT5G24140	-1.1956	0.5601	4.84E-10	2.00E-08	squalene monooxygenase 2 (SQP2)
AT4G11170	-1.2000	0.6780	1.19E-09	4.57E-08	Disease resistance protein (TIR-NBS-LRR class) family
AT3G19320	-1.2011	0.1408	4.04E-08	1.12E-06	Leucine-rich repeat (LRR) family protein
AT1G13609	-1.2012	3.9328	1.06E-03	7.15E-03	Defensin-like (DEFL) family protein
AT3G27920	-1.2029	-0.4205	6.98E-06	1.10E-04	myb domain protein 0 (MYB0)
AT1G13510	-1.2095	1.0911	5.31E-13	3.34E-11	Protein of unknown function (DUF1262)
AT1G11112	-1.2143	-0.3924	3.77E-06	6.50E-05	unknown protein
AT1G27940	-1.2206	1.2908	2.60E-13	1.70E-11	P-glycoprotein 13 (PGP13)
AT5G04000	-1.2235	-0.2762	2.19E-06	4.04E-05	unknown protein
AT4G15700	-1.2262	-0.8042	1.24E-04	1.27E-03	Thioredoxin superfamily protein

AT1G27140	-1.2271	2.4940	8.23E-21	1.19E-18	glutathione S-transferase tau 14 (GSTU14)
AT5G37478	-1.2296	-0.7308	3.87E-05	4.78E-04	TPX2 (targeting protein for Xklp2) protein family
AT2G30750	-1.2322	5.7324	2.55E-17	2.61E-15	cytochrome P450, family 71, subfamily A, polypeptide 12 (CYP71A12)
AT3G62430	-1.2331	-1.1433	6.47E-04	4.84E-03	Protein with RNI-like/FBD-like domains
AT1G53610	-1.2350	-1.1140	1.96E-04	1.85E-03	unknown protein
AT5G53380	-1.2360	-0.9747	9.14E-05	9.88E-04	O-acyltransferase (WSD1-like) family protein
AT3G45330	-1.2367	-0.7633	3.33E-05	4.21E-04	Concanavalin A-like lectin protein kinase family protein
AT1G21100	-1.2374	4.9610	2.01E-37	7.29E-35	O-methyltransferase family protein
AT3G02850	-1.2442	1.5416	6.06E-17	5.94E-15	II (inward rectifying channel): KAT1 (AT5G46240) and KAT2 (AT4G18290)
AT5G65030	-1.2461	-0.1750	6.11E-07	1.32E-05	unknown protein
AT3G09960	-1.2481	0.2442	1.15E-08	3.60E-07	Calcineurin-like metallo-phosphoesterase superfamily protein
AT4G24340	-1.2496	1.9500	1.49E-19	1.89E-17	Phosphorylase superfamily protein
AT3G22570	-1.2509	1.2060	7.38E-15	5.77E-13	Bifunctional inhibitor/lipid-transfer protein/seed storage 2S albumin superfamily protein
AT5G46890	-1.2532	3.9441	2.89E-33	8.99E-31	Bifunctional inhibitor/lipid-transfer protein/seed storage 2S albumin superfamily protein
AT2G37025	-1.2600	1.4416	7.92E-12	4.27E-10	TRF-like 8 (TRFL8)
AT1G65680	-1.2605	-1.1431	2.74E-04	2.40E-03	expansin B2 (EXPB2)
AT4G27570	-1.2606	-0.5780	1.15E-05	1.68E-04	UDP-Glycosyltransferase superfamily protein
AT5G45960	-1.2625	1.0386	2.72E-13	1.77E-11	GDSL-like Lipase/Acylhydrolase superfamily protein
AT2G28860	-1.2741	-0.9189	5.61E-05	6.52E-04	cytochrome P450, family 710, subfamily A, polypeptide 4 (CYP710A4)
AT1G26410	-1.2876	1.8064	6.17E-14	4.34E-12	FAD-binding Berberine family protein
AT1G54790	-1.2909	1.4390	3.37E-17	3.35E-15	GDSL-like Lipase/Acylhydrolase superfamily protein
AT4G10310	-1.2923	2.6218	9.08E-17	8.81E-15	high-affinity K+ transporter 1 (HKT1)
AT1G16370	-1.2927	0.1787	1.44E-08	4.41E-07	organic cation/carnitine transporter 6 (OCT6)
AT2G25220	-1.2939	1.0919	3.39E-14	2.46E-12	Protein kinase superfamily protein
AT1G63295	-1.2964	1.1990	2.09E-13	1.38E-11	Remorin family protein
AT3G45430	-1.2994	1.2266	1.04E-15	8.74E-14	Concanavalin A-like lectin protein kinase family protein
AT5G38910	-1.3015	2.3190	2.87E-16	2.58E-14	RmlC-like cupins superfamily protein
AT1G09500	-1.3185	1.1002	3.06E-14	2.24E-12	NAD(P)-binding Rossmann-fold superfamily protein
AT1G22590	-1.3214	2.7739	1.08E-32	3.23E-30	AGAMOUS-like 87 (AGL87)
AT3G25655	-1.3247	-0.7664	1.98E-05	2.68E-04	inflorescence deficient in abscission (IDA)-like 1 (IDL1)
AT1G72450	-1.3310	4.1603	8.00E-47	4.36E-44	jasmonate-zim-domain protein 6 (JAZ6)
AT5G02540	-1.3371	2.3435	1.53E-27	3.48E-25	NAD(P)-binding Rossmann-fold superfamily protein
AT5G43520	-1.3379	1.7669	1.64E-18	1.89E-16	Cysteine/Histidine-rich C1 domain family protein
AT1G34510	-1.3437	-0.2667	1.41E-07	3.53E-06	Peroxidase superfamily protein
AT5G59510	-1.3481	0.3754	1.12E-10	5.10E-09	ROTUNDIFOLIA like 5 (RTFL5)
AT5G23990	-1.3565	3.5055	7.82E-47	4.36E-44	ferric reduction oxidase 5 (FRO5)
AT5G65600	-1.3602	-0.3133	2.98E-07	6.98E-06	Concanavalin A-like lectin protein kinase family protein
AT5G48400	-1.3646	0.4143	4.40E-11	2.13E-09	ATGLR1.2
AT1G09240	-1.3658	0.1144	1.46E-09	5.51E-08	nicotianamine synthase 3 (NAS3)

AT4G20210	-1.3699	-0.2562	9.35E-08	2.41E-06	Terpenoid cyclases/Protein prenyltransferases superfamily protein
AT1G52790	-1.3701	-0.9291	3.16E-05	4.05E-04	contains PF03171 2OG-Fe(II) oxygenase superfamily domain
AT1G66460	-1.3711	-0.1710	5.13E-08	1.40E-06	Protein kinase superfamily protein
AT3G05155	-1.3824	-0.0523	5.15E-09	1.73E-07	Major facilitator superfamily protein
AT3G27940	-1.3850	-0.9293	3.35E-05	4.22E-04	LOB domain-containing protein 26 (LBD26)
AT5G64120	-1.3901	6.6920	5.15E-45	2.66E-42	Peroxidase superfamily protein
AT3G13540	-1.3937	-0.6963	2.61E-06	4.69E-05	myb domain protein 5 (MYB5)
AT1G06100	-1.4075	1.3263	9.73E-09	3.09E-07	Fatty acid desaturase family protein
AT1G52000	-1.4143	5.9465	4.65E-61	4.80E-58	Mannose-binding lectin superfamily protein
AT3G61840	-1.4159	-0.7791	4.16E-06	7.10E-05	Protein of unknown function (DUF688)
AT1G15050	-1.4182	-0.9590	1.40E-05	1.99E-04	indole-3-acetic acid inducible 34 (IAA34)
AT1G48470	-1.4183	-0.8716	1.48E-05	2.09E-04	glutamine synthase isozyme
AT1G12570	-1.4254	2.1274	2.90E-26	5.81E-24	Glucose-methanol-choline (GMC) oxidoreductase family protein
ATCG00630	-1.4256	-1.1337	4.15E-05	5.09E-04	PSAJ
AT3G21800	-1.4330	-0.8274	5.48E-06	9.01E-05	UDP-glucosyl transferase 71B8 (UGT71B8)
AT1G17380	-1.4370	-0.3164	4.18E-08	1.16E-06	jasmonate-zim-domain protein 5 (JAZ5)
AT3G52550	-1.4437	0.0395	6.61E-10	2.67E-08	Similar to ovate family protein 18
AT4G12520	-1.4492	2.3952	1.75E-26	3.57E-24	Bifunctional inhibitor/lipid-transfer protein/seed storage 2S albumin superfamily protein
ATCG00800	-1.4519	-0.0158	1.61E-09	6.00E-08	RESISTANCE TO PSEUDOMONAS SYRINGAE 3 (RPS3)
AT2G29130	-1.4532	1.4152	3.54E-21	5.21E-19	laccase 2 (LAC2)
AT1G05650	-1.4559	1.1739	1.87E-14	1.39E-12	Pectin lyase-like superfamily protein
AT2G22330	-1.4598	5.6156	4.40E-78	7.20E-75	cytochrome P450, family 79, subfamily B, polypeptide 3 (CYP79B3)
AT5G02170	-1.4618	1.4327	1.24E-21	1.92E-19	Transmembrane amino acid transporter family protein
AT5G23780	-1.4630	-0.8384	6.95E-06	1.09E-04	DOMAIN OF UNKNOWN FUNCTION 724 9 (DUF9)
AT2G35980	-1.4635	1.9214	1.25E-25	2.47E-23	YELLOW-LEAF-SPECIFIC GENE 9 (YLS9)
AT3G05730	-1.4638	5.5233	5.89E-62	6.80E-59	LOCATED IN: endomembrane system
AT5G42600	-1.4905	3.8827	3.78E-29	9.88E-27	marneral synthase (MRN1)
AT3G46300	-1.4909	-0.7601	8.49E-07	1.75E-05	unknown protein
AT5G62420	-1.4943	0.0404	1.72E-10	7.58E-09	NAD(P)-linked oxidoreductase superfamily protein
AT2G19060	-1.4943	0.6967	1.80E-14	1.35E-12	SGNH hydrolase-type esterase superfamily protein
AT2G26370	-1.5053	-0.8923	4.07E-06	6.96E-05	MD-2-related lipid recognition domain-containing protein
AT1G62280	-1.5069	1.7071	4.45E-24	8.32E-22	SLAC1 homologue 1 (SLAH1)
AT4G40020	-1.5078	-0.1742	1.11E-09	4.28E-08	Myosin heavy chain-related protein
AT1G26390	-1.5087	3.9480	5.88E-20	7.89E-18	FAD-binding Berberine family protein
AT5G40330	-1.5098	1.1624	9.93E-20	1.29E-17	myb domain protein 23 (MYB23)
AT2G02300	-1.5111	-1.0316	8.30E-06	1.27E-04	phloem protein 2-B5 (PP2-B5)
AT4G22212	-1.5130	2.1309	4.23E-32	1.22E-29	Arabidopsis defensin-like protein
AT5G36130	-1.5245	1.0306	2.65E-17	2.70E-15	Cytochrome P450 superfamily protein
AT1G47890	-1.5338	-0.4674	2.17E-08	6.39E-07	receptor like protein 7 (RLP7)

AT2G20870	-1.5366	-0.6778	1.66E-07	4.11E-06	cell wall protein precursor, putative
AT1G26700	-1.5380	-0.7302	3.44E-07	7.85E-06	MILDEW RESISTANCE LOCUS O 14 (MLO14)
AT3G21660	-1.5494	-0.3750	1.29E-08	3.97E-07	UBX domain-containing protein
AT5G65340	-1.5498	-0.8470	1.35E-06	2.65E-05	Protein of unknown function, DUF617
AT4G12510	-1.5578	1.7651	1.26E-23	2.30E-21	Bifunctional inhibitor/lipid-transfer protein/seed storage 2S albumin superfamily protein
AT1G63710	-1.5635	1.0489	1.07E-18	1.26E-16	cytochrome P450, family 86, subfamily A, polypeptide 7 (CYP86A7)
AT1G18990	-1.5671	-0.7428	3.59E-07	8.12E-06	Protein of unknown function, DUF593
AT5G46350	-1.5720	-0.2723	3.21E-09	1.13E-07	Group II-c
AT4G15690	-1.5754	-0.2437	5.70E-10	2.33E-08	Thioredoxin superfamily protein
AT5G28630	-1.6049	-0.8200	4.15E-07	9.25E-06	glycine-rich protein
AT3G44860	-1.6058	0.8195	1.27E-16	1.21E-14	farnesoic acid carboxyl-O-methyltransferase (FAMT)
AT1G36622	-1.6083	0.5551	1.70E-15	1.40E-13	unknown protein
AT2G19500	-1.6091	0.2448	1.58E-13	1.07E-11	cytokinin oxidase 2 (CKX2)
AT4G15990	-1.6455	-0.2976	4.05E-10	1.69E-08	unknown protein
AT3G61390	-1.6486	0.5546	1.90E-15	1.53E-13	RING/U-box superfamily protein
AT3G01175	-1.6528	-0.8894	4.96E-07	1.09E-05	Protein of unknown function (DUF1666)
AT5G23830	-1.6629	3.9546	4.07E-35	1.35E-32	MD-2-related lipid recognition domain-containing protein
AT4G12545	-1.6677	3.1511	2.47E-59	2.42E-56	Bifunctional inhibitor/lipid-transfer protein/seed storage 2S albumin superfamily protein
AT1G52400	-1.6794	7.3349	6.54E-56	5.83E-53	beta glucosidase 18 (BGLU18)
AT3G59010	-1.6853	2.6636	8.21E-40	3.36E-37	pectin methylesterase 61 (PME61)
AT5G10946	-1.7012	0.5355	1.71E-16	1.58E-14	unknown protein
AT1G13500	-1.7306	-1.2265	3.91E-06	6.71E-05	Protein of unknown function (DUF1262)
AT5G33370	-1.7307	3.1851	3.93E-19	4.73E-17	GDSL-like Lipase/Acylhydrolase superfamily protein
AT5G64667	-1.7567	-1.0904	1.49E-06	2.90E-05	inflorescence deficient in abscission (IDA)-like 2 (IDL2)
AT5G49870	-1.7675	-1.0672	3.08E-07	7.16E-06	Mannose-binding lectin superfamily protein
AT5G24780	-1.8124	4.7860	1.13E-79	2.01E-76	vegetative storage protein 1 (VSP1)
AT3G62950	-1.8151	0.6961	5.36E-20	7.30E-18	Thioredoxin superfamily protein
AT1G52820	-1.8400	3.0356	3.33E-21	4.99E-19	2-oxoglutarate (2OG) and Fe(II)-dependent oxygenase superfamily protein
AT3G28220	-1.8938	5.8677	3.54E-50	2.40E-47	TRAF-like family protein
AT5G24770	-1.8968	7.3739	3.99E-34	1.28E-31	vegetative storage protein 2 (VSP2)
AT1G73325	-1.9036	-0.5192	3.64E-11	1.79E-09	Kunitz family trypsin and protease inhibitor protein
AT1G58320	-1.9506	0.8418	9.98E-25	1.90E-22	PLAC8 family protein
AT1G14250	-1.9665	4.7699	7.44E-62	8.11E-59	GDA1/CD39 nucleoside phosphatase family protein
AT4G33120	-1.9861	1.6907	1.55E-37	5.74E-35	S-adenosyl-L-methionine-dependent methyltransferases superfamily protein
AT4G12550	-1.9959	3.8635	2.82E-100	9.23E-97	Auxin-Induced in Root cultures 1 (AIR1)
ATCG01020	-2.0024	-0.8700	1.76E-09	6.48E-08	ribosomal protein L32 (RPL32)
AT5G48430	-2.0092	2.4552	2.55E-39	1.00E-36	Eukaryotic aspartyl protease family protein
AT1G77530	-2.0455	2.7134	2.99E-31	8.37E-29	O-methyltransferase family protein
AT3G21460	-2.0829	0.1032	3.18E-18	3.54E-16	Glutaredoxin family protein

AT4G22214	-2.2144	1.3997	1.49E-39	5.95E-37	Defensin-like (DEFL) family protein
AT2G28210	-2.2579	0.0898	1.85E-19	2.33E-17	alpha carbonic anhydrase 2 (ACA2)
AT4G36700	-2.2905	1.2058	6.88E-07	1.46E-05	RmlC-like cupins superfamily protein
AT5G23840	-2.3106	1.7418	1.33E-52	1.00E-49	MD-2-related lipid recognition domain-containing protein
AT2G04032	-2.3241	0.9097	1.64E-28	4.07E-26	zinc transporter 7 precursor (ZIP7)
AT5G55720	-2.4027	0.1140	6.01E-22	9.91E-20	Pectin lyase-like superfamily protein
AT1G65450	-2.4737	1.5125	3.40E-51	2.47E-48	HXXXD-type acyl-transferase family protein
AT4G17470	-2.4884	1.4711	2.02E-48	1.24E-45	alpha/beta-Hydrolases superfamily protein
AT3G05950	-2.6155	-1.2816	7.18E-10	2.87E-08	RmlC-like cupins superfamily protein
AT2G39330	-2.7390	1.8900	5.95E-70	7.77E-67	jacalin-related lectin 23 (JAL23)
AT2G24850	-3.1492	-0.7427	2.25E-18	2.55E-16	tyrosine aminotransferase 3 (TAT3)
AT1G52030	-3.5464	1.8504	2.62E-95	7.35E-92	myrosinase-binding protein 2 (MBP2)
AT5G06900	-3.6952	-0.6516	2.39E-23	4.22E-21	cytochrome P450, family 93, subfamily D, polypeptide 1 (CYP93D1)
AT3G16670	-3.7452	3.9900	4.95E-181	2.43E-177	Pollen Ole e 1 allergen and extensin family protein
AT1G52040	-5.4508	3.5315	1.04E-200	6.80E-197	myrosinase-binding protein 1 (MBP1)
AT2G38540	-6.0115	8.9814	0.00E+00	0.00E+00	lipid transfer protein 1 (LP1)
AT4G04950	-7.6232	4.2675	0.00E+00	0.00E+00	PICOT1

FC, fold change; CPM, counts per million; FDR, false discovery rate